ProQuest LLC.
789 East Eisenhower Parkway
P.O. Box 1346
Ann Arbor, MI 48106 – 1346

An investigation into the effect of the piston-liner interface upon the particulate emissions from a turbo charged diesel engine

P.W.Yates

A thesis submitted in partial fulfilment of the requirements of
Sheffield Hallam University
For the degree of Doctor of Philosophy

November 1999

Collaborating organisation: AE Goetze

Abstract

The continuing tightening of emission regulations has encouraged extensive research into fuel spray vaporising and combustion. This thesis is an investigation into the effect that the cylinder boundaries have upon the quantity and composition of the unburnt hydrocarbons present in the exhaust gas and particulate matter.

To determine the cylinder boundaries' effect on the exhaust hydrocarbon content a series of engine tests was completed. The engine used for these experiments was a modern four cylinder turbo charged direct injection diesel engine, operated at five steady state test points. The test consisted of two standard engine builds to determine the accuracy of measurement and to supply a base point for comparison. The second test used standard pistons with modified oil control rings to increase the oil film thickness. The final test used pistons with the top ring moved nearer the top of the piston by 5.5 mm to reduce the top land crevice volume by ≈55%.

The composition of the particulate soluble organic fraction (SOF) for the test using the low tangential load oil control piston ring was shown to have a greater fuel content than for other tests, showing that adsorption of the fuel in the lubricating oil contributes to the particulate. The reduction of the top ring crevice volume produced similar quantities of particulate SOF but it consisted of generally lighter hydrocarbon species.

The effects of these changes were replicated in a mathematical model which calculated the in cylinder values for fuel, soot, temperature and hydrocarbons. The model also simulated the oxidation of hydrocarbons at the cylinder boundary and consisted of 3 primary zones; the combustion chamber, crevice volume and oil film.

This research shows that careful design of engine components can influence the quantity and composition of the particulates exhaust gas and allow the reduction of regulated components.

Acknowledgements

Firstly I would like to thank Maggie France for all the support and encouragement that she has given throughout this research program. I would also like to thank the following people who have made this thesis possible.

Dr Peter Foss	Director of studies
Prof D.H Tidmarsh	Director of studies
Dr Mick Willcock	Industrial adviser
Mr Simon Gazzard	Industrial adviser

I would also like to thank David Douce for all the assistance in developing my chemical analysis skills and the technical staff in the School of Engineering for their support and contributions to the test program. Without Dave Allen, Richard Wilkinson and Brian Palmer the test equipment would not have functioned as well as it did.

AE Goetze for their financial and equipment contributions.

Finally I would like to thank my parents for their encouragement to return into further education and the support they gave throughout all my studies.

Nomenclature

ρ	Density	kg/m^3
Φ	Equivalence ratio	
γ	Specific heat ratio c_p/c_v	
A	Area	m^2
c	Specific heat	kJ/kgK
C^*_{eq}	mass fraction of fuel in oil at equilibrium	
C^*	mass fraction of fuel in oil	
Cmax-Cmin	total fuel emitted from oil in a cycle	
d	Diameter	m
d_{mf}	the incremental mass of oil emitted	
D	Hydraulic diameter	m
D_c	Cylinder liner diameter	m
E	Absolute internal energy	kJ
F/A	Fuel Air ratio	
FBR	Fuel Burning Rate	
FPR	Fuel Preparation Rate	
h	Height	m
K	Equilibrium constant	
k	adsorption coefficient	
m	Mass	kg
N	Crankshaft rotational speed	rpm
N_{HC}	Henry Constant	
p	Pressure	N/m^2
p'_{O2}	partial pressure of oxygen	N/m^2
Q	Heat transfer	kJ
R	Specific gas constant	kJ/kgK
Ra	Arithmetical mean deviation of the departure above and below the profile	
Rz	The average distance between the 5 highest peaks and the 5 lowest valleys	
S	Spray penetration	m
T	Temperature	K
t	Time	s
U	Internal energy	kJ
u	Specific internal energy	kJ/kg
v	Specificvolume (volume per unit mass)	m^3/kg
V	Volume	m^3
W	Width	m
X	Oil layer thickness	μm
Z	Thickness	m

subscripts

n	nozzle
g	gas
f	fuel

Abbreviations and Terms

DI	Direct Injection
FID	Flame Ionisation Detector
GC-MS	Gas Chromatography with Mass Spectomety
HPLC	High Pressure Liquid Chromatography
IDI	Indirect Injection
NA	Naturally Aspirated
PAH	Polycyclic Aromatic Hydrocarbon
hr	Hour
SI	Spark Ignition
SOF	Soluble Organic Fraction
TC	Turbo Charged

Nozzle sac volume is the volume within the injector that is open to the combustion chamber when the injector needle is on its seat.
Molecular weight is the total of the atomic weights of the atoms within the compounds.

ECE-R 49/01 13 mode cycle is a combination of 13 steady state operation conditions in which each operation point is held for 6 minutes. Only the final minute of each operation point is used for emission testing. The operation points are as follows

Mode N^{o}	Engine Speed	Per cent load	Mode weighting factor
1	idle	0	0.25/3
2	peak torque	10	0.08
3	peak torque	25	0.08
4	peak torque	50	0.08
5	peak torque	75	0.08
6	peak torque	100	0.25
7	idle	0	0.25/3
8	max power	100	0.10
9	max power	75	0.02
10	max power	50	0.02
11	max power	25	0.02
12	max power	10	0.02
13	max power	0	0.25/3

Federal Test Procedure (FTP) 75 a simulated drive cycle which corresponds to typical urban driving speeds and loads. All testing is carried out using a computer controlled chassis dynamometer.

Sauter mean diameter is the droplet size of a hypothetical spray of uniform size, such that the volume and the overall volume to surface area ratio is the same

Contents

Appendices

1) Piston and liner dimensions
2) Values for CO CO_2 and NOx
3) Model input parameters
4) Listing of model code
5) Papers published

List of Figures

List of tables

1.0 Introduction

The diesel engine is at present dominant in the bus and truck prime mover market. The advantage this type of engine has over its competitors is that it is more durable, reliable and fuel efficient. The present environmentalists are condemning the diesel engine as polluting and dangerous to health. The diesel engine has to shake off its dirty and polluting image whilst retaining its fuel efficiency.

The contribution of different sources to the total UK emissions of the six main pollutants is shown in Figure 1.1-6 and shows that current diesel vehicles contribute significant quantities to the total NO_X and black smoke emissions. The total quantity of SO_2 and CO_2 emitted for each diesel vehicle group is solely dependent on the quantity of fuel burnt and so is directly proportional to the number of units in use, thus the influence of engine design does not alter the results. However, the contribution to NOx emissions by heavy goods vehicles is significantly higher and thus each diesel unit produces more NOx.

Diesel particulates are increasingly being labelled as a health hazard. Exhaust particles are generally less than 1μm in diameter and typically 0.1-0.5 μm. They are deposited mainly in the alveolar part of the lung and, to a lesser extent, in the nose and throat. These small particles have a greater potential to adversely affect human health than larger particles as they remain in contact with the lungs for longer periods. Particles in the air aggravate diseases such as bronchitis, asthma and cardiovascular problems. It has been estimated that 1 in 5 of the British population are sensitive to the effects of particulate pollution.

In 1970 the diesel engine accounted for only 9% of the total black smoke emitted. The Clean Air Act and other methods of control upon domestic sources has halved the

majority of emissions from other sources so that by the early 1990's the diesel engine accounted for 39%. Another reason for the increase in the contribution is that the total quantity of black smoke from diesel engines has doubled from the early 1970's to over 200 kilotonnes per annum through an increase in diesel engine vehicle sales.

The power output from diesel engines is regulated by the quantity of fuel injected directly into the working cylinder and therefore the engine does not need any restrictions in the induction system. The restriction caused by the throttle on Spark Ignition(S.I.) is one of the primary reasons for its lower fuel conversion efficiency($\eta_{f,i}$) (energy lost pumping sub-atmospheric pressure intake gases past a part open throttle valve[1]). Figure 1.7 shows the effect of load upon the specific fuel consumption of the three main engine types. The $\eta_{f,i}$ is also directly related to the engine's compression ratio; the higher the compression ratio the higher the $\eta_{f,i}$. Typical compression ratio values for spark ignition(S.I.) engines are 8 to 12 and compression ignition(C.I.) engines 12 to 24. There is no theoretical limit to the compression ratio for the diesel engine because only air is compressed, but as the compression ratio increases it necessitates an increase in weight of the major components, reducing the maximum engine speed and acceleration and increasing vehicle weight.

Emissions regulations and market acceptability have become strong motivators for controlling pollutants from diesel engines through increasing public awareness of the impact the combustion of fossil fuels has on the environment and the health of the population within cities. There is increasing evidence[(2)] that hospital admissions are directly related to urban air quality. Figure 1.8 shows the relation between sulphur dioxide levels and the admissions to hospitals. The results for this graph are for all of November and December. The reason for the increase in atmospheric air pollution is the weight of traffic combined with a weather system producing minimal wind speed.

The main pollution concerns for diesel vehicles are nitrogen oxides and particulates. Carbon monoxide emission levels are significantly lower than petrol engines with similar power output because the engine always operates at fuel-air mixtures with more than the stoichiometric air requirement. The only area where there is insufficient air for the complete oxidation of the fuel is within the fuel spray . CO_2 and hydrocarbon emissions are less than comparable power output petrol engines because of their better specific fuel consumption.

The particulate matter present in the exhaust of a diesel engine is primarily comprised of two components, dry soot (solids of carbon) and adsorbed organic matter (unburnt hydrocarbons). The solids of carbon are primarily formed in the fuel rich areas within the combustion chamber and, therefore, the fuel is the predominant source, with some contribution from the lubricating oil. The adsorbed matter consists of unburnt fuel, oil, water and trace amounts of sulphur, zinc, phosphorus, calcium, iron, silicon and chromium. The lubricating oil has a high molecular weight and any entering the exhaust gas will become a major contributor to the adsorbed particulate matter. The boiling point for the majority of the adsorbed component of the collected particulate is lower than the temperature of the gases exiting the cylinder at high loads. As the temperature decreases below 500°C the higher molecular weight organic compounds condense and adsorb onto the solids of carbon.

Hence the focus of research and development has centred around NOx and particulates. The primary components of the measured NOx are nitrogen dioxide (NO_2) and nitric oxide (NO). NOx can be reduced by retarding the injection timing, thus lowering the combustion temperature, but this action increases the dry soot, CO_2 and increases fuel consumption for the same power output. To reduce the levels of NOx to those proposed in forthcoming legislation, the use of oxidation catalysts within the exhaust will be used.

As the proportion of particulates produced from the incomplete combustion of fuel decreases, the reduction of lubricating oil consumption becomes an increasingly important issue.

The contributions of fuel and lubricating oil to particulate emissions vary with engine load such that, with light engine load, there will be a higher contribution from the lubricating oil of up to 40% [3]. The contribution of oil to the particulate emissions is much greater than would be expected, based on relative consumption rates of oil and fuel (approximately 0.25% by mass). At the high speed low load condition the oil contribution is approximately 100 times greater than that predicted from the relative oil fuel consumption rate. Depending on test conditions a given amount of engine oil can supply from 50 to 280 times as much material to the particulate emissions as does an equal amount of fuel. It can be seen that although the oil consumption is relatively small compared to that of the fuel, the oil can still have a significant effect on particulate emissions.

The oil that enters into the combustion chamber has low inertia and flows into a relatively cool area. This low inertia and temperature does not allow for complete oxidation and the oil molecules are subject to the effects of pyrolysis. The oil and fuel used in diesel engines have molecular weights that are closer than those found in spark ignition engines. The closer the molecular weights of the adsorbent and adsorbate the faster and greater the quantity of matter can be adsorbed. The facility for the fuel to adsorb into the oil within a diesel engine is not available for the same period of the engine's cycle as with homogeneous charged engines, and so the effect is less prominent. It is therefore important to establish the transport mechanisms that allow oil to pass into the combustion zone, and their contribution to the total particulate emission.

Experimental work has been undertaken to enable the development and calibration of a mathematical model to predict the effects of the changes made to the in-cylinder geometry to the hydrocarbon and soot emissions. The model uses the measured cylinder pressure to calculate the conditions present in the working cylinder. Using previously developed and verified equations for the formation and possible oxidation of the main exhaust gas components as the starting point, the effect of the modifications can be replicated. The results from the model are compared to those obtained experimentally and used to optimise the design of the piston and cylinder liner.

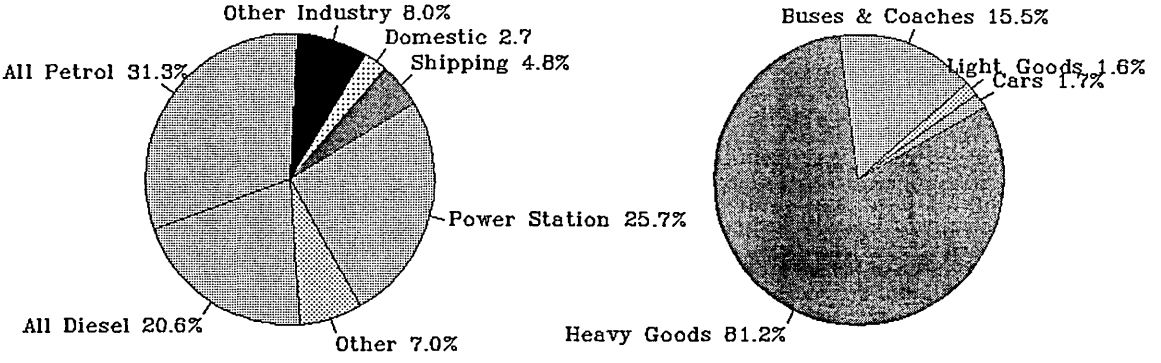

UK National Air Pollutant Emissions 1991 (Data From Warren Springs Laboratory)

Figure 1.1 UK NOx Emissions

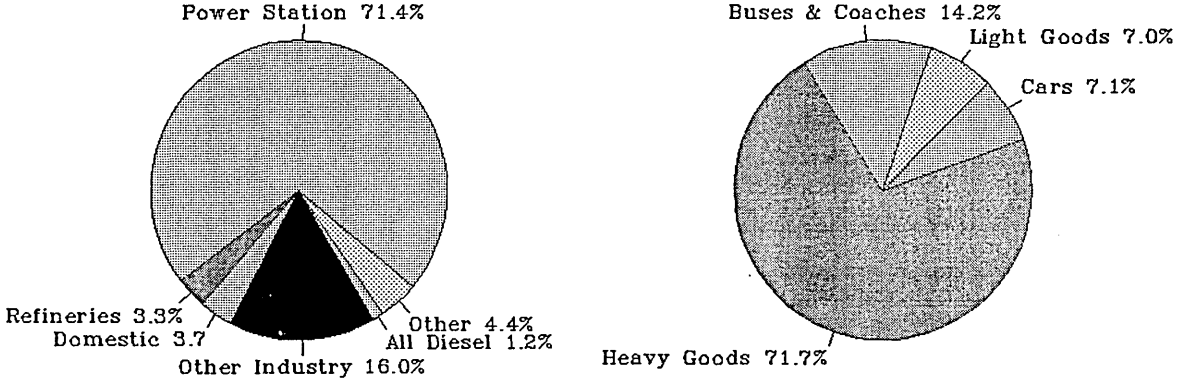

Figure 1.2 UK SO2 Emissions

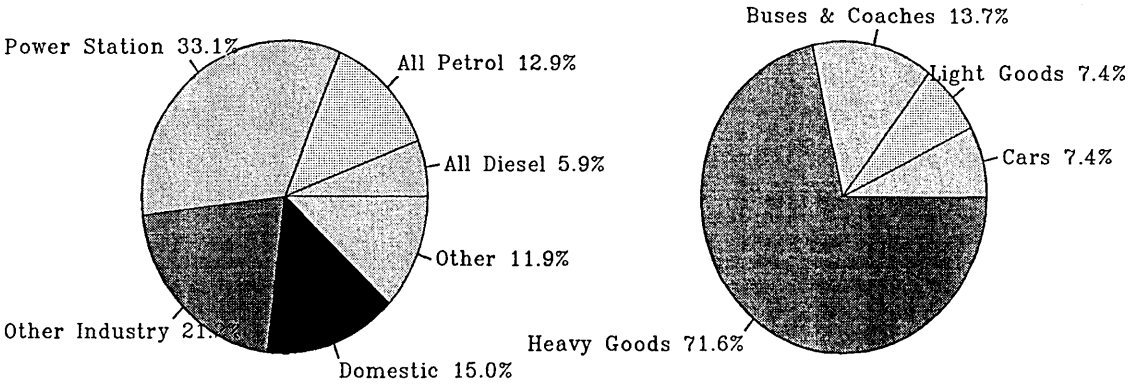

Total CO2 Emissions Diesel Emissions of CO2

UK National Air Pollutant Emissions 1991 (Data From Warren Springs Laboratory)

Figure 1.3 UK CO2 Emissions

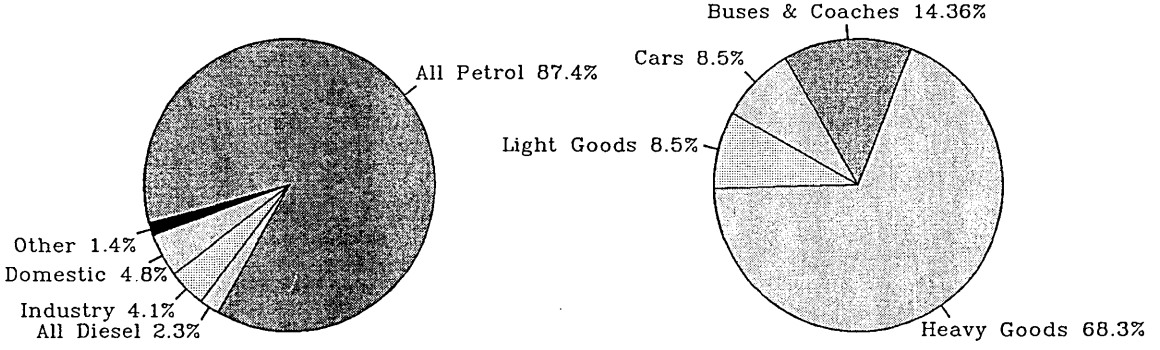

Total CO Emissions Diesel Emissions Of CO

Figure 1.4 UK CO Emissions

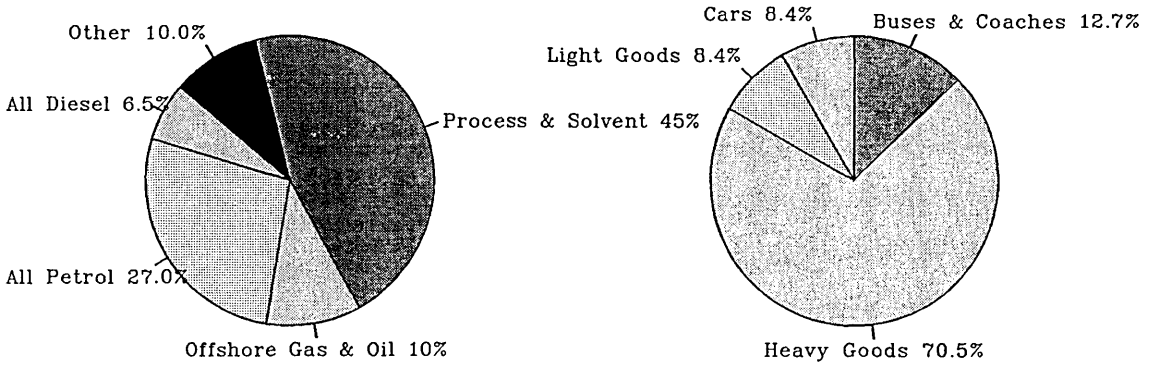

UK National Air Pollutant Emissions 1991 (Data From Warren Springs Laboratory)

Figure 1.5 Volatile Organic Compounds

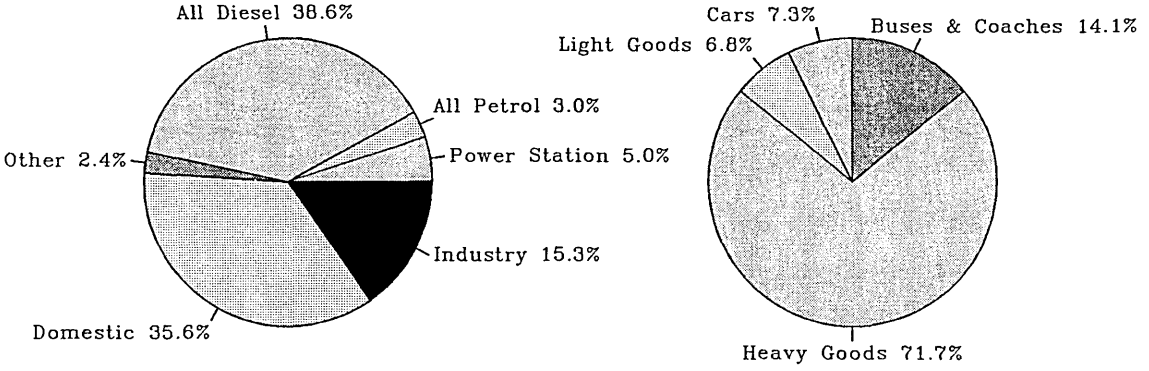

Figure 1.6 UK Black Smoke

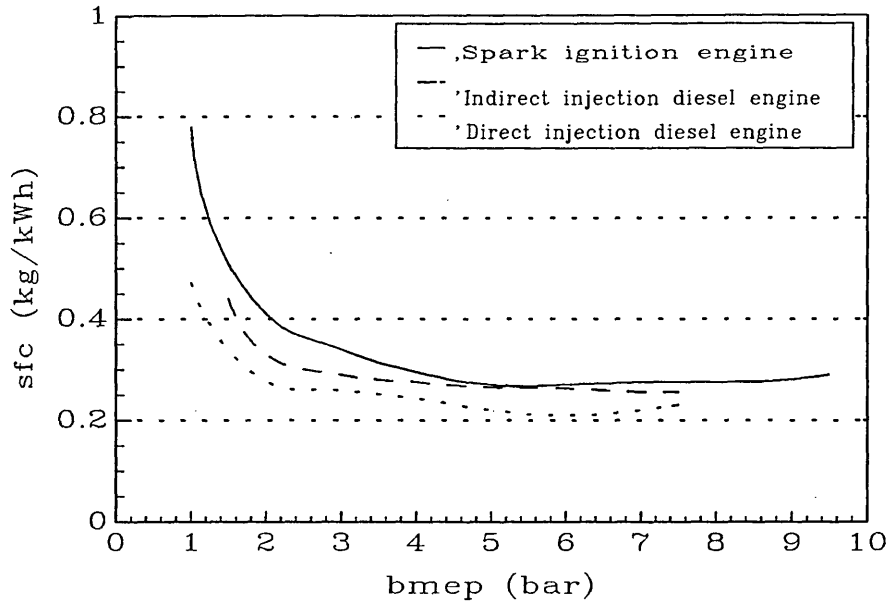

Data from Stone R. Motor Vehicle Fuel Economy, Macmillan, London.

Comparison of the part specific fuel consumption 2000 RPM

Figure 1.7 The effect of part load upon specific fuel consumption

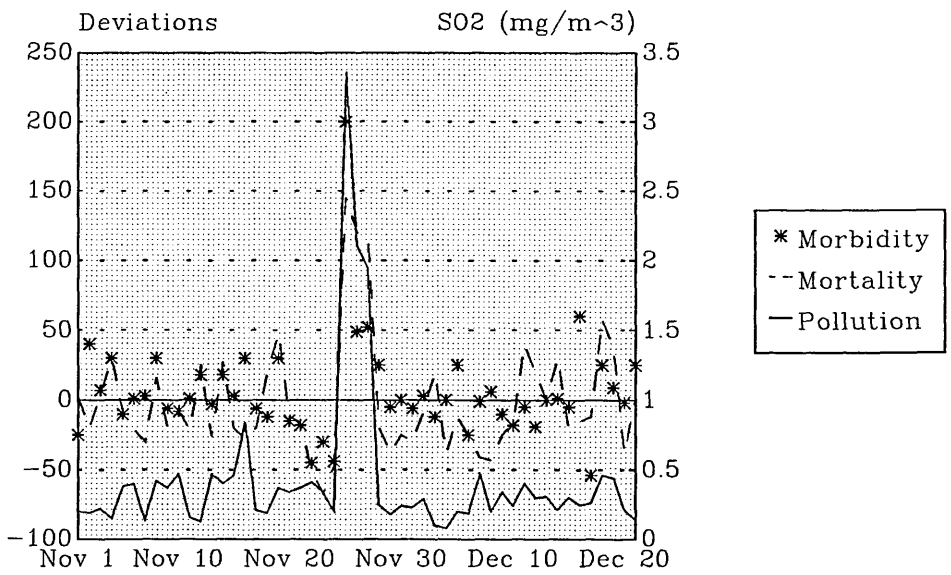

Daily Average Sulphur Dioxide Concentrations and Hospital Admissions London 1962

Figure 1.8

2.0) Origins of Hydrocarbon Emissions from a Diesel Engine.

There are two main types of diesel engine, direct injection (D.I.) and indirect injection (IDI). The indirect injection system was developed to overcome the poor mixing of the fuel/air mixture in small engines. The size of the engine determines the maximum available fuel injection pressure; the larger the engine the higher the fuel injection pressure. Diesel engines were not suitable for small vehicles until the development of improved high pressure fuel injection equipment combined with the IDI combustion configuration. The small quantity of air within the cylinder did not have sufficient inertia to allow complete mixing and clean combustion, and thus the higher fuel pressures were required to provide the necessary in-cylinder mixing. These developments have allowed the more efficient direct injection engine to be applied to small vehicles. Any given vehicle with a D.I. engine may be up to 20% more fuel efficient than with an IDI diesel engine and up to 40% more than when fitted with a spark ignition engine. The loss in efficiency of the IDI engine when compared to the D.I. is primarily because of the turbulent flow (flow with a high Reynolds number) through the throat connecting the combustion chamber to the working cylinder.

The hydrocarbon emissions from diesel engines are typically lower than those from a spark ignition engine, but with exhaust after treatment the exhaust gas from a spark ignition(S.I.) engine that enters the atmosphere contains comparable levels. Oxidation catalysts that are fitted to S.I. engines will not function on D.I. engines because of the lower exhaust gas temperatures, the possibility of blockage through soot and the quantity of oxygen present in the exhaust gas.

The emissions from vehicles for use in Europe were not a problem for manufacturers until July 1970 when the first European Community directive (70/220/EEC) was implemented. It was not until 1988 and 88/436/EEC,L214 was implemented when the particulate emissions from diesel engines were first legislated, and this legislation did

not discriminate between the two types of Diesel engine. IDI and DI engines were not treated separately until 1996 and 96/44/EC,L210.

Combustion in a D.I. engine is in three general stages:

1. Delay (the time between the start of injection and the start of combustion).
2. Rapid combustion (the burning of the fuel injected during the delay period) .
3. Controlled combustion (fuel burning as it is injected).

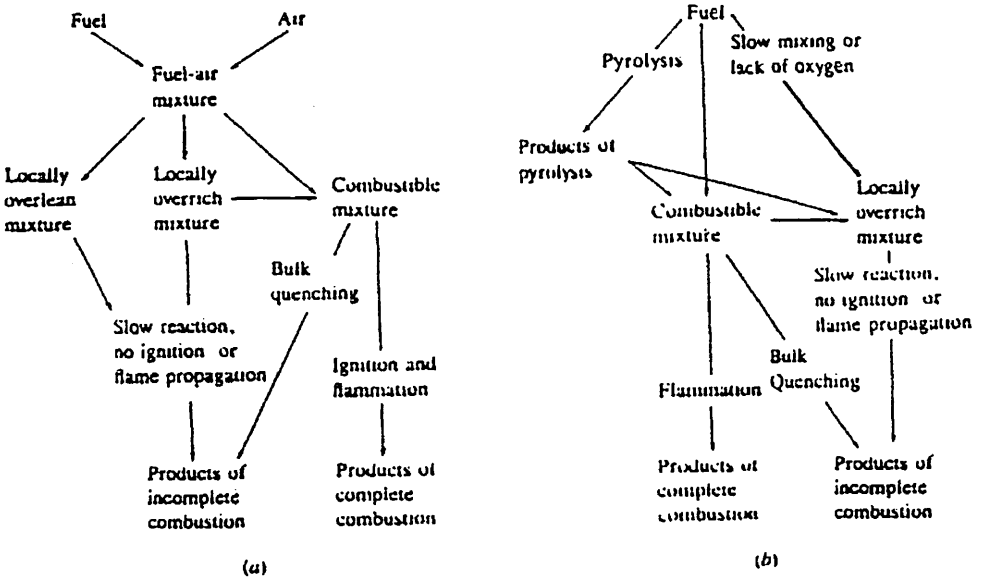

Schematic representation of diesel hydrocarbon formation mechanisms: (*a*) for fuel injected during delay period; (*b*) for fuel injected while combustion is occurring.

2.1 uHC formation mechanisms

The unburnt hydrocarbon(uHC) formation mechanisms for each of these stages are different. The speculated routes have been shown by Yu [4]. These are shown in fig 2.1 which does not show the effects of the system boundaries, i.e. wall quench and adsorption/desorption of the fuel into the lubricating oil. Daniel and Whitehouse [5, 6] used in-cylinder sampling to determine the distribution of hydrocarbons. Their tests showed that as the sample point neared the cylinder wall the hydrocarbon concentrations increased, indicating wall quench. Multi spray D.I. diesel engines delivering high fuel quantities can allow the fuel spray to penetrate too far into the combustion chamber so that it impinges onto the cylinder wall or piston crown. Excessive impingement upon the piston crown can cause cavitation bubbles to form

within the fuel spray. These turbulent conditions have been shown to cause damage to the piston crown. Conditions in this area are relatively cool with poor or no air swirl and the fuel will not ignite until later in the cycle. High speed photographic studies[7] on four types of combustion chambers showed that by 5° ATDC flammation has reached the cylinder boundary in all designs. The Meurer type of direct injection chamber produced a rim of flame between the soot cloud and the cylinder bore; thus fuel rich areas of combustion chamber gases do not reach the boundary and "Unburnt air seems to be reaching the gap between soot and bore, but how it gets there is puzzling". This implies that there is fuel air mixture in close proximity to the lubricating oil on the cylinder boundary for much of the duration of flammation. Lyn and Valdmanis [8] varied injector hole size, nozzle type and its geometry but none of these affected the ignition delay. When the hole size was doubled and the injection pressure remained constant, the fuel flow rate increased by a factor of four and the droplet size increased by approximately 30 percent.

A source of UHC also associated with the injector is that of the fuel remaining in the injector nozzle after injection. This is most significant at low fuel injection volumes where there is little overmixing. Greeves [9] found that a $1mm^3$ nozzle sac volume gave 350 ppm C_1, and he also stated that $1mm^3$ of fuel gave 1660 ppm C_1. He postulated that the volume may not be filled with fuel and the higher boiling point fractions of the fuel remained in the nozzle. The relationship between nozzle sac volume and exhaust HC is linear, with its intercept for zero HC at $-1.8mm^3$ for a speed range of 1700 - 2800 rpm. Farrar-Khan[10] used differing types of injector to investigate the effect the nozzle sac volume has upon the composition of the fuel derived SOF. The results from this did not correlate to previous studies. The change in injector type also changed the Sauter mean diameter of the fuel spray and caused other spray cone variations. The results showed that a valve covered orifice type of injector produced the lowest emission results. The results from this paper are shown in table 2.1. The effect that the changes to the fuel spray geometry had on the

emissions were analysed and the authors concluded that the levels of UHC, particulate and the particulate SOF were reduced by having a smaller nozzle sac volume.

		% Survivability		
PAH(Fuel ppm)	STD	Reduced Sac Volume	Minisac	Valve Covered Orifice
Phenathrene(700)	0.17	0.07	0.28	0.08
Fluoranthene(100)	0.55	0.11	0.33	0.09
Pyrene(100)	0.23	0.10	0.32	0.14
Chrysene(10)	1.12	0.21	0.74	0.00
Benzo(a)pyrene(1)	10.10	0.00	4.30	0.00

Table 2.1 Hydrocarbon species survivability with nozzle sac volume.

The rate of fuel injection in the majority of production diesel engines is constant after the injector needle has attained its fully open condition. Vollenweider [11] completed a series of tests using a two spring injector. This style of injector allowed a small amount of fuel to be injected before the main quantity and this reduced the heat release within the premixed combustion stage. The net result in emissions was a reduction of HC and NOx but an increase in particulates. In a study of "in use" motor vehicles Williams [12] reported that injectors that had a lower opening pressure than the standard specification produced higher levels of emitted particulate matter. This is because the lower kinetic energy of the particle allows it to slow in the air stream, removing its supply of oxygen. The highest concentrations of soot within the combustion chamber of a diesel engine are in the core region of each of the fuel sprays. This is where the local equivalence ratios are very rich. The formation of the soot particle initiates with a fuel molecule containing 12 to 22 carbon atoms and a H/C ratio of approximately 2 and progresses through the two stages proposed by Haynes[13],

i) Particle formation - the first condensed phase of the material formed by oxidation and pyrolysis. The typical components of these are unsaturated hydrocarbons, i.e. acetylene and its multiples($C_{2n}H_2$), and polycyclic aromatic hydrocarbons (PAH).

These particles are very small (d < 2nm).

ii) Particle growth - by surface growth (gas phase material condensing and being incorporated) and agglomeration of smaller particles.

Studies [14] with combustion bombs have shown three different paths to soot formation depending on combustion temperature. At the lowest temperatures (>1700 °C) only aromatics or highly unsaturated aliphatic compounds of high molecular weight are very successful in forming solid carbon through pyrolysis. At intermediate temperatures typical of diffusion flames (<1800 °C), all normally used hydrocarbon fuels produce soot if burned at a significantly rich mixture. At very high temperatures (above the range found in diesel engines) a nucleation process utilising carbon vapour is the primary formation mechanism.

The reduction of the delay and combustion period to a negligible period by pre-heating the fuel to 550°C can produce hypergolic combustion[15]. This type of fuel preparation reduced smoke emissions and the peak combustion temperature and thus a reduction in particulates and NOx. The problems associated with this method of emission reduction is that fuel deposits build up in the fuel heater and the handling of the hot fuel. Hoppie[16] speculated that the use of hypergolic combustion would enable the thermal efficiency of an engine to be increased by optimising the rate of heat release.

2.1) The Effect Of Fuel Properties

The complex cocktail of hydrocarbons that combine to give a fuel the properties that are required for effective combustion also influence the quantity of unburnt hydrocarbons present in the exhaust. The key elements in the fuel that affect the exhaust emissions are sulphur content, cetane number, density and total aromatic content; the distillation characteristics only have a minimal influence. The conversion of the fuel sulphur into the particulate sulphates is engine dependent but for all engines 1.0% to 2.0% of the fuel sulphur is measured as particulate matter. The

density of the fuel influences the particulate emissions, depending upon the fuelling characteristics of the engine.

a) Engines that have an increase in specific particulate emissions when approaching full rack have decreasing particulate emissions with decreasing density when measured on the standard R49 cycle and constant torque 13 mode cycles.

b) Engines with a flat 60% speed load range characteristic are insensitive to density when measured on the standard R49 cycle and constant torque 13 mode cycles.

c) Engines with complex engine management systems particulate matter can increase or decrease when measured on the standard R49 cycle and constant torque 13 mode cycles.

The improvement of emissions through the use of advanced fuels will not benefit all engines because these effects vary with each combustion chamber shape and fuel injection system.

2.2) Lubrication oil contribution to exhaust emissions

Studies[17] using a similar engine to the one used for this research project showed that the lubricating oil contributed between 10% and 50% of the SOF. The values for the contribution were determined by motoring the engine for 15 minutes after a period of normal running to obtain the normal running temperature. The average molecular weight of engine lubrication oil is nearly two and one half that of the fuel [18], therefore the contribution of lubricating oil to exhaust particulate is considerable when compared to relative consumption rates. The relative importance of the control of engine oil is also increasing with the tightening of emission regulations. In 1980 Mayer [19] found that the 25 mass percent of the collected particulate matter was oil

derived. Wachter[20], using a 1991 specification engine, obtained 32 percent. The surface area of the oil exposed in the working chamber influences the exhaust components. Cartellieri [21] used a lubrication oil particulate index (LPI) to express particulate emission in grams/(mile x cyl wall area). The conversion equation used assumed a bore stroke ratio of 1 for simplicity and is as follows:-

A = Wall Area B = Bore
V = Total Cyl Displacement Z = No of cylinders

$$A = B^2 \times \pi \times Z \qquad (1)$$

And

$$V = B^3 \times \pi/4 \times Z \qquad (2)$$

rearranging to give B and substituting equation 2 into 1 gives

$$A = V^{2/3} \times Z^{1/3} \times \pi^{1/3} \times 4^{2/3}$$

Thus

$$A = V^{2/3} \times Z^{1/3} \times 3.691 \qquad (3)$$

When the figures were corrected to these results, the engine configurations with the greatest number of cylinders showed a reduction in exhaust emissions, but these results implied a target of 0.002 to 0.003 g / (mile x cm^2) to comply with the FTP75 emission test.

The surface area oil losses are also influenced by cylinder liner distortion. Zelenka[22] showed that bore distortion can produce in excess of a three fold increase in the oil derived particulates. The engines for these tests were measured in a cold static state at two points 10 and 30 mm below the fire deck. The engine with a bore distortion of ±5μm produced 0.064 g/KW-hr where the engine with a bore distortion of ±10μm produced 0.22 g/KW-hr.

The oil film thickness above the ring pack can be controlled in many ways, i.e. liner surface finish and piston ring surface pressure. Jakobs[23] used identical ring profiles in a series of tests but altered the oil ring surface pressure. An increase in pressure from 1.56 N/mm^2 to 3.5N/mm^2 produced a reduction in oil consumption from 0.26

g/KW-hr to 0.09 g/KW-hr. Essig [24] found that a 25 percent reduction in oil consumption could be obtained by fine honing of the cylinder bore. For these tests the Ra value was reduced from 1.43μm to 0.64μm and the Rz from 8.48μm to 4.75μm. The Abbot curve for the smoother liner was also flatter.

2.3 Oil consumption measurement techniques

The consumption of lubricating oil of engines is of primary importance to engine developers. The high molecular weight of the oils used causes any oil loss to contribute considerably to the particulate matter. The lubrication oil will always be present in the working cylinder because, even with improvements in material technologies and design, the top piston ring will always require oil above it to prevent detrimental sliding contact between it and the cylinder wall and to stop the ring from being impacted into the piston ring groove.

The method of measuring lubrication oil consumption that has been the most widely used is the drain and weigh method. This method is easy to use but requires the engine to be run for a minimum of 6 hours to provide the level of oil consumption that can be weighed with any degree of accuracy. There have been several variations on this method proposed where there is an external oil reservoir that is attached to a load cell or spring balance. The engine is either fitted with a "dry sump" where the lubricating oil is removed from the base of the engine before any significant quantity can accumulate or the sump is modified so that there is a constant volume of oil in the sump, this level being maintained by a two pump system connected to an external reservoir, a typical configuration of which is shown in figure 2.2 [25]. This system was also checked by the drain and weigh and proved to be approximately 5% accurate over a 15 minute period where the oil consumption was 50 gm/hr. The engine was run for durations of approximately 12 hours for each test. The greatest disadvantage of the drain and weigh system is that for transient engine testing the oil consumption

for each test point cannot be accurately determined. The use of radioactive tracers within the lubricating oil has provided a faster method of determining the oil consumption[26,27,28] but the materials used are not suitable for the typical engine test facility.

The measurement of elements present in the lubrication oil have provided suitable solutions. The cost and complexity of the measuring equipment has prohibited these methods from being accepted by many engine testing facilities. The elements that have been measured are hopanes[29](alkanes that were produced by bacteria in ancient sediments), sulphur[30] and the metals[31] present in the lubrication oil additive package. The sample time required for this type of technique is significantly lower than that for the drain and weigh method and is normally 20 minutes. Because the sample that is analysed is a very small component of the total emitted over the sampling time these methods are prone to measurement error, but with operator familiarity can produce reasonable results.

2.4) The Effect of piston design upon emissions.

The most influential component of the piston design upon combustion noise and regulated emissions from diesel engines is the combustion chamber in the crown. This part of the piston is designed to complement the fuel injection equipment and for this research program the piston crown and fuel injection equipment have remained as fitted in the standard build. The combustion chamber influences the piston's temperature considerably; the smaller the surface area the cooler the piston temperature for similar operating conditions. The primary function of the combustion chamber is to promote air movement. As the engine size increases and thus the quantity of fuel injected increases, the combustion chamber has less effect upon the movement of the charge in the cylinder. The increase in size of components with

increasing engine size allows for easier machining of the fuel injection equipment to allow higher fuel injection pressures. These higher pressures and greater quantities of fuel injected per cycle are the primary mechanism of charge movement within the working cylinder. The necessity for the combustion chamber to produce the sufficient charge movement in medium sized diesel engines has produced pistons with a re-entrant bowl shape. This type of piston is prone to cracking around the bowl rim. The cracks are caused through thermal and mechanical cyclic loads. The higher thermal loads on the bowl edge are caused by the smaller heat path from the bowl to the ring pack. The following table 2.2[32] shows the typical details for six engine sizes.

System	<-------- Direct Injection ------>				<-- Indirect Injection --->	
	Quiescent	Medium swirl	High swirl "M"	High swirl multi spray	Swirl chamber	Pre- chamber
Size	Largest	Medium	Medium - smaller	Medium - Small	Smallest	Smallest
Cycle	2/4-stroke	4-stroke	4-stroke	4-stroke	4-stroke	4-stroke
Aspiration	TC/S	TC/NA	TC/NA	NA/TC	NA/TC	NA/TC
Maximum engine speed (RPM)	120-2100	1800-3500	2500-5000	3500-4300	3600-4800	4500
Bore (mm)	900-150	150-100	130-80	100-80	95-70	95-70
Stroke/bore	3.5-1.2	1.3-1.0	1.2-0.9	1.1-0.9	1.1-0.9	1.1-0.9
Compression ratio	12-15	15-16	16-18	16-22	20-24	22-24
Combustion chamber	Open or shallow dish	Bowl in piston	Deep bowl in piston	Deep bowl in piston	Swirl pre chamber	Single/multi orifice pre chamber
Air-flow pattern	Quiescent	Medium swirl	High swirl	Highest swirl	Very high swirl in pre chamber	Very turbulent in pre chamber
Number of nozzle holes	Multi	Multi	Single	Multi	Single	Single
Injection Pressure	Very high	High	Medium	High	Lowest	Lowest

TC = Turbo Charged
S = Super Charged
NA = Naturally Aspirated
Table 2.2 Engine configuration with size

2.5) The piston ring pack.

The main design criteria for a piston ring pack are:-

1) To provide a seal between the piston and the cylinder liner, retaining the gas pressure and minimise blow by.

2) To allow sufficient lubrication to the cylinder surface while sustaining high thrust and gas force loads and control oil consumption to acceptable levels.

3) To control piston temperature by assisting heat transfer to the cylinder.

The operating principle of piston rings is such that there are high shear forces between the ring and the lubricating oil and at the limit of the stroke there is asperity contact between the piston ring and cylinder liner. The work done by the engine to overcome these components of friction can account for 45% of the total engine friction. The piston assembly and connecting rod typically account for 66% of the total engine friction. The number of piston rings found in typical engines has been reduced to improve efficiency. Modern engines now have 3 piston rings (2 compression and 1 oil scraper). Previously it was not uncommon to have five piston rings on diesel engines (3 compression and 2 oil scraper). Piston ring pack assemblies for 4 stroke S.I. engines using only 2 rings have been developed.[33]

The piston rings are a clearance fit in the ring grooves and this allows axial movement, depending upon local gas pressures and acceleration of the assembly. This motion is an important factor in providing the required sealing [34, 35]. Typical movement of the compression rings are shown in figure 2.3 [24]. The movement of the top ring is influenced by the design of the second ring, the inter ring pressure between the two compression rings being the predominant factor. The reduction of the pressure in the second land produces a top ring motion with an increased residence on the bottom face and a reduction in lubricating oil consumption. The correlation of top ring lift and oil consumption was further emphasised by Furuhama[36,37]. The factors that influence the 2nd land pressure are the crevice volume and the 2nd ring end clearance. These factors are shown by the International Harvesters patent for the

balanced pressure concept[38] where the increase in 2nd land volume and the increase in the 2nd ring end gap has produce a significant reduction in lubricating oil consumption over a considerable operating time. Operating time has a significant effect on the oil consumption. A new engine with the components in an "as machined" finish has a higher oil consumption than when the engine has been run in correctly. The oil consumption starts to increase again as the engine wears and the combustion deposits build up. It is well documented that high levels of piston crown deposits are often linked to high oil consumption[39 - 42] but Burnett[43] found that the increase in carbon around the second land had beneficial effects on the top ring motion and oil consumption in particular circumstances with a two compression ring pack. The results for the two compression ring test engine showed that as the carbon deposits built up, the second ring had a greater duration of the cycle off the bottom ring groove face but the top ring was displaced from the bottom face for a lesser time. The effect of top land clearance influences engine life as well as emissions. A piston with minimal clearance allows the carbon deposits to be embedded into the piston material and the hard carbon particles act as polishing medium, removing the oil bearing honing marks. The absence of the lubrication leads to rapid engine wear and premature failure.

The study of worn cylinder liners using a scanning electron microscope will show these following wear features[44]:-

1) Hard phases standing proud of the surface at T.D.C. caused by abrasive wear.

2) The pearlite/phosphide/graphite structure of the cast iron is readily observed indicating surface etching with little or no abrasive wear.

3) At B.D.C there is no chemical etching and little abrasive wear.

2.6) Exhaust hydrocarbon species

Following injection of the fuel it is subjected to increasing pressures and temperatures. These conditions initiate very marked pre-reactions prior to combustion. After these reactions have begun, the additional increase promotes more reactions, such as cracking, dehydrogenation and polymerisation. A portion of the fuel is changed to oxides of carbon, water and oxygenated products during this pre-reaction period, thereby reducing the thermal value of the charge in the cylinder. The extent of these pre-reactions is a function of the fuel and of the engine operating variables. All paraffin fuels undergo these pre-reactions to a certain extent, but isooctane(C_8H_{18}) is much more resistant than normal heptane(C_7H_{16}). Aromatic fuels are fairly stable and resist pre-reaction. These pre-reactions increase with the severity of engine operation, increase in intake air temperature and higher compression ratios.

Research[45] using a single hydrocarbon fuel, isooctane, in S.I. engines produced 11 different types of hydrocarbon species in the exhaust, Sweeney[46] listed approximately 225 different organic compounds that have been identified as being present in vehicle exhaust gases and there are many more to identify.

The majority of research into the speciation of the diesel engine's exhaust particulate has been centred on the aromatic compounds, because these were the first components of the emitted matter to be identified as being a hazard to health[47-49]and because of their stability, as discussed above. Aromatic Compounds are closed chain, cyclic or ringed compounds. Aromatic hydrocarbons are based on the Benzene molecule and are unsaturated, thus they will undergo substitution or addition reactions where the double or triple bonds between carbon atoms will be replaced by atoms of another reactant.

The polycyclic aromatic hydrocarbons (PAH) present in the fuel are the largest contributor to the aromatic component of the particulate matter. Typically 0.2 to 1.0% of these compounds survive the combustion process. The principal PAH compounds present in the diesel fuel used in the UK are napthalene, fluorene and phenathrene and their alkyl substituted homologues[50]. Benzo[a]pyrene and benzo[a]anthracene are typically found in concentrations of < 1 ppm[51,52].

Combustion studies using tetradecane and tetradecane with 10 volume % α-methylnapthalene showed that the increase in the aromatic content caused an increase of measured soot[53]. The use of a fast sampling valve in this research showed that the in cylinder levels of acetylene and carbon monoxide increased throughout the cycle. This was attributed to the aromatic oxidation chemistry which initially starts as side-chain oxidation and ring breaking. There was a similar increase in pyrolytic products which showed that the aromatic compounds influence the oxidation of the aliphatic compounds.

Each hydrocarbon species by the nature of the elemental bonds and composition will survive combustion at differing rates. Research based on a Perkins 4-236 engine showed that the survivability of n-alkanes varied with molecular weight and engine speed and load. The results from this research are shown in table 2.3[17]. Results show only the hydrocarbons collected on a filter paper sample obtained from a dilution tunnel. The gas phase hydrocarbons that are present in the gas stream are generally lighter than those found in the particulate SOF having a carbon number distribution from C1 to C25 where the particulate SOF has a carbon number distribution between C14 and C40[54].

Cn	N-alkane Identification	Fuel composition µg/g	%Survivabilty 1500 rpm 52 Nm Torque	%Survivabilty 2000 rpm 52 Nm Torque
C_{16}	Hexadecane	15142	0.003	0.005
C_{17}	Heptadecane	15008	0.004	0.0096
C_{18}	Octadecane	13227	0.008	0.0169
C_{19}	Nonadecane	12080	0.017	0.025
C_{20}	Eicosane	9600	0.03	0.039
C_{21}	Henicosane	7633	0.06	0.041
C_{22}	Tricosane	3094	0.13	0.019
C_{23}	Tetracosane	1564	0.15	0.019
C_{24}	Pentacosane	676	0.12	0.02

Table 2.3 Hydrocarbon species survivability with load

Air samples collected in road tunnels[55] that were analysed for non-methane hydrocarbons showed that the alkane range measured when the tunnel was used for predominantly heavy duty vehicle engines was between elements with between 9 and 20 carbon atoms. The majority of the tests showed that the most prolific component was dodecane with typical rates of 25% of the sample. There were exceptions to these results, i.e. where vehicles that showed visible signs of combustion inefficiency passed through the tunnel the peak of the alkane sample was then tetradecane. The authors concluded that heavy duty vehicles emit approximately 50% of the total hydrocarbon emissions above C_{10}.

2.7) Modelling

Pressure data heat release.

The analysis of cylinder pressure data to determine the mass fraction burnt is based on a method first developed in the 1930's by Rassweiler and Withrow [56] for spark ignition engines, using high speed photographs. An empirical method for defining the polytropic index was developed. Also by comparing the difference between measured pressure and that calculated from polytropic compression or expansion is taken to be proportional to the mass fraction burnt. This method was enhanced by comparing the differences between pV^n calculated during combustion and pV^n at the end of compression[57,58]. The main disadvantage of this method is that the energy changes of the cylinder charge are never accurately determined.

The rate of heat release during the combustion process was researched during the 1960's by Lyn[59,60,61] and co-workers. This was by analysing the rate of fuel injection and heat release diagrams for a range of engine speeds and loads, and the following combustion properties were observed.

1) The total burning period is longer than the injection period by a significant margin.

2) The absolute burning rate increases proportionally with the increase in engine speed.

3) The initial heat release peak is dependent on the delay period; the greater the delay the greater the heat release peak.

The rate of heat release is dependent upon which of the four combustion phases is predominant at that instant in time. A typical rate of heat release diagram is shown in figure 2.4. The studies by Lyn also proposed three basic injection, mixing and burning patterns for the fuel injected.

1) Fuel enters the combustion chamber with considerable momentum.
Mixing starts instantaneously as the fuel enters the chamber there is negligible combustion.

2) Fuel deposited on the combustion chamber walls.
During the delay period little evaporation and minimal mixing. After ignition, evaporation becomes rapid and its rate is controlled by the access of the hot gases to the surface. Radial mixing is by centrifugal forces.

3) Fuel distributed near the combustion chamber wall.
There is limited mixing at a rate lower than 1, after ignition mixing is the same as 2.

The complexity of the combustion process and the interaction of all the factors that determine the combustion rates produces measurable cycle to cycle variations in both cylinder pressure and the rate of heat release. These variations can cause the calculated rate of heat release to become negative as combustion is completed. This is more predominant when the engine is operating with fast burning cycles[62]. This anomaly was attributed to either the heat transfer correlation, the method that was used to represent the thermodynamic properties of the working fluid, or temperature effects upon the pressure transducer.

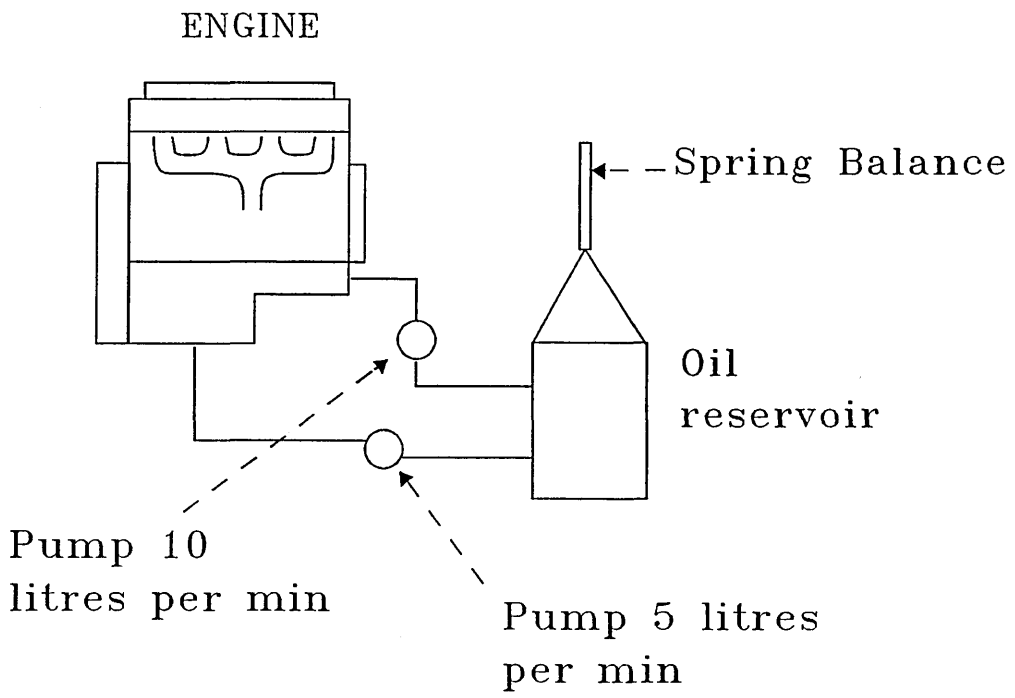

Figure 2.2 Oil consumption measurement system

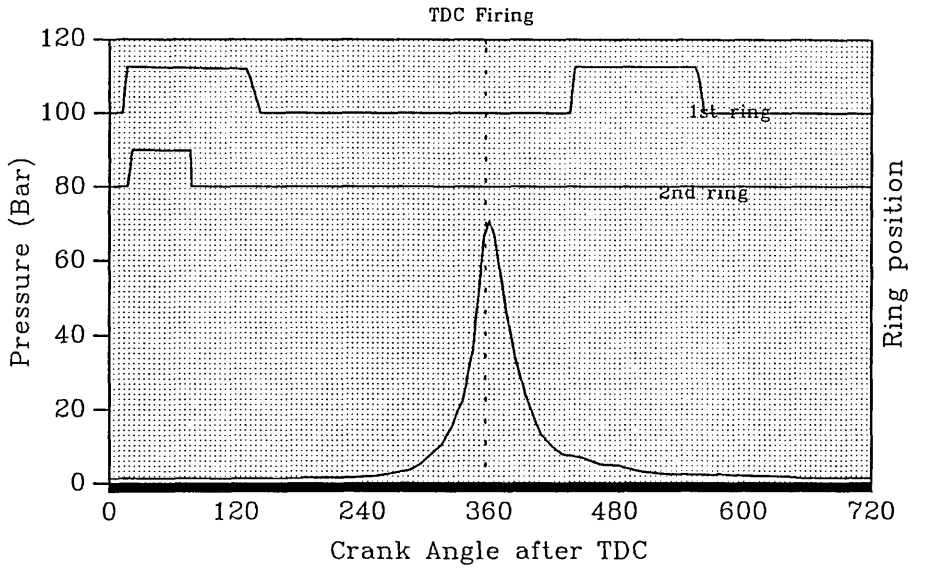

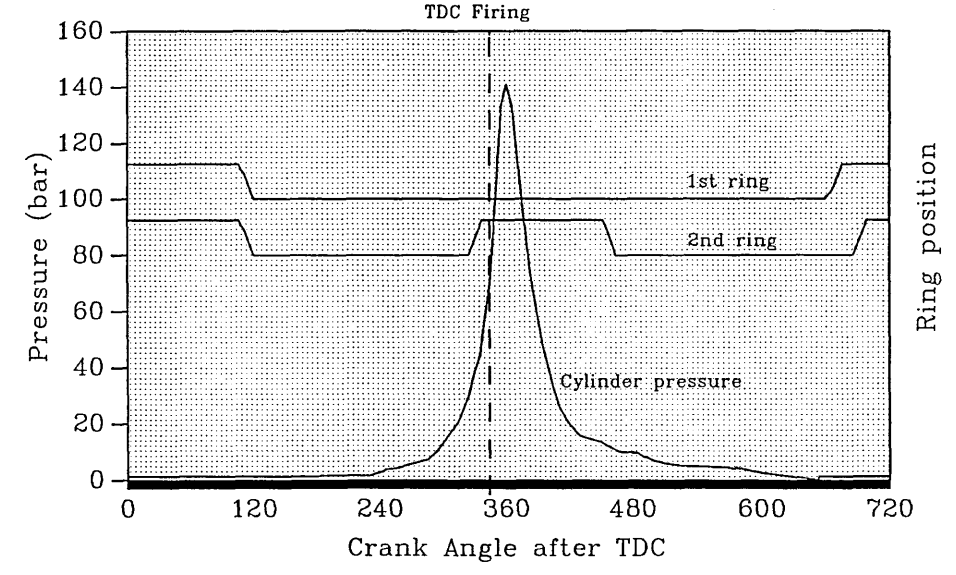

Figure 2.3 Piston ring motion

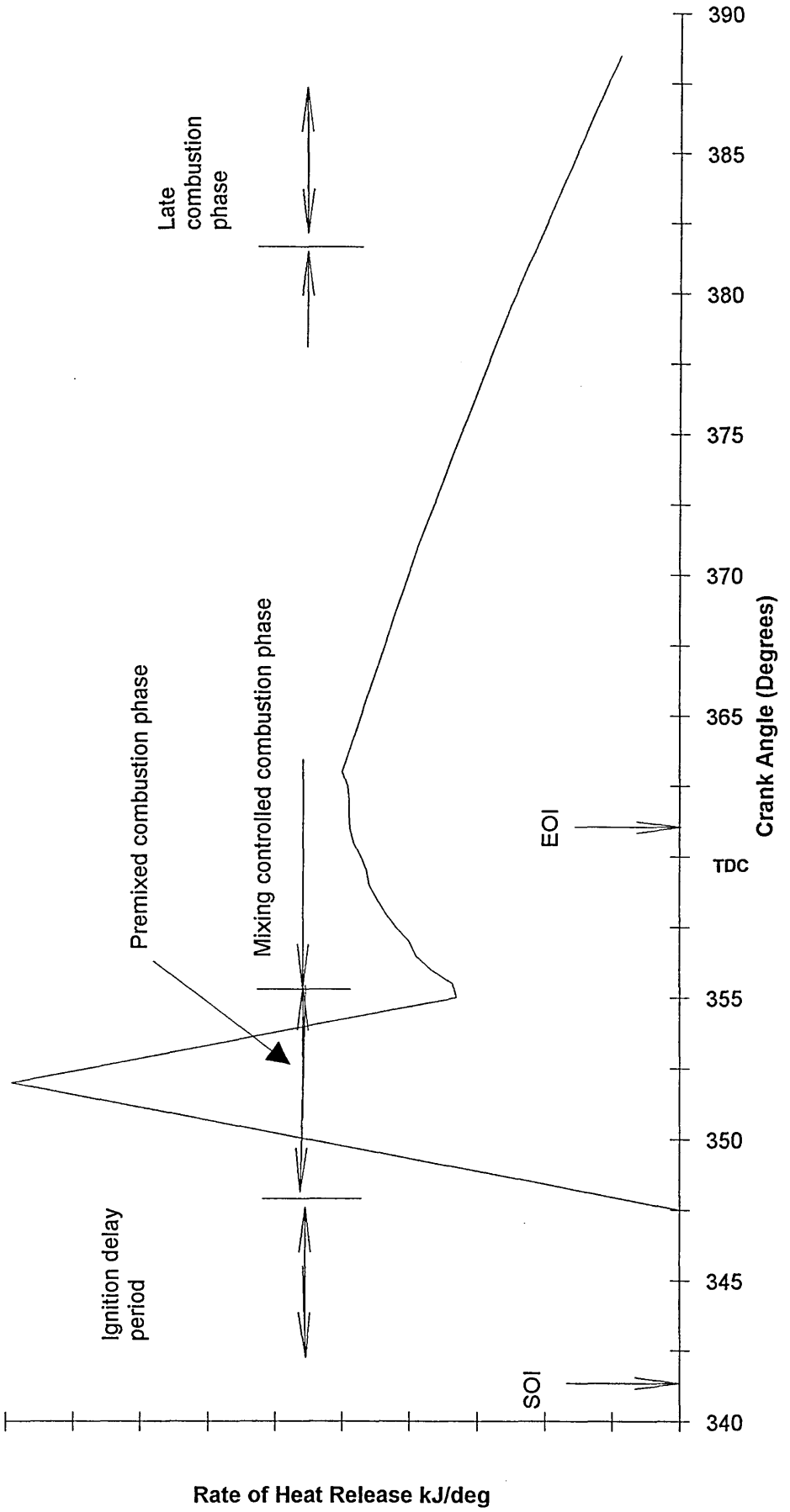

Figure 2.4 Typical rate of heat release

3.0) Experimental Facility

The engine was located in a purpose built air conditioned sound proof booth, with the majority of the instrumentation and analysis equipment located on its outside within the operators area. The air supply to the booth when the engine was not operating was fully air conditioned with reasonable control on the temperature and humidity. When the engine was running the heat and fumes were removed by additional make-up air which was filtered external air. There were three fans for the positive extraction of the exhaust gases and the waste air from the booth. A simplified layout of the test cell is shown in figure 3.1.

3.1) The Engine

The engine used in this research was a Perkins Phasor 110T. This engine has a displacement of 4 litres and a typical power output of 110 horsepower (80 kW) at 2600 RPM. This engine was chosen because the cylinder liners could be obtained pre-finished and, therefore, could be replaced without the engine being shipped to a machine shop for the new liners to be bored and honed. The pistons for the test program were to be modified naturally aspirated (N.A.) piston castings from the Perkins Phasor 80 the major dimensions of the pistons used are shown in shown in figure 3.2. The only significant design difference between the N.A. and turbocharged (T.C.) rough piston casting is the angled small end bearings. The reason for the inclusion of pistons from a N.A. engine is that AEGoetze did not manufacture the pistons for T.C. Perkins engines. A turbo charged engine was required for this research because AEGoetze would benefit from the knowledge base to a far greater extent than research on a naturally aspirated engine. Of particular interest was the contribution to the particulate matter from the turbocharger. The piston ring pack and ring groove dimensions were manufactured to T.C. specification. The engine was originally supplied with a Schwitzer S2A turbocharger. This unit was found to have excessive clearance on the turbine shaft, leading to significant oil loss into the exhaust

gas, and was replaced by a Garret T4 which is a direct replacement for this engine.

The cylinder head was instrumented to allow the measurement of the combustion chamber pressure in cylinders three and four. It has been proved that the maximum observed peak cylinder pressure is determined by the position of the pressure transducer relative to the cavity centre (63). To facilitate the precise positioning of the pressure transducers the cylinder head was first modelled on a computer aided draughting system to determine the position of water paths and material thickness. The positions for the transducers now determined, allowed the surfaces of the cylinder head to be machined, giving datum points and surfaces for precise measurement. The original drawings from the engine supplier utilised the valve guide centres as the reference point for all machining. When measured, the cylinder head had distorted slightly through use and the valve guides showed that there was a significant deviation from a straight line. The computer model was recreated with this deviation taken into consideration. The final positioning of the transducers was to within 0.02 mm.

To ensure that the pressure data was of sufficient accuracy, cylinder three was also fitted with a pressure transducer in the same relative position. The additional crevice volume that was added by the fitting of the transducers was significantly less than 1%. The fuel injection pressure was also monitored by a Kistler 602 piezo-electric transducer. The injector pipe length was required to be the same as all the other injector pipes because during the injection process there are reflected pressure waves generated. This pressure wave is a function of the harmonic property of the system and to ensure that the inclusion of the injector produce different harmonics for the one cylinder and thus alter the injection characteristics of that cylinder the high pressure fuel pipe for cylinder three was shortened to retain the same pipe length and a suitable holder fabricated and fitted at the injector end.

The air flow into the engine was measured by a calibrated Cussons laminar flow meter. The air flow was calculated by measuring the pressure differential across a

laminar flow element. The pressure drop through the air filter was also required to calculate the air flow. This pressure drop also provided an indication of the air cleaner element condition and effectiveness.

The uncorrected air flow rate in litres per second was obtained from the following equation:

$$\text{Flow} = (d_p \times 0.8842) - 0.5947$$

Where d_p is the pressure difference in mm of water.

The mass flow of air and fuel flowing into the engine was required for the model, emission calculations and to check operating conditions, thus any gas that is not present in the exhaust stream would alter all of the above, therefore, gases from the crankcase breather were measured by a rotameter. The pressure fluctuations caused by the movement of the pistons and the blow by gases were damped by a large volume plenum chamber situated between the engine and the rotameter.

The fuel injection duration and rate influences the total emissions. To minimise any changes in fuel density and viscosity the fuel was cooled before entering the fuel filter, which was heated to a constant 45°C for all tests. The combustion properties of diesel fuels are influenced by any products of partial oxidation or pyrolysis introduced before the start of combustion[64]. To avoid the local overheating of the fuel in the fuel heater and limit the effects of the heating the fuel heater was constructed of a large mass to allow easier temperature control and a constant temperature. The fuel consumption was obtained using a stop watch and a calibrated measure. The calibrated measure was constructed such that there was a significant change in the liquid level at the start and end of the known quantity. The temperature of the fuel in the measure was recorded and all the volumes corrected for any deviation from the standard 45°C . A diagram of the fuel flow system is shown in figure 3.3.

3.2) Exhaust gas analysis

The cylinder head fitted to the test engine had two pairs of siamesed exhaust ports. To obtain a sample from each cylinder the stainless steel sample pipe for each cylinder was taken through the exhaust manifold wall and along the top of the ports. The sample pipe was then taken into the area directly above the exhaust valve. Where there was some cross contamination of the exhaust gases between cylinders, a fault on one cylinder made only a perceivable change in its pair. To study the effect of the exhaust system on the exhaust gases further sampling points were fitted to the engine; one in the mid-stream of the gas flow into the turbocharger and another one meter from the turbocharger exit in the middle of the gas flow. All sample pipes faced into the gas flow. The sample pipes were connected to a stainless steel manifold and the sample point selected by a stainless steel ball valve. The pipes were routed close to the exhaust system to allow similar temperatures in the sample system as those present in the exhaust system. A schematic representation of the sample system is shown in figure 3.4.

The sample gas was transported to the gas analysers from the sample manifold by a heated sample line to restrict the condensation of the heavier gas phase matter. To avoid the excessive build up of the carbon solids in the line a heated pre-filter was fitted between the manifold and the line. The temperature of the sample line was 180°C and the pre-filter was at 186°C. The heated sample line, filter, manifold and sample pipes were purged using compressed air in the reverse direction to normal flow between each test sample and while the engine's temperatures were stabilising after a change in speed or load.

3.3) Gas phase emission measurement

The hydrocarbon content of the gas stream was measured by a Flame Ionisation Detector (F.I.D.) based analyser. CO_2, CO, O_2, were measured using a Non

Dispersive Infra Red (N.D.I.R.) analyser and NOx by a chemiluminescent analyser.

The calibration of all of the devices was by supplying a calibration gas directly to the detector. The calibration gases for each detector are as follows

Detector	Calibration Gas
F.I.D. and N.D.I.R.	CO_2 16%, CO 8% Propane 1600 ppm Nitrogen Balance
Chemiluminescent detector	NO2 4000ppm, Nitrogen balance

Table 3.1 Calibration Gases

The instruments were calibrated at the start of each test series and during the engine stabilisation period between test points. The reliability and accuracy of the sample system was checked by admitting the calibration gases at varying points in the system. The sample system pre-filter was replaced at the start of each daily test series and the analysers' internal filters were replaced after five tests.

3.4) Particulate measurement

The exhaust gas immediately leaving the tail pipe of a diesel engine is composed primarily of elemental carbon and organic compounds and, when at normal operating temperature, these exist separately. The purpose of a dilution tunnel is to simulate the mixing of the exhaust gas with the external air, thus cooling the exhaust and allowing the organic compounds to condense. The maximum permissible sampling temperature for a dilution tunnel is 52°C. This is the mid point between the boiling points of pentane (Bp 36.1°C) and hexane (Bp 68.7°C). To reduce the sample gas temperature further to the boiling point of pentane, the dilution ratio would have to be increased to a region above that of the optimum ratio for the collection of the extractable fraction. The dilution ratio for the collection of the maximum amount of the extractable organic fraction is approximately 5:1. The reasons for this are that, as the dilution ratio increases from unity, the effect of the decreasing temperature on the

number of active sites dominates the condensation process. When the dilution ratio becomes higher the decreasing partial pressure causes the extractable mass to fall again. Condensation will occur whenever the vapour pressure of the gaseous phase hydrocarbons exceeds its saturated vapour pressure. Increasing the dilution ratio decreases the hydrocarbon concentrations and hence the vapour pressure. The tunnel used for these tests was 3 metres from the injector to the start of the isokinetic probe and 0.2 metres in diameter.

Because the exhaust gas quantity emitted from the engine is in excess of the maximum flow through the dilution tunnel an exhaust gas splitter was required. This device consisted of a "Y" junction with a throttle valve on each branch of the "Y". The measurement of the gas flow down each branch of the splitter is critical because any error in the measurement of the flow influences the dilution ratio calculations and the total exhaust particulate emissions. After changing either the engine speed or load the throttle that restricted the exhaust gas flow to atmosphere was closed until the pressure in the system reached 40 mm H_2O above the ambient pressure. The throttle to the tunnel was then opened to allow some of the exhaust gas to flow into the tunnel. At low exhaust gas flows the throttle that controlled the exhaust back pressure would then require adjustment to return the exhaust back pressure to its level.

The installation of the measurement orifice for the exhaust gas into the tunnel complied to British Standard 1042 and is shown in figure 3.5.

The NOx present in the exhaust gas was used for error checking. The NOx formed in the combustion chamber of diesel engine is frozen earlier in the cycle than in petrol engines. The critical equivalence ratio for the formation of NOx in high temperatures and high pressures is close to stoichiometric and the critical time period is when the burned gas temperatures are at a maximum; i.e. between the start of combustion and

shortly after peak pressure. After the period of peak pressure the burned gas temperature decreases as the cylinder gases expand. The decreasing gas temperature is due to both expansion and the mixing of high temperature gas with air or cooler air or burned gas.

Because the gas is "frozen" and not much decomposition will occur in the exhaust pipe, there will be a direct correlation between the concentration in the diluted and undiluted exhaust gas sample. During particulate sampling the NOx analyser was used to take a sample from close proximity to the particulate sample pipe. This sample was then compared to that taken directly from the exhaust pipe. The ratio between the two samples provided a very close approximation of the exhaust gas dilution ratio present within the tunnel. This reading was monitored thoughout the particulate sampling tests and would indicate if any malfunctions or discrepancies had occurred.

The correlation between exhaust smoke and particulate solid content has been shown by Fosberry [65]. These are displayed in graphical form figure 3.6, using the results from a hot sample to a Bosch smoke meter. The calculated results from the dilution tunnel, combined with the NOx error checking, has provided an accurate measurement of the particulate matter.

3.5) Solvent Extraction

Solvent extraction is one of the most common analytical methods for the determination of the soluble organic fraction present in diesel engine exhaust particulate matter. The main extraction process used the Soxholet apparatus (Fig 3.7). The operating principle of this is to wash solvent over the sample. The solvent used for this test program was dichloromethane.

Because of the small amount of material collected for the majority of the test points,

the optimum method to determine the amount of material removed by the extraction process was to weigh the filter before and after the process. Because the filter can contribute to the weight difference, blank filters also have to be subjected to the extraction process. The overall calculation for the soluble organic fraction by weight was :-

SOF(filter weight loss) = (W_{be} - W_{ae} - Av_b)

W_{be} = Weight before extraction

W_{ae} = Weight after extraction

Av_b = Average weight loss of blank filters

To remove the solvent and to stop any mutation or oxygenation of the remaining matter prior to weighing, the papers were dried in a nitrogen atmosphere. Before any weighing of the filter papers they must be subjected to the same ambient conditions, therefore papers were stored in temperature and humidity controlled conditions overnight to equilibrate before any weighing process.

3.6) Clean up procedure[66]

A high performance liquid chromatography(HPLC) system using an alumina column-activated, basic, Brockmann 1 (150 mesh, 250 x 5 mm) was used to separate the hydrocarbons of interest, i.e. C_8 to C_{30} from any other emitted by the engine, i.e. aromatic and substituted aromatic compounds known to be released by incomplete combustion. Fractionation was achieved on a Varion isocratic HPLC system using a UV detector set at 254 nm. To separate the sample into these groups, low pressure liquid chromatography utilising different eluants was used. Table 3.2 shows the eluant with the corresponding group

Isocratic Eluant	Group
Hexane	Alkanes
Dichloromethane	Polycyclic Aromatic Hydrocarbons (PAH)
Acetronitrile	Polar PAH & Nitro PAH
Acetronitrile & Methanol (3:1)	Very polar PAH

Table 3.2 Isocratic eluants for hydrocarbon groups

3.7) Capillary GC/MSD Analysis

The residual weights of the test samples varied with the speed/load conditions, i.e. depending upon the contribution to the total collected weight of the soluble fraction, these samples were then diluted with Dichloromethane to give similar concentrations. A 1μl. sample of this was then used for analysis. The instrument used was a Hewlett Packard 5890 (Series II) coupled with a HP 5971A Mass Selective Detector. Electron impact mass spectra were obtained at 70eV and processed using an HP ChemStation data system. The GC conditions used are shown in table 3.3.

Gas Capillary Chromatographic Conditions	
Carrier gas	Helium
Analytical column	18m x 0.25mm (id), 5% biphenyl fused silica
Film thickness	0.25μm
Oven temperature program	50°C (2 mins) ramped at 10°C/min to 280°C (5 mins)
Volume injected	1μl. splitless

Table 3.3 Gas Capillary Chromatographic Conditions

The identification of the abundance peaks on the chromatograms produced was initially by the comparison to the retention times of a standard. After the calibration test engine build a comprehensive library of hydrocarbon species was used to search

and identify the components of the sample. To allow the mass of each individual component of the sample to be determined, a known quantity of each species that was under investigation, combined with two additional hydrocarbon species (one lighter and one heavier than those under investigation) were analysed with each batch of samples. Each sample that was analysed was doped with the lighter and heavier hydrocarbon species to allow the accurate measurement of the mass composition.

3.8) Temperature measurement

All engine temperatures were monitored by type K thermocouples (the positions are shown in table 3.4). The output voltage from these were conditioned to compensate for the temperatures of any junctions in the cabling and the output signal then linearised. The thermocouple positioned in the fuel filter directly controlled the fuel filter band heater via a temperature controller and maintained the temperature of the fuel filter to approximately 45°C. The temperature of the gases flowing into and out of the engine were logged on a P.C. based data acquisition system. This data was shown on the P.C. screen in the form of line graphs. Temperatures that were critical to the testing of emissions and the engine set up were continuously displayed on the engine and dynamometer control panel.

Group and number of thermocouples		Position
Cooling System	(2)	Top hose and bottom hose
Induction System	(2)	Air flow meter and inlet manifold
Exhaust system	(5)	All exhaust valves and after turbocharger
Fuel system	(2)	Fuel filter and measure
Particulate sampling system	(2)	At sample point and measuring orifice
Lubrication system	(1)	Sump

Table 3.4 Engine thermocouple positions

3.9) Pressure measurement

The cylinder and fuel line pressure was recorded on an AVL 646 high speed data acquisition system. This system used an optical shaft encoder fitted to the crankshaft

pulley to provide the trigger for recording. The encoder's resolution allowed pressure measurements of up to 3600 per crankshaft revolution. The software for the AVL 646 enabled the averaging of pressure traces for each cylinder over a number of cycles to remove the effect of cycle to cycle variability. The data was then transferred to a P.C. by a RS232 link.

3.10) Injection Timing

The pressure trace from the high pressure fuel line could not be used to give an accurate indication for the start of injection, because there is a rise in pressure in the fuel line before the injector needle is raised from its seat. Injection was assumed to have started when the injector needle had just moved from its seat. To determine this an injector fitted with a Hall effect sensor was fitted to cylinder four. This injector was not used during the emission measurement tests to allow all pressure measurements to be taken with the same amount of wear and carbon deposit on the injector. The standard injector was used for all emission tests. The results from the injector and crankshaft encoder were captured by an oscilloscope and then printed to allow the start of injection to be accurately determined during testing (Fig 3.8), thus allowing any inaccuracies in the set up of the engine for that test to be rectified; a sample is shown below.

3.11) Engine preparation.

The engine was prepared in the same manner for each test session. The pistons and liners were measured for accuracy of form before and after each test. The liners were fitted to the cylinder block in the same orientation of the measurements for each engine build. After dismantling, all components were cleaned thoroughly to remove all traces of the old lubricating oil and any carbon deposits were removed from the combustion area and injector nozzles. Before the start of any emission testing, the engine was subjected to a strictly controlled running period to ensure the same surface finish of any new components. This program is detailed in table 3.5.

step	time mins	total time mins	speed RPM	load kW	Approx. % load
1	10	10	1000	none	none
check oil flow to rockers rectify oil leaks etc.					
2	20	30	1300	10	15
3	30	60	1600	17	28
4	30	90	1800	28	40
5	30	120	2100	36	50
6	30	150	2350	48	68
7	30	180	2500	58	83
8	30	210	2600	70	100

Table 3.5 Engine running in program

3.12) Test Procedure

The atmospheric conditions can vary significantly over a long term engine test programme and combined with combustion variability could provide an unacceptable margin of error if the engine test is not suitably controlled. A strict routine was developed to ensure that the engine had been subjected to the same conditions for a reasonable period of time before any measurements were taken, and that all sample lines and filters had undergone the same degree of sample flow. The data was recorded on computer spread sheets and specifically designed forms. The recording of the data by this method instructed the operator to follow the same routine and time between measurements.

The test points chosen for this test were based on a fraction of the peak power output. Full power testing was omitted because the operating temperatures could not be controlled for the duration of the earlier tests and the results were not repeatable. The test points are shown in table 3.6.

Test point	Speed RPM	Torque (Nm)	BMEP (bar)	Power (kW)	Approx. % load
A	Idle	0	0	0	none
B	1600	89	2.86	14.9	25
C	1600	179	5.72	30	50
D	1600	268	8.59	44.9	75
E	2500	234	7.49	61.2	75

Table 3.6 Engine test points

The gas phase exhaust samples were initially taken from each of the exhaust valve sample points (1,2,3,4) singularly then simultaneously (All4). The measurements were then taken progressively down the exhaust system at the turbocharger inlet (PreTurbo) and at 1 metre from the turbocharger outlet (1metre). The engine was run at the required speed and load for 10 minutes before any measurements were taken. If any of the displayed temperatures were outside the expected level the engine was allowed to run for longer. The inlet air temperature was corrected by increasing or decreasing the air flow from the air conditioning system into the test cell. The fuel and water temperatures were controlled by heater and coolers which could be adjusted manually.

When all the gas phase samples had been recorded and the flow to the measuring devices had been stopped, a proportion of the exhaust gas was diverted to the dilution tunnel. The flow to the tunnel was allowed to flow into the tunnel until all the measured temperatures and flows stabilised before the sample was taken. The clean and used sample filters were stored in a desiccator jar during the test procedure before being placed in a temperature and humidity controlled environment prior to analysis. During the testing of the particulate, any deviation of the test equipment from normal would render the test invalid and all the flows and filters would be reset and the test repeated.

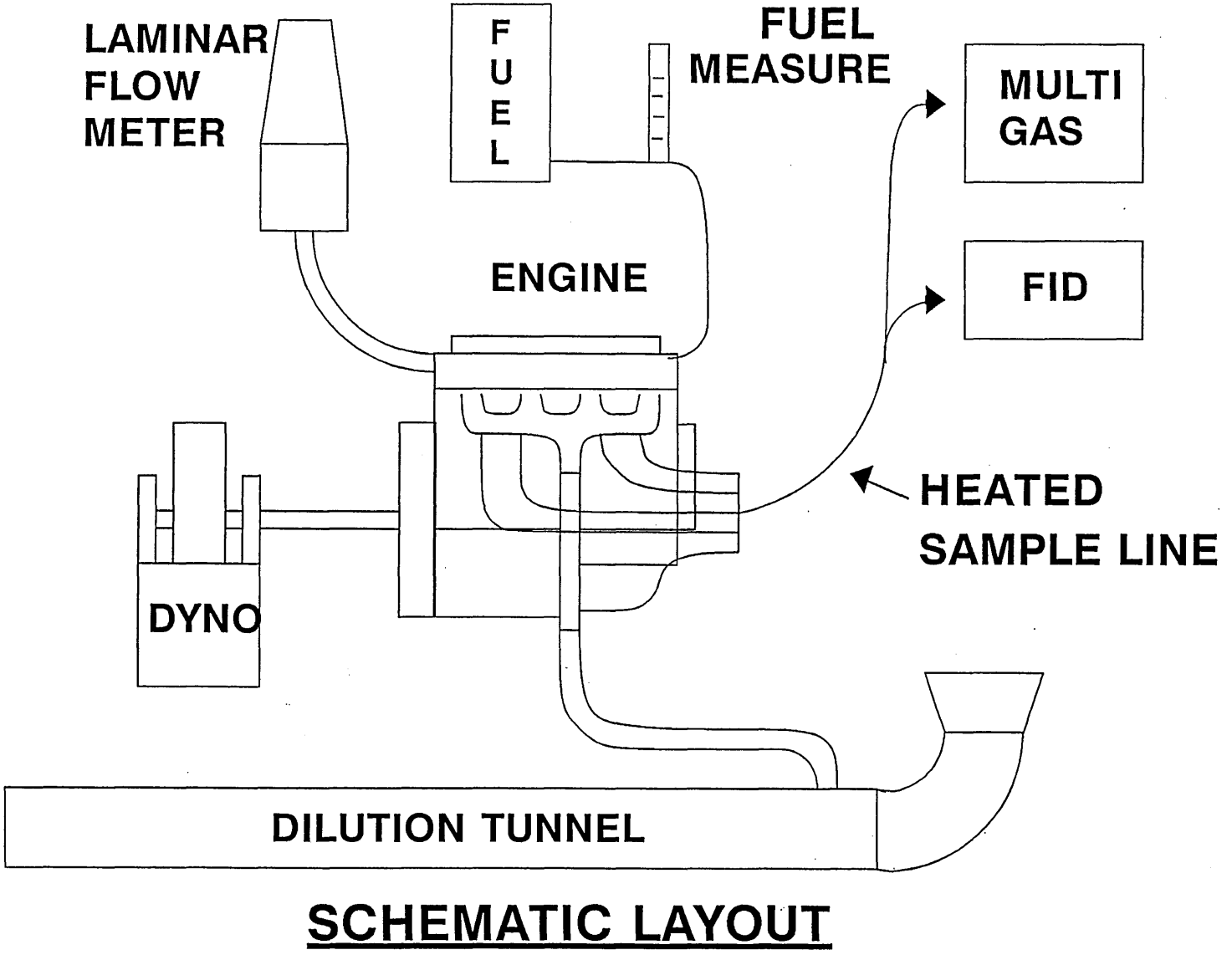

Figure 3.1 Layout of test cell

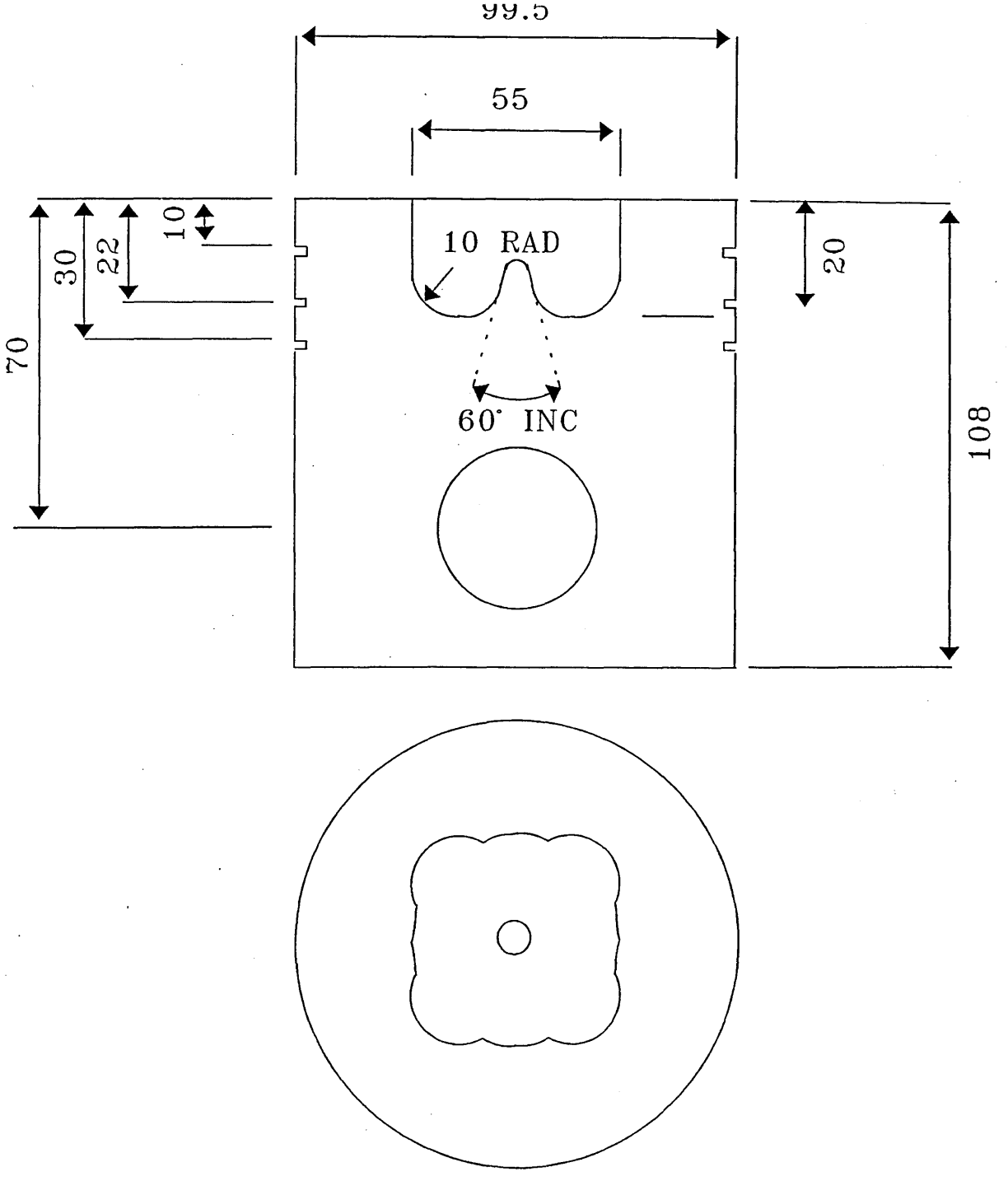

Top ring grove 4.5 by 3.5 mm
2nd ring grove 4.5 by 2.5 mm
Oil ring grove 5.5 by 4.0 mm

All dimensions are approximate

Figure 3.2 Simple drawing of a standard piston

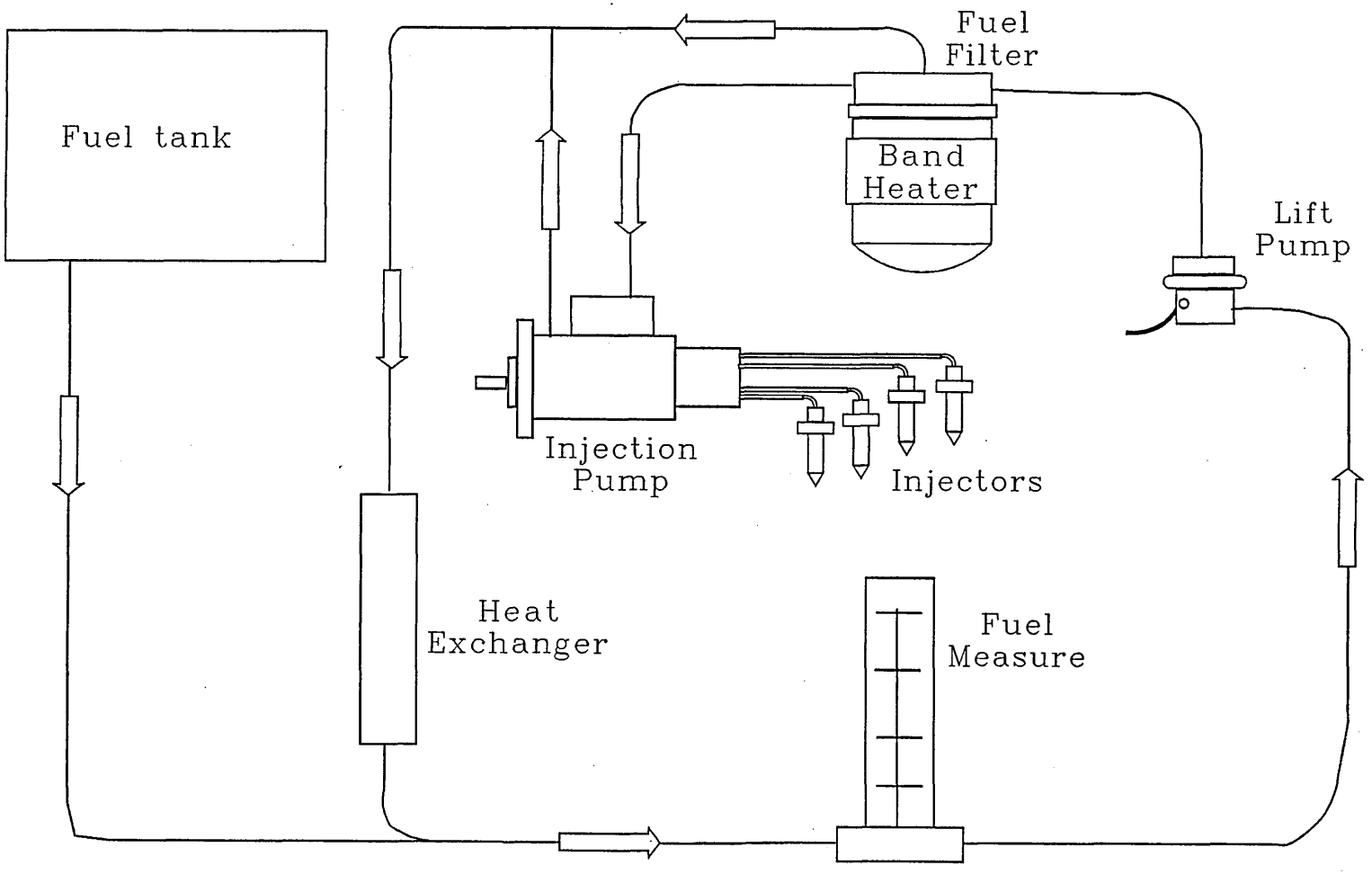

Figure 3.3 Fuelflow system for test cell

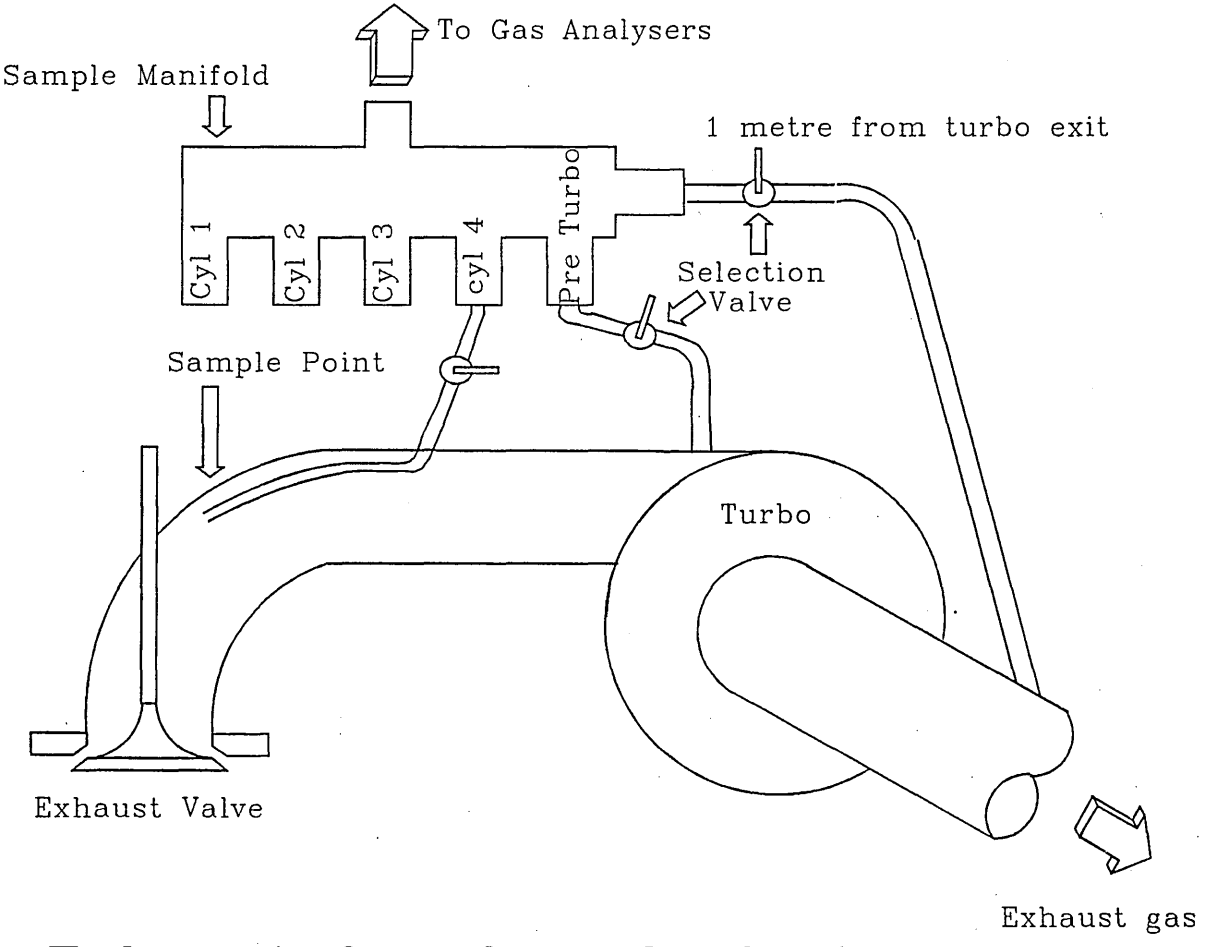

Exhaust Gas Sample System

Figure 3.4 Exhaust gas sampling system

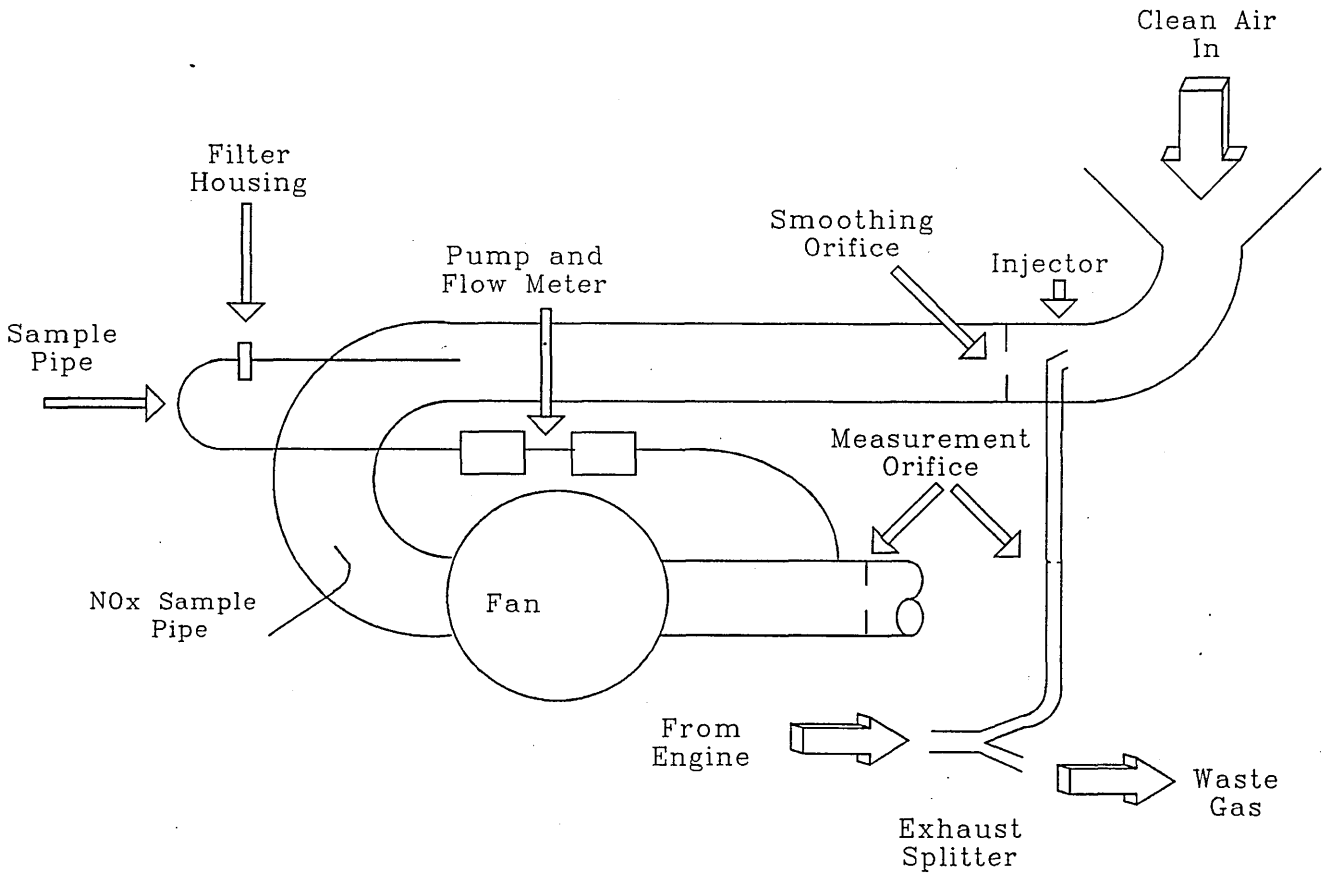

Tunnel Schematic

Figure 3.5 Dilution tunnel sample flow system

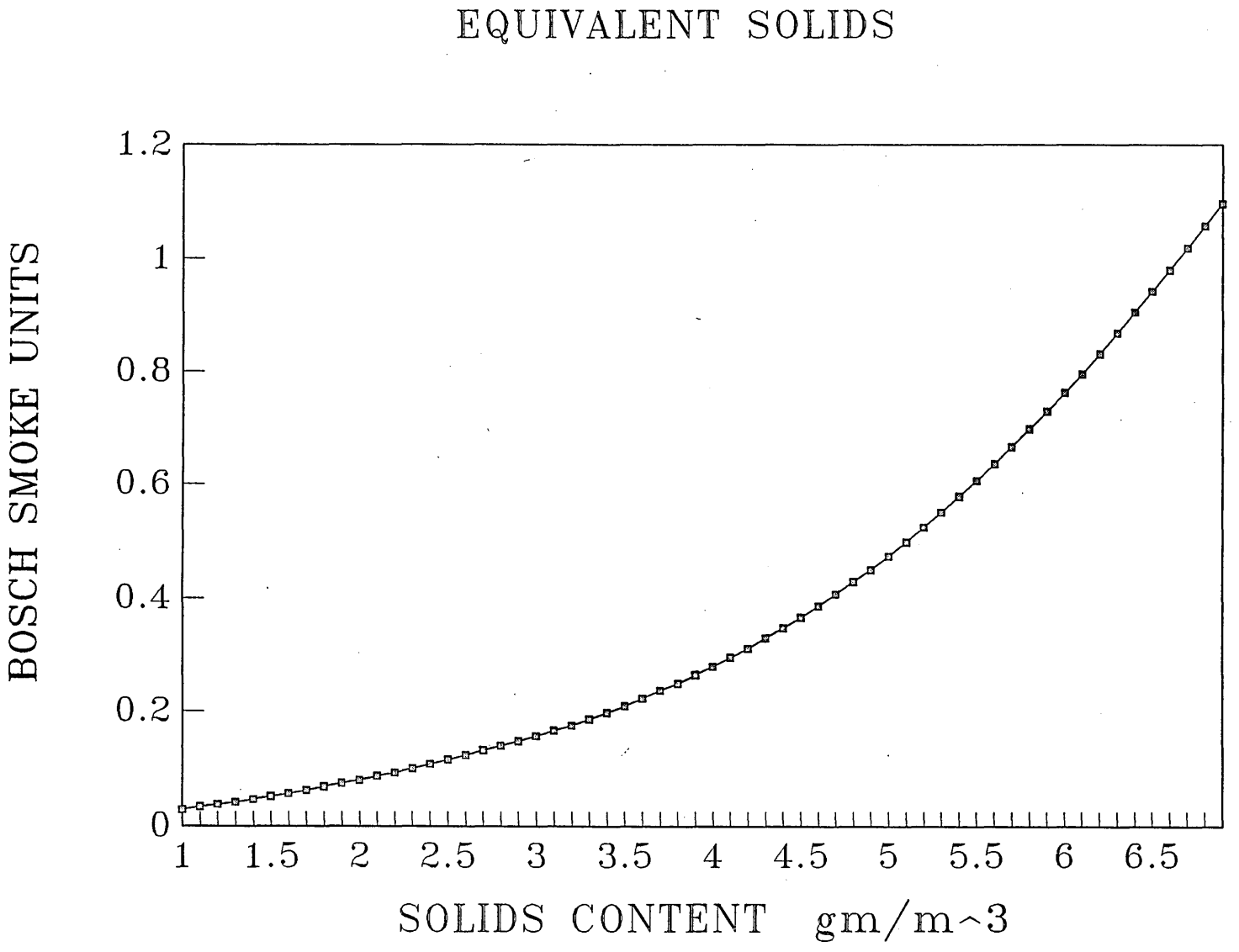

Figure 3.6 Correlation between smoke and particulates

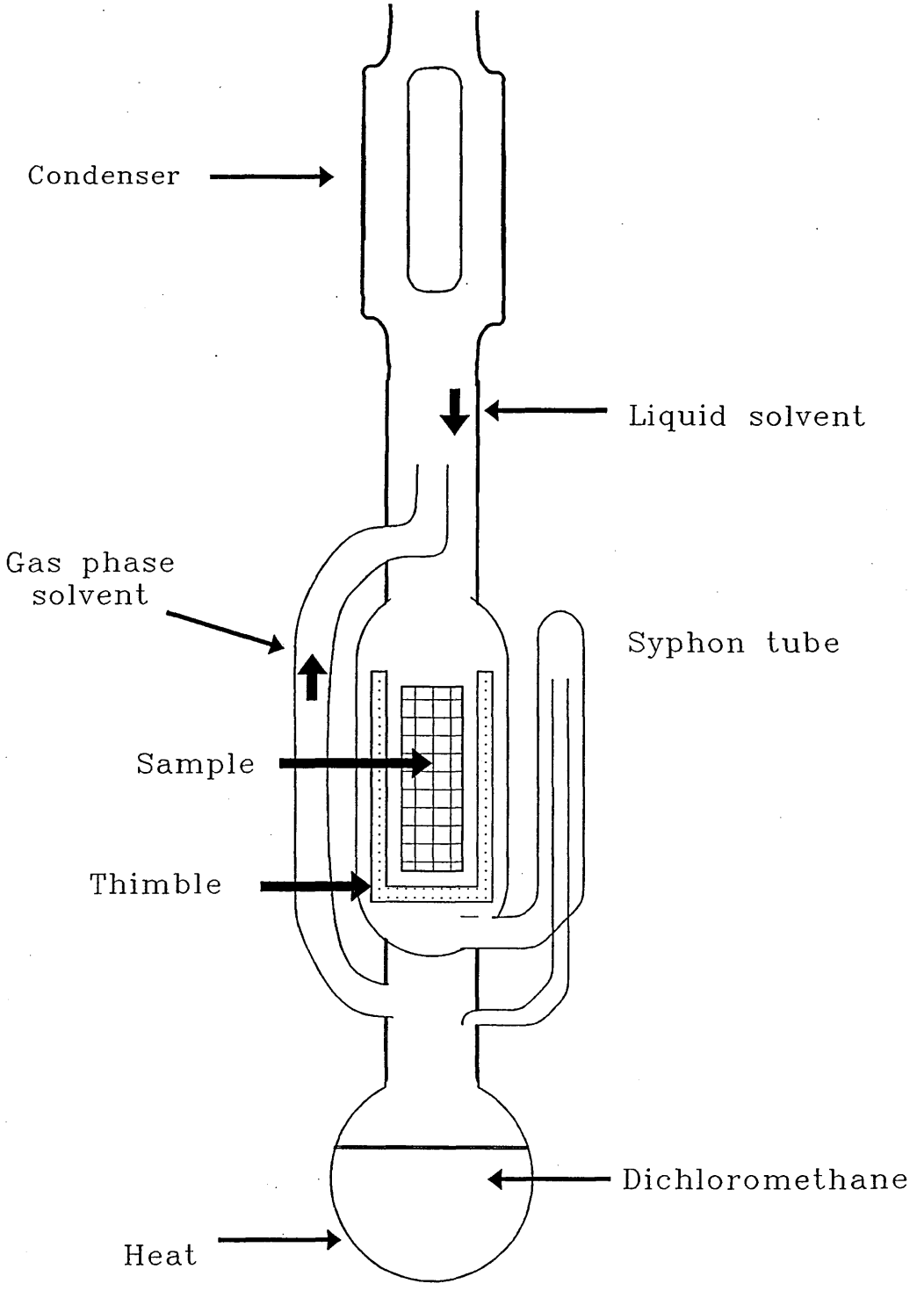

Figure 3.7 Soxholet apparatus

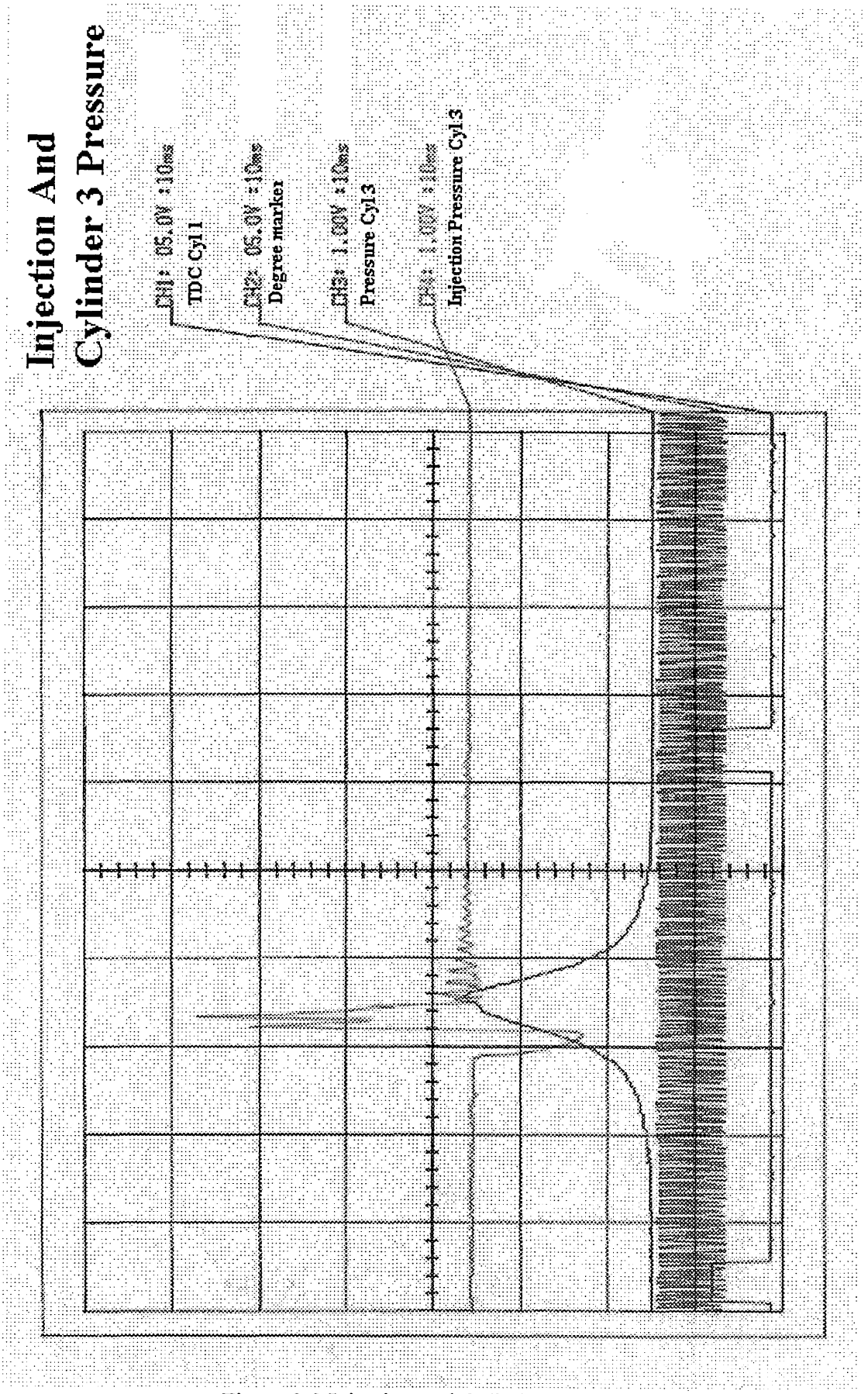

Figure 3.8 Injection and Cylinder Pressure

4.0) Mathematical Model

4.1) The development of a computer model

To complement the engine test program a computer model has been developed to test the theories used for the selection of each piston design. The model is of the single zone, pressure driven type. In order to provide the necessary data and to validate the theoretical model results, experimental data was taken from a test engine. The cylinder pressure from an engine test is recorded at one degree intervals. This data is used as a known variable for each of the routines used to derive each unknown. The fuel injection pressure was also recorded to allow the determination of the start and end of injection. This pressure trace, combined with the cylinder pressure trace, allowed the ignition delay angle for each operation point to be obtained. The logic flow chart used for the development of this model is shown in figure 4.1 and the definition of the zones in figure 4.2.

Many of the equations used within this model were derived with constants that allowed the equation to be "fine tuned" to match the engine and operating condition. These constants were obtained by comparing the model's results to that obtained from practical observations for the standard engine configuration until the results were within the required levels of accuracy. These constants were not changed when the model was used to predict the emission levels for the other engine configurations. The additional data required for the model has been obtained from:-

Variable	Origin
Piston Dimensions	Original Drawings
Liner Dimensions	Original Drawings
Engine Speed/Load	Engine Testing
Inlet Air Conditions	Engine Testing
Ambient Air Conditions	Engine Testing
Fuel Injection Limits	Engine Testing
Combustion Duration	Engine Testing
Piston/Liner Temperature	Literature[43,67, 68, 69,87]

Because of the complexity of the combustion process within a diesel engine, this model includes some assumptions,

1) The piston is completely circular and positioned centrally in the circular liner.
2) The gas flow into the crevice is isothermal.
3) The gas in the crevice volumes are at the piston temperature.
4) The gas in the crevice volume is unburnt mixture.
5) The gas entering the crevice is air until the fuel penetration reaches the liner radius.
6) The gas entering the crevice volume with fuel contained has the same average equivalence ratio as the cylinder.
7) The piston rings remain on the base of the ring groove
8) There is no gas flow past the 2nd ring.
9) The cylinder contents are at a uniform temperature.

4.2) The derivation of the heat release equation

For this type of engine the cylinder contents are assumed to be a single open system. The only mass that flows across the boundaries (while all the valves are closed) are the fuel and crevice gases.

The first law for an open system is

$$\frac{dQ}{dt} - p\frac{dV}{dt} + m_f h_f = \frac{dU}{dt} \qquad \text{Eqn 1}$$

Since $h_f = 0$, no enthalpy change of the fuel, equation 1 becomes

$$\frac{dQ}{dt} = p\frac{dV}{dt} + \frac{dU}{dt} \qquad \text{Eqn 2}$$

If the contents are modelled as an ideal gas equation 2 becomes

$$\frac{dQ}{dt} = p\frac{dV}{dt} + mc_v\frac{dT}{dt} \qquad \text{Eqn 3}$$

From the ideal gas law , pV=mRT, with R assumed constant it follows that

$$\frac{dp}{p} + \frac{dV}{V} = \frac{dT}{T} \qquad \text{Eqn 4}$$

Equation 4 can be used to eliminate T from equation 3 to give

$$\frac{dQ}{dt} = (1 + \frac{C_v}{R})p\frac{dV}{dt} + \frac{C_v}{R}V\frac{dp}{dt}$$

or

$$\frac{dQ}{dt} = \frac{\gamma}{\gamma-1} p \frac{dV}{dt} + \frac{1}{\gamma-1} V \frac{dp}{dt} \qquad \text{Eqn 5}$$

The mass of the crevice volume gases is small and therefore assuming that it is at the cylinder wall temperature including crevice volumes[32] equation 5 becomes with

$\gamma(T) = a + bT$

$$\frac{dQ}{dt} = \frac{\gamma}{\gamma-1} p \frac{dV}{dt} + \frac{1}{\gamma-1} V \frac{dp}{dt} + V_{CR}\left[\frac{T}{T_W} + \frac{T}{T_W(\gamma-1)} + \frac{1}{bT_W} \ln\left(\frac{\gamma-1}{\gamma-1}\right)\right] \frac{dp}{dt} + \frac{dQ_{ht}}{dt} \qquad \text{Eqn 6}$$

Where $\gamma = \frac{C_p}{C_v}$

4.3) Fuel mass burning

With the internal energy of the cylinder known, then by comparing it to a consistent datum the difference is equivalent to the fuel mass burning rate. The routine used was developed by Krieger and Borman[70] and is as follows,

m = mass, u = specific internal energy , Φ= equivalence ratio.

$$\frac{d}{dt}(mu) = -p\frac{dV}{dt} + \frac{dQ}{dt} + h_f \frac{dm}{dt}$$

$dm/dt = m_f$

The internal energy of a gas is a function of its temperature, pressure and the equivalence ratio thus u=u(T,p,Φ) and R=R(t,pΦ)

Therefore

$$\frac{du}{dt} = \frac{\partial u}{\partial T}\frac{dT}{dt} + \frac{\partial u}{\partial p}\frac{dp}{dt} + \frac{\partial u}{\partial \Phi}\frac{d\Phi}{dt} \qquad \text{Eqn 7}$$

$$\frac{dR}{dt} = \frac{\partial R}{\partial T}\frac{dT}{dt} + \frac{\partial R}{\partial p}\frac{dp}{dt} + \frac{\partial R}{\partial \Phi}\frac{d\Phi}{dt}$$

also $$\Phi = \Phi_0 + \left(\frac{m}{m_0} - 1\right)\frac{1+(F/A)_0}{(F/A)_s} \qquad \text{Eqn 8}$$

and $$\frac{d\Phi}{dt} = \frac{1+(F/A)_0}{(F/A)_s m_o}\frac{dm}{dt}$$

F/A is fuel air ratio, 0 denotes initial value prior to fuel injection, s denotes stoichiometric value. It then follows that

$$\frac{1}{m}\frac{dm}{dt} = \frac{-(RT/V)(dV/dt) - (\partial u/\partial p)(dp/dt) + (1/m)(dQ/dt) - CB}{u - hf + D(\partial u/\partial \Phi) - C[1+(D/R)(\partial R/\partial \Phi)]}$$

where

$$B = \frac{1}{p}\frac{dp}{dt} - \frac{1}{R}\frac{\partial R}{\partial p}\frac{dp}{dt} + \frac{1}{V}\frac{dV}{dt}$$

$$C = \frac{T(\partial u/\partial T)}{1+(T/R)(\partial R/\partial T)}$$

$$D = \frac{[1+(F/A)_o m]}{(F/A)_s m_o}$$

4.4) Fuel injection

The accurate prediction of the fuel behaviour within the injection system requires a sophisticated model. Ofner[71] showed that by splitting the complete fuel injection system into individual parts and then describing each component as a general physical model each component model could be allowed to be called when required. This type of model requires the physical dimensions of the complete fuel injection system to provide suitable results.

For this model the fuel injected is based on quasi steady, one dimensional and incompressible flow through a nozzle.

mass of fuel injected (m_f) is determined by

$$m_f = C_D A_n \sqrt{2\rho\Delta p}\frac{\Delta\Theta}{360N}$$

where Θ is nozzle open period in degrees, N is engine speed.

The discharge coefficient for the injector for the model was taken to be constant. Where this provides suitable accuracy the model could be enhanced by using an instantaneous value. Timoney[72] showed that the kinetic energy of the fuel droplets have a significant effect on the mixing rate of the fuel and air and hence the

combustion characteristics. The kinetic energy of the fuel droplets is controlled by the discharge coefficient. It has been shown that this varies throughout the injection process[73]. At the start of injection the value is approximately 0.82 and drops to 0.65 when the injector needle is at maximum lift with maximum fuel flow.

4.5) Fuel spray penetration

Fuel penetration into quiescent air within diesel engines (S)

This model used the formula developed by Dent[74]

$$S = 3.07\left(\frac{\Delta p}{\rho_g}\right)^{1/4}(td_n)\left(\frac{294}{T_g}\right)^{1/4}$$

4.6) Fuel adsorption and desorption

The next routine that was developed and incorporated into the model was to observe the effect of the fuel entering and leaving the oil film on the liner surface. There was not a model previously developed for a diesel engine for this and the model by Korematsu[75] was modified to allow for the change in molecular weight of the fuel air charge. The model for S.I. engines is as follows,

$$d_{mf} = (C_{\max} - C_{\min}) \times \pi D_c \times X \times \rho \times C^*_{eq} \times dy \qquad (9)$$

where

dy = the incremental piston movement in the y axis

d_{mf} = the incremental mass of fuel emitted

C^*_{eq} = mass fraction of fuel in oil at equilibrium

C^* = mass fraction of fuel in oil

Cmax-Cmin = total fuel emitted from oil in a cycle

D_c =Cylinder liner diameter

X = Oil layer thickness

ρ = oil density

The values for Cmax and Cmin were initially extrapolated from the data supplied by Korematsu[75] but these values produced results that were not within tolerable limits. A simplified version of the model was then produced that calculated the quantity of fuel adsorbed/desorbed using the method of Dent and Lakshminarayanan[76].

$$\frac{dm_i}{dt} = m^{"} A_i + \rho_o Z_o \sum m_{fFi} \frac{dA_{i,j}}{dt}$$

where

$$m^{"} = \frac{g_G^* g_F^*}{N_{HC} g_G^* + g_F^*} \left[m_{FG} - m_{fF} N_{HC} \right]$$

g_G^* = gas phase mass transfer conductance

g_F^* = liquid phase mass transfer conductance

m_{FG} = mass concentration of fuel vapour in bulk gas state

m_{fF} = mass concentration of fuel vapour in the oil film

N_{HC} = Henry Constant

A_i = Area i

ρ_o = Oil density

Z_o = Oil thickness

m_{fFi} = Mass fraction fuel in region i

$\frac{dA_{i,j}}{dt}$ = The rate of change caused by boundary regions

This method used four areas for the calculation:

1) The area in contact with the unburned gas
2) The area that was in contact with the unburned gas and now covered by the piston
3) The area in contact with the burned gas
4) The area that was in contact with the burned gas and now covered by the piston

The adsorption of the fuel into the oil could only occur when the crevice volume around the piston contained unburnt fuel particles. The desorption of the fuel could occur over the remainder of the cycle.

Figure 4.3 shows the change in adsorbed / desorbed matter caused by changing the oil film thickness from 5μm to 4μm. The sudden increase in matter migrating into the oil at 347 degrees is because the fuel from the start of injection (342 degrees) can travel to the oil film.

To determine the solubility of the fuel into the oil film a variation of Henrys Law was used. Henrys Law states that the amount of gas dissolved in a given quantity of liquid is directly proportional to the gas pressure above the solution. This law cannot apply to substances that will react with each other and is only correct for oxygen and inert gases, i.e. group 8 of the periodic table. Henrys Law is represented by the following equation.

$$c = kP$$

Where

c = molarity (mol litres $^{-1}$)
k = absorption coefficient
P = pressure.

The variant of Henrys Law used for the model was

$$Hc = \frac{P_f}{n_f}$$

This variant was used because the variable suited those previously calculated within the model,

Where

Hc = the Henry Constant (N/m²)
Pf = the partial pressure of fuel vapour (N/m²)
nf = Mol fraction of fuel dissolved in oil film.

Both the lubricating oil and the fuel used throughout testing were complex combinations of many different hydrocarbons and other elements. To allow the determination of the Henry constant they were both assumed to be comprised of a single species hydrocarbon. The lubricating oil was assumed to be squalane $C_{30}H_{62}$ and the fuel octadecane $C_{18}H_{38}$.

Dent and Lakshminarayanan [76] used the results from Chappelow and Prausnitz [77] to extrapolate the Henry constant for a range of pure hydrocarbon species. Using these results gave the following relationship:-

$$\text{Log (Hc)} = -1.82 + 0.0125.(T - 300) \tag{10}$$

4.7) Flow into the 2nd land area

The area that provides the main mass flow into this region is the ring gap and this has been modelled as an orifice.

Using the conservation of energy to develop a formula for the flow through an orifice:-

Mass flow = $\dot{V}\rho = AV\rho$

Therefore

$$A_1 V_1 \rho_f = A_2 V_2 \rho_f \tag{11}$$

and

$$\frac{P_1}{\rho} + \frac{V_1^2}{2} = \frac{P_2}{\rho} + \frac{V_2^2}{2} \tag{12}$$

Rearranging eqn 12 to give V_1

$$V_1 = \frac{A_2 V_2}{A_1} \tag{13}$$

Substituting eqn 13 into eqn 12 gives

$$\frac{P_1}{\rho} + \frac{A_2^2 V_2^2}{A_1^2 2} = \frac{P_2}{\rho} + \frac{V_2^2}{2} \tag{14}$$

Rearranging eqn 14 to give V_2

$$V_2 = \sqrt{\frac{2\Delta P}{\left\langle \frac{A_2^2}{A_1^2} - 1 \right\rangle \rho}} \tag{15}$$

To include friction for some areas of the model a coefficient of discharge(Cd) is added to equation 15 ,

$$V_2 = Cd\sqrt{\frac{2\Delta P}{\left\langle \frac{A_2^2}{A_1^2} - 1 \right\rangle \rho}} \qquad (16)$$

4.8) The molecular weight of the fuel air mixture

The fuel is injected during the cycle, therefore the properties of the contained gas change. To facilitate the mass of hydrocarbons in any one area to be calculated the number of moles of each compound flowing into or out of it needs to be obtained. The ideal gas law is used to determine the number of moles of fuel and air present at each program step, the step normally being 1 degree.

m(mass) = η(number of moles) x M(molecular weight)

The mass per molecule is designated M* and the number of molecules per mole No, thus the mass per mole is

$$\frac{m}{\eta} = \text{M*No} = \text{M}$$

$$\text{No} = \frac{M}{M^*}$$

No = Avogadro's number = 6.022045 x10^{23} molecules/g mol.

4.9) Flow into the area behind the top ring

The flow into the area behind the top ring is primarily through the area between the ring and the ceiling of the ring groove, For this model this area of flow is treated as a long thin channel. with compressible isothermal laminar flow with friction. The following formula was developed by Shapiro[78] and used in other models [79, 80].

$$\left(\frac{\dot{m}}{A}\right)^2 = \frac{p^2{}_u - p^2{}_d}{RT\left(\frac{4fW}{D} + 2\ln\left(\frac{p_u}{p_d}\right)\right)} \qquad (23)$$

For laminar flow

$$f = \frac{24}{\mathrm{Re}} \qquad \text{and} \qquad \mathrm{Re} = \frac{m \times D}{A \times \mu_{gas}}$$

to simplify the equation Namazain[79] assumed that

$$2 \times \ln\frac{p_u}{p_d} << \frac{4Wf}{D}$$

and that the hydraulic diameter D = 2h

Therefore equation 23 becomes

$$\left(\frac{\dot{m}}{A}\right) = \frac{h^2}{24 \times W \times \mu_{gas} R \times T}\left(p^2{}_u - p^2{}_d\right)$$

Where

$\dot{m}$ = mass flow rate A = area (m^2)

h = height of narrow gap

p = pressure u = up, d= down (N/m^2)

R = universal gas constant

T = temperature of gas (K)

W = length of the channel (m)

D = hydraulic diameter (m)

$\mu_{gas} = 3.0 \times 10^{-7} \times T^{0.7}$ (Ns/m^2)

4.10) Crevice mass

Increasing the 2nd land volume by 8.812×10^{-6} m^3 effectively doubling the original, reduced the observed pressure by one half, but this reduction in pressure allowed the gases to flow into this region for a longer period at the same mass flow rate. This increase in time for the flow allowed a greater mass of gas to accumulate in this region before being released later in the cycle, than the gas from a standard piston. The entrained mass was slightly more than double that of the standard piston. The mass in the second land contributes more to the total than that of the top ring.

4.11) Soot, soluble fraction and particulates.

The inclusion of a soot formation routine required a different method for the calculation for the preparation and combustion of the injected fuel. For this the combustion has been modelled using the approach suggested by Whitehouse[81]. This model is comprised of two parts; the first based on the Arrhenius equation predicts the fuel burning rate and the second predicts the fuel preparation rate.

$$FBR = \frac{K}{N} \times \frac{p'_{o2}}{\sqrt{T}} \exp\left(-\frac{E_a}{T}\right) \int (FPR - FBR) d\Theta \qquad (24)$$

Where

$$FPR = K' \times m_i^{(1-x)} \times m_u^{x} \times (p'_{O2})^{z} \qquad (25)$$

p'_{O2} = Partial pressure of oxygen
mi = mass of fuel injected
mu = mass of fuel yet to be injected

Also within the derivation of the model are the ranges of the constants and these are as follows:

$$0.01 < x < 1$$

$$z = 0.4$$

$$0.008 < K < 0.020 \text{ (bar}^{-2}\text{)}$$

$$1.2 \times 10^{10} < K' < 65 \times 10^{10} \text{ (K}^{½}\text{/bar s)}$$

$$Ea = 1.5 \times 10^{4} \text{ (K)}$$

Within this equation the term (FPR - FBR)dΘ is equal to the quantity of fuel within the cylinder that has been prepared but not yet burnt. For each step the value of FBR is calculated using the value of $\sum$(FPR - FBR)dΘ

The full formation mechanism of the soot produced within the combustion chamber of a diesel engine are not fully understood but the controlling factors have been identified; these are gas temperature and oxygen availability. Because the full formation mechanism is not understood, there is no generally accepted method for the calculation of soot levels. Because of the structural similarities between soot and pyrographites, the oxidation rates should be similar. Studies based on the Nagle and Strickland-Constable[82] oxidation mechanism have shown a reasonable correlation for temperatures between 1100 and 2500 K and when the oxygen partial pressure is below one atmosphere. The operating fundamentals of this mechanism are based on the theory that as oxidation progresses, the sites available on the carbon for oxygenation change from the reactive type A sites to the less reactive type B sites. The operating conditions found within the combustion chamber of a diesel engine are not within the range that have been proved accurate for this mechanism. The partial pressure of oxygen is in the region of several atmospheres and the temperature attains a peak of approximately 2800K.

The soot formation mechanism used within the model has been developed by Nishida[83], and is as follows.

$$\frac{dms}{d\Theta} = \frac{dmsf}{d\Theta} - \frac{dmsc}{d\Theta} \qquad (26)$$

where

$$\frac{dmsf}{d\Theta} = A_{sf} \times m_{fv} \times P_{cyl}^{0.5} \times \exp(-6313/T) \qquad (27)$$

and

$$\frac{dm_{sc}}{d\Theta} = A_{SC} \times m_s \times PPo2 \times P_{cyl}^{1.8} \times \exp(-7070/T) \qquad (28)$$

and

dms = the incremental mass of soot
dmsf = the incremental mass of soot formed
dmsc = the incremental mass of soot consumed
Asf = constant for soot formation
Asc = constant for soot consumption
T = Gas temperature (K)
PPO2 = oxygen partial pressure (N/m^2)
Pcyl = Cylinder pressure (N/m^2)

ms = mass of soot (g/m^3)

mfv = mass of fuel vapour (g/m^3).

The results from this equation produce a soot concentration curve for the complete cylinder, that has the same form as a soot concentration curve as the global average for a three dimensional model. Because soot formation is a direct function of fuel vapour within the cylinder, the injection timing and duration can influence the total quantity considerably.

The soot content that enters the atmosphere is assumed to be the same as the concentration within the cylinder when the exhaust valve opens. This soot mass concentration can be converted to other units i.e. Bosch smoke units.

The correlation used within the model was derived by Matsui[84]:

$$BSU = 40.03231\rho_{s,ntp} - 221.9747\rho_{s,ntp}^2 + 819.641\rho_{s,ntp}^3 - 1758.072\rho_{s,ntp}^4 \quad (29)$$
$$+2195.714\rho_{s,ntp}^5 - 1574.006\rho_{s,ntp}^6 + 599.589\rho_{s,ntp}^7 - 93.9501\rho_{s,ntp}^8$$

This method was preferred to that proposed by Greeves[85] because it provided a closer correlation to the results obtained experimentally. The equation that Greeves derived was a best fit to a straight line using the weight of the smoke collected by a Bosch smoke meter and the concentration of unburnt hydrocarbons. The equation is as follows.

$$\text{Particulate } (g/m^3) = 1.024 \times \text{Smoke } (g/m^3) + 0.505 \times \text{uHC } (g/m^3) \quad (30)$$

The soluble organic fraction is related to the unburnt hydrocarbon(uHC) mass concentration within the cylinder when the exhaust valve opens; this mass is comprised of :-

1) Fuel from regions where the concentration was not sufficient to promote combustion.
2) Fuel from regions where the temperature was not sufficient to allow combustion to complete.
3) Fuel from locally over rich areas.
4) Fuel adsorbed and desorbed from the lubricating oil film.
5) Fuel entering the crevice volumes and emerging after flame extinction

The contribution to the UHC from items 1,2 and 3 are derived from the combustion model.

4.12) Oxidation of crevice mixture.

The fuel that avoids combustion by entering the crevice volumes is still subjected to partial oxidation upon re-entering the cylinder. The oxidation rate is determined by the cylinder gas temperature and the rate of the gases mixing. During combustion there are large temperature gradients within the cylinder gases, i.e. there are distinct areas of flammation. Calculating the temperature of the region where the crevice gas enters the cylinder gas within a single zone model requires the assumption of certain mixing ratios.

The end of oxidation for the crevice gases is determined by the sudden freezing temperature of the mixture. Above this temperature all uHC from the crevices will be oxidised: and below this temperature oxidation will halt because the time required for the reaction will be to great. Oxidation can occur in the absence of oxygen, as a molecule is said to be oxidised if it loses a hydrocarbon atom. This temperature is given by[86] :

$$Tsf = \frac{1320}{\left(1 + 0.02 \times \ln(F_{O2} \times 100 \frac{P_i}{P_o})\right)} \qquad (32)$$

Where

F_{O2} = Percentage Oxygen present in the exhaust gas
Pi = Inlet manifold pressure
Po = Atmospheric Pressure

A calibrated version of the model was generated for each test point and the only variables that were changed are shown in Figure 4.4. This figure shows the variable input screen from the model. A complete table of the actual values used for each model run is shown in chapter 6 Model Results.

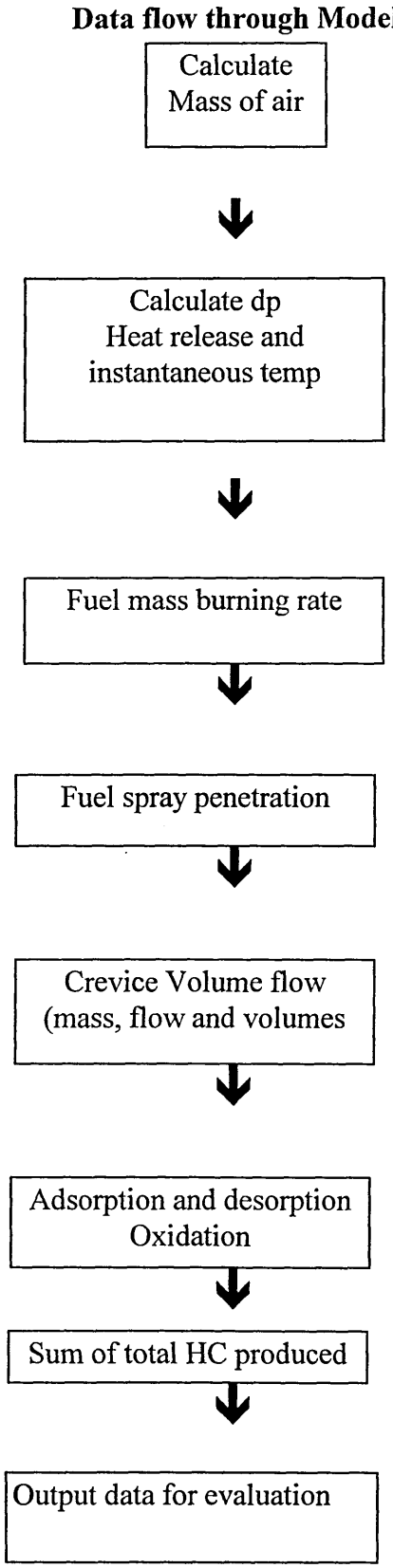

Figure 4.1 Data flow through model

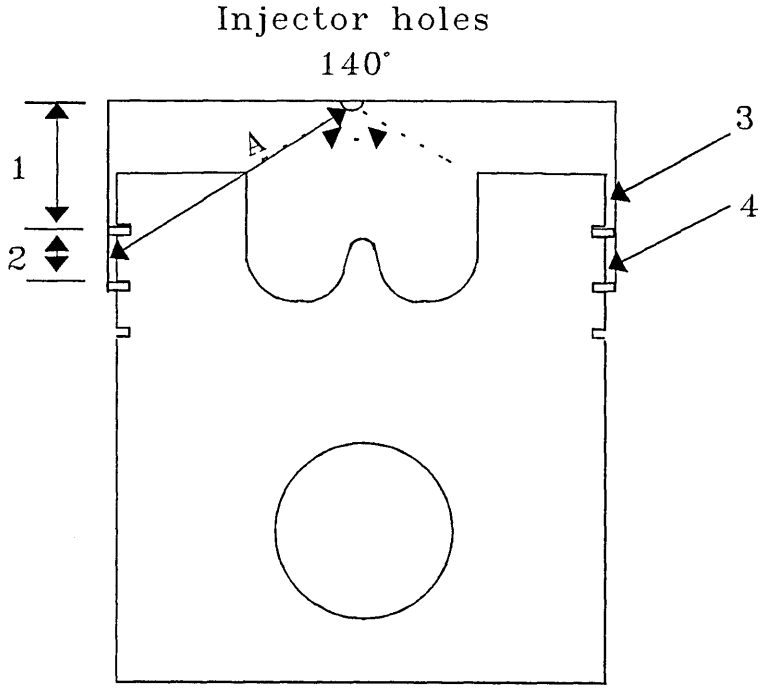

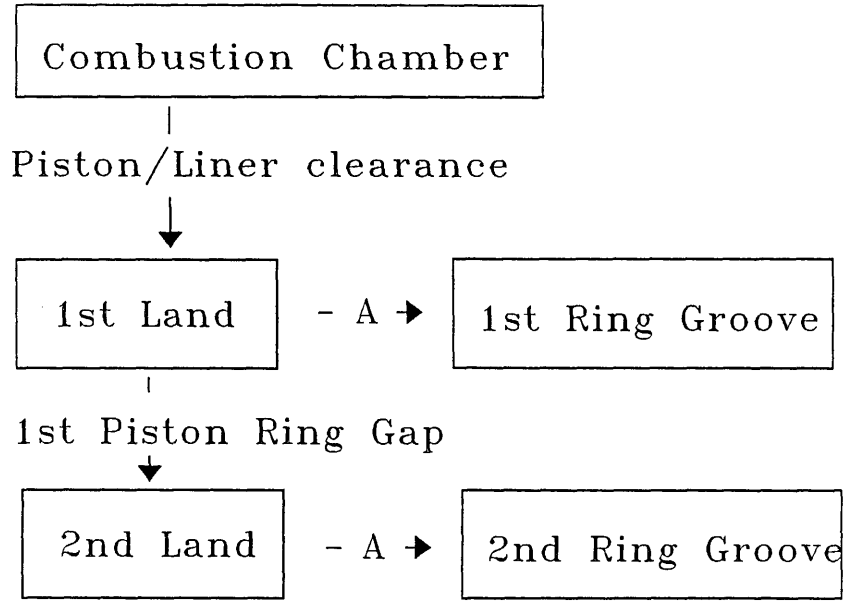

Figure 4.2 The zones within the model

Area 1 Adsorption desorption part a
Area 2 Adsorption desorption part b
Area 3 Crevice volume including 1st ring grove
Area 4 Crevice volume including 2nd ring grove

All flow past piston rings is through ring gap
Flow A is flow through ring/groove clearance
There is no flow past 2nd ring

The area above the piston and within combustion chamber is of uniform air/fuel ratio
Line A is the distance used for the fuel to travel to contact the oil film

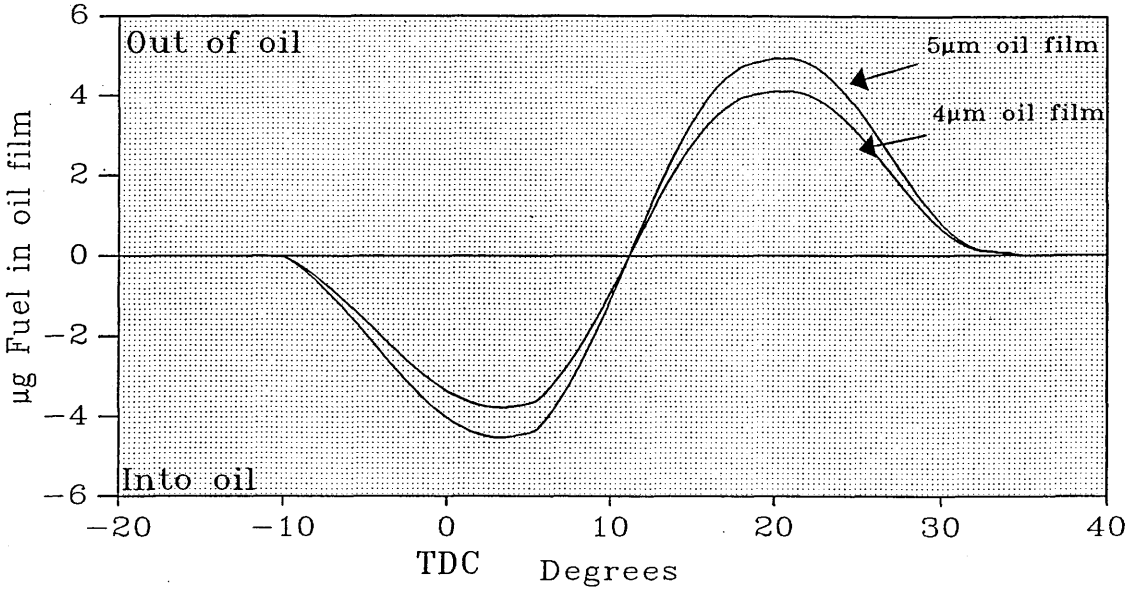

Figure 4.3 The effect of oil film thickness

Screen shot of variables determined at run time

F1 RESTORE DEFAULT F10 TO QUIT		F5 TO CONTINUE ENTER TO EDIT	
TEST NO	88	CON ROD Lth(m)	0.219
BORE (m)	0.1	STROKE(m)	0.127
COMP RATIO	16.5	SPEED(RPM)	2500
LOAD(Nm)	234	PISTON DIA(m)	0.099286
LINER DIA(m)	0.1	MANIFOLD P(mmHg)	280
AIR TEMP(C)	67	AIR P(mbar)	999
OIL LAYER (um)	0.244	LAND HT (m)	0.01
2ND LAND DIA(m)	0.09952	2ND LAND VOL(m^3)	0
PISTON TEMP (K)	505	EXHAUST O2 (%)	10.74

Figure 4.4

5.0) Engine Testing

5.1) Introduction

For the purpose of this research a series of four tests using different piston and liner combinations was developed and are shown in table 5.1.

Number	Piston	Ring	Liner
1	Standard	Standard	Standard (liners finished in bore)
2	Standard	Standard	Standard (pre-finished liners)
3	Standard	Reduced tangential load oil control rings	Standard (pre-finished liners)
4	High top ring	Standard	Standard (pre-finished liners)

Table 5.1 Engine piston / liner combinations for each test

The initial test was used to test the suitability and reliability of the test facility and the results were not used for any other purpose. This test also fulfilled the following criteria.

1) To allow the operators to learn how to use the test equipment reliably, accurately and safely.
2) To test for repeatability of the test technique and allow any improvements.
3) To ensure that the equipment had a suitable resolution and operated reliably and was correctly installed and operating within acceptable limits.
4) To ensure any modifications to the engine did not compromise its operating characteristics.

5.2) Repeatability between tests and engine builds

To allow the comparison between engine builds, the engine must be operating at conditions that are as close to that of the other builds as practically possible, but

because of the modifications to the in cylinder geometry some minor changes were expected. The first test showed that the turbocharger produced differing levels of boost over a significant period of time, if the engine was set to a test point greatly increasing the fuelling rate, to that observed by reducing the fuelling rate by a similar amount. The engine speed was controlled by the dynamometer to 0.5% of the desired speed at 1600 rpm. The engine torque was set by the engine governor. This is achieved by balancing fuel pressure to that of a compressed spring and this was susceptible to changes in the fuel volume caused by any change in the fuel temperature. The temperature of the fuel in the main fuel filter was controlled to ± 2.5°C and the volume flow measured during the emission sampling. The careful control and monitoring of the engine operating parameters allowed any significant change in engine performance to be observed and the engine re-set to the test point.

5.3) Pistons And Liners

The manufacture of pistons and liners requires the machining of complex shapes to a high degree of accuracy and thus there are variations in all dimensions. To allow each liner to be matched to a piston, more pistons than required were manufactured. The pistons were matched to a liner by selecting the smallest piston and matching it to the smallest liner that gave a similar clearance. The piston and liner combinations for each build were selected by separating the combinations into four groups. One piston and liner was then chosen from each group. The smallest piston and liner from each group was then fitted to cylinder one and the next largest fitted to cylinder two. The mean diameter of the piston and liner increased as the cylinder number increased.

5.4) Standard test

The objective of this test was to produce a set of reference values that the subsequent engine builds were to be compared against, because this was the reference test a large

number of test runs were completed to provide the accuracy of data, and the average of the six tests that showed the most similarity were used for the reference. The piston and liner combinations for all the builds were selected to provide a similar clearance fit and thus have a relatively constant crevice volume. The dimensions of the pistons and liners used for this test are shown in figure 5.1. A more comprehensive listing of the piston and liner dimensions are shown in appendix (1).

Piston Number	Dia "A1" (mm)	Dia "G" (mm)	Dia "F" (mm)	Liner Number	Effective Diameter (mm)	Oil Control Ring Tangential Load (N)
5	99.952	99.296	99.328	10	100.0495	94.8
14	99.949	99.298	99.329	8	100.0570	92.9
6	99.950	99.298	99.363	3	100.0615	96.0
10	99.950	99.300	99.363	12	100.0695	91.7

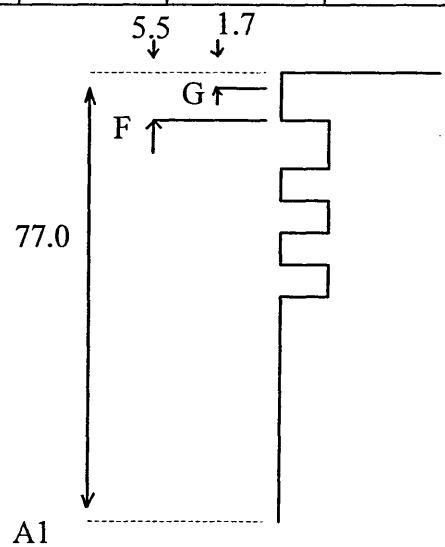

Figure 5.1 Measurement points for piston dimensions

5.4.1) Standard test results

The emission and operating conditions for each test point were noted, the accumulated data for each test point within acceptable operation limits averaged and the standard deviation calculated. The mass of gas phase hydrocarbons emitted for all the test points are shown in figures 5.2 a - e and the brake specific emissions are shown in figures 5.3 a - d. The deviation between cylinder readings increased as the gas temperature increased. This is partly through the heavy molecules of the fuel sample

pipes leading to the sample pre filter condensing onto the pipe wall, but the primary cause is the slight manufacturing differences in the injectors and the profile of the high pressure cam within the fuel injection pump. The evidence of fuel condensing onto the sample pipes is shown by the reading for the "ALL CYLS"; because the gas flow is split between four sample pipes the mass flow rate is not sufficient to transport the gases quickly enough to stop them condensing, thus the reading for this point is not a true average of separate cylinder values averaged. The values of CO_2 and NOx are shown in appendix(2). These graphs follow the trends stated in many publications and show the level of combustion efficiency and in cylinder gas temperature.

5.4.2) Particulate Emissions

The particulate emissions were collected and processed using the method stated in chapter 3. The effect of fuel velocity and equivalence ratio can be clearly observed. At low speeds and low fuelling rates the fuel can overmix with the air within the cylinder and avoid combustion. This unburnt fuel contributes to the soluble organic fraction and thus at these speeds and loads the soluble organic fraction forms the greater component of the particulate matter. Conversely when the fuelling rates are increasing there is less time for the fuel air to mix and the fuel within the spray cannot combine with any free oxygen and forms the soot particles. The results for the mass per hour are shown in figure 5.4 a-c and the brake specific results are shown in figure 5.5 a - c.

5.4.3) Gas chromatography

The direct injection of the fuel within the working cylinder of a diesel engine limits the time for the fuel and air to mix and, therefore, a road use diesel engine is never operated at stoichoimetric value for the fuel and air, thus there is always a significant quantity of available oxygen. The silica that forms the stationary phase of the gas

chromatograph column degrades quickly with any free oxygen and thus for this research the samples were analysed using the soluble organic fraction from the particulate matter.

Carbon chains exist in many forms in the alkanes (paraffins). They may be straight, branched or cyclic. The straight chained alkanes are termed normal or (n-alkanes) and they do not have any double or treble bonds and are deemed saturated. The family of n-alkanes forms a homologous series and thus the physical properties of the series vary in a regular way. The physical properties for the n-alkane series is shown in figure 5.6. The melting point for the n-alkane series shows the typical homologous sawtooth pattern where the n-alkane with an odd number of carbon atoms has a slightly lower melting point with respect to the even numbered molecules. On an exaggerated graph the even carbon molecules are on a separate higher curve than the odd carbon molecules. The reason for this behaviour is that the van der Waals forces among the molecules in the odd carbon molecule are weaker than that in the even carbon molecule.

Branched chain hydrocarbons tend to have lower melting points than the linear ones because the branching interferes with the regular packing in the crystal. When a branched molecule has a substantial symmetry its melting point is relatively higher because of the ease that the molecules fit together within the crystal. The effect of the change symmetry has upon melting point of various C_6H_{14} molecules are shown in table 5.3.

Name	Symmetry	Molecular formula	Melting point
neohexane	High	$C_2H_5C(CH_3)_3$	-76°C
hexane		$CH_3(CH_2)_4CH_3$	-95°C
2-methylpentane	Low	$CH_3CH_2CH(CH_3)_2$	-154°C

Table 5.3 Melting points of various C_6H_{14} molecules

The species of hydrocarbons present in the exhaust particulate include molecules that were not present in the fuel, these molecules being the product of pyrolysis, pyrosynthesis and other mechanisms. The number of different hydrocarbon compounds is dependent upon the fuel composition but other researchers have identified over 70 different compounds. The reference fuel used for this research comprised mainly n-alkanes, and this research concentrated on the survivability of these species. The properties of these species are shown in table 5.3 and the percentage composition in figure 5.7. Throughout testing tricosane was not present in quantities that could be measured accurately. Samples of the GC-MS plots are shown in figures 5.8 a - d. The molecular weight of the hydrocarbon species decreases as load increases. This is because at idle the measured species accounts for 80% of the total SOF but when the speed and load have been increased to 2500 RPM 7.49 Bar (BMEP) the contribution of the measured species to the total is only 30%. The survival rates of the n-alkane species is also comparable to the measured quantity of the significant fuel species present in the SOF (fig 5.4). The composition of the SOF at idle is primarily n-alkane based (81%). The fuel is composed of 86.1% of these n-alkane species, and assuming that there is little or no separation of n-alkane species from the lubricating oil this indicates that at idle the fuel is contributing 94% of the SOF. It is well documented that at low injection rates fuel can easily overmix with the air and not allow any combustion. Also the temperature of the gases during the expansion and exhaust stroke is insufficient to continue the oxidation process. Another significant contributor to the SOF is the injector nozzle sac volume. This contributes a constant quantity of incorrectly mixed fuel throughout the speed load range. The measured values for the n-alkanes species present in the SOF are shown in figure 5.9 a - e for g/hr and in figure 5.10 a -d for g/kW.hr. The percentage survival for each of the hydrocarbon species injected for this test is shown in figure 5.11.

The improvement in combustion efficiency with increasing fuelling rates is shown by the quantity of the fuel species being present in the SOF. At 2500RPM 7.49 BMEP bar the fuel species only account for 32% of the SOF, the remainder being composed of fuel derived products of incomplete combustion and pyrolysis, with a significant contribution from the lubricating oil which will not separate into individual species.

Name	Chemical Formula	Boiling Point	Molar Mass
Dodecane	$C_{12}H_{26}$	216	170.34
Tetradecane	$C_{14}H_{30}$	253	198.40
Hexadecane	$C_{16}H_{34}$	290	226.45
Heptadecane	$C_{17}H_{36}$	302	240.48
Octadecane	$C_{18}H_{38}$	317	254.50
Nonadecane	$C_{19}H_{40}$	330	268.53
Eicosane	$C_{20}H_{42}$	340	282.56
Heneicosane	$C_{21}H_{44}$	355	294.57
Docosane	$C_{22}H_{46}$	369	310.61
Tricosane	$C_{23}H_{48}$	380	324.64
Tetracosane	$C_{24}H_{50}$	391	338.66

Table 5.4

5.5) Low Tangential Load Oil Control Ring Test

The effect oil film thickness has upon petrol engine emissions is well documented and the mechanisms that change the unburnt hydrocarbon emissions understood. Conversely the only research on diesel engines that has been undertaken is based on oil consumption and not on any effect of the fuel and its combustion.

The pistons and liners used for this test were from the same batch as the reference engine's. The only modification was to remove some material from the oil control rings expander spring reducing the force that forces the ring onto the liner wall. The standard oil control ring produces a tangential load of approximately 3.1 N without

the spring and 93 (N) with the spring. The modified spring produced a load of 75% of the standard. The tangential load was measured by compressing the complete oil control ring to a diameter of 100 mm. The piston and liner dimensions for this engine build are as follows, please refer to figure 5.1 on page 70.

Piston Number	Dia "A1" (mm)	Dia "G" (mm)	Dia "F" (mm)	Liner Number	Effective Diameter (mm)	Oil Control Ring Tangential Load (N)
11	99.95	99.298	99.361	1	100.0275	57.5
12	99.949	99.294	99.357	11	100.0405	60.5
13	99.949	99.297	99.361	6	100.0565	48.6
9	99.95	99.299	99.362	9	100.0665	64.2

5.5.1) Low Tangential Load Hydrocarbon Emissions

The measured values for the unburnt hydrocarbons are shown in figure 5.12 a - e for g/hr and in figure 5.13 a -d for g/kW.hr. The differences between this engine build and the standard build are shown in figure 5.14

The gas phase hydrocarbons showed significant increases for all test points. The graphs show that the greatest increase occurs at the highest speed and load. The effect of the crevice volume (if cylinder 3 is disregarded) is that the change is greater for the cylinders with the largest cold crevice volume, i.e. the cylinder with the largest change has the largest crevice volume when measured cold. Cylinder 3 for all tests of each build showed higher levels of gas phase hydrocarbons than the other cylinders, this was attributed to the injector not allowing correct fuel vaporisation. The increase with emissions also increases with load until the 1600 RPM 8.59 Bar (BMEP) test point. One possible explanation for the reduction after this point is that the higher combustion temperatures allow combustion to occur nearer the cylinder boundaries and thus the fuel or oil at these boundaries can be burnt. The larger increase at the 2500 RPM 7.49 Bar (BMEP) point shows that the engine speed allows the larger oil

film created by the increase in hydrodynamic force and any fuel present within it to avoid combustion. The highest value for unburnt hydrocarbons is from the point before the turbocharger, which remained constant for all tests and showed that the fuel is still being broken down by pyrolysis. The heated sample lines temperature will allow any large hydrocarbon molecules to condense out, if the fuel and oil are still being broken down into smaller molecules and thus the boiling point of these molecules will be lower. These lighter molecules can then be transported through the heated sample line to the analyser and detected. Further actions of heat upon the hydrocarbons as they pass through the turbocharger and exhaust pipe reduces them further and some of the molecules are oxidised fully and thus the readings for 1 metre are lower than the pre turbo.

5.5.2) Particulate Emissions

The results for the mass per hour are shown in figure 5.4 b and the brake specific results are shown in figure 5.5 b.

The reduction of friction through the lower tangential load of the oil control ring could be the main contributing factor to the significantly lower quantity of particulate matter emitted at idle. The composition of the particulate matter for this test showed that soluble organic fraction contributed a greater quantity than the other builds, this contribution being more significant as the engine power increased above 1600 RPM 2.86 Bar (BMEP). The greatest increase was at 1600 RPM 8.59 Bar (BMEP) where the SOF contributed more to the total matter than the soot. The total particulate weight for this speed and load only increased by over 10% when compared to the standard while the SOF percentage contribution increased from 32% to 52%. The percentage contribution by the SOF to the particulate for this engine build was higher than the standard at all test points except idle.

5.5.3) Gas chromatography

The measured values for the n-alkanes species present in the SOF are shown in figure 5.16 a - e for g/hr and in figure 5.17 a -d for g/kW.hr.

The chromatograms for this build showed that the species that contributed the most to the soluble organic fraction increased in molecular weight from that of the standard engine. The standard engine produced SOF that had nonadecane as the most abundant species where as the low tangential engine produced eicosane as the most abundant. The quantities of dodecane and tetradecane present in the SOF for this build were significantly lower and the values were such that quantification of any reasonable level were deemed too inaccurate to be presented. The effect of increasing the combustion temperature removed all the lighter species from the standard engine SOF. The low tangential load engine produced an increasing quantity of hexadecane as the engine output increased above 1600 RPM 5.72 Bar (BMEP). Figure 5.15 shows the survivability of each species of n-alkanes for this test.

5.6) High Top Ring

A set of pistons with a higher top ring was manufactured to investigate the effect of the first land on emissions. The pistons for the Perkins Phasor uses an Alfin insert to stop the top ring from enlarging the top ring groove. The harder material is used because there is insufficient lubricating oil to absorb the ring's kinetic energy when the ring moves. The high top ring pistons were manufactured by placing this Alfin insert into the piston mould upside down. This had the effect of moving the top ring up 5 mm producing a top land height of 4.5 mm. The second and oil control ring's position remained the same as the standard pistons. The value for the second top land measurement point "F" is not shown because it is in the middle of the top ring

groove for this piston type. The movement of the top ring has caused a reduction of top land crevice volume of approximately 29% for all cylinders but the second land crevice volume increased to 150% of the original. The larger reduction of the top land clearance when compared to the increase of the second land is that the liners were selected to be a closer fit for this build to reduce crevice volumes even further.
The piston and liner dimensions for this engine build are as follows, please refer to figure 5.1.

Piston Number	Dia "A1" (mm)	Dia "G" (mm)	Dia "F" (mm)	Liner Number	Effective Diameter (mm)	Oil Control Ring Tangential Load (N)
1h	99.952	99.292	N/A	2	100.0400	93.4
6h	99.949	99.290	N/A	7	100.0515	96.4
5h	99.950	99.290	N/A	4	100.0555	93.3
2h	99.951	99.292	N/A	5	100.0375	91.6

5.6.4) High Top Ring Hydrocarbon Emissions

The mass of gas phase hydrocarbons emitted for all the test points are shown in figures 5.18 a - e and the brake specific emissions are shown in figures 5.19 a - d. The change in quantity of uHC emitted between this engine build and the standard is shown in figures 5.20 a - e.

The gas phase hydrocarbon emissions for 5 successful and repeatable tests were obtained. The hydrocarbon readings for all the tests and most of the sample points showed that there was a slight increase. The measured levels of unburnt hydrocarbons for this build do not differ from the standard by a sufficient quantity to determine if there is any change. The increase of the measured hydrocarbons could be attributed to the higher levels of the lighter species being present in the gas stream and thus are more easily transported to the analyser by the heated sample system.

5.6.5) Particulate Emissions

The results for the mass per hour are shown in figure 5.4 and the brake specific results are shown in figure 5.5. The particulate emissions for this build showed that there was a slight increase in the SOF at the lower power test points and 1600 RPM 8.59 Bar (BMEP). The only test point that showed a conclusive reduction was at 1600 RPM 5.72 Bar (BMEP). The weight of the total collected particulate matter showed that there was little change and the changes are within the margin of error for the measurement and calculation of the total weight and thus could indicate no change.

5.6.6) Gas chromatography

The low power chromatograms showed that the species with the highest contribution to the SOF was the same as the standard. The total weight of the measured species for the idle and 1600 RPM 2.86 Bar (BMEP) test point was lower for this build when compared to the standard. The measured values for the n-alkanes species present in the SOF are shown in figure 5.21 a - e for g/hr and in figure 5.22 a -d for g/kW.hr. The percentage survival for each of the hydrocarbon species injected for this test is shown in figure 5.23.

uHC Emissions Idle

a

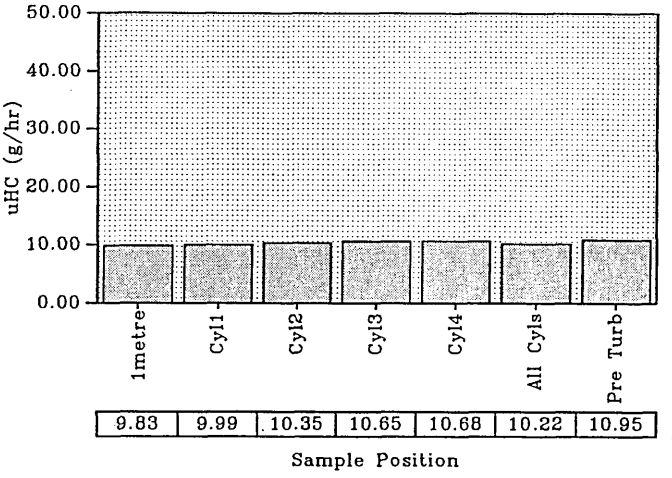

Standard Build
uHC Emissions 1600 RPM 2.86 Bar (BMEP)

b

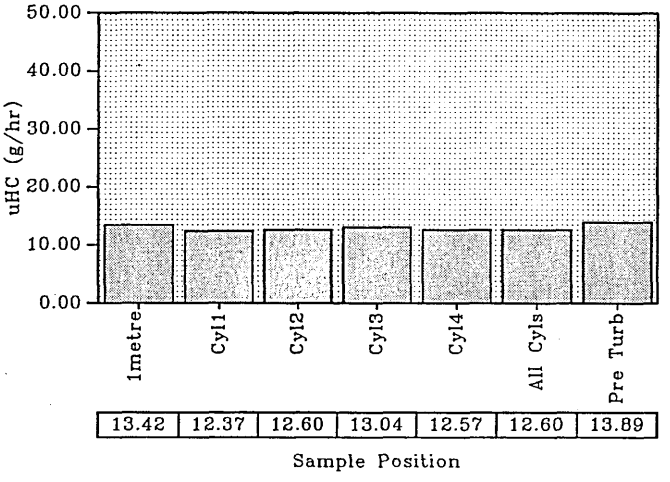

Standard Build
uHC Emissions 1600 RPM 5.72 Bar (BMEP)

c

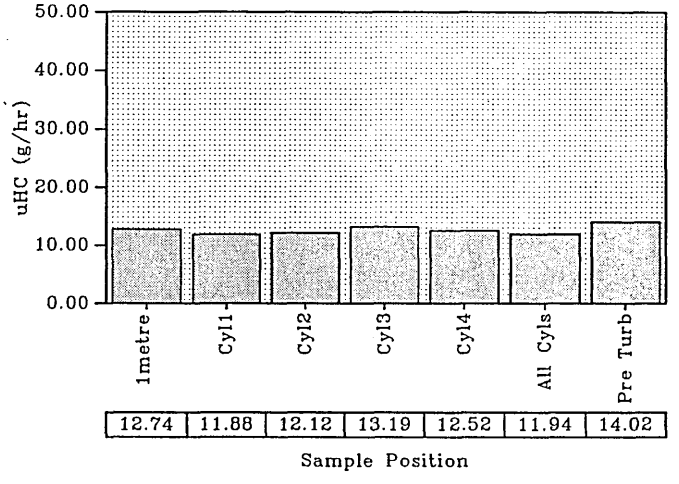

Figure 5.2 Standard build hydrocarbon emissions (g/hr)

d

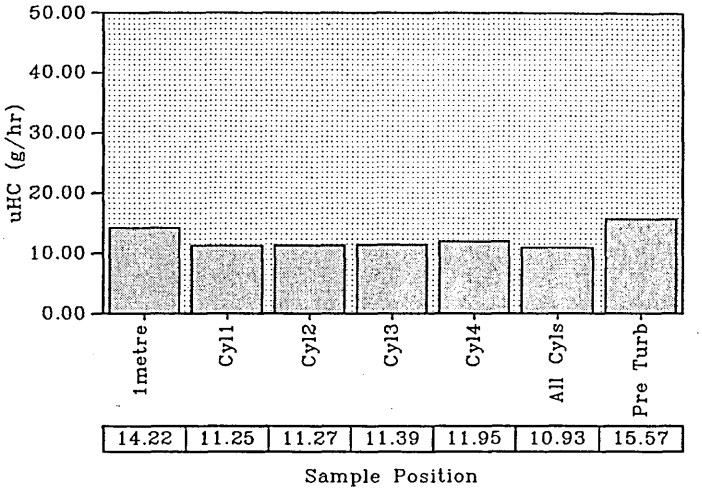

e

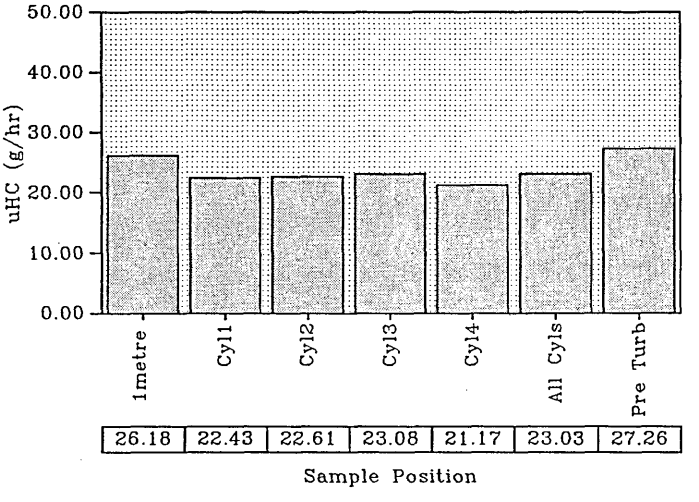

Figure 5.2 Standard build hydrocarbon emissions (g/hr)

a

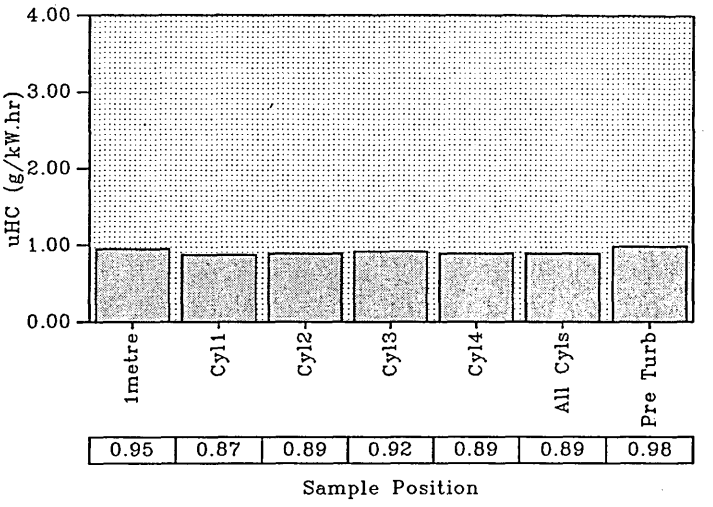

b

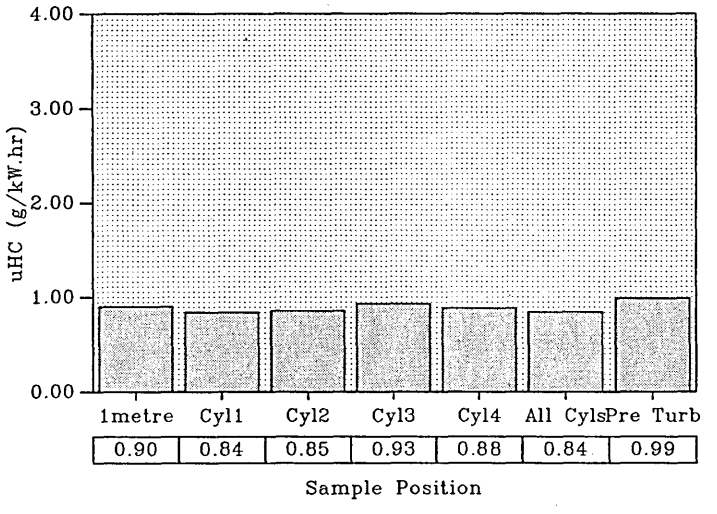

Figure 5.3 Standard build hydrocarbon emissions (g/kW.hr)

c

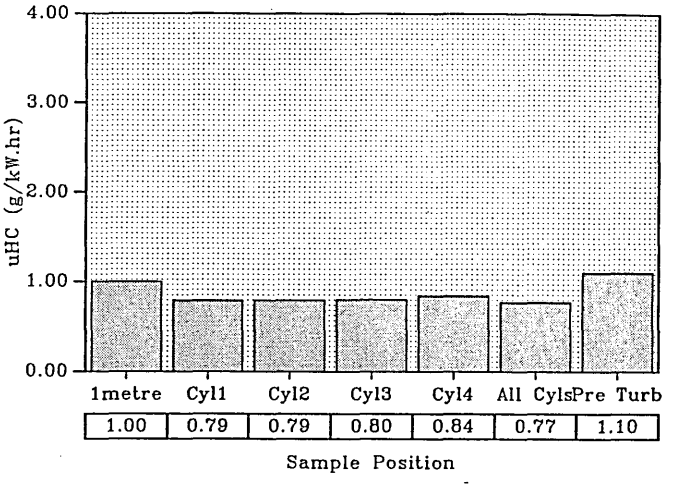

d

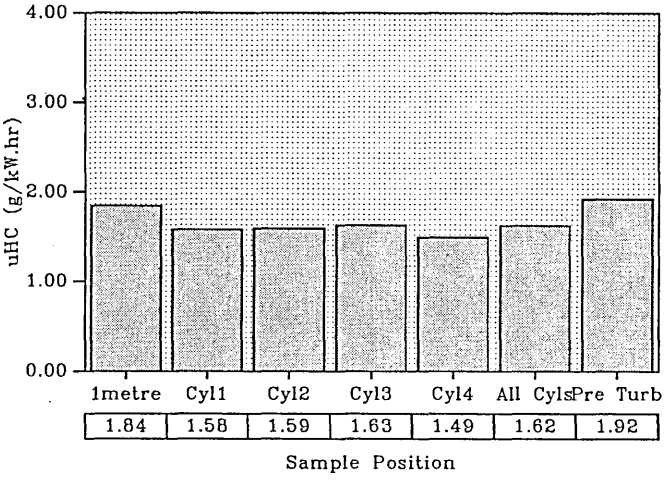

Figure 5.3 Standard build hydrocarbon emissions (g/kW.hr)

Particulate Emissions

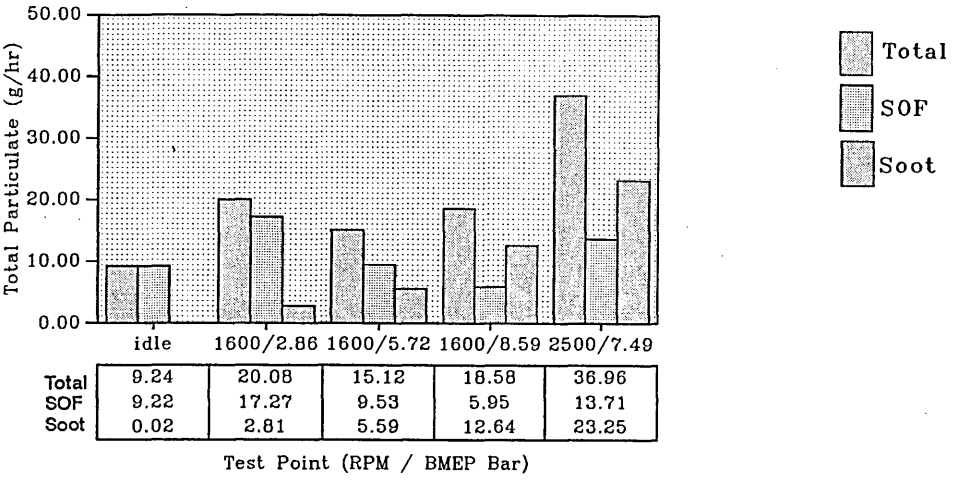

	idle	1600/2.86	1600/5.72	1600/8.59	2500/7.49
Total	9.24	20.08	15.12	18.58	36.96
SOF	9.22	17.27	9.53	5.95	13.71
Soot	0.02	2.81	5.59	12.64	23.25

Test Point (RPM / BMEP Bar)

Low Tan Load Build
Particulate Emissions

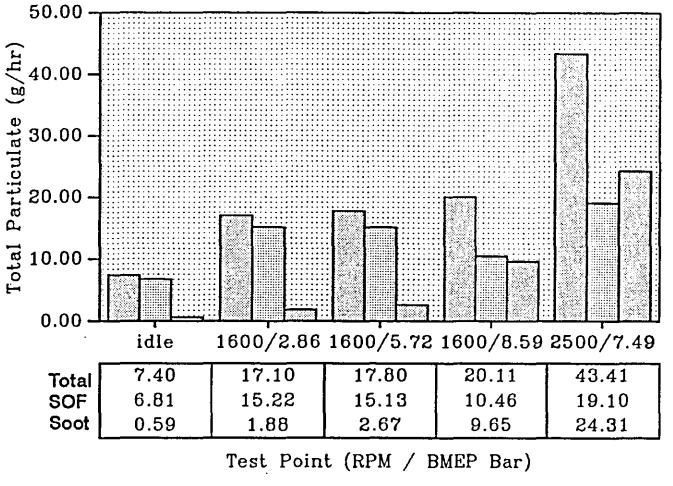

	idle	1600/2.86	1600/5.72	1600/8.59	2500/7.49
Total	7.40	17.10	17.80	20.11	43.41
SOF	6.81	15.22	15.13	10.46	19.10
Soot	0.59	1.88	2.67	9.65	24.31

Test Point (RPM / BMEP Bar)

High Top Ring Build
Particulate Emissions

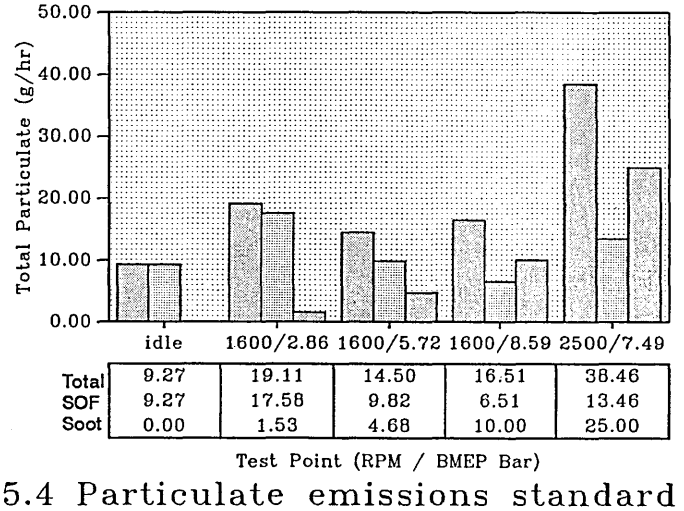

	idle	1600/2.86	1600/5.72	1600/8.59	2500/7.49
Total	9.27	19.11	14.50	16.51	38.46
SOF	9.27	17.58	9.82	6.51	13.46
Soot	0.00	1.53	4.68	10.00	25.00

Test Point (RPM / BMEP Bar)

Figure 5.4 Particulate emissions standard build (g/hr)

Particulate Emissions

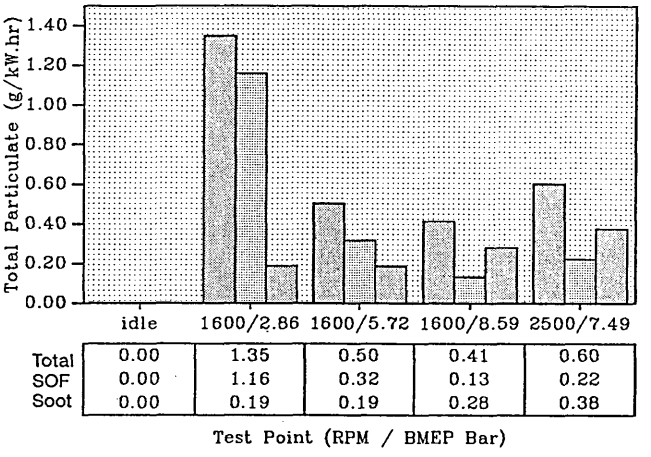

Total	0.00	1.35	0.50	0.41	0.60
SOF	0.00	1.16	0.32	0.13	0.22
Soot	0.00	0.19	0.19	0.28	0.38

Test Point (RPM / BMEP Bar)

Low Tan Load Build
Particulate Emissions

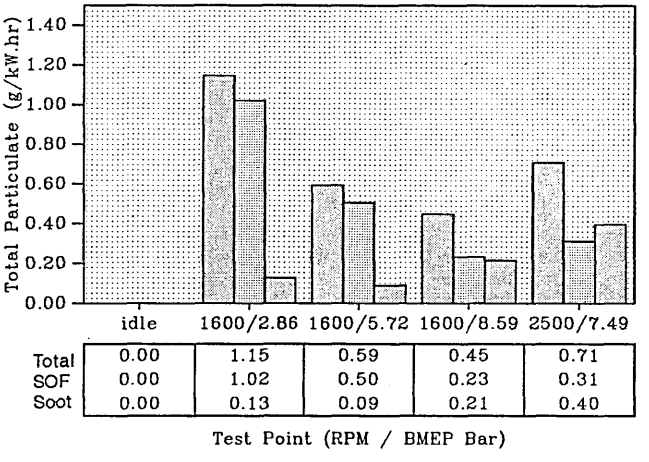

Total	0.00	1.15	0.59	0.45	0.71
SOF	0.00	1.02	0.50	0.23	0.31
Soot	0.00	0.13	0.09	0.21	0.40

Test Point (RPM / BMEP Bar)

High Top Ring Build
Particulate Emissions

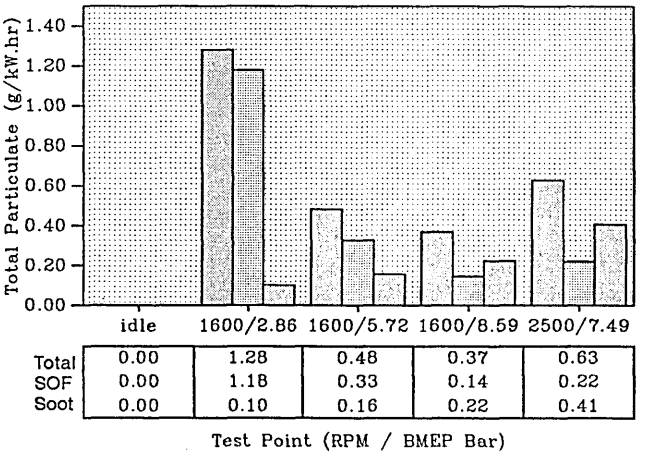

Total	0.00	1.28	0.48	0.37	0.63
SOF	0.00	1.18	0.33	0.14	0.22
Soot	0.00	0.10	0.16	0.22	0.41

Test Point (RPM / BMEP Bar)

Figure 5.5 Particulate emissions standard build (g/kW.hr)

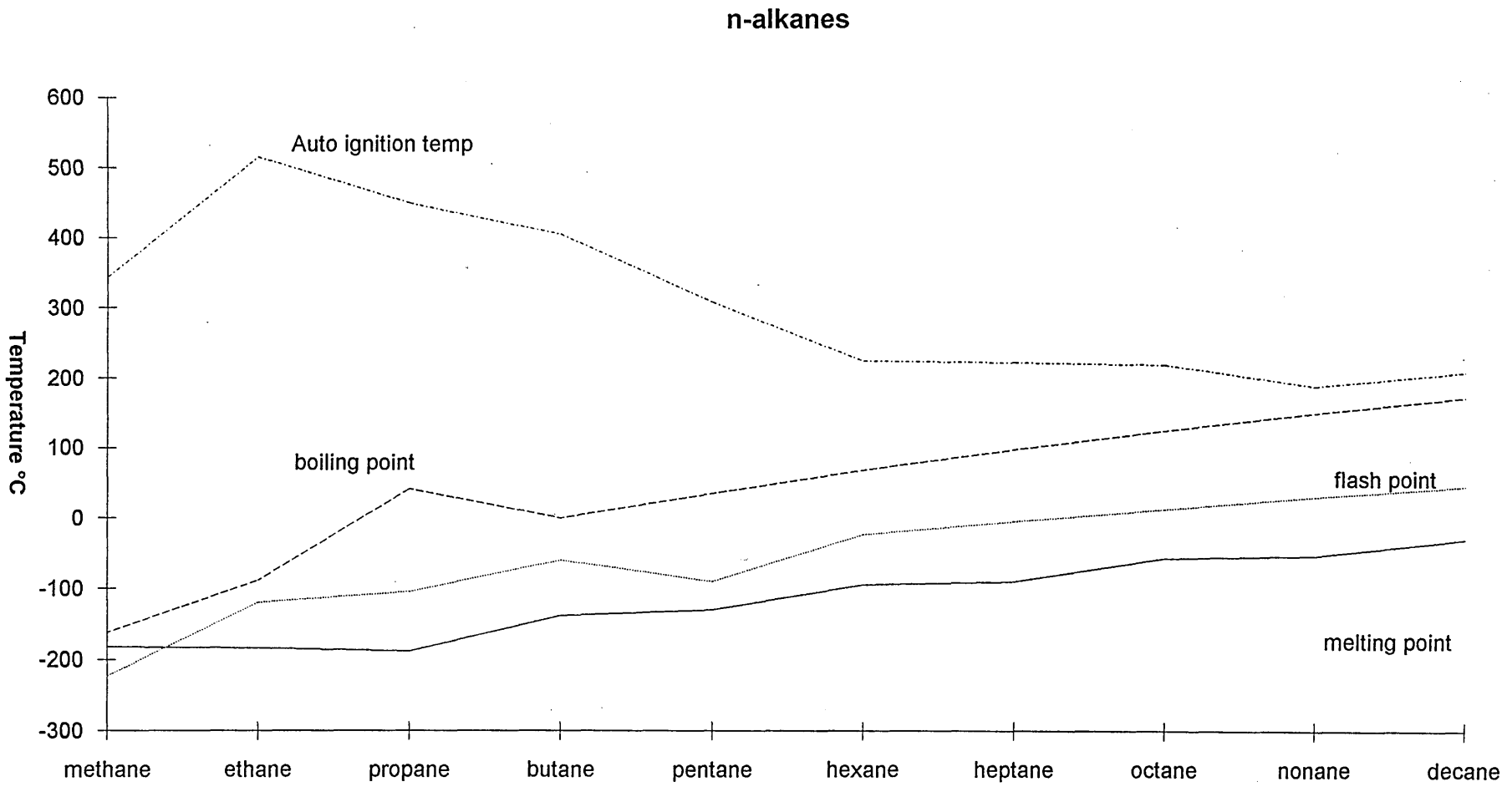

Figure 5.6 Properties of n-alkanes

Fuel n-alkane composition (%)

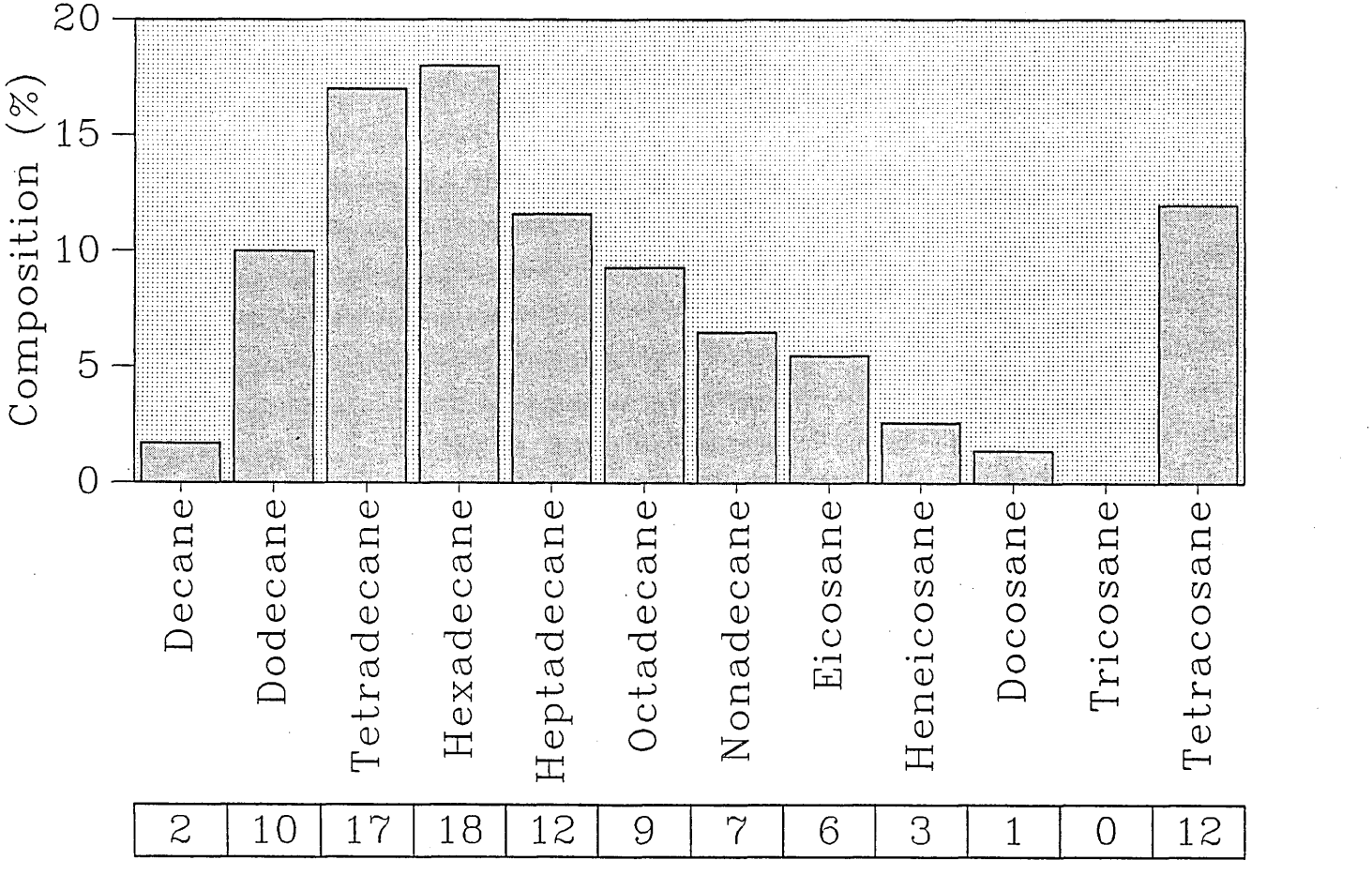

Figure 5.7 Percentage composition of fuel n-alkanes

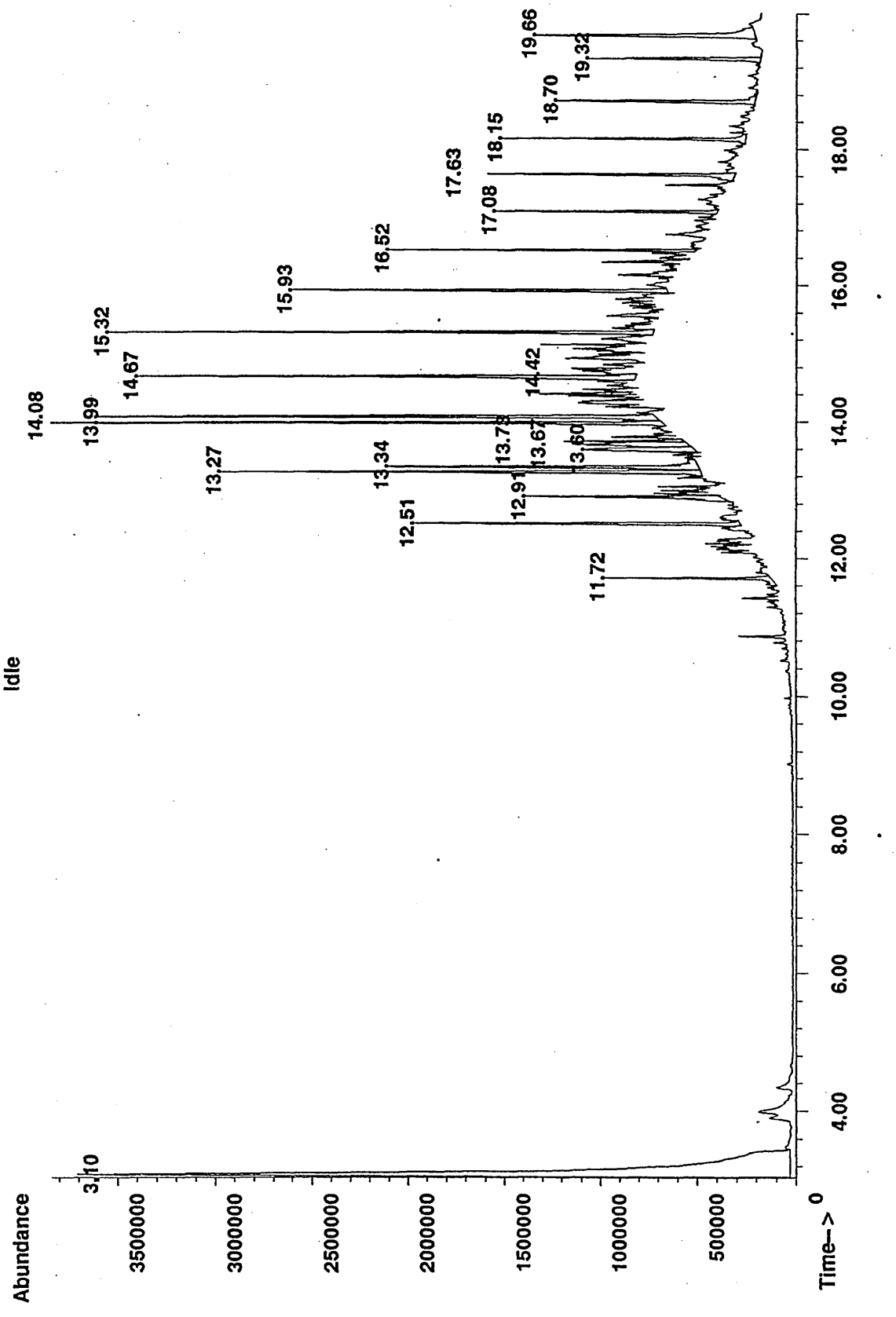

Figure 5.8 Sample plots from GC-MS

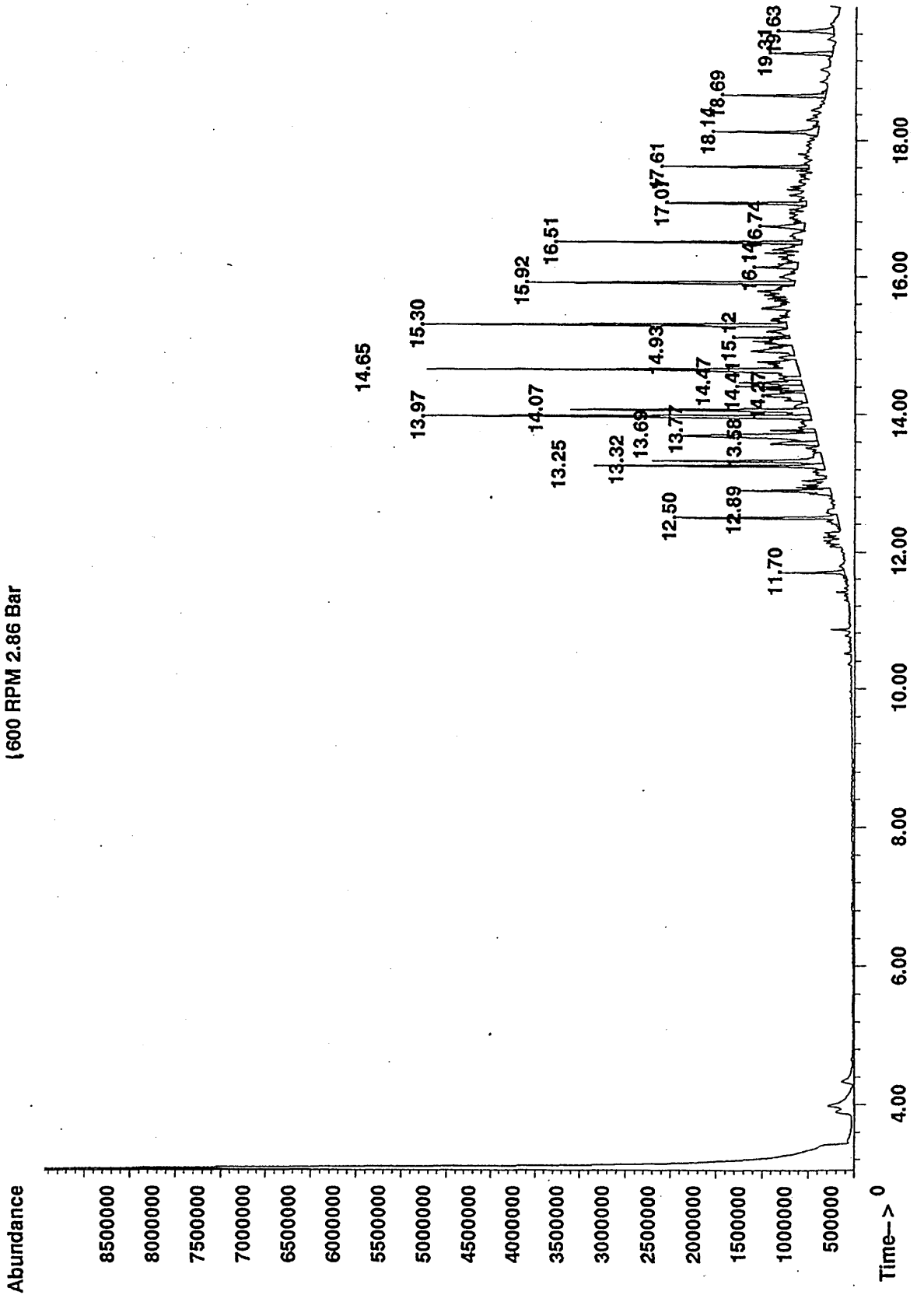

Figure 5.8 Sample plots from GC-MS

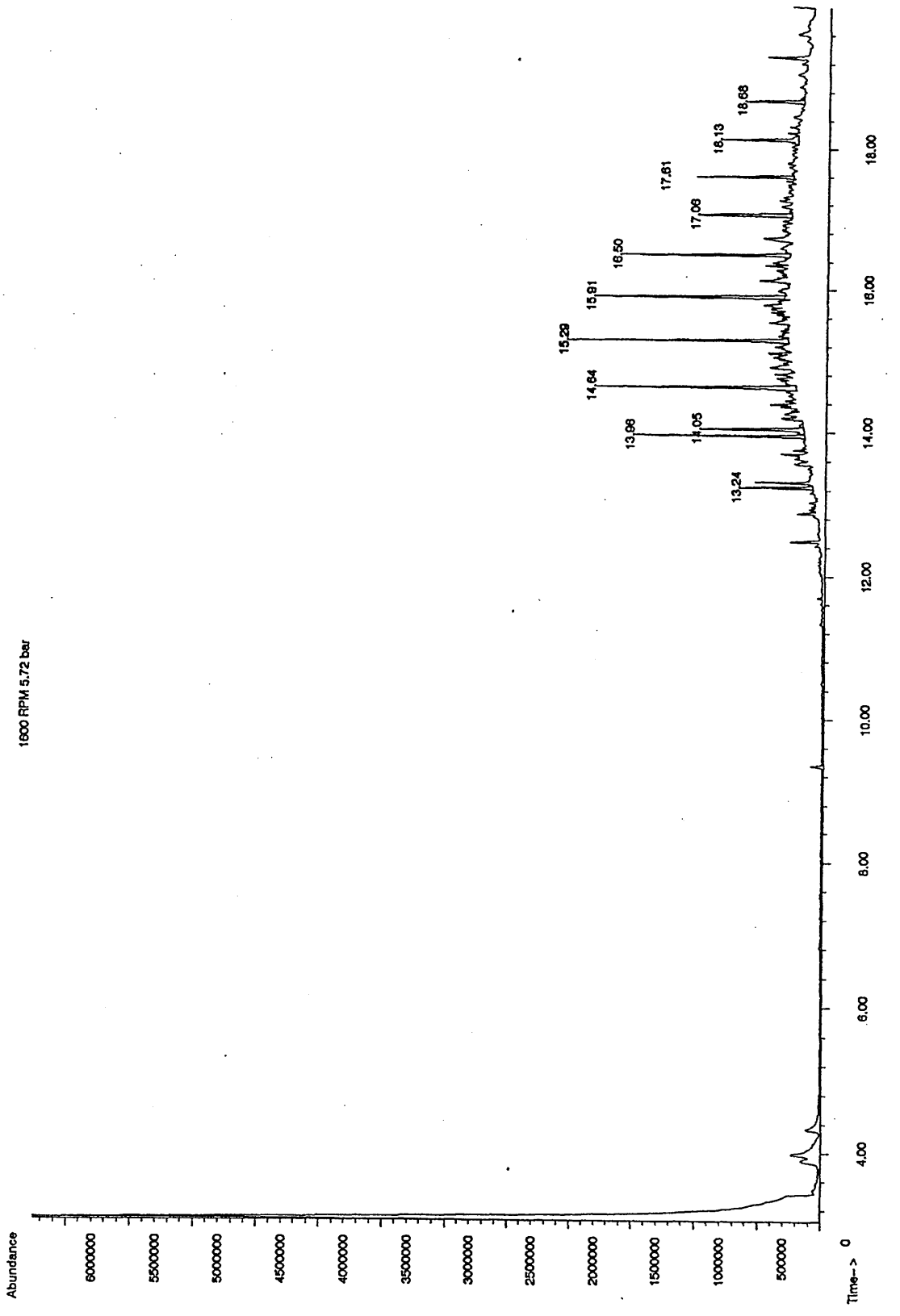

Figure 5.8 Sample plots from GC-MS

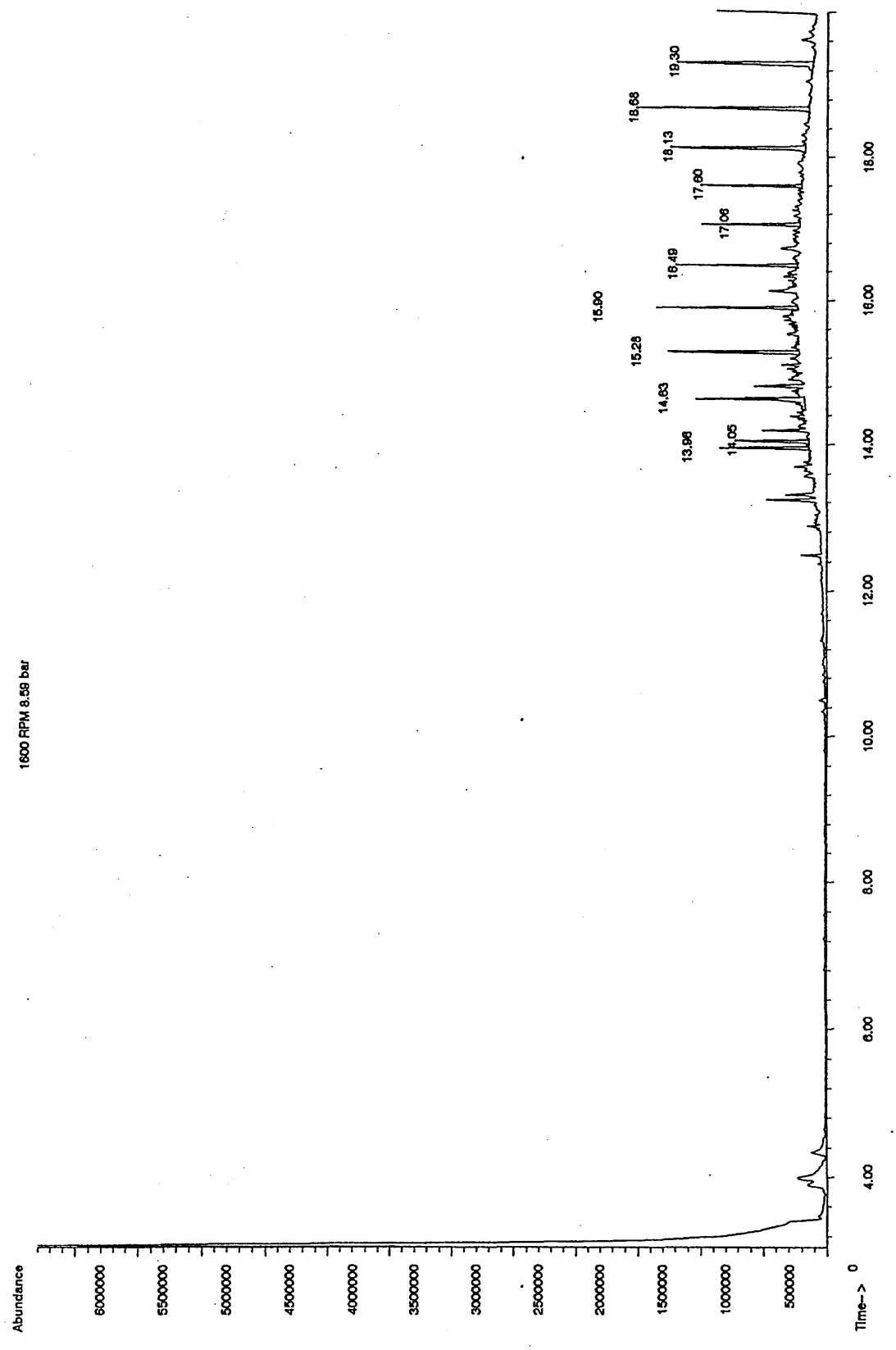

Figure 5.8 Sample plots from GC-MS

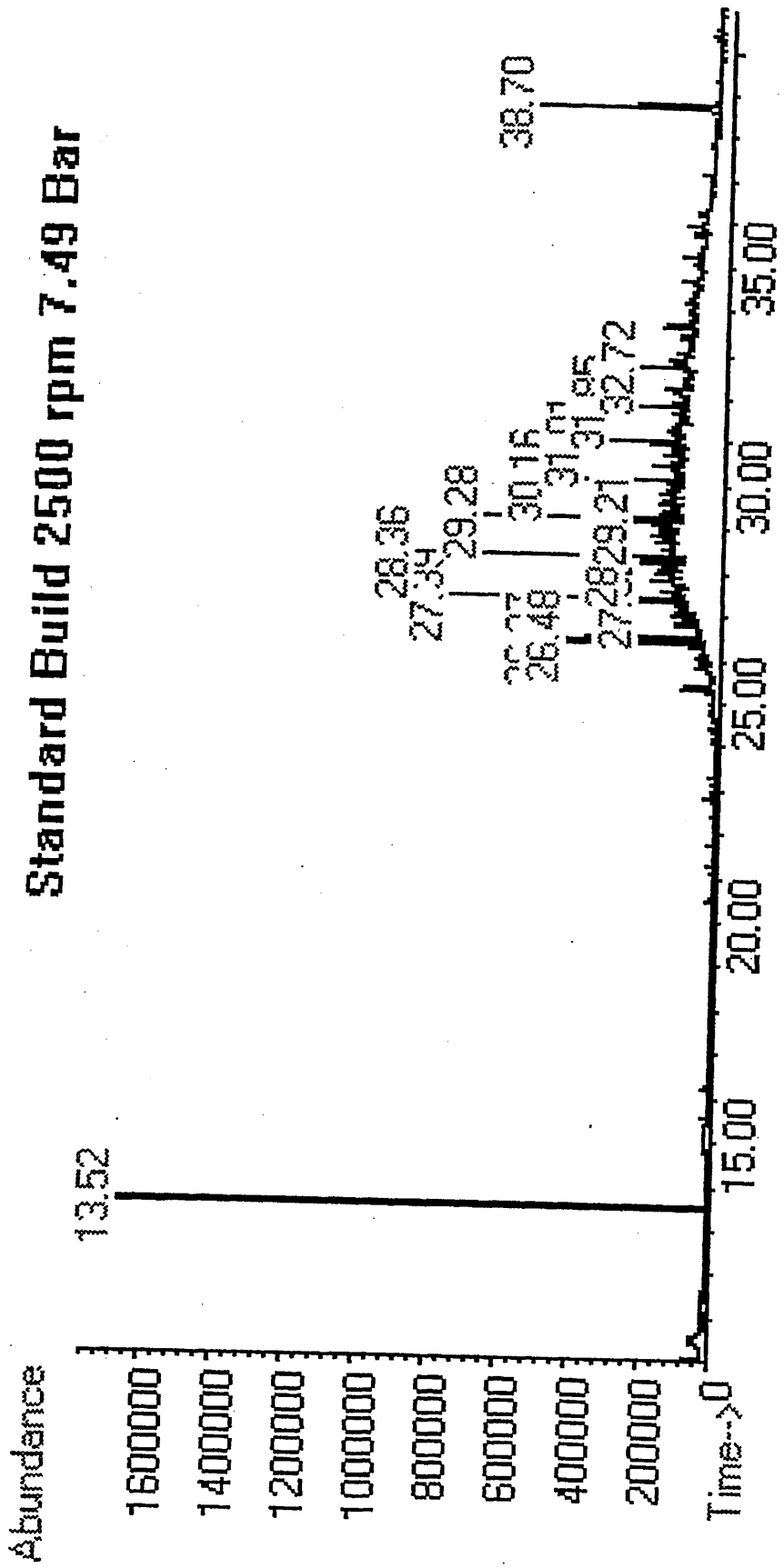

Figure 5.8 Sample plots from GC-MS

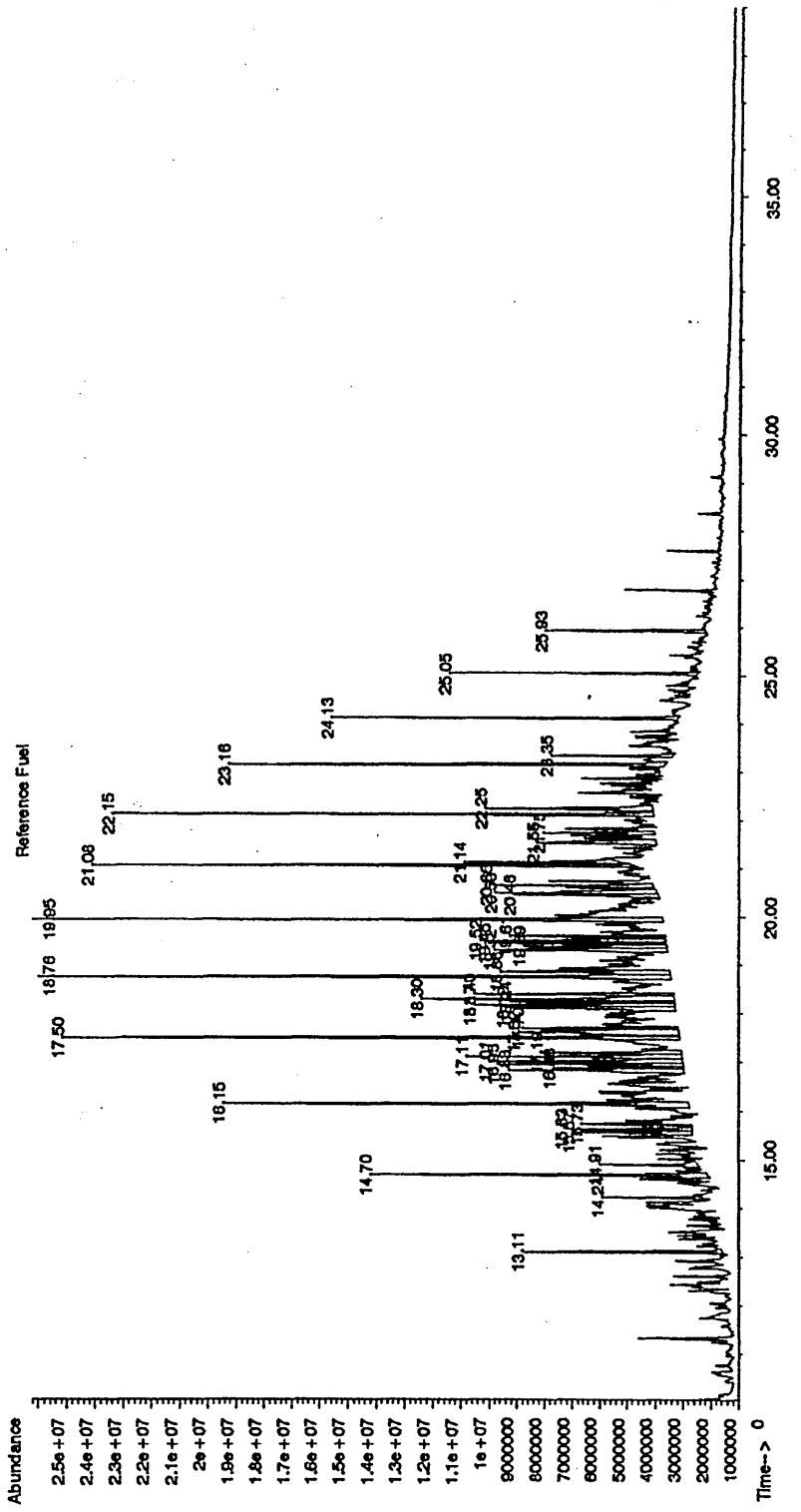

Figure 5.8 Sample plots from GC-MS

SOF alkane species Idle

a

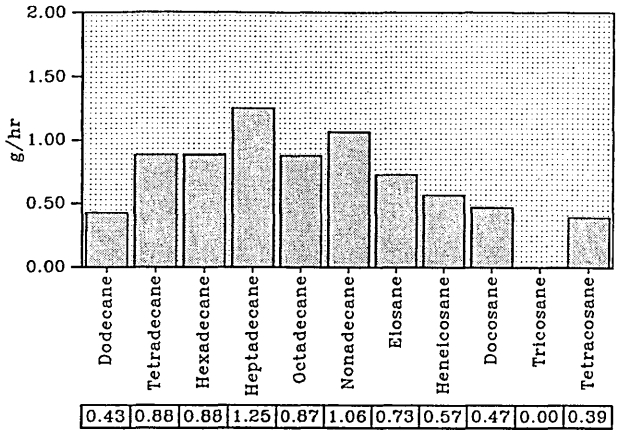

Standard build
SOF alkane species 1600 RPM 2.86 Bar(BMEP)

b

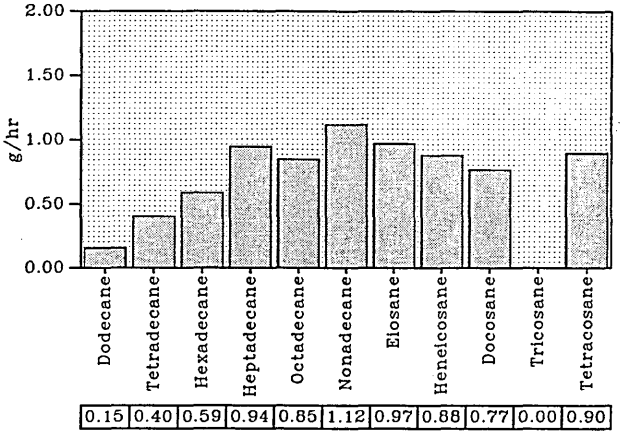

Standard build
SOF alkane species 1600 RPM 5.72 Bar (BMEP)

c

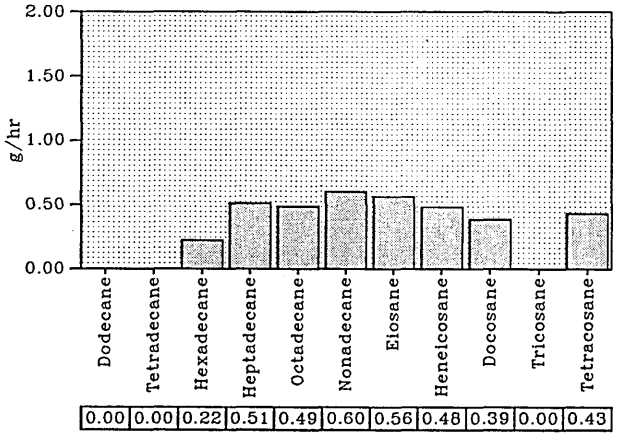

Figure 5.9 Standard build n-alkane species from SOF (g/hr)

d

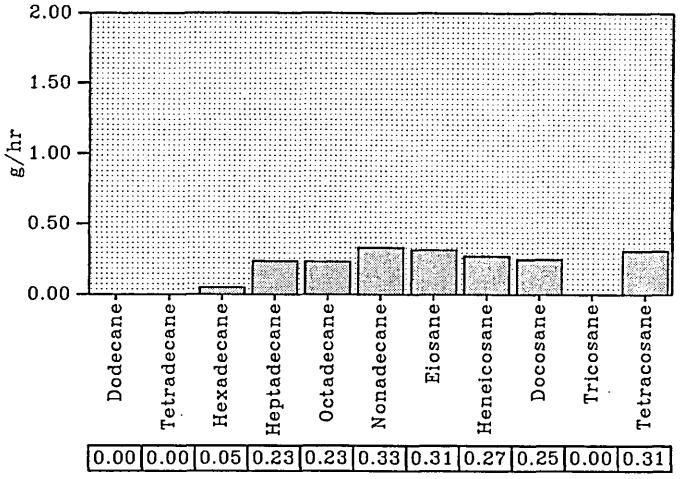

e

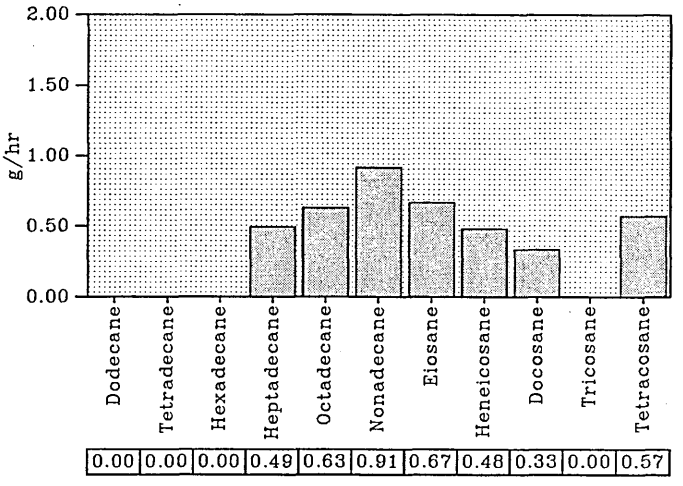

Figure 5.9 Standard build n-alkane species from SOF(g/hr)

Standard Build
SOF alkane species 1600 RPM 2.86 Bar (BMEP)

a

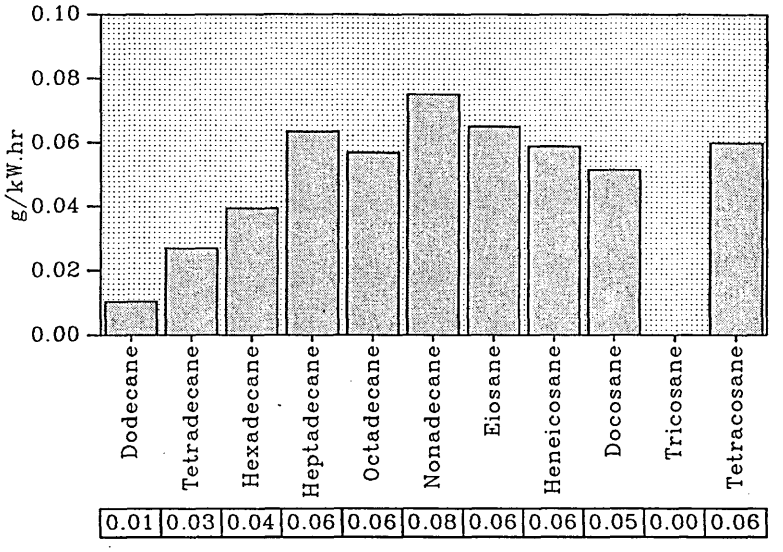

Standard Build
SOF alkane species 1600 RPM 5.72 Bar (BMEP)

b

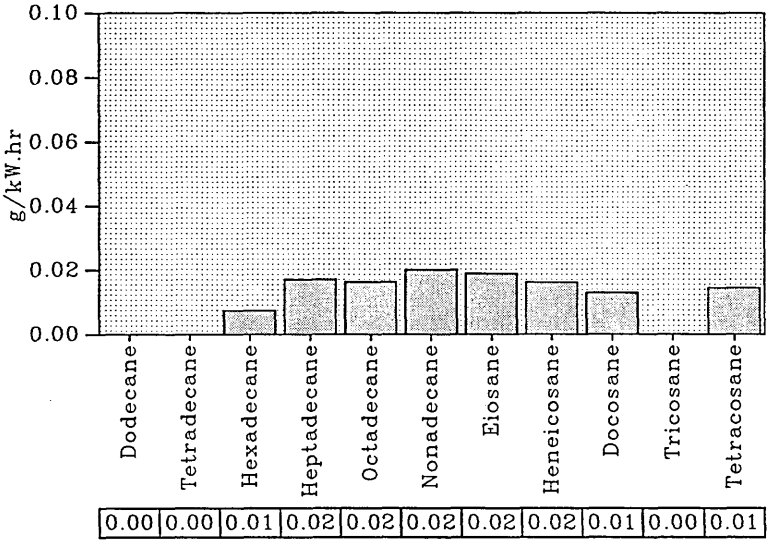

Figure 5.10 Standard build n-alkane species from SOF(g/kW.hr)

SOF alkane species 1600 RPM 8.59 Bar (BMEP)

c

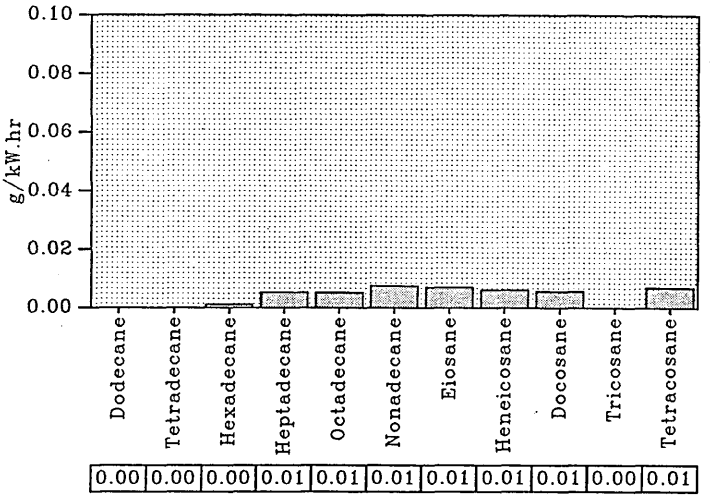

Standard Build

SOF alkane species 2500 RPM 7.49 Bar (BMEP)

d

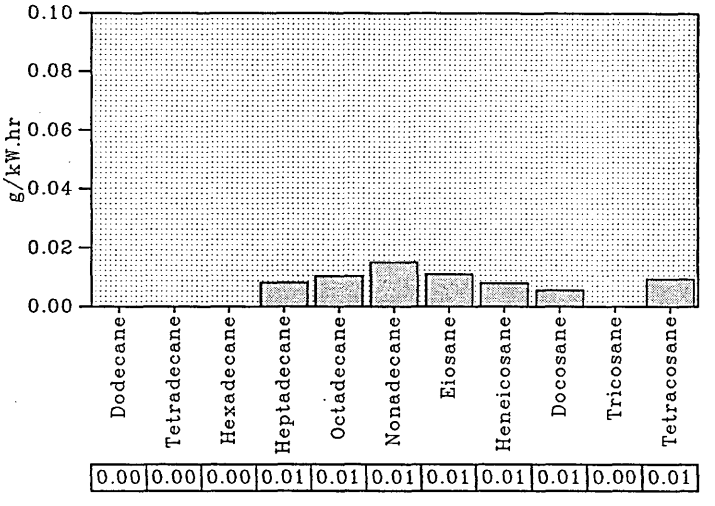

Figure 5.10 Standard build n-alkane species from SOF(g/kW.hr)

% Survival of injected alkanes
Standard Build

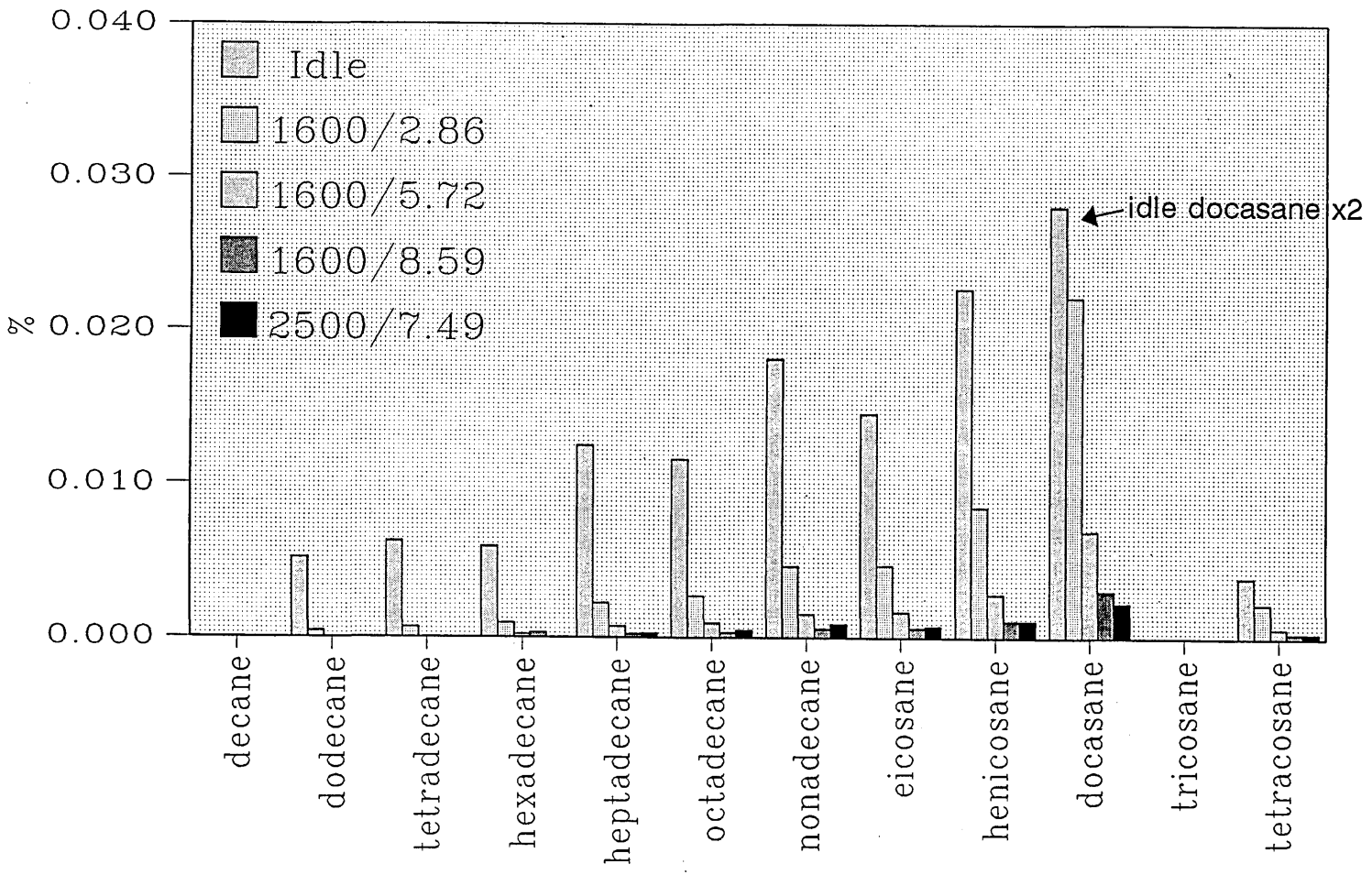

Figure 5.11 Survival of species standard build

uHC Emissions Idle

a

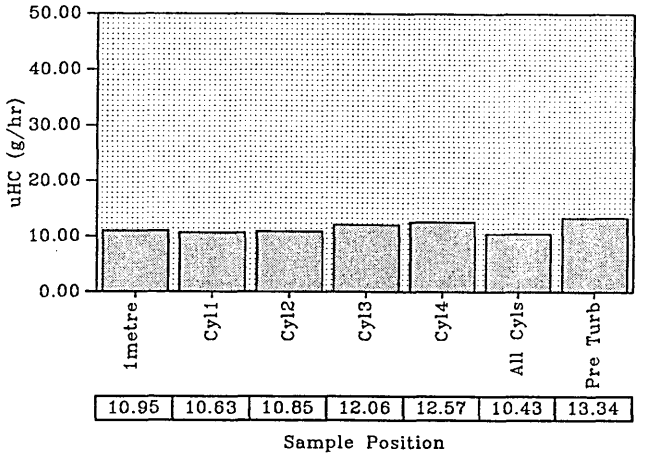

Low Tan Load
uHC Emissions 1600 RPM 2.86 Bar (BMEP)

b

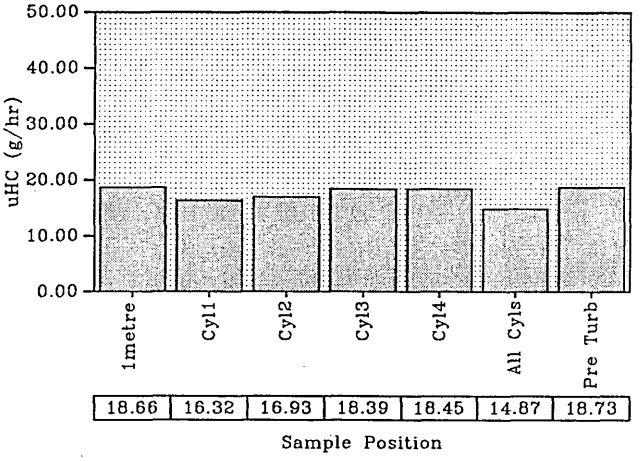

Low Tan Load
uHC Emissions 1600 RPM 5.72 Bar (BMEP)

c

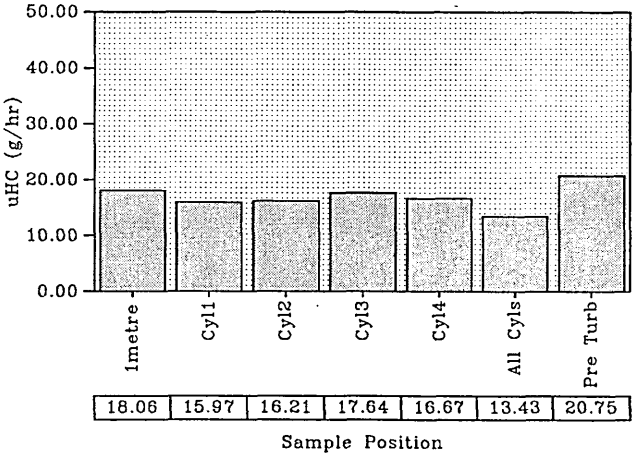

Figure 5.12 Low tangential oil ring build gas phase hydrocarbons emitted

uHC Emissions 1600 RPM 8.59 Bar (BMEP)

d

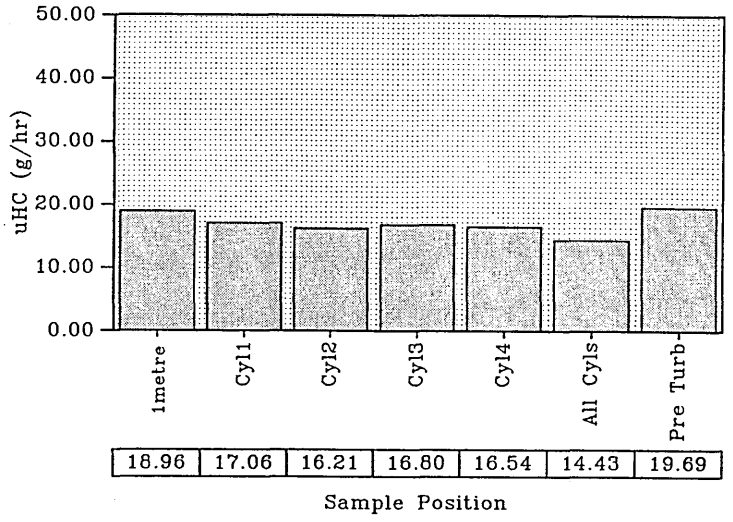

Low Tan Load

uHC Emissions 2500 RPM 7.49 Bar (BMEP)

e

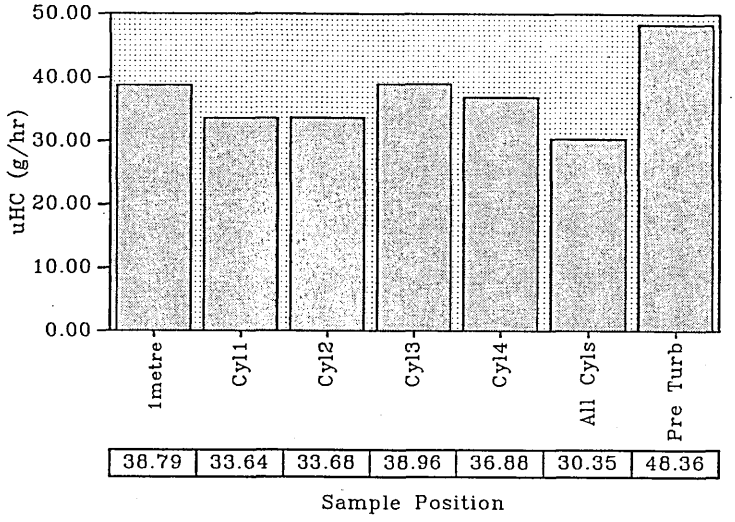

Figure 5.12 Low tangential oil ring build gas phase hydrocarbons emitted

uHC Emissions 1600 RPM 2.86 Bar (BMEP)

a

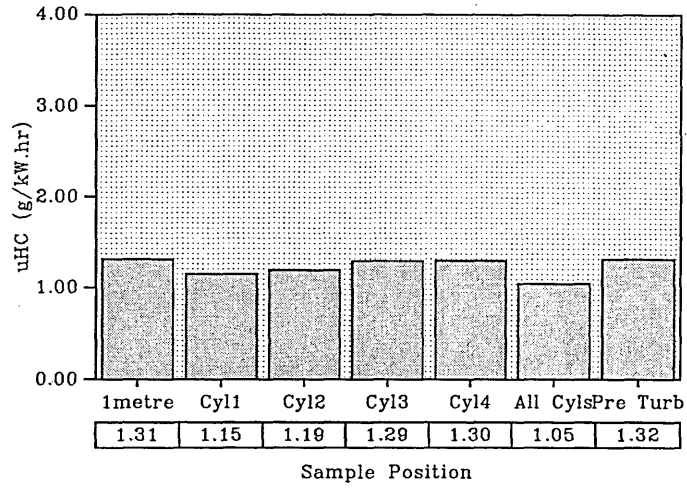

Low Tan Load

uHC Emissions 1600 RPM 5.72 Bar (BMEP)

b

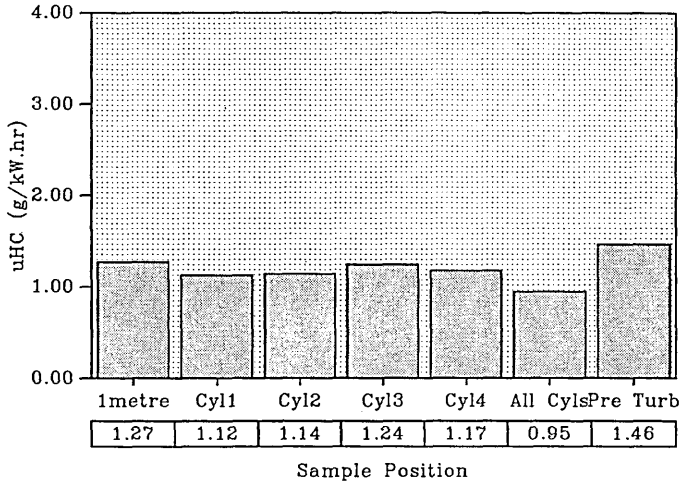

Figure 5.13 Low tangential oil ring build gas phase hydrocarbons emitted(g/kW.hr)

uHC Emissions 1600 RPM 8.59 Bar (BMEP)

c

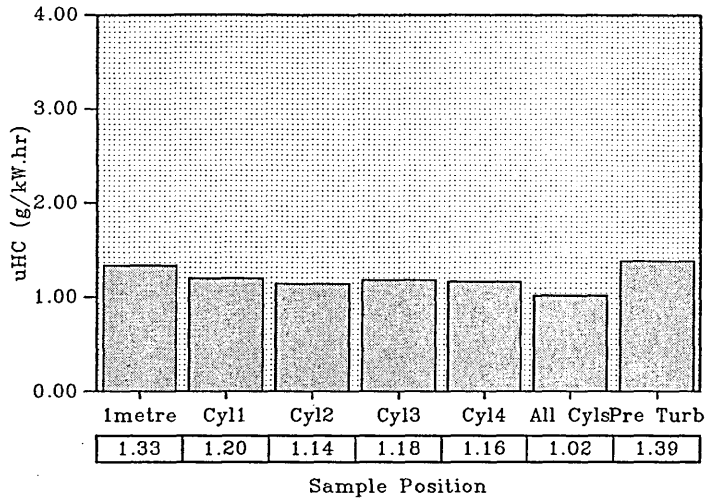

Low Tan Load

uHC Emissions 2500 RPM 7.49 Bar (BMEP)

d

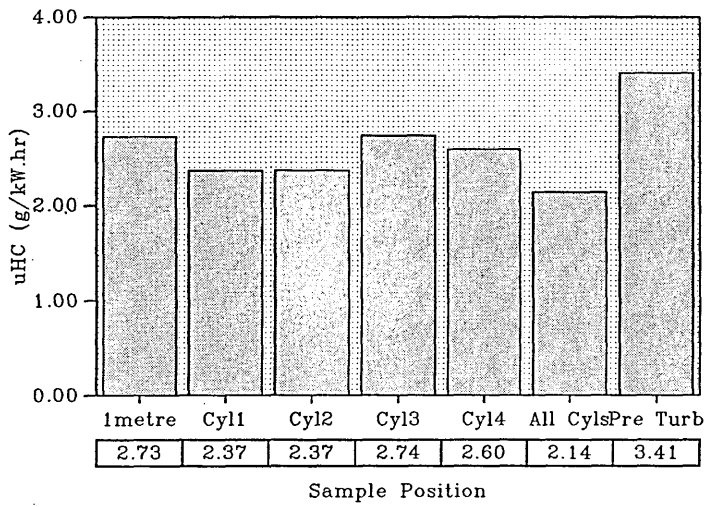

Figure 5.13 Low tangential oil ring build gas phase hydrocarbons emitted(g/kW.hr)

a

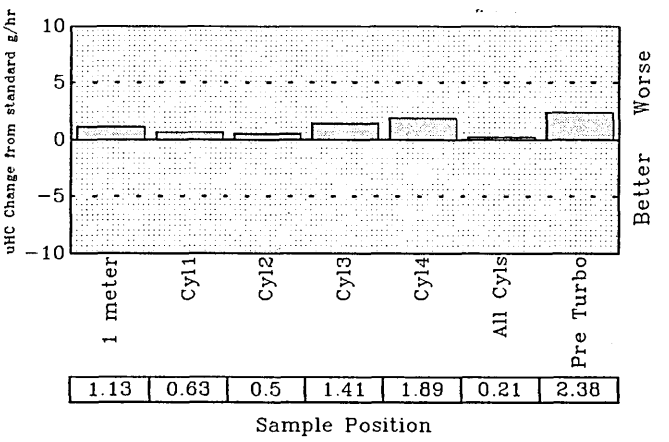

b

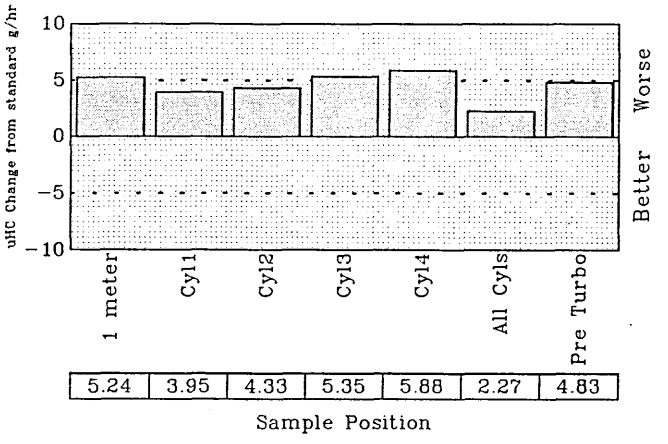

c

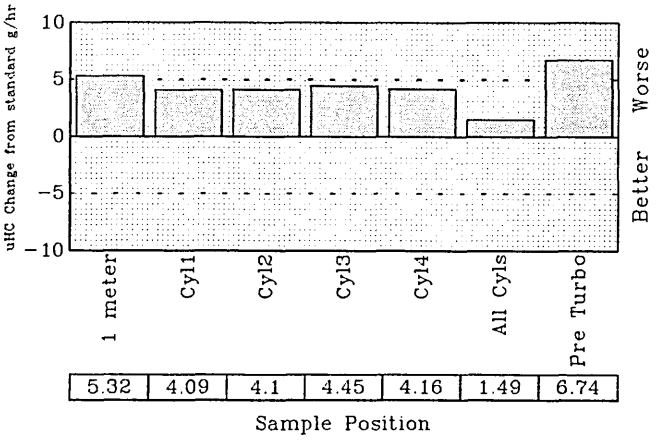

Figure 5.14 uHC emissions change from standard

d

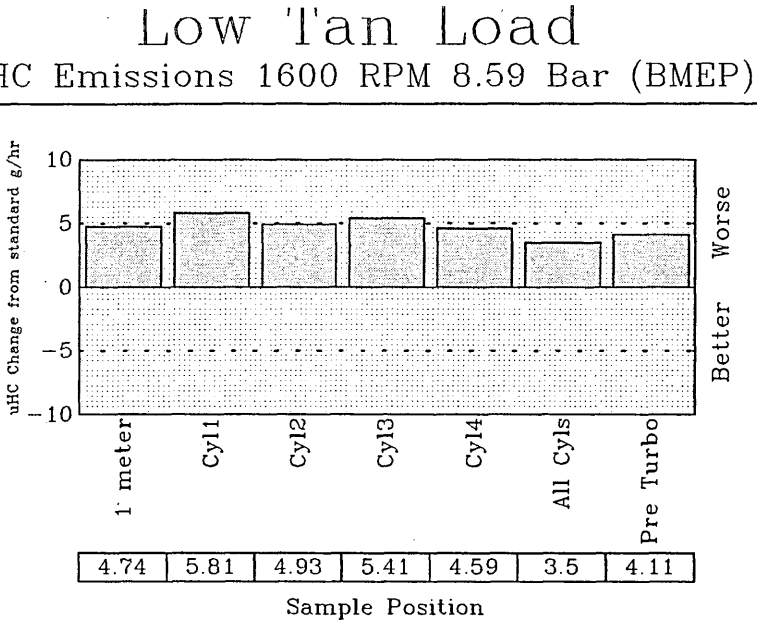

e

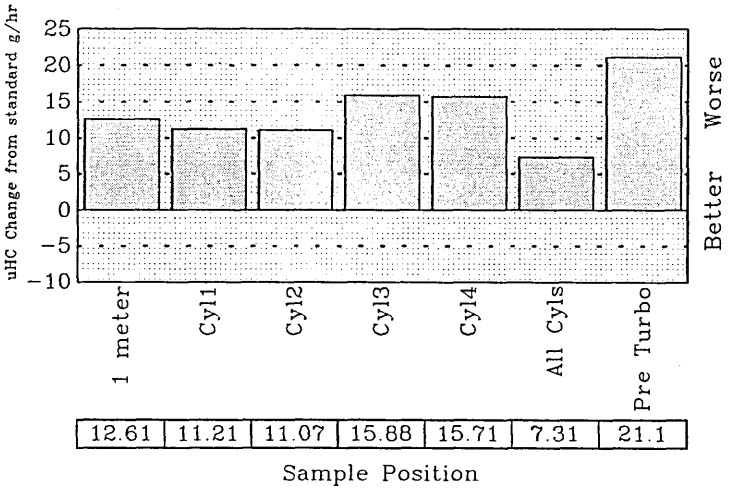

Figure 5.14 uHC emissions change from standard

Percentage survival of fuel species
Low tan load rings

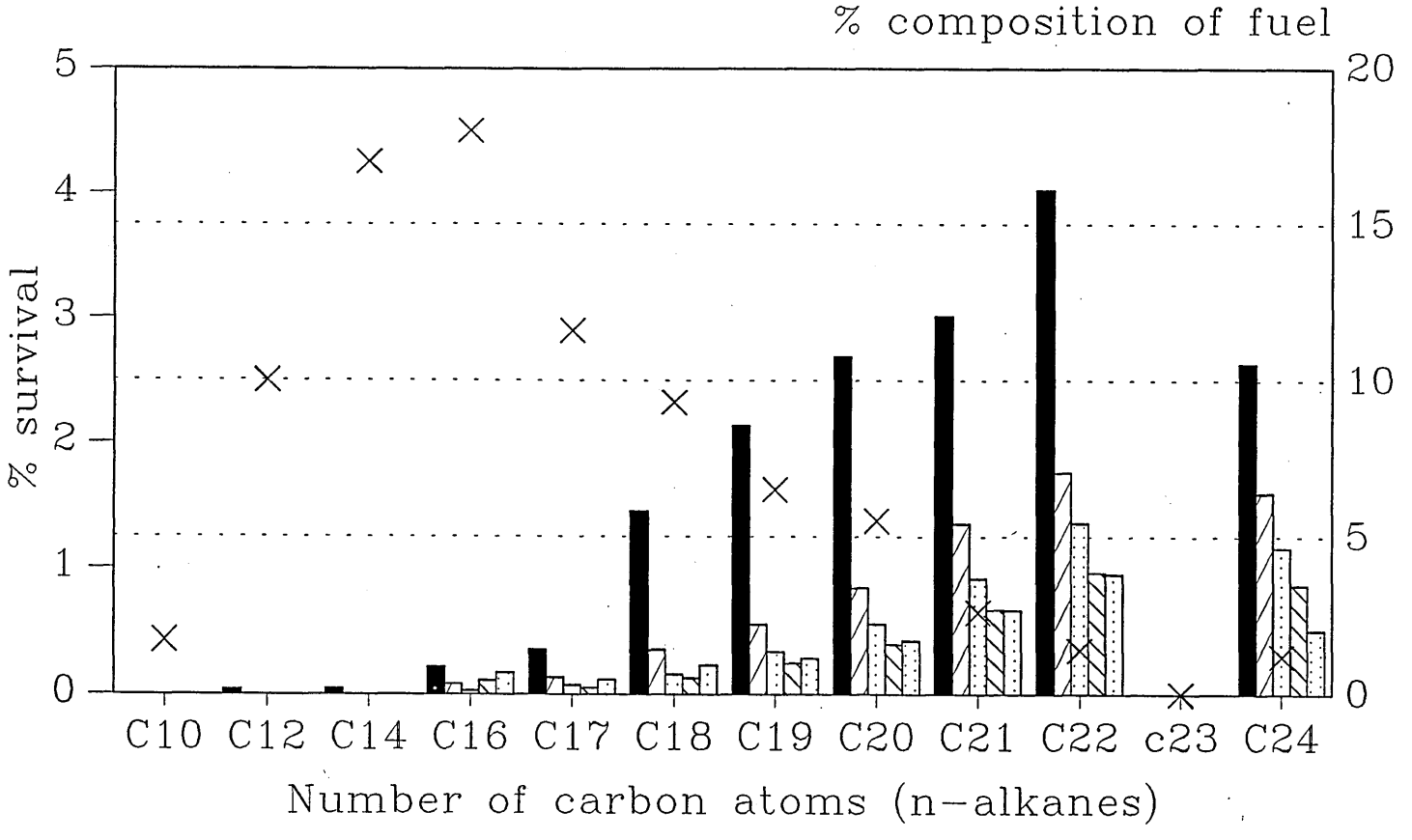

SOF alkane species Idle

a

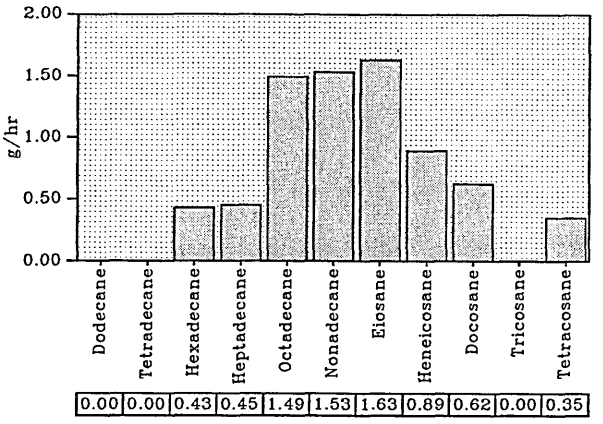

Low Tan Load
SOF alkane species 1600 RPM 2.86 Bar(BMEP)

b

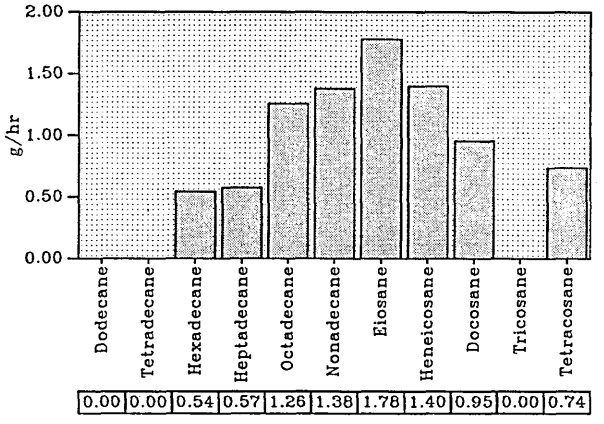

Low Tan Load
SOF alkane species 1600 RPM 5.72 Bar(BMEP)

c

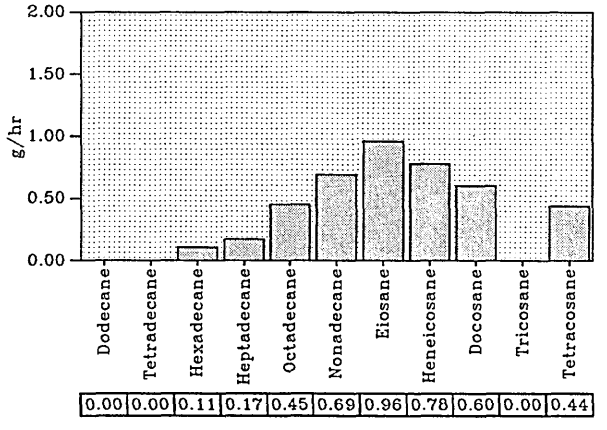

Figure 5.16 Survival of fuel species Low tangential oil ring engine

SOF alkane species 1600 RPM 8.59 Bar(BMEP)

d

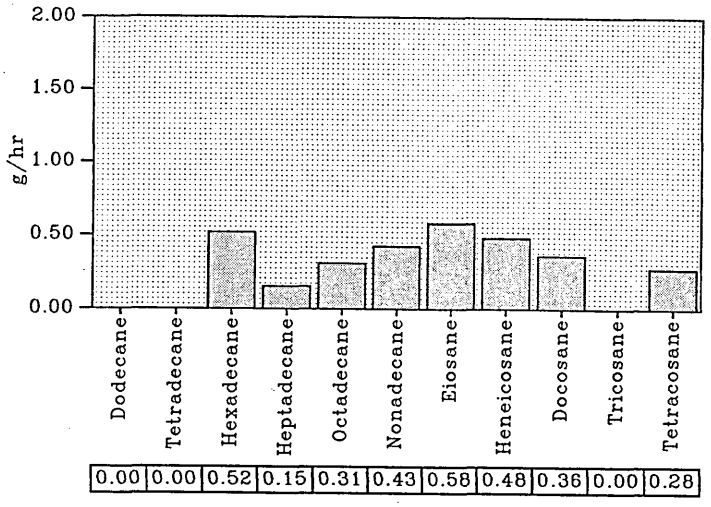

Low Tan Load

SOF alkane species 2500 RPM 7.49 Bar(BMEP)

e

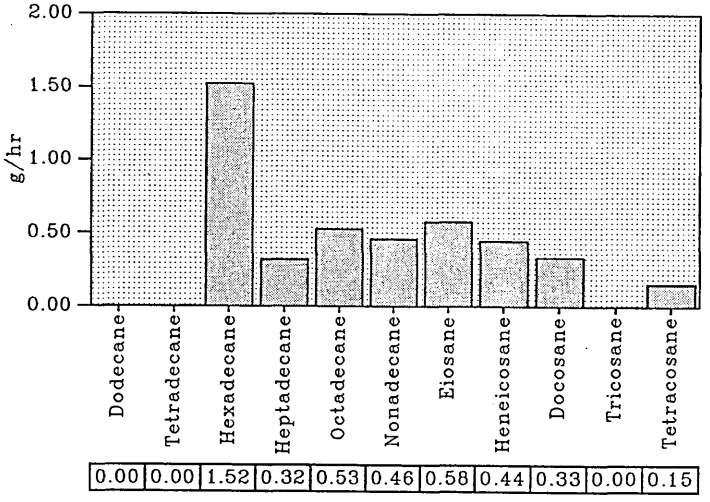

Figure 5.16 Survival of fuel species Low tangential oil ring engine

SOF alkane species 1600 RPM 2.86 Bar (BMEP)

a

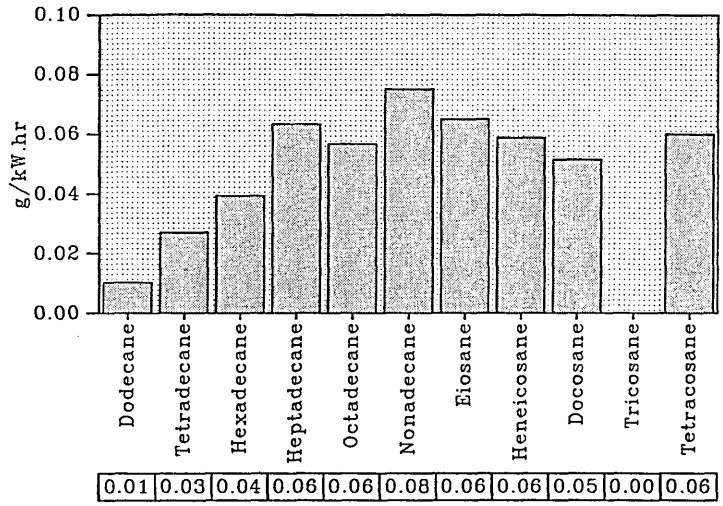

Low Tan Load

SOF alkane species 1600 RPM 5.72 Bar (BMEP)

b

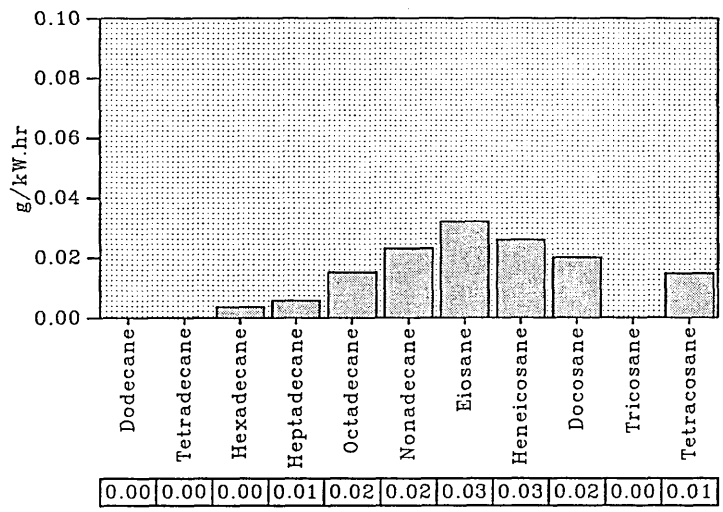

Figure 5.17 Survival of fuel species Low tangential oil ring engine(g/kW.hr)

SOF alkane species 1600 RPM 8.59 Bar (BMEP)

c

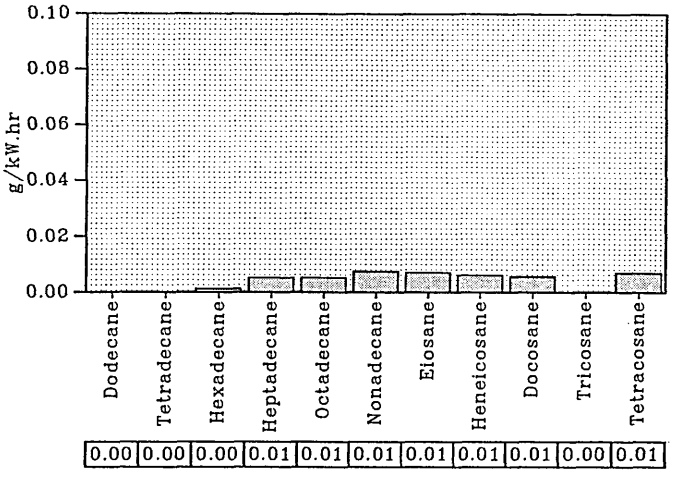

Low Tan Load

SOF alkane species 2500 RPM 7.49 Bar (BMEP)

d

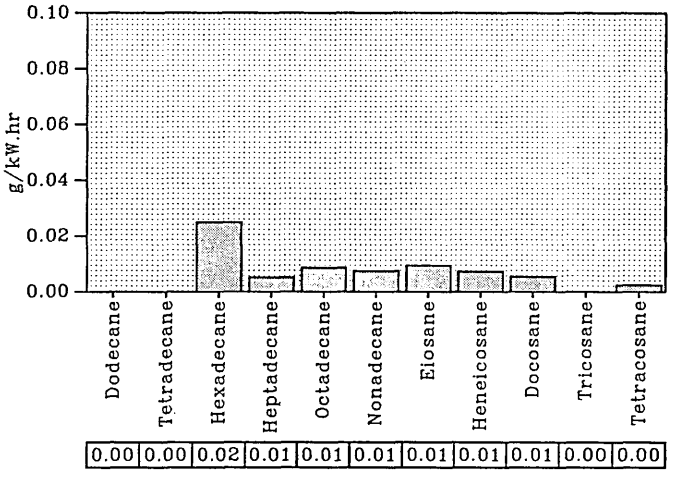

Figure 5.17 Survival of fuel species Low tangential oil ring engine(g/kW.hr)

uHC Emissions Idle

a

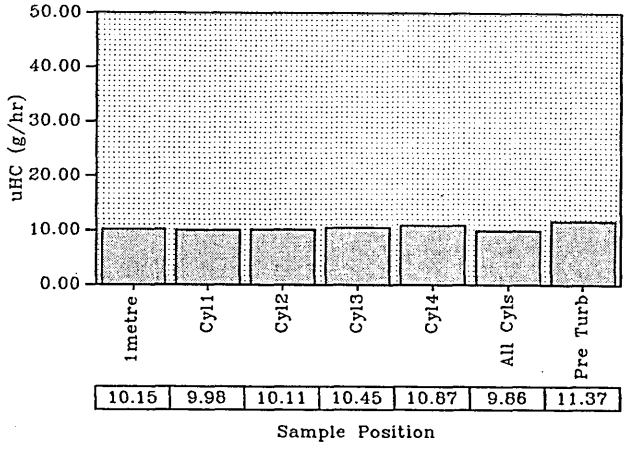

High Top Ring
uHC Emissions 1600 RPM 2.86 Bar (BMEP)

b

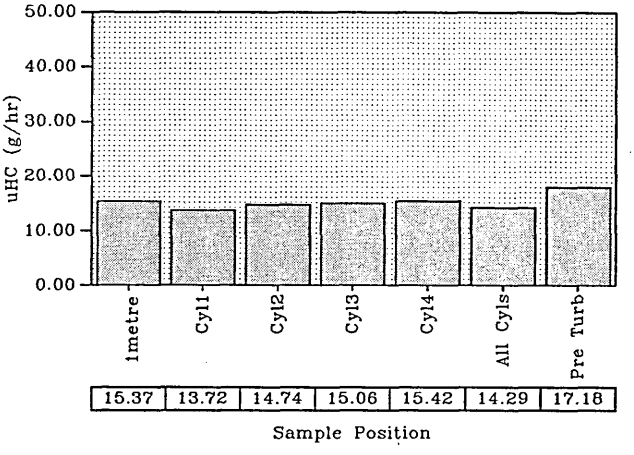

High Top Ring
uHC Emissions 1600 RPM 5.72 Bar (BMEP)

c

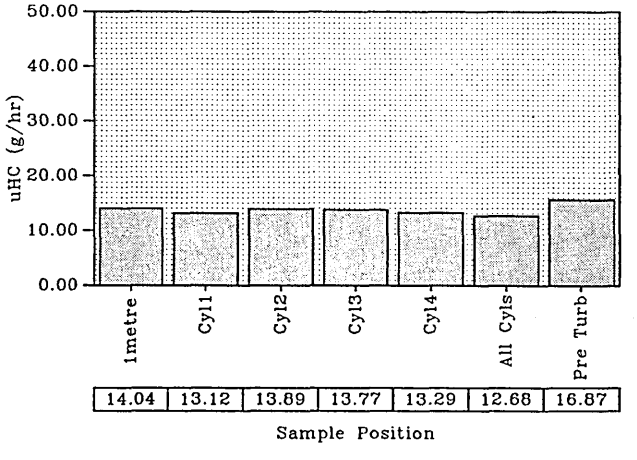

Figure 5.18 High top ring build gas phase hydrocarbons emitted (g/hr)

d

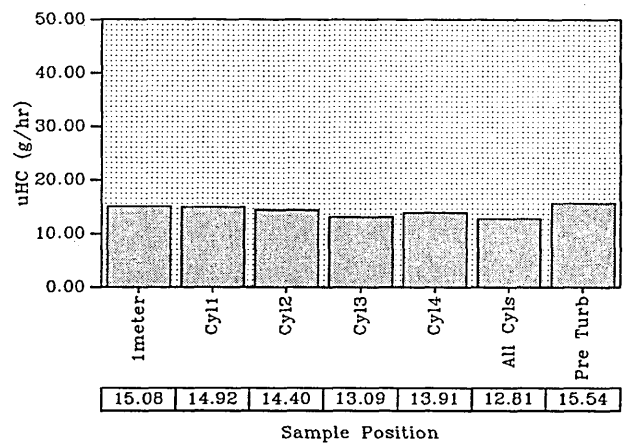

e

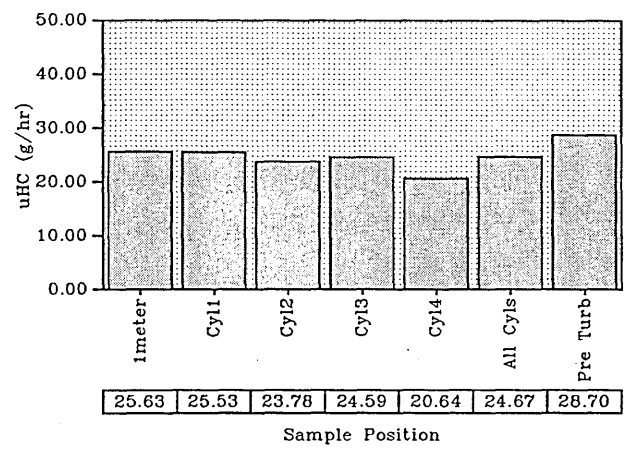

Figure 5.18 High top ring build gas phase hydrocarbons emitted (g/hr)

uHC Emissions 1600 RPM 2.86 Bar (BMEP)

a

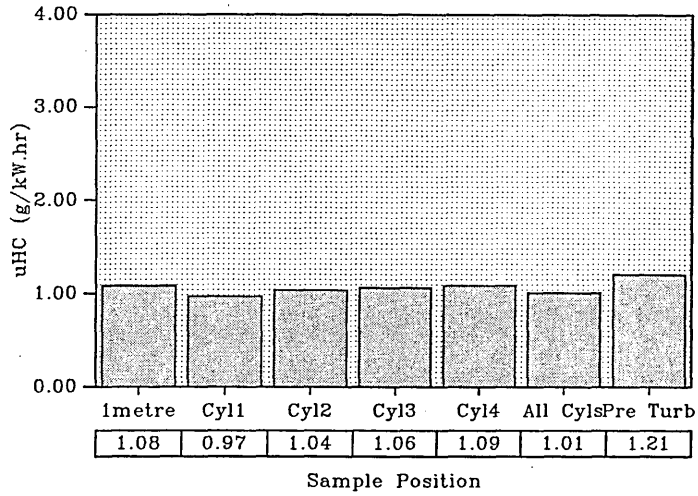

High Top Ring
uHC Emissions 1600 RPM 5.72 Bar (BMEP)

b

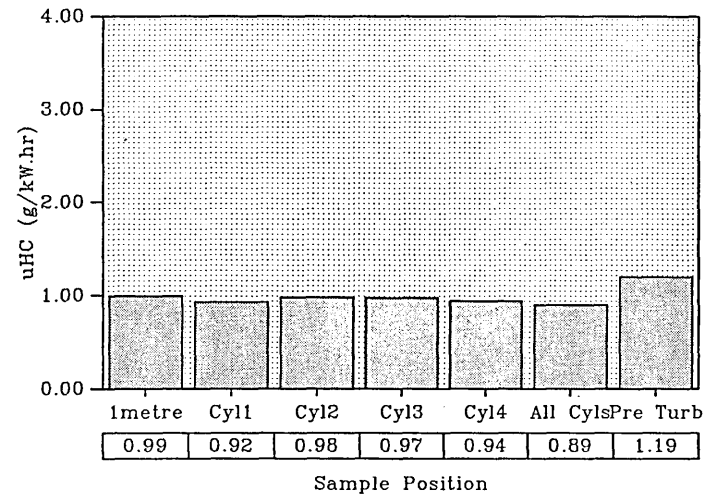

Figure 5.19 High top ring build gas phase hydrocarbons emitted (g/kW.hr)

uHC Emissions 1600 RPM 8.59 Bar (BMEP)

d

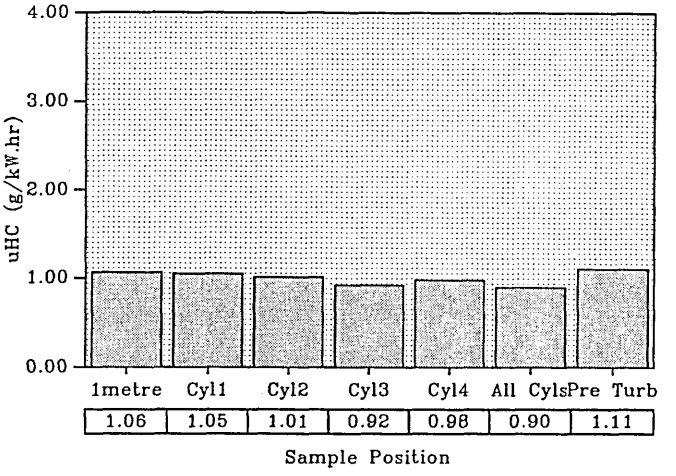

High Top Ring
uHC Emissions 2500 RPM 7.49 Bar (BMEP)

e

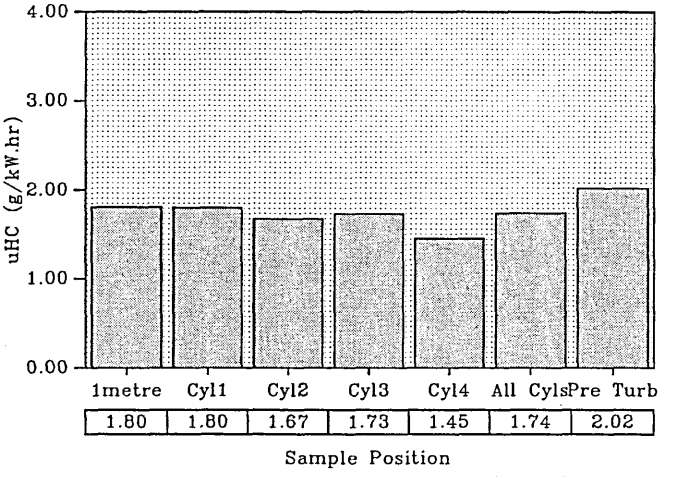

Figure 5.19 High top ring build gas phase hydrocarbons emitted (g/kW.hr)

High Top Ring
uHC Emissions Idle

a

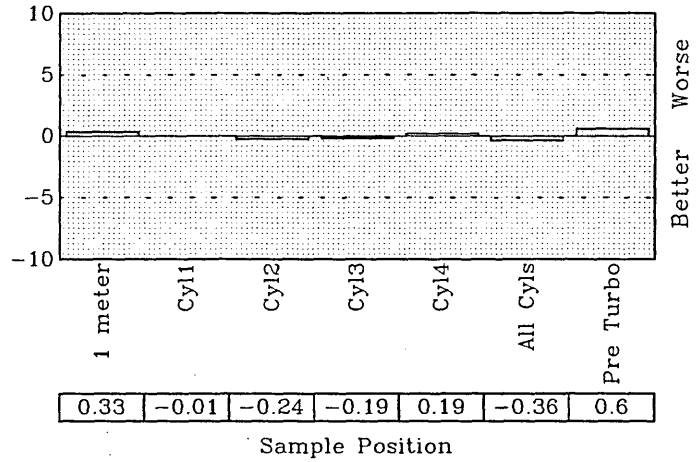

High Top Ring
uHC Emissions 1600 RPM 2.86 Bar (BMEP)

b

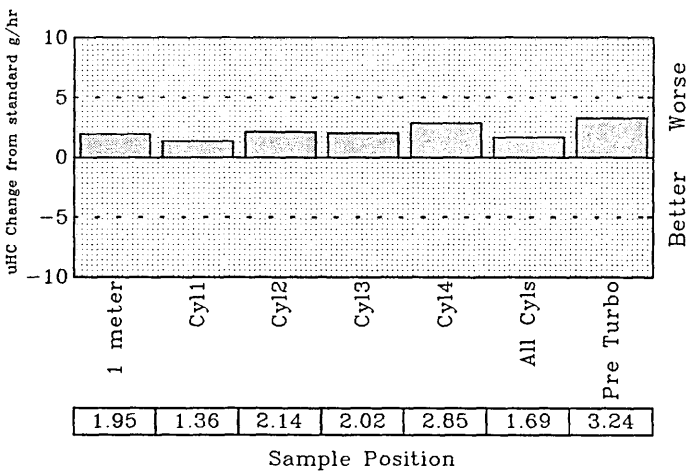

High Top Ring
uHC Emissions 1600 RPM 5.72 Bar (BMEP)

c

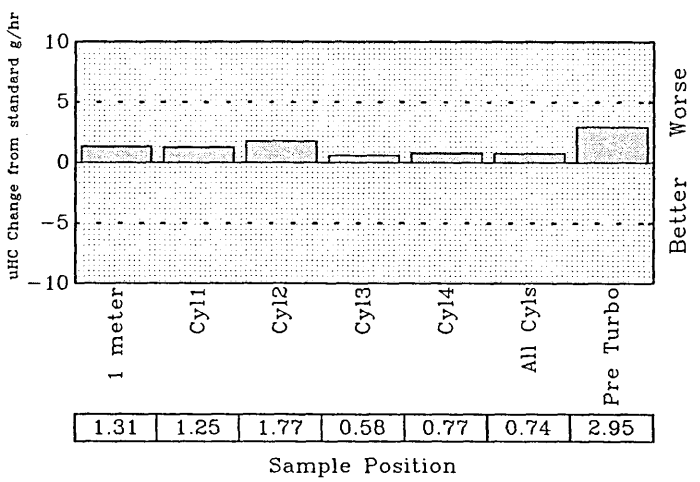

Figure 5.20 High top ring uHC emissions change from standard

High Top Ring
uHC Emissions 1600 RPM 8.59 Bar (BMEP)

d

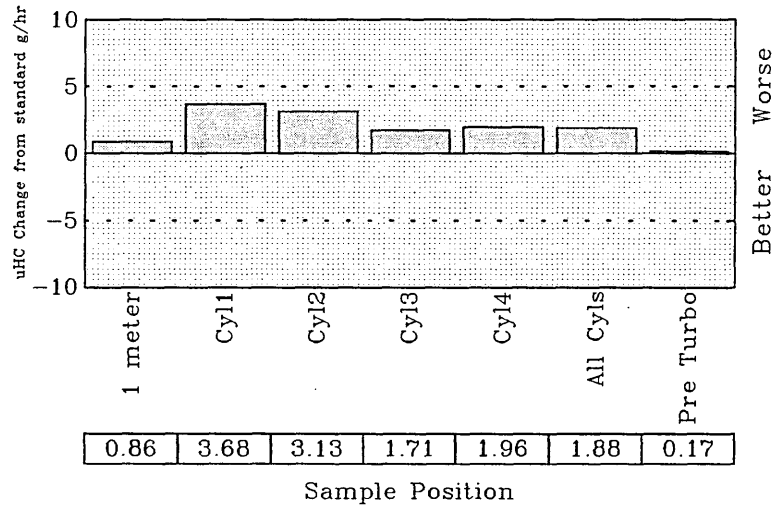

High Top Ring
uHC Emissions 2500 RPM 7.49 Bar (BMEP)

e

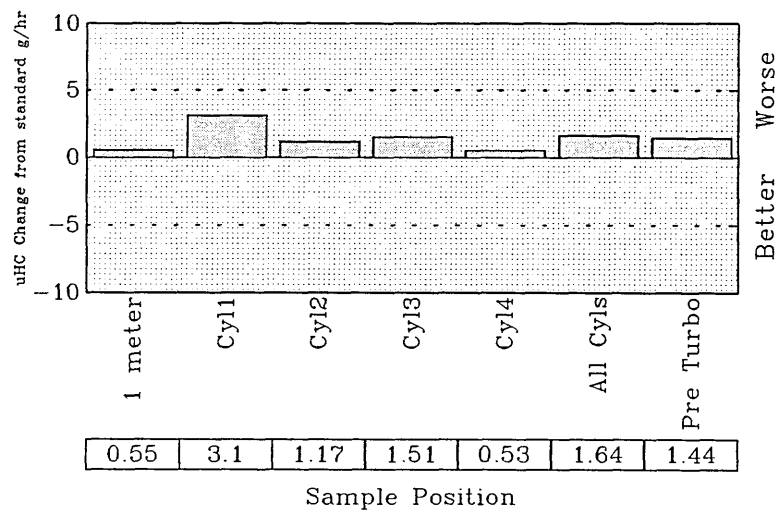

Figure 5.20 High top ring uHC emissions change from standard

SOF alkane species Idle

a

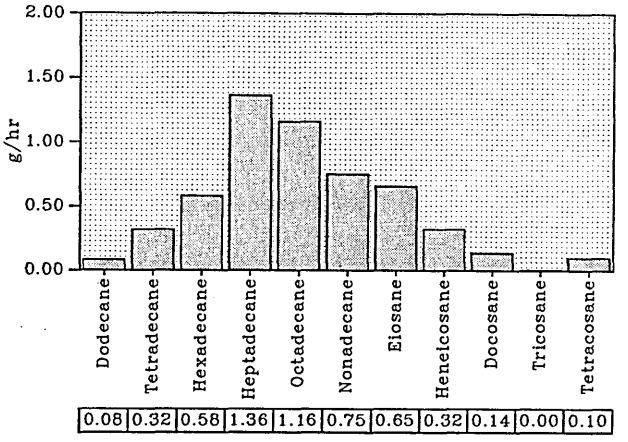

High Top Ring
SOF alkane species 1600 RPM 2.86 Bar (BMEP)

b

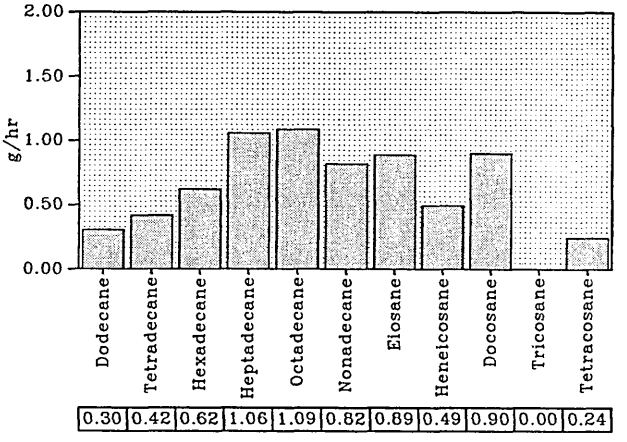

High Top Ring
SOF alkane species 1600 RPM 5.72 Bar (BMEP)

c

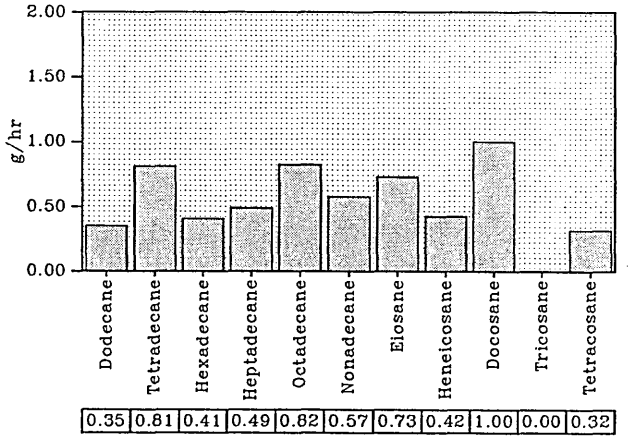

Figure 5.21 High top ring build
n-alkane species from SOF(g/hr)

SOF alkane species 1600 RPM 8.49 Bar (BMEP)

d

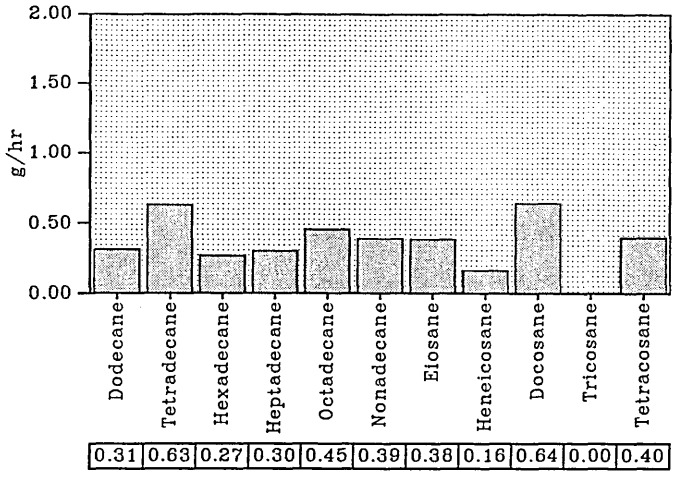

High Top Ring

SOF alkane species 2500 RPM 7.49 Bar (BMEP)

e

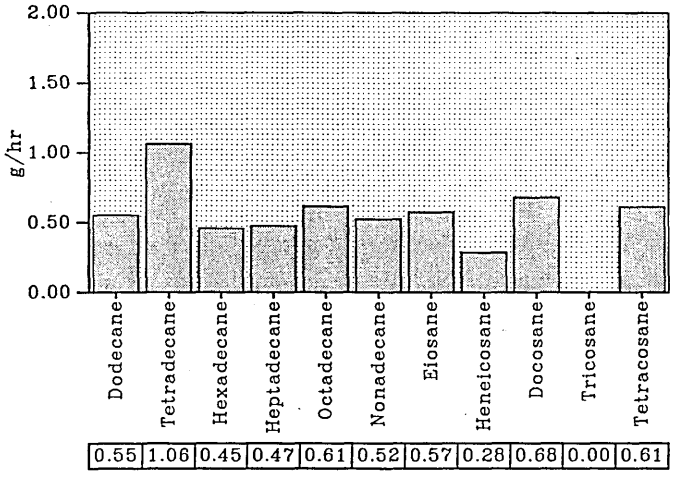

Figure 5.21 High top ring build n-alkane species from SOF(g/hr)

a

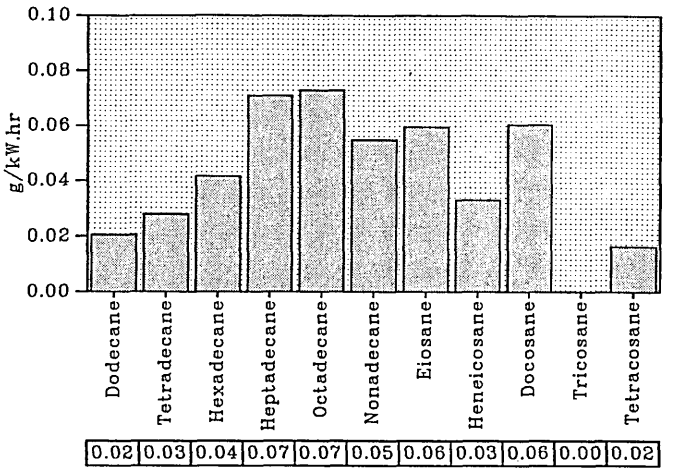

b

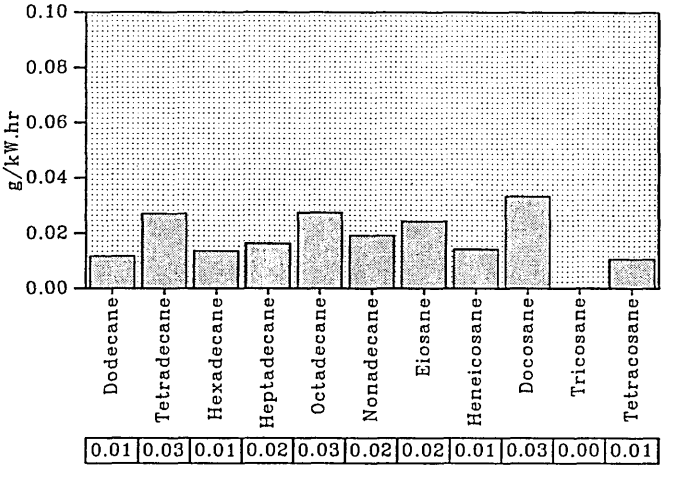

Figure 5.22 High top ring build n-alkane species from SOF(g/kW.hr)

c

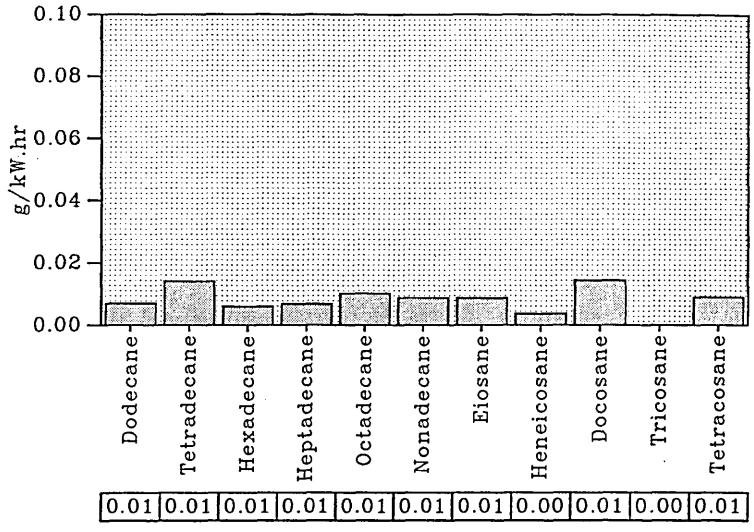

d

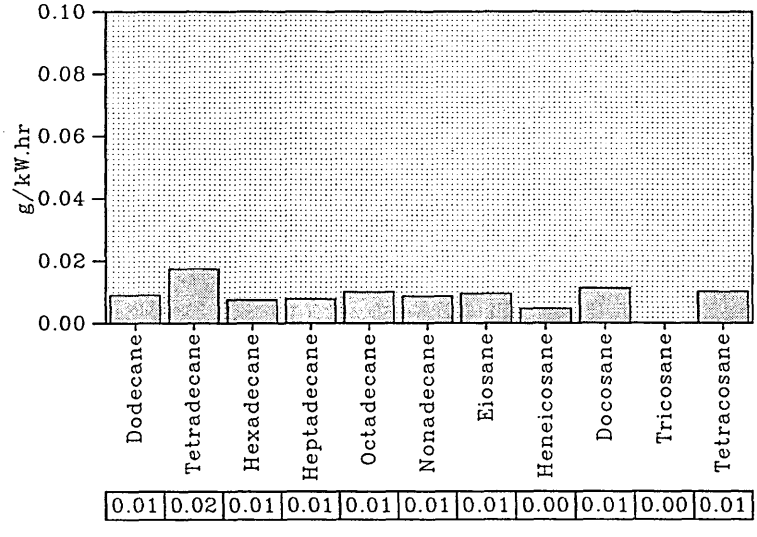

Figure 5.22 High top ring build n-alkane species from SOF(g/kW.hr)

% Survival of injected alkanes
High Top Ring

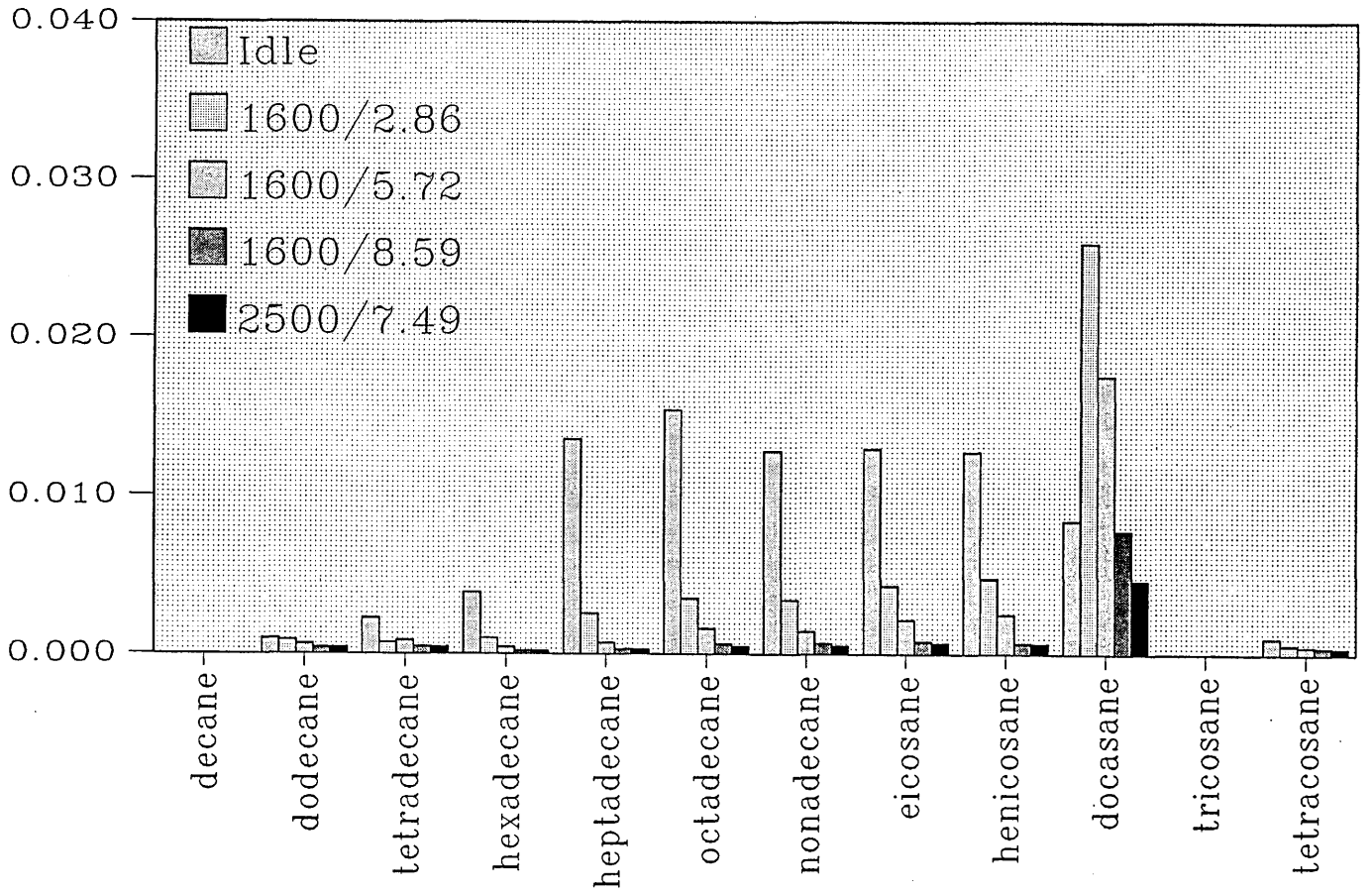

5.23 Survival of fuel species high top ring

6.0) Model results

6.1) Introduction

The model was calibrated to provide results that compared to that obtained experimentally and then three versions of that model were cloned and then modified to reflect the change made to the engine for each of the test runs. The major changes between the three models are shown in table 6.1.

	Oil film thickness (μm)	Top land height(m)	Top land volume(m^3)	Second land height(m)	Second land volume(m^3)
Standard	0.244	0.01	$1.12x10^{-6}$	0.01	$0.752x10^{-6}$
Low Tan Load	0.488	0.01	$1.12x10^{-6}$	0.01	$0.752x10^{-6}$
High Top Ring	0.244	.00045	$0.503x10^{-6}$	0.0155	$1.16x10^{-6}$

Table 6.1 Engine parameters changed for each model run.

A complete table for all the input parameters for the model can be seen in Appendix 3. The majority of the input data for the model testing was obtained from the physical engine test results. The most significant exception to this list was the piston and liner temperatures. These temperatures were obtained from test results presented by Barr[87].

The model was run for all the test points used in the empirical testing. This was to allow the study of the effects of differing fuelling rates, pressure and combustion temperature and produce a greater understanding of the influence of the component on the total hydrocarbon emission.

6.2) Standard Engine Dimensions

The parameters that allowed the tuning of the model allowed the results for this set of tests to provide results within the range from this type of model. The tuning parameters were generally around the mid point of the range suggested by the equation's author. The model used data at 1° intervals, and the sum of the exhaust gas components present in each of the calculated regions at exhaust valve opening was taken to be that which would be measured at the tail pipe.

The folowing section refers to figure 6.1 to figure 6.6 and table 6.2.

6.2.1) Unburnt hydrocarbon emissions.

The results for these could be tuned to provide similar results to that of the empirical testing. The final result was the total hydrocarbon weight contained in the three areas calculated at the point when the exhaust valve opened. The three areas were

1) In the gases within the combustion chamber.
2) Within the gases in the crevice volumes (ring grooves and lands)
3) Retained in the lubrication oil film.

When the model was in this mode the effect of the cylinder boundaries was insignificant. The reason for this is that the model does not have a suitable procedure for the transport of the fuel from the injector to the cylinder boundaries. To provide the boundary effect the results from the empirical testing were used to extrapolate the effect of the boundary and then applied to the model, providing the approximate magnitude for the unburnt hydrocarbon emissions for the cylinder boundaries.

6.2.2) Soot emissions.

The emissions of carbon solids for this model produced results similar to the empirical testing for changes in speed and load when the correlation proposed by Whitehouse[81] was used. The effect of the injector's geometry, the injection pressure

and the duration of the injection period has a significant effect of the formation of the soot within the cylinder. The temperature of the combustion gases and the availability of free oxygen are the main factors in the consumption of the soot particles during the combustion process.

6.3) Low Tan Load Oil Control Ring .

The model for this engine configuration used all the tuning parameters calibrated for the standard engine. The low tangential oil ring simulation was applied to the model by increasing the oil film thickness

6.3.1 Unburnt hydrocarbon emissions.

The primary component of the uHC emissions is from the fuel that overmixes with air and forms a mixture that cannot sustain combustion. The crevice volumes contribute significantly more than that adsorbed and then desorbed from the oil film. The effect of adsorption and desorption is not significant except at high speeds and loads. The predicted levels from the model regarding these results are the most unreliable because the model does not include a routine for the bulk loss of the oil. The results from the model produce similar values for uHC for this configuration to those predicted in the standard configuration.

6.3.2 Soot emissions.

The calculated values for the soot from this model configuration was the same as that for the standard build.

6.4) High Top Ring Piston .

The model for this engine configuration used all the tuning parameters calibrated for the standard engine. The high top ring simulation was applied by changing the dimension for the vertical position of the first ring groove in the piston. This piston configuration had a larger second land and this acted as a reservoir that released gases later in the cycle than if it had been contained within the top land. It has been proved

that the higher up the piston the top ring is sited, the higher the temperature that the ring operates at for a given operating condition. The ring running at a higher temperature causes a greater quantity of heat to flow into the liner throughout the whole operating cycle. This greater flow of heat causes the piston to operate at a lower temperature.

6.4.1 Unburnt hydrocarbon emissions.

The model significantly under predicted the effect of the crevice volumes for the reasons discussed earlier in this chapter. The mass of the gases contained within the crevices increases by a factor of over 2.5 times from the start of injection to peak pressure when the model simulates the higher power output test points. This continuous increase in the crevice mass is for over 25° and allows the fuel to be transported to the combustion chamber boundaries. The contribution the boundaries made to the total hydrocarbon emissions was calculated by the same method used in the standard model runs. The normalised values for the hydrocarbon emissions from the crevices produced results that produced the same trends as the empirical testing.

6.4.2 Soot emissions.

The calculated values for the soot from this model configuration was the comparable to that for the standard build.

Test Point	Engine Build	Model uHC (g/hr)	Actual uHC (g/hr)
Idle	Standard	9.96	9.82
	Low tan load		10.9
	High top ring		10.15
1600/2.86	Standard	15.36	13.4
	Low tan load		18.6
	High top ring		15.3
1600/5.72	Standard	14.016	12.7
	Low tan load		18.1
	High top ring		14.04
1600/8.59	Standard	15.56	14.02
	Low tan load		18.95
	High top ring		15.08
2500/7.49	Standard	25.5	26.1
	Low tan load		38.7
	High top ring		25.62

Table 6.2 Engine and model uHC emissions

Predicted Soot

All test points

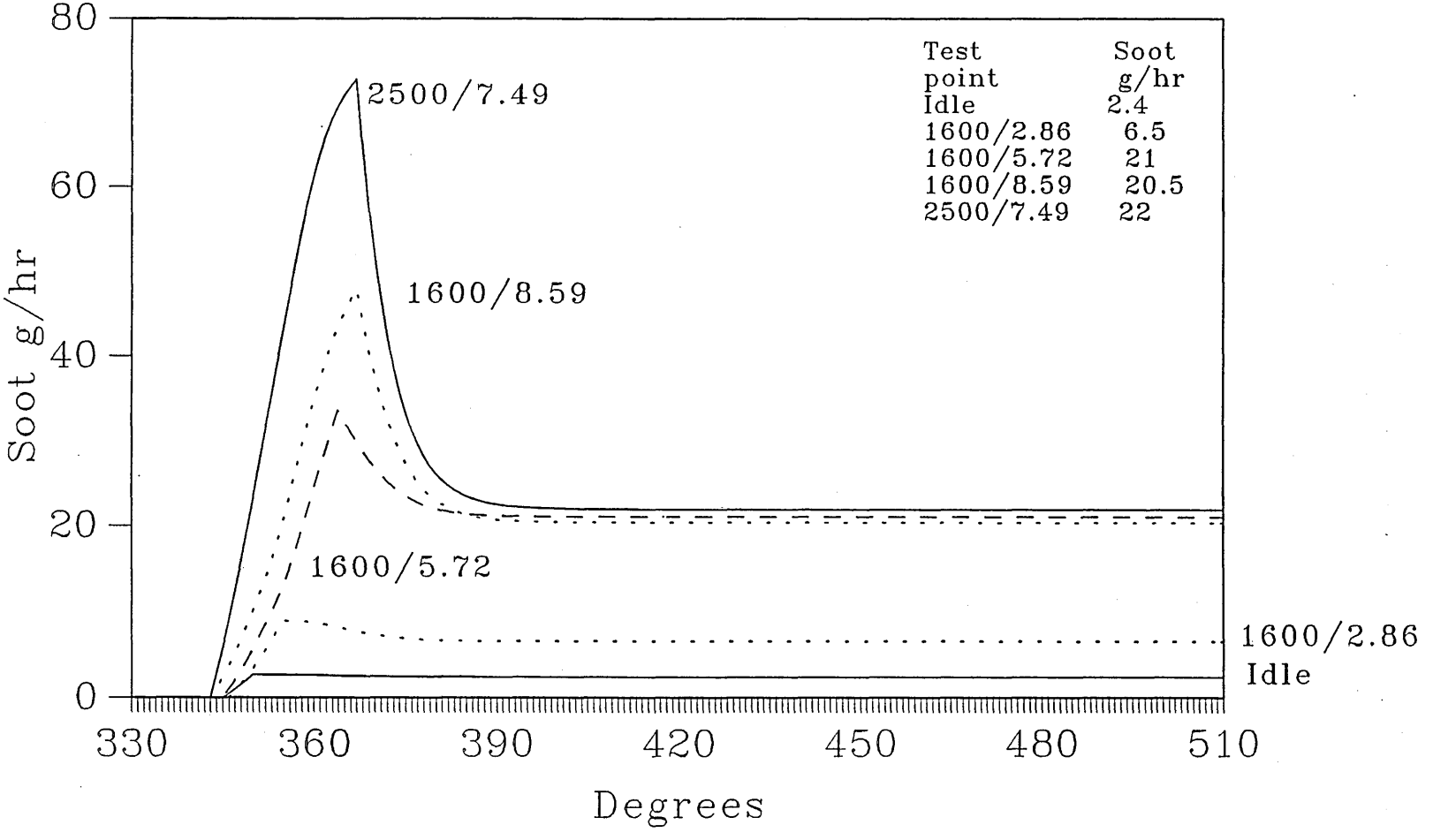

Figure 6.1 Predicted soot levels all test points

Standard (Model)

Crevice uHC Emissions Idle

a

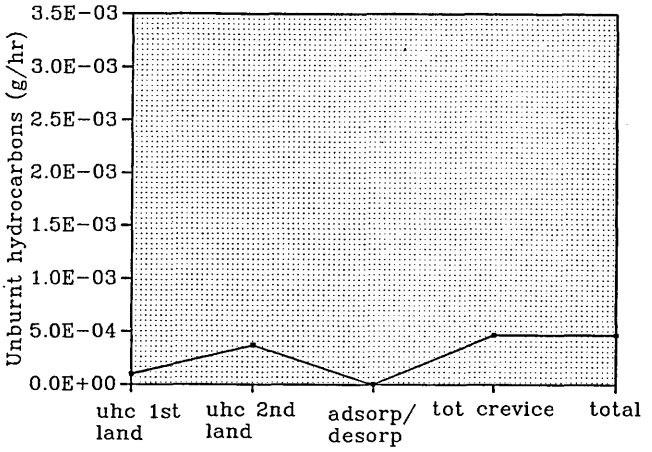

Low tan Load (Model)

Crevice uHC emissions Idle

b

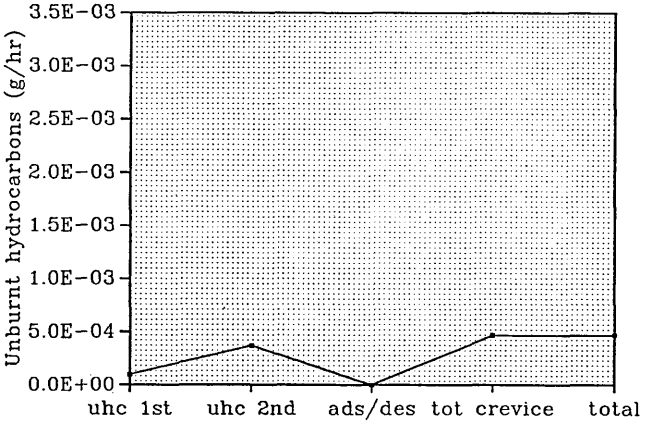

High Top Ring (Model)

Crevice uHC Emissions Idle

c

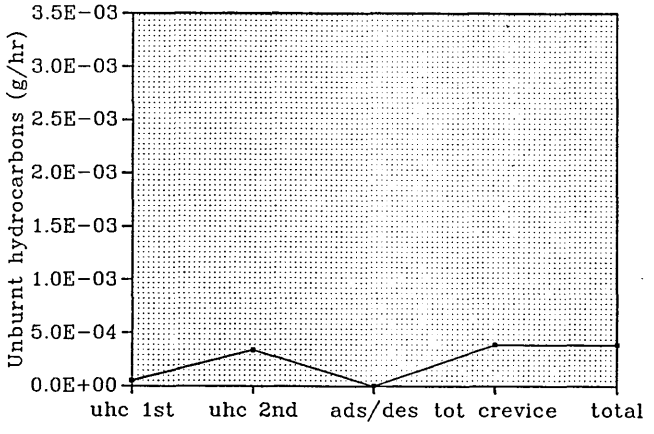

Figure 6.2 Predicted crevice uHC(idle)

Standard (Model)
Crevice uHC Emissions 1600 2.86 Bar (BMEP)

a

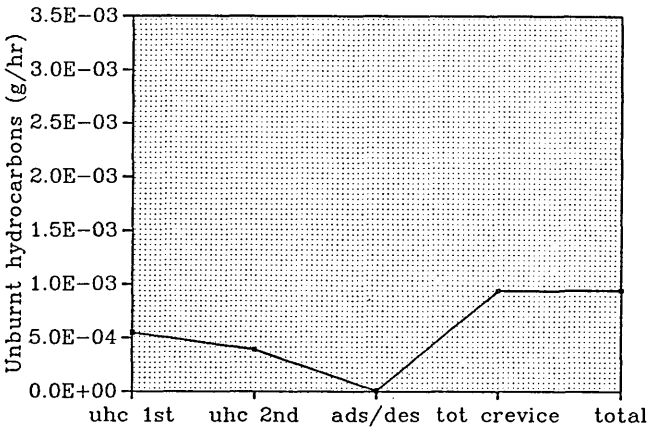

Low Tan Load (Model)
Crevice uHC Emissions 1600 2.86 Bar (BMEP)

b

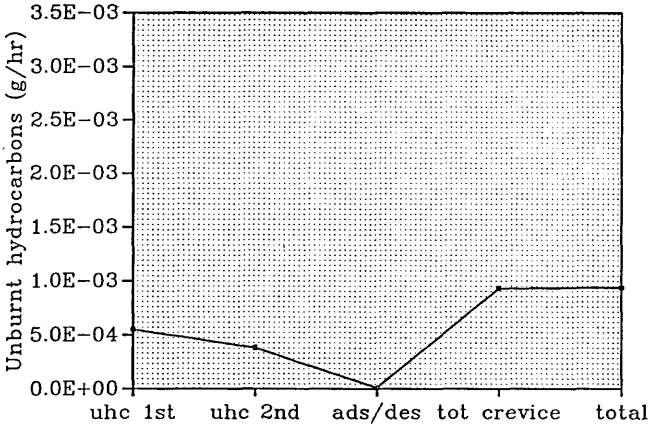

High Top Ring (Model)
Crevice uHC Emissions 1600 2.86 Bar (BMEP)

c

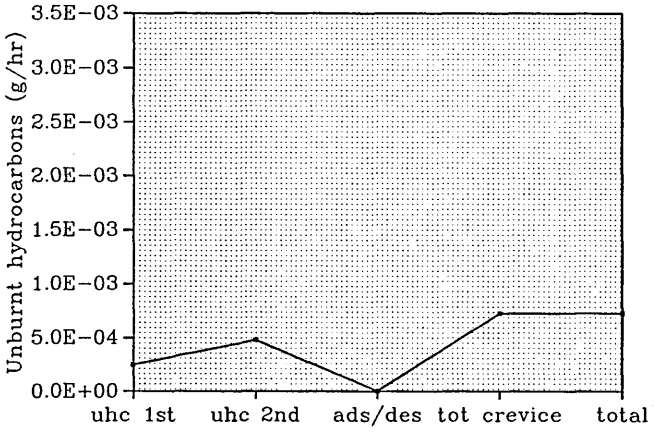

Figure 6.3 Predicted crevice uHC(1600 RPM 2.86 bar(BMEP))

Standard (Model)
Crevice uHC Emissions 1600 5.73 Bar (BMEP)

a

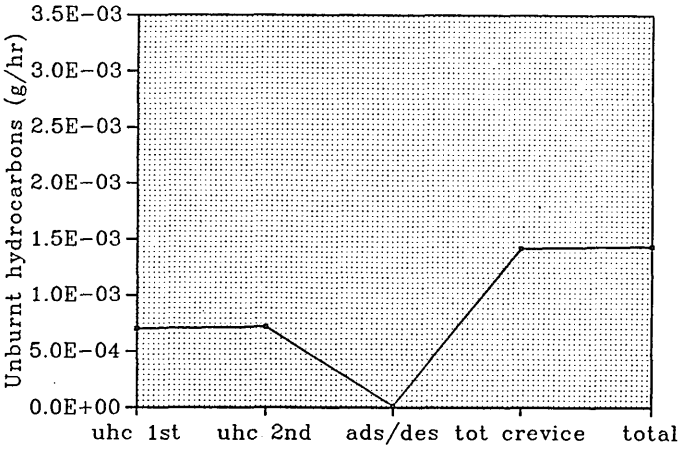

Low Tan Load
Crevice uHC Emissions 1600 5.73 Bar (BMEP)

b

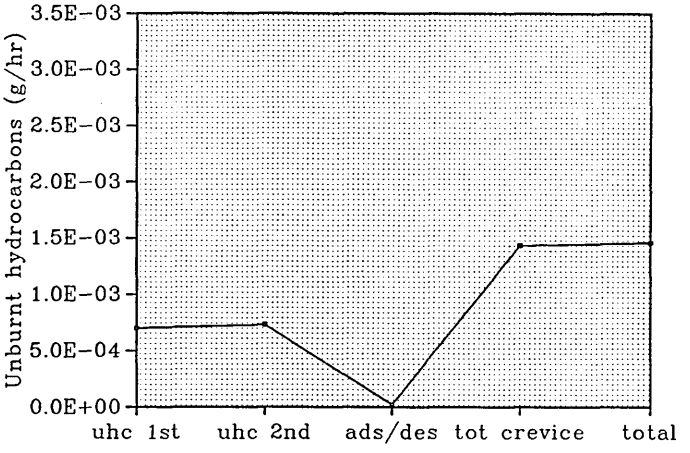

High Top Ring
Crevice uHC Emissions 1600 5.73 Bar (BMEP)

c

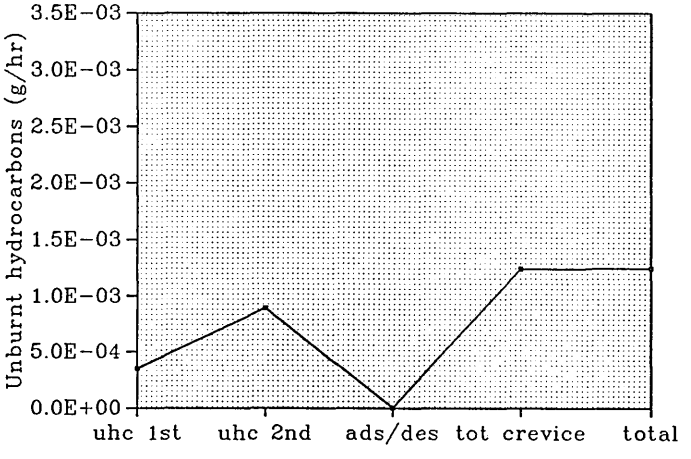

Figure 6.4 Predicted crevice uHC(1600 RPM 5.73 bar (BMEP))

Standard (Model)
Crevice uHC Emissions 1600 8.59 Bar (BMEP)

a

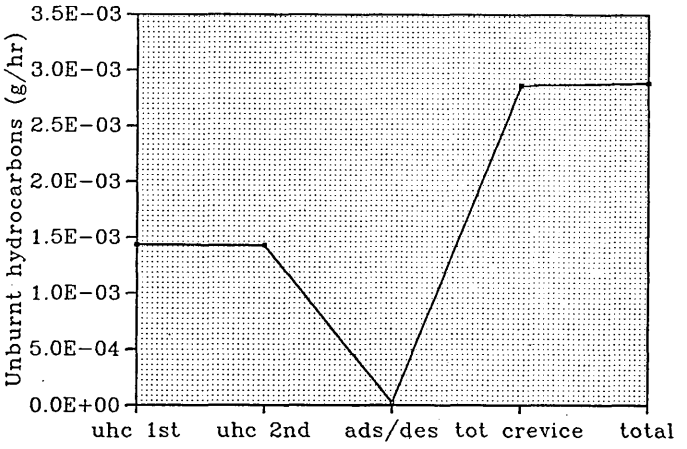

Low Tan Load (Model)
Crevice uHC Emissions 1600 8.59 Bar (BMEP)

b

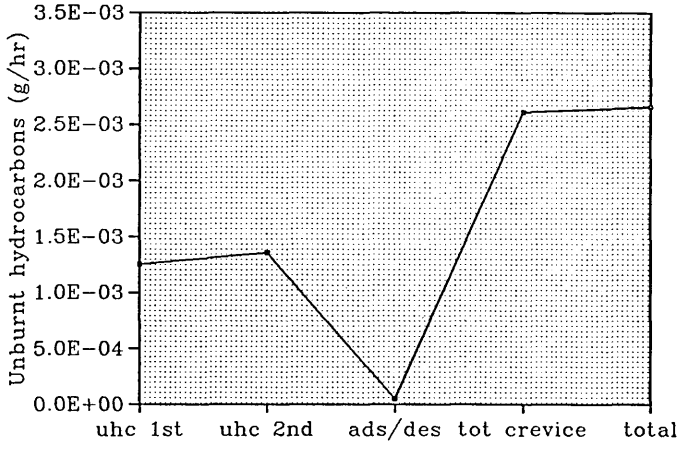

High Top Ring (Model)
Crevice uHC Emissions 1600 8.59 Bar (BMEP)

c

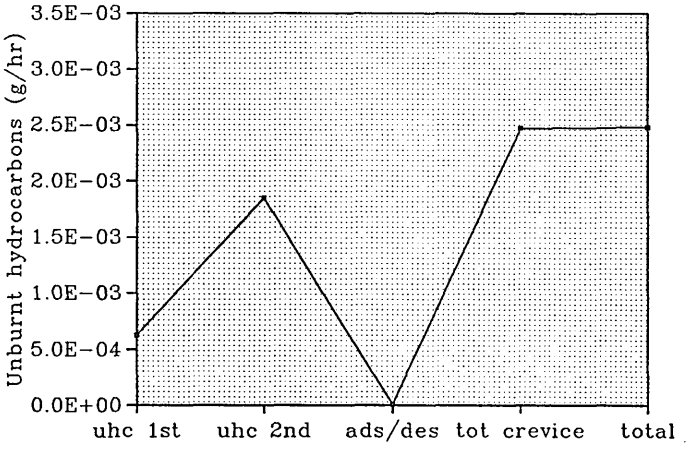

Figure 6.5 Predicted crevice uHC(1600 RPM 8.59 bar (BMEP))

Crevice uHC Emissions 2500 7.49 Bar (BMEP)

a

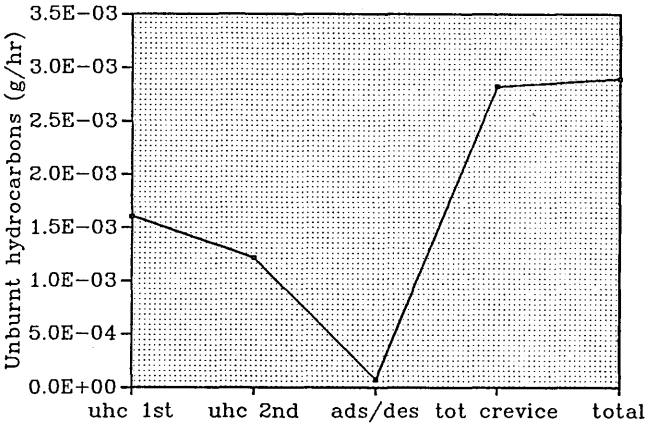

Low Tan Load (Model)

Crevice uHC Emissions 2500 7.49 Bar (BMEP)

b

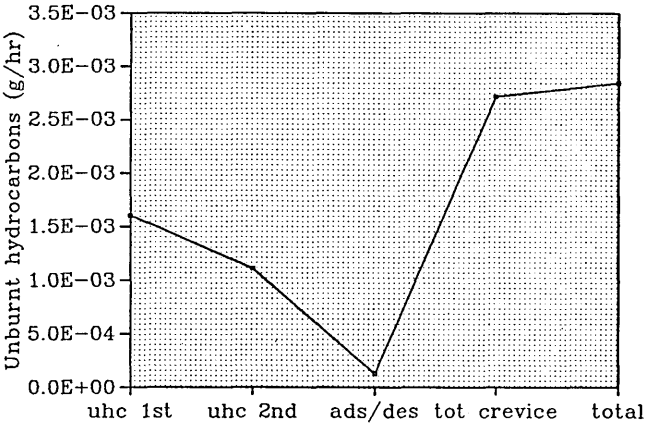

High Top Ring (Model)

Crevice uHC Emissions 2500 7.49 Bar (BMEP)

c

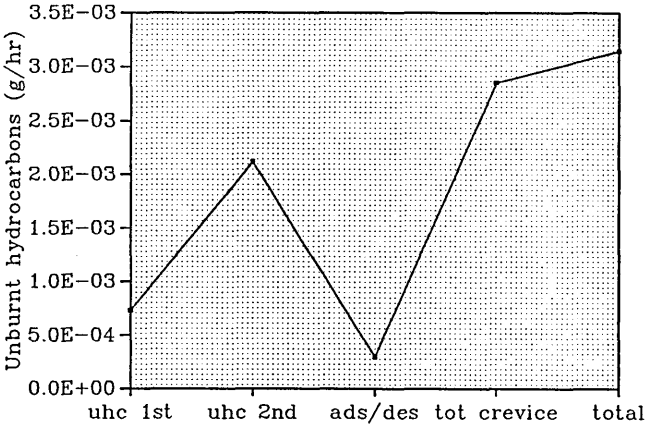

Figure 6.6 Predicted crevice uHC(2500 rpm 7.49 bar (BMEP))

7.0) Discussion

7.1) Introduction

The results from the empirical testing and those predicted by the model have been presented in earlier chapters. The comparison of these results within this chapter shows how the changes to the combustion chamber boundaries affect the measured pollutants.

Common factors to all empirical tests

Throughout all the tests certain trends were observed that applied to all engine builds. These are:-

Post combustion pyrolysis of hydrocarbons.

The gas phase hydrocarbon measurements obtained by the FID consistently showed that the sample taken at the entry to the turbocharger was consistently the highest of all the measurement points. The n-alkane component of the reference fuel used for these tests was from decane($C_{10}H_{22}$) to tetracosane($C_{24}H_{50}$). Decane is the lightest component with a boiling point of 174°C. This is only 6 degrees below that of the heated sample line and prefilter that was used to transport the sample to the FID. Thus any fuel particles that had not undergone any type of reaction in the combustion chamber could not be transported to the FID. When comparing the exhaust port and pre-turbo measurements the measurement just before the turbo charger was 5% to 28 % higher. The higher the gas temperature in the exhaust system the greater the change between the two points, the only exception to this being when the engine speed was increased. The increase in engine speed produced an increase in gas flow in the exhaust system thus there was a shorter time period between the measuring points and less time for any reaction to take place. The measurement at 1 metre showed a drop of

between 4% and 18% to that at the turbo charger for all test points. The 18% drop was at idle where the gas temperatures are the lowest and this drop was attributed to the hydrocarbons condensing before reaching the sample point.

The effect of pyrolysis was postulated because there is insufficient time to allow the oxidation of the hydrocarbons. To oxidise gas phase hydrocarbons, a residence time of 50ms or longer is required at temperatures at or above 600°C. The air motion and combustion properties within a diesel combustion chamber are such that areas where flammation has occurred are rapidly mixed with air from much cooler regions, producing a quenching effect. This quenching effect was used in the model as a basis for the temperature of sudden freezing. The measured exhaust port gas temperatures are shown in table 7.1, and it can be seen that even the highest of these is below that required for the oxidation of gas phase hydrocarbons.

Test Point RPM/BMEP (bar)	Idle	1600/2.86	1600/5.72	1600/8.59	2500/7.49
Exhaust port temperature °C	103	258	375	490	580

Table 7.1 Exhaust port temperatures

Thus the fuel molecules that would condense within the exhaust gas sample system are broken down by the action of the heat. The further down the exhaust system the longer the fuel particles are exposed to this heat and the greater the number of fuel molecules broken down. The molecules formed by pyrolysis will be smaller and thus have a boiling point below that of the sample system, allowing delivery to and detection by the FID.

7.2) Particulate SOF speciation.

The composition of the SOF n-alkane species changed with operating conditions. At idle the quantities of individual n-alkane species closely matched the relative

quantities found in the fuel. The only exception to this was tetracosane at idle. The quantities measured for this species were significantly lower than those present in the fuel. With increasing engine power output the percentage of species present in the fuel falls considerably from 81.7% at idle to 29.5% at 2500 RPM and 7.49 Bar (BMEP) .

As the fuelling rates increased, the average molecular weight of the SOF sample increased and the two lighter n-alkanes measured for this research decreased considerably. The contribution of tetracosane was typically never the greatest at even the highest combustion temperatures and pressures.

The heavier the alkane molecule the greater the contribution in weight to the SOF and the higher the level of survivability from oxidation and/or pyrolysis. The exception to this is tetracosane, the heaviest alkane studied. The quantity detected in the SOF was considerably smaller than that injected into the cylinder by weight.

7.3) Exhaust Manifold unburnt hydrocarbons.

The level of measured gas phase hydrocarbons at the three points measured along its path in the exhaust system showed that the levels were higher just prior to the inlet of the turbocharger at all test points. The difference became more apparent as the exhaust port temperatures increased with the power output.

The measurement where all the exhaust ports were sampled simultaneously showed significant variation and the results were not comparable to the sum of the individual readings. The value for the simultaneous sample was typically 5% to 15 % lower then the average for the four individual port values. It was hypothesised that the flow rate in the individual sample pipe, being reduced to one quarter when sampling from all four ports, allowed the sample to either condense or undergo reactions. The addition

of a second sample pump to increase the flow to the sample selection manifold could solve this but it was not implemented during this research.

When the engine was operating at high loads this longer transport time allowed the sample to undergo pyrolysis for a longer period before reaching the sample line. At lower speed the sample pipes were not at the same elevated temperature and there was the potential for the sample to condense.

There was always a variation in the individual exhaust port measurements. As expected there was not a repeatable trend between cylinders 1, 2 and 4 but throughout all the tests cylinder three was consistently the highest. Cylinder 3 was the cylinder that had a pressure transducer placed in the injection pipe, as described in chapter 3. The engine was run with the original injection pipe but where the difference to other ports was reduced, cylinder 3 still produced higher levels of unburt hydrocarbons.

Hydrocarbon mass emissions.

The rate of fuel consumption had a direct relationship with the mass of unburnt hydrocarbons. The highest hydrocarbon mass emission was at the highest engine power output. The trend for all tests was for an increase in the mass emissions of hydrocarbons with increasing fuelling rates.

7.4) Standard Build

Unburnt hydrocarbon Emissions

The level of brake specific uHC was expected to drop as the engine was taken through each of its test programs, but the level started to rise after half load until at 2500 RPM 7.49 Bar (BMEP) it was twice the level of that at 1600 RPM 5.72 Bar (BMEP) . It is generally assumed that the level of unburnt hydrocarbons decreases as the engine load increases. This is because the main factor in the formation of unburt hydrocarbons is

the mixture being allowed to mix over lean. As load increases there is less volume within the combustion chamber where the mixture can reach these equivalence ratios. The engine's fuel injection system was suspected to be the cause because it was built from various sources and the components may not have been matched properly and, whilst serviceable, some had been used for earlier testing.

Particulates

The level of soot increased as the level of power was increased with each successive test point. The contribution by the SOF diminished with this increase in load until the engine speed was altered to 2500 RPM when the level increased. This reduction in SOF levels follows the trend that was expected for the unburnt hydrocarbons. The increase in the soot is due to the quantity of fuel injected. The greater the fuel injected the more the fuel enters into an oxygen depleted area and thus more soot is produced. The dilution ratios for the samples taken at 2500 7.49 Bar (BMEP) were approximately 5.5:1. This is just above the optimum for the collection of the maximum quantity of the extractable fraction. The dilution ratios for all the samples for this engine test were within the range of 3.3:1 and 5.5:1 and the calculated level of change in collected extractable material was negligible.

SOF speciation

At idle the measured species of hydrocarbons present in the fuel accounted for 81.7% of that found in the SOF. This quantity was 0.1286% of the total fuel injected during the sample period. The largest contributor to this fraction was docasane which accounted for one third of the sample. Docasane was the largest contributor to all samples of the SOF.

The survival rates for all the alkanes for all test points exhibit a saw tooth pattern similar to that of the melting points for the alkanes but instead of the odd numbered carbon molecules having the lower levels, it is the even numbered molecules that exhibit this trait. The reason for the saw tooth pattern in the melting points is that

even numbered solid state carbon alkanes have stronger van der Waals forces then those with odd numbers.

The measured hydrocarbon species accounted for only 0.04912 % of the total fuel injected during the sample period when the engine was operated at 1600 RPM 2.86 Bar (BMEP) although the same number of alkane species were present.

Model

The values for both soot and uHC correlated well with that obtained empirically. The calculation for the uHC present in the cylinder at exhaust valve opening showed that the fuel spray element was the main contributor. The calculated quantity of fuel injected per cycle was within –1.6% to + 15% of the actual value. The fuel injection pressure was either 0 or the mean value taken from the fuel line measurements while the injector needle was not on its seat. This injection pressure profile would give a far greater velocity to the fuel spray in the early stages of injection than in the empirical tests. This greater velocity would in practice give a larger quantity of fuel being overmixed at light loads, because the model used the percentage burnt to calculate the unburnt fuel component from the area above the piston, therefore the effect of the fuel injection pressure was deemed unimportant for these results.

The results for the unburnt hydrocarbon emissions for this configuration showed that at idle the crevices contributed ≈1/21,000 of the calculated unburnt hydrocarbon. This is because the quantity of fuel injected is so small and the velocity so low that the fuel spray could not reach the crevices before peak pressure. The test point that produced the greatest crevice contribution to the unburnt hydrocarbons was 1600 RPM 8.59 Bar (BMEP) which was ≈ 1/5,000 of the total, this measurement is higher than that at 2500 RPM 7.49 Bar (BMEP) because the time for the fuel spray to reach the crevices is 2/3 that for 1600 RPM even with the higher injection pressures.

7.5) Low Tan Load

Unburnt hydrocarbon Emissions

The levels recorded of gas phase hydrocarbons present in the exhaust system showed elevated quantities at all sample points for all the engine tests. The largest change from the standard build was at 2500 RPM 7.49 Bar (BMEP). The effect of the change in piston ring tangential load was to increase the oil film thickness on the combustion chamber wall. The quantity of this oil that was present in the gas phase hydrocarbons in the exhaust system was not determined. This oil would still be in its liquid state at the temperatures found in the sample system and should not be recorded by the FID, therefore the increase in the levels was attributed to the fuel being adsorbed and desorbed in the oil in the combustion chamber. The effects of pyrolysis on the lubricating oil produced small hydrocarbon molecules that could be transported to the detector. The thicker oil film would also lead to a greater quantity of bulk loss oil. Bulk loss is where the oil is removed from the surface in the form of droplets. The region that contributes the most to this is the area around the piston ring gap. The gas flow through the ring gap has a higher velocity than the gases flowing around the ring groove. This velocity is sufficient to transport the oil into the combustion chamber.

Particulates

The level of total particulate at idle was the highest of all the engine builds and this engine test was the only test to show an obvious level of soot within the particulate matter at idle.

There was a discernible drop in the soot level at all test points except the 2500 RPM 7.49 Bar (BMEP) where the levels were the same. This drop did not match the values for the total particulate values and showed an increase at the three highest engine output test points.

When compared to the standard engine the quantity of SOF increased with load at all test points at 1600 RPM until at 8.59 Bar (BMEP) the mass emissions were twice that

of the standard engine. The increase in the SOF component of the particulate measurement was attributed to the bulk loss oil being transported to the filter and this oil contributing to the adsorbtion and desorbtion effects. The lower total particulate measurement at idle could be partially due to the lower friction of the ring pack. The fuel consumption for this test was always at or below the lower levels for the standard test but the difference could not be accurately determined.

SOF speciation

The measured alkane species for this build were reduced in the number that were detected, i.e. the levels of dodecane and tetradecane were indistinguishable from the base line of the chromatogram and thus impossible to integrate. The base line of the chromatograms for this set of samples showed the largest amount of base line drift. The increase in drift had the same profile as a chromatogram of neat engine oil. Engine lubricating oil does not separate into its constituent parts within the type of gas chromatograph and column used for this series of tests and therefore, the resulting chromatogram is just a large 'hump'. If used oil was analysed the fuel desorbed within it showed as spikes. The survivability percentage for the species octadecane through to docasane at idle were the highest of any of the tests. The greatest change was Hexadecane for the standard build. As the exhaust port temperature increased the levels decreased until at 2500 RPM 7.49 Bar (BMEP) there was insufficient quantity to measure. For this build the hexadacane measurement for Idle was only 50% of that of the standard build. For the test point 1600 RPM 2.86 and 5.72 Bar (BMEP) the levels were approximately the same but for the next two test points the level increased dramatically. At 1600 RPM 8.59 Bar (BMEP) the level was 10 times that of the standard engine. Where the hexadecane level was 0 for 2500 RPM 7.49 Bar (BMEP) with the standard engine for this test, the level was 1.52 g/hr.

Model

The model predicted the same levels of soot particles as the standard build for the low tangential build.

The contribution the cylinder boundaries made to the uHC was not of significance to show any change in the total levels. The model showed that the increase in oil film thickness allows more of the fuel stored in the fuel air mixture at the cylinder wall to enter into the oil film and be released later in the cycle into a cooler region and not be subjected to oxidation and/or pyrolysis. The oil film having twice the thickness gave an increase in the adsorbed fuel of between 50 and 63% . The greatest increase was at 1600 RPM 5.72 Bar (BMEP). It was expected that the highest value would be for the highest load at 1600 RPM but this was not so. The greater pressure differential between each data point for the higher load allowed the adsorbed fuel to desorb quicker. The faster desorption rate reduced the quantity of fuel remaining in the oil when the exhaust value opened. The increase in adsorption of the fuel into the oil at higher engine loads produced a drop in the unburnt fuel in the 1^{st} and 2^{nd} lands. This is because the quantity of the fuel flowing into the crevice volumes was the same for this build as the standard but the oil film could adsorb more.

7.6) High Top Ring

Unburnt hydrocarbon Emissions

The uHC results for this build showed very similar results to those of the standard build. Where a reduction in uHC was expected these results were typically slightly higher for this test than the standard, except at 2500 7.59 Bar (BMEP) where there was a slight reduction. Any effect the reduction in the crevice volume had on the uHC emissions was negated by the presumed reduction in piston temperature, producing lower evaporation rates of any fuel that had impinged on the combustion

chamber wall. The effect that the enlarged second land had on the crevice gases and the motion and stability of the ring pack could also contribute to this increase.

Particulates

The levels of both soot and SOF were very similar to those from the standard tests. The only test that showed any significant variation was 1600 RPM 8.59 Bar (BMEP) where the soot level was approximately 16% lower.

SOF speciation.

The two lower speed test points produced lower levels of measured alkanes than the standard engine but the three other samples recorded much higher levels of all alkanes. The levels of the alkanes that were too low to determine in the standard engine were clearly detected and quantified for this test. Where the measured alkanes within the SOF at idle for the standard build accounted for 81.7%, this test only produced 58.9% of these alkanes. The test points that showed low levels of the measured range of alkanes on the standard test, i.e. where the exhaust and thus the combustion temperatures were higher, showed elevated levels on this test. The rise in these alkanes for this test was attributed to the lower piston temperature. The increase in the combustion temperature corresponds to the increase in fuel quantity and to achieve sufficient fuel flow the duration of injection is longer and the injection pressure is high. This increase in fuel flow will allow more fuel to impinge on the piston crown. Any fuel molecules in the proximity of the cooler piston crown would be subjected to much lower levels of pyrolysis. The higher top ring gave a shorter heat path from the piston crown to the liner and this allows the heat to be transferred from the piston more quickly. It was expected that this would reduce the temperature of the gas during the compression stroke and produce a longer delay period. Additionally during the expansion stroke the cylinder pressure was expected to drop at a greater rate. Both these effects were not detectable from the cylinder pressure readings and the change was assumed to be smaller than the cycle to cycle variability.

The measurement of the cylinder pressure was an average of many cycles, typically 50, to remove this variation.

Model

The pressure within the second land reaches its maximum later in the cycle than when compared to the standard build and the pressure attained was significantly lower also. There have been many studies on the effect of inter ring gas pressures on the stability of the ring pack. The model does not have the facility to replicate the movement of the rings but future work could incorporate this. This lower pressure for a longer duration implies that the top ring would move from off its lower face later in the cycle. This later ring movement, combined with the later release of the crevice gas within the cycle, allows an increase in the hydrocarbons retained within the crevice volumes to be released into a cooler combustion chamber. The higher pressure within the second land allowed the fuel to have a longer period in contact with the oil at pressures that allow adsorption. The pressure being released later in the cycle allows all fuel that is retained in the oil below the first ring to enter into the combustion chamber and there is little or no oxidation of the fuel. The results from the model showed that at 2500 RPM 7.49 Bar (BMEP) this pressure produced four times the adsorption/desorption component for unburnt fuel than the standard build. At all other speeds and loads the adsorption/desorption component was approximately one third of the standard result.

The results for this model produced a drop in top land and first ring groove unburnt hydrocarbons of 50% at idle to 70% at 1600 RPM 8.59 Bar (BMEP). The result for idle follows because the volume was reduced by 50%. The result for the higher speeds and loads was reduced because the fuel air mixture flowing into the first land in the latter stages of the expansion stroke are from a larger than standard second land and the concentration of the fuel is less.

8.0) Conclusion

8.1) Experimental

These experiments showed that the cylinder boundaries influence the composition of the unburnt hydrocarbons present in the exhaust gas stream and with careful design these emissions could be reduced. The changes to the total mass emissions were typically small but the composition of the particulate SOF was clearly discernible. The large change in the particulate SOF composition indicated that the contribution to the uHC by each formation mechanism had changed and that these changes had cancelled each other. The emphasis of the research was to determine the effects of the changes to the cylinder boundaries and any reduction in the engine out emissions would be a bonus.

To achieve the same degree of reduction in exhaust gas composition with modifications to the fuel injection equipment would be both easier and quicker to attain. The influence that the low tangential load oil control ring had on other factors relating to the emissions were determined but not accurately. The main factors that changed were that the FMEP of this engine build was reduced considerably and there was a noticeable increase in the lubricating oil content of the SOF sample. The high top ring produced results that were similar to the standard test but the larger volume below the top ring in the second land would change the ring pack dynamics and alter the temperature profile of the piston. Any benefit from the reduced top land crevice was masked by these changes. The changes to the cylinder boundaries influenced many uHC formation mechanisms. These changes had the effect that where one could be beneficial the others could be detrimental to the same or lesser degree, and thus the net result would be no change.

The gas phase uHC emissions increased with engine load but, as shown in the graphs in chapter 5 of the hydrocarbon species, the average molecular weight of the hydrocarbon species also increased. This increase in molecular weight caused a greater component of the sample to have a boiling point above that of the sample

system, and thus the quantity of the sample that would condense in the sample system would rise and produce a reading lower that the true value.

8.2) Gas Chromatography

The analysis of the alkane species present in the particulate SOF by HPLC showed that the distribution of the species is sensitive to engine operating condition and in cylinder design considerations. The additional oil caused by the reduction of the oil control rings' tangential load and the possible additional oil in the combustion chamber had a pronounced effect on the measured species. The low speed levels of the eleven measured species was very similar to that of the fuel injected. The SOF from samples where the engine was operating at higher loads contained a greater quantity of hydrocarbon species that were not being measured when compared to those taken at lower speeds. The average weight of the alkanes in the SOF sample increased with increasing load or speed. The increase in load or speed also increases the pre-reaction rate of the charge, thus there will be a greater quantity of unburnt hydrocarbons in the particulate SOF that were not measured in these tests.
The testing of the hydrocarbon species could be enhanced considerably if the gas phase of the exhaust could be speciated using a traditional capillary gas chromatograph. At present this is not possible because the stationary phase used in the column is very sensitive to oxygen and there are always significant quantities present in the exhaust gas of a diesel engine. The elevated temperature used in the oven of a gas chromatograph causes any oxygen present in the sample to oxidise the stationary phase within the capillary column. Additionally the number of hydrocarbon species to be studied should be increased and should include aromatic hydrocarbons as these are more resistant to pre-reactions than alkanes, thus giving a greater indication of the in-cylinder events.

8.3) Modelling

The model produced results that correlated well with those obtained empirically. The model could reproduce the same trends as seen from the engine testing but the results for the boundary calculations were significantly smaller than those for the fuel spray and thus the value calculated did not represent the value obtained empirically . The reason for this lower value is that the model could not accurately repeat the movement of the fuel within the combustion chamber and thus the boundary effects were not repeated to the same extent. The model would be greatly enhanced if there were a greater number of calculated zones. The increase in the number of zones would allow greater accuracy of all calculated components, with the movement of the fuel molecules within the cylinder showing the largest benefit of this modification. The model predicted the same level of soot for each engine configuration whereas the engine tests produced differing results. The calculation for the soot only used the values for the main combustion chamber and did not include those for the crevice effects and the inclusion of these within the model would produce a better correlation of results.

8.4) Piston Design

The change that influenced engine emissions the most was the reduction of the oil control rings tangential load. Where the purpose of the test was to change the oil film thickness, it also increased the oil consumption which masked the effect of the oil film thickness to a certain degree. The high top ring produced results that were similar to the standard but the increase in lighter hydrocarbon species increased. This showed that the greater second land volume combined with the cooler piston crown allowed for slower evaporation of any fuel that impinged on the piston. Any fuel that entered into the crevices could re-enter the combustion chamber at a point where little or no reaction could take place. The influence of the piston land and ring pack design has a greater influence on service life of the components involved than exhaust emission

when oil control is ignored. The design of the ring pack for a successful piston design should concentrate on the following factors. These are not shown in any particular order as the priority changes for each different application.

1) Effective gas sealing
2) Durability and service life
3) Good oil control
4) Effective heat transfer
5) Ease of manufacture

8.5) Other Observations

Engine emission testing is very costly, time consuming and not a very accurate science. Emission measurement taken in one test facility cannot be accurately repeated at another facility using the same equipment, personnel and testing methods. During the period of this research the testing facility was moved to a new location. After the equipment was moved from the old facility to the new the results, although very similar, were not identical. Where the changes were small and some could be attributed to improved knowledge of the testing equipment and methods, the results from the first set of tests were not used in the preparation of this thesis.

Even with modern manufacturing methods two identical items cannot be made. Great care was taken in the selection and assembly of all components used for each engine build but there were still small variations that influenced the results to a minor degree. Fewer cylinders is the best route for engine testing. The more cylinders the greater the cost and complexity of the test facility. There is also data replication that causes unnecessary processing. Also there is more to go wrong and incorrectly functioning components of one cylinder alter the operating conditions of the other cylinders.

9.0) Recommendations for further work.

9.1) Areas of research

Where as this work has added to knowledge about the combustion processes within the diesel engine it supplies an insight into a very small area and many questions remain unanswered. This work has shown that the interaction of the piston and liner alter the composition and quantity of the exhaust gas hydrocarbons by changing one dimension on the piston or the mechanical property of one of the piston rings. Further work is required to develop the ideal dimensions for the complete ring pack. This area includes piston land dimensions, crevice volumes, piston ring profiles and liner finish. The lubricating oil that is present in the working cylinder also influences the emissions and further studies on the oil film thickness and the solubility of the fuel within the oil should be implemented.

The combustion chamber within the piston has a major influence on the emissions and changes within the ring pack can alter the emissions from both the crevice volumes and the combustion chamber. To evaluate the influence of this, a study of the heat flow from the combustion chamber to the ring pack and temperature gradients within the piston during the operating cycle would provide a more accurate data source for the model developed within this research.

9.2) Development of modelling

During the period of this research the cost of computing has fallen dramatically and there have been significant improvements in the area of Computational Fluid Dynamics (CFD). CFD can be easily utilised to determine the air movement within the cylinder and models with moving boundaries can also be implemented to model

the complete cycle. A multi zone model version of the one produced for this research would provide a greater insight into the effects of the in cylinder changes and reproduce in cylinder conditions to a far greater accuracy.

9.3) Analytical techniques

The speciation of the hydrocarbons for this research was from a sample that has been stored in temperature and humidity controlled conditions before being immersed in a strong solvent. During this period the sample would have undergone slight changes. The development of a method that could take gas phase samples and produce the same quantitative analysis would allow the analysis of exhaust gases to be completed quicker and allow all non methyl hydrocarbons to be included in the study.

References

1) Blakey S.C., Foss P.W., Basset M.D. and Yates P.W. "Improved automotive part load fuel economy through late intake valve closing". XIV National Conference on I.C. Engines and Combustion, Puna India, December 8-10 1995.

2) Advisory group on the medical aspects of air pollution episodes (1992) second report: Sulphur Dioxide, Acid aerosols and particulates. HMSO, London.

3) Nakajima. M., Shimoda M. and Nakagome. K. "Relationship between particulates and black smoke / hydrocarbons in diesel engines". Int J. of Vehicle Design, Vol 10, no 3. 1989.

4) Yu R.C., Wong V.W. and Shahed S.M.: " Sources of hydrocarbon emissions from direct injection engines. S.A.E Paper 800048 1980.

5) Daniel, W.A., Wentworth, J.T.: " Exhaust gas hydrocarbons Genesis and Exodus". S.A.E. 486B ,1962.

6) Whitehouse, N.D., Clough, E., and Uhunmwangho, S.O.: " The development of some gaseous products during diesel engine combustion". SAE Paper 800028, 1980.

7) Alcock J.F. and Scott W.M.: "Some more light on diesel combustion". Proc. Auto Div., Institution of Mechanical Engineers, No 5, pp 179 - 191, 1962 - 1963.

8) Lyn, W.T., and Valdmanis, E.: "Effects of physical factors on ignition delay". S.A.E. 680102, 1968.

9) Greeves, G., Khan, I.M. , Wang, C.H.T. and Fenne, I.: " Origins of hydrocarbon emissions from diesel engines". SAE Paper 770259.

10) Farrar-Khan J.R., Andrews G.E., Williams P.T and Bartle K.D.: "The influence of nozzle sac volume on the composition of diesel particulate fuel derived SOF". SAE Paper 921649 1992.

11) Vollenweider, J.:" Emission-optimized fuel injection for large diesel engines-expectations, limitations and compromises ". Proc IMechE C448/003, 1990.

12) Williams, D.J., Milne, J.W, Quigley, S.M.and Roberts, D.B.: "Particulate emissions from "in use" motor vehicles-II Diesel Vehicles". Atmospheric Environment Vol 23, No12, pp 2647-2661 1989.

13) Haynes, B.S. and Wagner, H.G.: "Soot formation" Prog Energy Combustion Science, Vol 7, pp 229 - 273, 1981.

14) Amann, C.A., and Siegla, D.C.: "Diesel particulates-What they are and why." Aerosol Science Technology, vol , pp 73-101, 1982.

15) Schrnweber D.H. and Hoppie L.O.: "Hypergolic combustion in an internal combustion engine". SAE Paper 850089, 1985.

16) Hoppie L.O., Min Y.K., Srinivasan N. and Wu S.H.: "Opimum heat release for a reciprocating internal combustion engine". SAE Paper 870572, 1987.

17) Abbass M.K, Andrews G.E., Ishaq R.B. and Williams P.T.: "A comparison of the particulate composition between turbocharged and naturally aspirated DI diesel engines". SAE Paper 910733, 1991.

18) Schreck R., McGrath J., Swarin S., Herring W., Groblicki P. and MacDonald, "Characterisation of diesel exhaust particulate for mutagenic testing", General Motors Publication GMR 2755, June 25, 1978.

19) Mayer W.J., Lechman D.C.: "The contribution of engine oil to diesel exhaust particulate emissions". SAE Paper 800256, 1981.

20) Wachter W.F., " Analysis of transient emission data of a modelyear 1991 heavy duty diesel engine". Sae Paper 900443, 1990.

21) Cartellieri W. and Tritthart P.: " Particulate Analysis of light duty diesel engines (IDI&DI) with particular reference to the lube oil particulate fraction. SAE Paper 840418, 1984.

22) Zelenka P., Kriegler W., Herzog P.L. and Cartellieri W.P.: " Ways toward the clean heavy duty diesel", SAE paper 900602, 1990.

23) Jakobs R. J. and Westbrooke K.: "Aspects of influencing oil consumption in diesel engines for low emissions". SAE Paper 900587, 1990.

24) Essig G., Kamp H. and Wacker E.: "Diesel engine Emissions reduction-The benefits of low oil consumption design. SAE Paper 900591, 1990.

25) Cooke V. B.: "Lubrication of low emission diesel engines Part 1 and Part 2". SAE Paper 900814, 1990 ISSN: 0148-7191.

26) Kawamoto J., Yamamoto M. and Ito Y.:"Continous measurement of engine oil consumption rate by the use of ^{35}S tracer". SAE Paper 740543 1974.

27) Mayer W.S., Moore C.P Krause C.P., Lange W.H. and Murphy C.B.:"Rapid, Precise measurement of engine oil economy by a radiometric method". SAE Paper 660058, 1966.

28) Guinn V.P. and Coit R.A.:"Measuring oil consumption with tritium tracers". Nucleonics, Vol 17 No 12, 1559, p112.

29) Trier C.J., Petch G.S., Fussey D.E. and Shore P.R.:"Assessing the contribution of lubricating oil to diesel exhaust particulates using geochemical markers. C341/87 pp109 - 117, 1987.

30) Hanaoka M., Ise A., Osawa H., Arakawa Y. and Obata T.:"New method for measurement of engine oil consumption(S-Trace method)". SAE Paper 790936. 1979.

31) Elamir I.E., Andrews G.E. and Williams P.T.:" Determination of diesel engine lubricating oil consumption through analysis of the calcuim in diesel particulates.

32) Heywood J.B.: "Internal Combustion Engine Fundamentals". McGraw-Hill, ISBN 0-07-100499-8.

33) Furuhama,S. Kojima, M. Enomoto,Y. and Yammaguchi,Y: "Some studies on two ring pistons in an automobile turbocharged gasoline engine". SAE Paper 840183 1984.

35) Miyachika M., Hirota K. amd Kashiyama K.: "A consideration on piston second land pressure and oil consumption of internal combustion engine". SAE Paper 840099 1984.

36) Furuhama S. and Hiruma M.: "Some factors on engine oil consumption through a piston". Proc JSLE Int Trib Conf, Tokyo July 8 - 10 p301 1985.

37) Furuhama S.: "Tribology of reciprocating internal combustion engines". JSME Int Journal, vol 30 no 266 pp1189 - 1199 1987.

38) Curtis J.M.: "Piston ring dynamics and its influence on the power cylinder performance". SAE Paper 810935 1981.

39)McGeehan J.A.: "The effect of piston deposits, fuel sulphur and lubricant viscosity on diesel engine oil consumption and cylinder bore polishing". SAE Paper 831720, 1983.

40) Hercamp R.D.: "Premature loss of oil consumption in a heavy duty diesel engine". SAE Paper 831720, 1983.

41) Dowling M., Prichard J.R. and Crawley.: "A severe single cylinder diesel engine test for SHPD oils". SAE Paper 812033, 1981.

42)Furuhama S., Hiruma M. and Enomoto Y.: " The effect of enlarged piston top land clearance on lubricating oil consumption". Bull. JSME vol 29 no 254 1981.

43) Burnett P.J.: "Relationship between oil consumption, deposit formation and piston ring motion for single cylinder diesel engines". SAE Paper 920089, 1992.

44) Eyre T.S., Dent N. and Dale R.: "Wear characteristics of piston rings and cylinder liners". ASLE/ASME Conterence New Orleans Louisiana, Oct 5-7 1981.

45) Siegl W.O., Jensen T.E: "Advanced emission speciation methodologies for auto/air quality improvement". SAE Paper 920320, 1992.

46) Sweeney E.G., Baudino J.H. Schmidt C.H.: "Composition of vehicle emissions - An analytical speciation program" SAE Paper 922253, 1992.

47) Lewton J.:"Toxicological effects of emissions from diesel engines". Elsever, New York, 1982.

48) National Research Council: "Impacts of diesel powered light duty vehicles". Diesel Technology US Govenment printing office, Washington, DC 1982.

49) National Reserch Council: "Health effects of exposure to diesel exhausts". US Govenment printing office, Washington, DC 1981.

50) Williams P.T., Bartle K.D. and Andrews G.E.: " The relationship between polycyclic aromatic compounds in diesel fuels and exhaust particulates". FUEL Vol 65, pp1150 - 1158, August 1986.

51) Lipkea W.H., Johnson J.H. and Vuk C.T.: SAE Paper 780108, 1978.

52) Williams R.L. and Swarin S.J. SAE Paper 790419, 1979.

53) Ciajolo A., D'anna A., and Barbella R.:"Combustion of tetradecane and tetradecane/α-methylnapthalene in a diesel engine with regard to soot and PAH formation". Combustion Science and Technology 1992 Vol 87 pp127-137.

54) Abbass M.K, Andrews G.E., Bartle K.D and Williams P.T.: "Condensible unburnt hydrocarbon emissions from a DI diesel engine", Proc international centre for heat and mass transfer pp 643-655 1989 ISSN 0272-880x.

55) Sagebiel J.C., Zielinska B., Pierson W.R. and Gertler A.W.: "Real world emissions and calculated reactivities of organic species from motor vehicles". Atmospheric Environment Vol 30, No 12 pp2287 - 2296, 1996.

56) Rassweiler G.M. and Withrow L: "Motion pictures of engine flames correlated with pressure cards". SAE Paper 800131 (first presented in 1938).

57) Blizard N.C. and Keck J.C.: "Experimental and theroetical invesitgation of turbulent burning model for internal combustion engines". SAE Paper 740191, SAE Tranactions, Vol. 83, 1974.

58) Harrington J.A.: "Application of a new combustion analysis method in the study of alternative fuel combustion and emission charicteristics". Future Automotive Fuels, edited by J.M. Colucci & N.E. Gallopoulos, pp. 177-210, Plenum Press, 1977.

59) Lyn W.T.: "Calculations of the effect of rate of heat release on the shape of cylinder pressure diagram and cycle efficiency". Proc Inst Mech Engrs, No 1, pp 34-46, 1960-1961.

60) Austen A.E.W. and Lyn W.T.: "Relationship between fuel injection and heat release in a direct injection engine and the nature of the combustion process". Proc Inst Mech Engrs, No 1, pp 47-62, 1960-1961.

61) Lyn W.T.: "Study of burning rate and nature of combustion in diesel engines". IX Symposium (International) on Combustion, Proceedings, pp 1069-1082, the Combustion Institute, 1962.

62) Gatowski J.A., Balles E.N., Chun K.M., Nelson F.E., Ekchain J.A. and Heywood J.B.: "Heat release analysis of engine pressure data". SAE Paper 841359, 1984.

63) Ishida, M., et al: "Studies on combustion and exhaust emissions in a high speed DI diesel engine" SAE Paper 901614, 1990.

64) Boyce T.R., Karim G.A. and Moore N.P.W.: "The effects of some chemical factors on combustion processes in diesel engines." Proc Instn Mech. Engrs, Vol. 184, pt 3J, pp137 - 146.

65) Fosberry R.A.C. and Gee D. E., " Some Experiments on the Measurement of Exhaust Smoke Emission from Diesel Engines."
M.I.R.A. Report 1961/5, 1961.

66) Ciccioli, P et al. Journal of Chromatography, 351 (1986) pp 451 - 464

67) Furuhama S., and Suzuki H.: "Temperature distribution of piston rings and piston in high speed diesel engine." Bull JSME, vol 22, No 174, pp 1788 - 1795, 1979.

68) Woschini G.: "Prediction of thermal loading of supercharged diesel engines." SAE Paper 790821, 1979.

69) Li C-H.: "Piston Thermal deformation and friction considerations." SAE Paper 820086, 1982.

70) Krieger, R. B., and Borman, G. L.: "The computation of apparent heat release for internal combustion engines", ASME paper 66-WA/DGP-4, in Proc. Diesel Gas Power, ASME 1966.

71) Ofner H: "A general purpose simulation for high pressure fuel injection systems and other mechanical-hydraulic systems", IMechE 1991, C430/009, pp 269 - 282.

72) Timoney D.J.: "Energetics of fuel-air mixing in D.I. diesel engines", Proc ICHMT conference on heat and mass transfer in gasoline and diesel engines, Dubrovnik, Yougoslavia, 1987, Hemisphere Publishing Corp 1989, pp189 - 199.

73) Smith W.J., Timoney B.E. and D.J., " Fuel injection rate analysis using measured data", IMechE 1991, C430/057, pp 283 - 288.

74) Dent,J.C.: "Basis for the comparison of various experimental methods for studying spray penetration" SAE paper 710571, SAE Trans., Vol 80, 1971.

75) Korematsu,K: "Effects of fuel absorbed in oil film on unburnt hydrocarbon emissions from spark ignition engines". Japanese Society of Mechanical Engineers. 1990. Vol. 33. No.3 pp 606-614.

76) Dent,J.C. and Lakshminarayanan,P.A: A model for absorption and desorption of fuel vapour by cylinder lubricating oil film and its contribution to HC emissions. SAE paper 830652, 1983.

77) Chappelow,C.C. and Prausnitz,J.M: Solubilities of gases in high boiling hydrocarbon solvents. AIChE Journal. 1974. Vol 20, No 6. pp 1097-1104.

78) Shapiro H.: The dynamics and thermodynamics of compressible fluid flow Vol. 1. Ronald Press company New York, 1954.

79) Namazian M. and Heywood J.B.: Flow in the piston-cylinder-ring crevices of a spark-ignition engine: Effect on hydrocarbon emissions, Efficiency and power. SAE paper 820088, 1982.

80) Kue,T.W. Seenau,M.C. Theobald,M.A. and Jones,J.D: Calculation of flow in the piston-cylinder-ring crevices of a homogenous charge engine and comparison with experiment. SAE 890838, 1989.

81) Whitehouse N.D. and Way R.: "Rate of heat release in diesel engines and its correlation with fuel injection data", Proc Instn Mech Engrs, vol 184, pt 3, Paper 1, pp 17 - 27 1969-1970

82) Park C., and Appleton J. P.: "Shock tube measurements of soot oxidation rates." Combustion Flame, vol 20, pp 369-379, 1973.

83) Nishida K. and Hiroyasu H. "Simplified three dimensional modelling of mixture formation and combustion in a DI diesel engine". SAE 890269, 1989.

84) Matsui Y., Kanimoto T. and Matsuoka S. " Formation and oxidation processes of soot particles in a DI diesel engine - An experimental study via the two colour method". SAE 820464, SAE Trans., vol 91, 1982.

85) Greeves G. and Wang C.H.T. "Origins of diesel particulate mass fraction". SAE 810260, SAE Trans 1981.

86) Wiess P and Keck J.C.: "Fast sampling valve measurements of HC's in the cylinder of a CFR engine". SAE 810149.

87) Barr W.G: "Low heat rejection diesel engines". PhD thesis University of Notingham May 1990.

88) Nishida K. and Hiroyasu H. "Simplified three dimensional modelling of mixture formation and combustion in a DI diesel engine". SAE 890269, 1989 from modelling ref 11.

Std Pistons											
Piston No	Dia "A1"	Dia "G"	Dia "F"		Ave Top			Dia "D"	Dia "E"	Dia	Dia
		- From A1			Land Dia			- From A1		top 2 land	bot 2 land
15	99.943	0.659	0.586	99.357	99.321	99.284		-0.387	-0.456	99.556	99.487
12	99.949	0.655	0.592	99.357	99.326	99.294		-0.391	-0.459	99.558	99.49
5	99.952	0.656	0.592	99.36	99.328	99.296		-0.39	-0.46	99.562	99.492
13	99.949	0.652	0.588	99.361	99.329	99.297		-0.389	-0.458	99.56	99.491
14	99.949	0.651	0.589	99.36	99.329	99.298		-0.392	-0.46	99.557	99.489
11	99.95	0.652	0.589	99.361	99.330	99.298		-0.39	-0.458	99.56	99.492
6	99.95	0.652	0.587	99.363	99.331	99.298		-0.386	-0.455	99.564	99.495
9	99.95	0.651	0.588	99.362	99.331	99.299		-0.388	-0.454	99.562	99.496
10	99.95	0.65	0.587	99.363	99.332	99.3		-0.387	-0.455	99.563	99.495
4	99.953	0.652	0.588	99.365	99.333	99.301		-0.389	-0.455	99.564	99.498
7	99.95	0.648	0.586	99.364	99.333	99.302		-0.386	-0.453	99.564	99.497
2	99.955	0.653	0.59	99.365	99.334	99.302		-0.391	-0.457	99.564	99.498
1	99.958	0.653	0.592	99.366	99.336	99.305		-0.393	-0.459	99.565	99.499
High Top Ring Pistons											
1	99.952	0.66		99.952	99.622	99.292		0.393	0.46	99.559	99.492
2	99.951	0.659		99.951	99.622	99.292		0.392	0.46	99.559	99.491
3	99.951	0.66		99.951	99.621	99.291		0.393	0.459	99.558	99.492
4	99.95	0.66		99.95	99.620	99.29		0.392	0.46	99.558	99.49
5	99.95	0.66		99.95	99.620	99.29		0.39	0.461	99.56	99.489
6	99.949	0.659		99.949	99.620	99.29		0.391	0.459	99.558	99.49
7	99.948	0.663		99.948	99.617	99.285		0.393	0.462	99.555	99.486

Liner 1	Dist from top	"A" Axis	"B" Axis	Ave top
	0	100.001	100.054	100.0275
AVE "A"	12.5	100.072	100.049	
100.0505	25	100.054	100.045	
DEV "A"	50	100.051	100.044	
0.017495	75	100.055	100.041	
	100	100.056	100.039	
AVE "B"	125	100.053	100.04	
100.0453	150	100.051	100.034	
DEV "A"	175	100.05	100.046	
0.006754	200	100.053	100.049	
	215	100.059	100.057	
Liner 2	Dist from top	"A" Axis	"B" Axis	Ave top
	0	100.008	100.072	100.0400
AVE "A"	12.5	100.013	100.068	
100.0292	25	100.02	100.072	
DEV "A"	50	100.023	100.065	
0.012319	75	100.027	100.06	
	100	100.03	100.055	
AVE "B"	125	100.033	100.053	
100.0584	150	100.038	100.052	
DEV "A"	175	100.04	100.048	
0.009458	200	100.045	100.049	
	215	100.044	100.048	

Liner 3	Dist from top	"A" Axis	"B" Axis	Ave top
	0	100.068	100.055	100.0615
AVE "A"	12.5	100.056	100.041	
100.0495	25	100.055	100.045	
DEV "A"	50	100.054	100.052	
0.008104	75	100.05	100.057	
	100	100.046	100.062	
AVE "B"	125	100.043	100.069	
100.0628	150	100.042	100.075	
DEV "A"	175	100.042	100.076	
0.01387	200	100.043	100.079	
	215	100.046	100.08	
Liner 4	Dist from top	"A" Axis	"B" Axis	Ave top
	0	100.05	100.061	100.0555
AVE "A"	12.5	100.035	100.052	
100.0707	25	100.038	100.053	
DEV "A"	50	100.054	100.053	
0.023444	75	100.063	100.048	
	100	100.077	100.047	
AVE "B"	125	100.088	100.047	
100.0475	150	100.091	100.047	
DEV "A"	175	100.093	100.044	
0.007594	200	100.096	100.038	
	215	100.093	100.033	

Liner 5	Dist from top	"A" Axis	"B" Axis	Ave top
	0	100.03	100.045	100.0375
AVE "A"	12.5	100.034	100.037	
100.0357	25	100.037	100.038	
DEV "A"	50	100.04	100.043	
0.002936	75	100.039	100.043	
	100	100.036	100.04	
AVE "B"	125	100.034	100.037	
100.0417	150	100.034	100.038	
DEV "A"	175	100.034	100.04	
0.004541	200	100.036	100.047	
	215	100.039	100.051	
Liner 6	Dist from top	"A" Axis	"B" Axis	Ave top
	0	100.069	100.044	100.0565
AVE "A"	12.5	100.048	100.056	
100.058	25	100.048	100.055	
DEV "A"	50	100.048	100.053	
0.008854	75	100.05	100.05	
	100	100.053	100.049	
AVE "B"	125	100.058	100.047	
100.0517	150	100.063	100.052	
DEV "A"	175	100.065	100.053	
0.003823	200	100.068	100.055	
	215	100.068	100.055	

Liner 7	Dist from top	"A" Axis	"B" Axis	Ave top
	0	100.06	100.043	100.0515
AVE "A"	12.5	100.046	100.046	
100.0601	25	100.05	100.05	
DEV "A"	50	100.053	100.051	
0.009428	75	100.058	100.05	
	100	100.057	100.05	
AVE "B"	125	100.059	100.047	
100.0475	150	100.061	100.045	
DEV "A"	175	100.066	100.043	
0.002876	200	100.073	100.048	
	215	100.078	100.049	
Liner 8	Dist from top	"A" Axis	"B" Axis	Ave top
	0	100.063	100.051	100.0570
AVE "A"	12.5	100.05	100.048	
100.0567	25	100.052	100.051	
DEV "A"	50	100.057	100.058	
0.003797	75	100.053	100.058	
	100	100.056	100.064	
AVE "B"	125	100.06	100.069	
100.059	150	100.059	100.066	
DEV "A"	175	100.059	100.064	
0.006782	200	100.058	100.062	
	215	100.057	100.058	

Liner 9	dist from top	Axis A	Axis B	Ave top
	0	100.064	100.069	100.0665
AVE "A"	12.5	100.042	100.064	
100.0476	25	100.039	100.042	
DEV "A"	50	100.04	100.06	
0.010337	75	100.041	100.062	
	100	100.041	100.062	
AVE "B"	125	100.041	100.061	
100.0629	150	100.043	100.064	
DEV "A"	175	100.048	100.066	
0.008142	200	100.058	100.067	
	215	100.067	100.075	
Liner 10	dist from top	Axis "A"	Axis "B"	Ave top
	0	100.014	100.085	100.0495
AVE "A"	12.5	100.016	100.065	
100.0304	25	100.018	100.061	
DEV "A"	50	100.03	100.058	
0.01023	75	100.032	100.055	
	100	100.032	100.051	
AVE "B"	125	100.033	100.047	
100.0547	150	100.035	100.047	
DEV "A"	175	100.038	100.046	
0.012386	200	100.041	100.044	
	215	100.045	100.043	

Liner 11	dist from top	Axis "A"	Axis "B"	Ave top
	0	100.065	100.032	Ave top
AVE "A"	12.5	100.05	100.031	100.0405
100.047	25	100.052	100.035	
DEV "A"	50	100.052	100.04	
0.007987	75	100.049	100.042	
	100	100.045	100.043	
AVE "B"	125	100.04	100.043	
100.0452	150	100.038	100.046	
DEV "A"	175	100.037	100.051	
0.012368	200	100.043	100.064	
	215	100.046	100.07	
Liner 12	dist from top	Axis "A"	Axis "B"	Ave top
	0	100.081	100.058	100.0695
AVE "A"	12.5	100.064	100.046	
100.0668	25	100.071	100.056	
DEV "A"	50	100.075	100.064	
0.008693	75	100.07	100.063	
	100	100.071	100.068	
AVE "B"	125	100.071	100.072	
100.0667	150	100.065	100.075	
DEV "A"	175	100.06	100.077	
0.010384	200	100.056	100.077	
	215	100.051	100.078	

Speed/ Load	Build	Piston Temp °C (°K)	Liner Temp °C	Inlet air Temp °C	Man Pressure mm HG	Oil Temp °C	Oil Film Thickness um	Exhaust O2 %	Exhaust Temp °C	Top land height mm	2nd land height mm	Start of injection °	End of injection °	Injection pressure bar	Start of combustion °
Idle	Std	80 (355)	80	27	-5	78.6	0.244	18.95	113	10	4.5	347	351	99.7	359
	LTL	80 (355)	80	27	-5	78.6	0.488	18.95	103	10	4.5	347	351	99.7	359
	HTR	79 (354)	80	27	-5	78.6	0.244	18.95	113	4.5	10	347	351	99.7	359
1600/2.86	Std	114 (389)	89	34	41	84.6	0.244	15.68	263	10	4.5	348	356	128.7	361
	LTL	114 (389)	89	34	41	84.6	0.488	15.68	258	10	4.5	348	356	128.7	361
	HTR	112(387)	89	34	41	84.6	0.244	15.68	263	4.5	10	348	356	128.7	361
1600/5.72	Std	177 (452)	93	43	95	87.6	0.244	12.53	375	10	4.5	347	365	133.5	357
	LTL	177 (452)	93	43	95	87.6	0.488	12.53	375	10	4.5	347	365	133.5	357
	HTR	170 (445)	93	43	95	87.6	0.244	12.53	375	4.5	10	347	365	133.5	357
1600/8.59	Std	200 (475)	100	60	168	94.8	0.244	10.44	490	10	4.5	345	368	148	354
	LTL	200 (475)	100	60	168	94.8	0.488	10.44	490	10	4.5	345	368	148	354
	HTR	190 (465)	100	60	168	94.8	0.244	10.44	490	4.5	10	345	368	148	354
2500/7.49	Std	230 (505)	120	67	280	103.8	0.244	10.74	580	10	4.5	345	368	236	356
	LTL	230 (505)	120	67	280	103.8	0.488	10.74	580	10	4.5	345	368	236	356
	HTR	200 (475)	122	67	280	103.8	0.244	10.74	580	4.5	10	345	368	236	356

Appendix 2 Model input parameters

```
DECLARE SUB OXIDAT ()
DECLARE SUB SPRAY ()
DECLARE SUB CREVICE ()
DECLARE SUB INSCREEN ()
DECLARE SUB FILEIN ()
COMMON SHARED injdegs  'time for max fuel penertration
COMMON SHARED inflag, FILENAME$
DEFSNG A-Z
ON ERROR GOTO HANDLER

'*******************************************************
'****** Temperature and heat relese model ***************
'******     FINISHED version 31/05/98     ***************
'******     OXFLAG SET TO  0.1 AND 0.9    ***************
'*******************************************************
' demension arrays
 DIM SHARED avl!(24, 640)  'DEGREES(1) AND PRESSURE (2)GAS TEMP(3)
 DIM SHARED MOR!(2, 640)'Molar weight of combustion gasses 1,fuel dist 2
 DIM SHARED bit!(4, 24)' ODDS
 DIM SHARED NAM$(1, 18)' INSCREEN TITLE ARRAY
 DIM SHARED PWY$(40) 'FILENAMES
 DIM SHARED PWY2$(40) 'DIRECTORYS
 DIM SHARED AVE$(40)
 'COMMON D, n, Hg, Tgi, Pamb,
 'AND HEAT RELEASE PER CRANK ANGLE(4) AND TOTAL(5)  % burnt(6)
FUEL SPRAY(7)
 'MASS OF FUEL(8) MOR (9) MTOT(10) M1RG (11) M2nd(12 P2RG (130 M1ST
LAND (14
 ' SOOT (15) FUEL HC (16) ADS DES (17)
 DIM CROSS%(100)    ' CIRCLE ON SCREEN
'***Original data for engine
DATA 38, 0.219, 0.1, .127, 16.5, 1600, 179, .099286,0.1
DATA  95,43, 999,0.244 ,0.01, 0.09952, 0, 452 , 12.53
'*** read in constants
FOR Z% = 1 TO 18
        READ bit!(2, Z%)
NEXT Z%
'set flag (inscreen)
inflag = 0
'** CONSTANT NAME
DATA TEST NO,CON ROD Lth (m),BORE(m),STROKE(m),COMP
RATIO,SPEED(RPM),LOAD(Nm),PISTON DIA(m) ,LINER DIA(m)
DATA MANIFOLD P(mmHg),AIR TEMP(C),AIR P(mbar),OIL LAYER um,LAND
HT(m),2ND LAND DIA(m),2ND LAND VOL(m^3),PISTON TEMP(K), EXHAUST
(O2)
```

```
'*** read in constant names
FOR Z% = 1 TO 18
        READ NAM$(1, Z%)
NEXT Z%
9
ERASE avl!, MOR!
FOR Z% = 0 TO 24
   bit(3, Z%) = 0  ' Reset Max Values
NEXT Z%

injdegs = 0
flag = 0
'********************
'RESET THE MAX VALUE
FOR Z% = 1 TO 21
    bit!(3, Z%) = 0
NEXT Z%
CLS
'***GOSUB FILIN GET FILE NAME
FILEIN

'*** gosub to inscreen
INSCREEN
'*** check for quit flag
IF bit!(1, 4) = 99 THEN GOTO 1000
 '***Define Constants
     '***constants to calculate gamma
          CONST G1 = -6.214E-12, G2 = 5.26449E-08, G3 = -.000155656#
          CONST G4 = 1.44722
     '***crank shaft throw = r and con rod length = L
           R = bit!(4, 4) / 2
           L = bit!(4, 2)
     '***Univ. gas const = Ro  kJ/kg   mol Wt of mixture = Mr
          CONST Mr = 30.35, RO = 8.314, PI = 3.1415927#


CLS 0
PRINT "PLEASE WAIT , THE INITIAL VALUES ARE BEING CALCULATED"

 ' Calculate sub functions, Ma  mass air in chamber.
 ' manifold pressure ref atmosphere
 Mp = bit!(4, 12) * 100 + (13600 * 9.81 * bit!(4, 10) / 1000)
 bit!(1, 1) = Mp
 Inlet = 213 * PI / 180    'inlet valve closing
 ' ** Calculate swept volume
 VSW = (PI * bit!(4, 3) ^ 2 * .127) / 4
```

```
' ** Calculate trapped air volume
Vs2! = SQR(L ^ 2 / R ^ 2 - (SIN(Inlet)) ^ 2)
Vs1 = (PI / 4) * bit!(4, 3) ^ 2 * R * ((1 - COS(Inlet)) + L / R - Vs2!)
Vcyl = Vs1 + (VSW / (bit!(4, 5) - 1))
Tgi = bit!(4, 11) + 273
' **  Calculate mass of trapped air
ma = Mp * Vcyl / ((RO / Mr) * 1000 * Tgi)
bit!(1, 2) = ma
PRI = 110000
PVi! = .0003
nti = -.0004
'***************** The data file is from 123 using print file, there must be
'** read in data**  a blank colum between the two data colums. use as-displayed
'*****************  and unformatted
DII = 1
          OPEN "i", 2, FILENAME$
  DO WHILE NOT EOF(2)
             INPUT #2, A$
                B$ = A$
                deg! = VAL(LEFT$(B$, 5))
                   IF deg! < 180 THEN
                   DI2 = 1
                   GOTO 70
                   ELSE
                DI% = ((deg - .1) - 180) + .5
                rad = deg! * PI / 180
                avl!(1, DI%) = rad
                xs = LEN(A$)
                P = VAL(RIGHT$(A$, 9))
            PC = P * 100000
            avl!(2, DI%) = PC
                 END IF
                '*** get max pressure
                IF bit!(3, 2) > avl!(2, DI%) THEN GOTO 69
                IF avl!(2, DI%) < avl!(2, DI% - 1) THEN bit!(3, 2) = avl!(2, DI% - 1)
69
70
 LOOP
       CLOSE #2
```

```
'************************************************
'*** gas temperature and change in heat energy ***
'************************************************
dQtot = 0
FOR t1 = 2 TO 640
    deg! = avl!(1, t1) * 180 / PI
    IF avl!(1, t1) = 0 THEN avl!(3, t1) = Ta: GOTO 220
    ' ** Pc = current cylinder pressure N/m^2
    dp! = avl!(2, t1) - PRI
    ' ** Calcs to define volume
    V2S! = SQR(L ^ 2 / R ^ 2 - (SIN(avl!(1, t1))) ^ 2)
    PV! = PI / 4 * bit!(4, 3) ^ 2 * R * ((1 - COS((avl!(1, t1)))) + L / R - V2S!)
    VOL! = PV! + (VSW / (bit!(4, 5) - 1))
    REM calcs for gas temperature.
    IF PRI / avl!(2, t1) = 1 THEN
            nt = nti
            ELSE
            nt = LOG(PRI / avl!(2, t1))
    END IF
    nb = LOG(ABS(VOL! / PVi!))
    IF P < 4.5 THEN
            nu = 1.3
            ELSE
            nu = (nt * 1.1) / nb
    END IF
    ni = (nu - 1) / nu
    dT = (((avl!(2, t1) / PRI) ^ ni) - 1) * Tgi
    Tgc = Tgi + (dT * 2.2) 'MODIFY
    avl!(3, t1) = Tgc
                IF bit!(3, 3) > avl!(3, t1) THEN GOTO 136
                IF avl!(3, t1) < avl!(3, t1 - 1) THEN bit!(3, 3) = avl!(3, t1 - 1)
136


    ' calcs for heat release
    '**********************
```

```
    ' define gamma
    '*************
    gamma = G1 * Tgc ^ 3 + G2 * Tgc / 2 + G3 * Tgc + G4
    IF gamma < 1.28 THEN gamma = (G1 * Tgc ^ 2) + 1.2797
    ' heat release per crank angle dQ!
    ' set ignition start A = 341, B = 332 C=337, D & E = 340, F = 345
    IF deg! < 359 THEN
            dQ! = 0: GOTO 156
            ' set end of combustion
            ELSEIF deg! > 400 THEN
            dQ! = 0: GOTO 156
            ' CHANGE SIGN OF DP!
            ELSEIF dp! < 0 THEN
            dp! = dp! * -1: GOTO 150
            ELSE : GOTO 150
    END IF

150         dQ2 = ((1 / (gamma - 1)) * VOL! * dp!)
            dQ! = ((gamma / gamma - 1) * avl!(2, t1) * (PVi! - VOL!)) + dQ2
156
            '*** get max heat per degree
            avl!(4, t1) = dQ!
                IF t1 < 3 GOTO 166
                IF bit!(3, 4) > avl!(4, t1) THEN
                GOTO 166
                ELSE
                bit!(3, 4) = avl!(4, t1)
                END IF
166

    IF dQ! < 0 THEN
            dQtot = dQtot
            ELSE
            dQtot = dQtot + dQ!

    END IF
    PRI = avl!(2, t1)
    PVi! = VOL!
    nti = nt
    Tgi = Tgc
```

```
   IF dQall < dQtot THEN dQall = dQtot
   avl!(5, t1) = dQtot
                IF t1 < 3 GOTO 178
                IF bit!(3, 5) > avl!(5, t1) THEN
                GOTO 178
                ELSE
                bit!(3, 5) = avl!(5, t1)
                END IF
178

'**************************
'***FUEL SPRAY PENETRATION**
'**************************
' SET LIMITS OF INJECTION***
'**************************
'          q    EOI   mean Pressure BAR
'iDLE       347   351     99.77
'1600/2.86   348   356     128.7
'1600/5.72   347   365     133.48
'1600/8.59   345   368     148.2
'2500/7.49   345   368     247


        IF deg < 347 THEN GOTO 220       'START OF INJECTION
        IF deg! > 365 THEN : MF = 0: GOTO 220  'END OF INJECTION
' TIME STEP = Ts
        Ts = (bit!(4, 6) * 6) ^ -1
        RHOg = ma / VOL!   'GAS DENSITY  ,fuel density 860 kg/m
        DpF = (133 * 101300!) - avl!(2, t1) 'PRESSURE DROP ACROSS NOZZLE
'**********************
'AREA OF INJECTOR HOLES 4 HOLES DIA 0.31mm L=0.6mm
        An = (PI * .0031 ^ 2) / 4 * .006 * 4
        Cd = .68   ' VALUE FROM LUCAS
        MF = (Cd * An * Ts * SQR(DpF * 860))
'RATIO = ma / Mf
' FUEL JET PENETRATION = Sp from Dent J.C. SAE 710571
        IF flag = 1 THEN GOTO 220
        injdegs = injdegs + 1
        Sp = 3.07 * (DpF / RHOg) ^ (.25) * (Ts * ((.00031) ^ .5)) * (294 / avl!(3, t1) ^
(.25))
        SPmax = Sp + MOR!(2, t1 - 1)
        IF SPmax > .0517638 THEN SPmax = .0517638: flag = 1: GOTO 220
        IF SPmax < .0517638# THEN flag = 0
220
        MOR!(2, t1) = SPmax

        avl!(8, t1) = MF + avl!(8, t1 - 1)
                ' GET MAX VALUE
                IF t1 < 3 GOTO 211
```

```
                IF bit!(3, 8) > avl!(8, t1) THEN
                GOTO 211
                ELSE
                bit!(3, 8) = avl!(8, t1)
                END IF
211


NEXT t1
'heat
'Calculations for theoretical heat release
 ' mass of fuel injected = mf
         FOR B1 = 1 TO 640

        Qf = 42787000
         Qind = Qf * MF   ' quantity of heat injected
        IF avl!(5, B1) = 0 THEN
           GOTO 1460
           ELSEIF dQall - avl!(5, B1) < .00001 THEN
           GOTO 1460
           ELSE
           xburn = (avl!(5, B1) / dQall) * 100
   avl!(6, B1) = xburn
                ' GET MAX VALUE
                IF B1 < 3 GOTO 222
                IF bit!(3, 6) > avl!(6, B1) THEN GOTO 222
                IF avl!(6, B1) < avl!(6, B1 - 1) THEN bit!(3, 6) = avl!(6, B1 - 1)
                IF avl!(6, B1) > avl!(6, B1 - 1) THEN bit!(3, 6) = avl!(6, B1)
222


   END IF
1460
    IF avl!(6, B1) < avl!(6, B1 - 1) THEN avl!(6, B1) = avl!(6, B1 - 1)
    NEXT B1
'*****************
'goto subs
'*****************
CREVICE
SPRAY
OXIDAT
```

```
        IF bit!(4, 1) < 10 THEN va = 1 ELSE va = 2
        nam1$ = RIGHT$(STR$(bit!(4, 1)), va)
        outnam$ = "c:\bild-com\model\" + nam1$ + "thes98.prn"" + STR$(bit!(4, 1))
        OPEN outnam$ FOR OUTPUT AS #5

        FOR HEAD = 1 TO 18
        PRINT #5, NAM$(1, HEAD) + "   " + STR$(bit!(4, HEAD))
        NEXT HEAD
     PRINT #5, "Fuel Injected kg"; bit!(3, 8); "% Burnt"; avl!(6, 600)
            PRINT #5, "rads, fuel pen, Cyl Press, 1st r press, 2nd r press,  soot, uHC
NF1st  ,NF2nd , ads-des"
            FOR R1 = 1 TO 640
            PRINT #5, USING "##.###^^^^ "; avl!(1, R1); avl!(7, R1); avl!(2, R1);
avl!(21, R1); avl!(13, R1); avl!(15, R1); avl!(19, R1); avl!(23, R1); avl!(24, R1);
avl!(17, R1)
            NEXT R1
            CLOSE #5

'****((vol*density)/mass fuel)/(speed * no of cyls / 2) /2 for four stroke
        timfuel! = ((.000025 * 860) / bit!(3, 8)) / (bit!(4, 6) * 4 / 2)
'***************detect if wall impingement has occured
IF flag = 0 THEN injdegs = 360
'****
'*********************************
'**  Screen to select which graph
'*********************************

DO
CLS
COLOR 7, 1
PRINT "  WHICH GRAPH DO YOU REQUIRE   F5 TO RESTART          F10
TO QUIT"
PRINT ""
PRINT "  1 = FUEL kg.MOLES 1 st                IVC = 213 ATDC"
PRINT "  2 = FUEL kg.MOLES 2 nd                EVO = 488 ATDC"
PRINT "  A = ADSORPTION/DESORPTION"
PRINT "  B = PERCENT BURNT"
PRINT "  F = FUEL REACTION RATE"
PRINT "  G = GAS TEMPERATURE"
PRINT "  I = MASS OF FUEL"
PRINT "  L = MASS 1st LAND (kg)"
PRINT "  M = MASS 2nd LAND (kg)"
PRINT "  N = PRESSURE 1st LAND"
PRINT "  P = PRESSURE 2nd LAND"
PRINT "  R = HEAT RELEASE/DERGREE (J/DEG)"
PRINT "  S = SOOT"
PRINT "  T = MOLE FRACTION TOTAL CHANGE"
PRINT "  U = EXHAUST uHC"
PRINT ""
```

```
PRINT "  Time for 25cc fuel use (mins)", timfuel!
PRINT ""
PRINT "  Max fuel   (kg) ", bit!(3, 8); "   % Crevice uHC     ";
PRINT USING "##.##"; (avl!(19, 300) * 10000) / (bit!(3, 8) * (100 - (avl!(6, 308))))
PRINT "  Total uHC  (kg) ", bit!(3, 8) * (1 - (avl!(6, 308) / 100)); "   total crevice
uHC "; avl!(19, 300)
PRINT "  Degrees to wall impinge  ", injdegs
' DATA STARTS AT 180 DEG
   '**** Wait for key stroke and display graph ****
   DO
          KBD$ = INKEY$
          SELECT CASE KBD$
               CASE "1": : GJ% = 23:  TITLES$ = "kg.mol FU 1sT": GOTO 172
               CASE "2": : GJ% = 24:  TITLES$ = "kg.mol FU 2nd": GOTO 172
               CASE "A", "a": : GJ% = 17: TITLES$ = "ADS/DES": GOTO 172
               CASE "B", "b": : GJ% = 6: TITLES$ = "FUEL % BURNT": GOTO
172
               CASE "F", "f": : GJ% = 16: TITLES$ = "FUEL R RATE": GOTO 172
               CASE "G", "g": : GJ% = 3: TITLES$ = "GAS TEMP": GOTO 172
               CASE "I", "i": : GJ% = 8: TITLES$ = "M FUEL": GOTO 172
               CASE "L", "l": : GJ% = 14: TITLES$ = "M 1st LAND": GOTO 172
               CASE "M", "m": : GJ% = 12: TITLES$ = "M 2nd LAND": GOTO 172
               CASE "N", "n": : GJ% = 21: TITLES$ = "P 1st LAND": GOTO 172
               CASE "P", "p": : GJ% = 13: TITLES$ = "P 2nd LAND": GOTO 172
               CASE "R", "r": : GJ% = 4: TITLES$ = "HEAT/DEG": GOTO 172
               CASE "S", "s": : GJ% = 15: TITLES$ = "SOOT": GOTO 172
               CASE "T", "t": : GJ% = 20: TITLES$ = "MOLE FRAC": GOTO 172
               CASE "U", "u": : GJ% = 19: TITLES$ = "EXH uHC": GOTO 172
               CASE CHR$(0) + CHR$(63): GOTO 9
               CASE CHR$(0) + CHR$(68): GOTO 1000
               CASE "Q", "q": GOTO 1000
               CASE ELSE
               END SELECT
   LOOP
172
CLS
SCREEN 9
COLOR 1, 7
CIRCLE (20, 20), 6
GET (14, 14)-(26, 26), CROSS%
CLS
```

```
'* DRAW RED BOXS AND TEXT*
     PSET (137, 10)
     LINE -(266, 45), 6, BF
     PSET (297, 10)
     LINE -(396, 45), 6, BF
     PSET (450, 10)
     LINE -(600, 60), 6, BF
     PSET (20, 10)
     LINE -(130, 45), 6, BF
     PSET (2, 300)
     LINE -(637, 300)
     PSET (2, 50)
     LINE -(2, 300)
     LOCATE 3, 5: PRINT "PRESSURE UP"
     LOCATE 3, 20: PRINT TITLES$
     LOCATE 3, 40: PRINT "DEGREES"
     LOCATE 2, 60: PRINT "+\- = STEP SIZE"
     LOCATE 3, 60: PRINT "ARROWS = MOVE  "
     LOCATE 4, 60: PRINT "Q = EXIT       "
  pp1 = 300
  H1 = 1
  FOR H = 1 TO 640 STEP 2
 '  ***PLOT POINTS****

  PSET (H, 300 - (180 * (avl!(2, H) / bit!(3, 2)))), 5
     ' PRINT AVL!(GJ%, H), BIT(3, GJ%)
        pp = 300 - (200 * (avl!(GJ%, H) / bit!(3, GJ%)))
PLOTP:
        IF pp < 10 THEN
        pp = 10
        ELSEIF pp > 310 THEN
        pp = 310
        END IF
   PSET (H, pp): LINE -(H1, pp1), 4
   '*** set TDC point
   IF CINT(avl!(1, H) * (180 / PI)) = 361 THEN PSET (H, 301): LINE -(H, 310):
LOCATE 23, H / 8.1: PRINT "TDC"
PLOTH:
   H1 = H
   pp1 = pp
   NEXT H
CLOSE #1
```

```
'********************
'**trace the curves**
'********************
 J = 1
 s! = 50
N1! = 1
 PUT (N1!, s!), CROSS%, XOR

        DO
          DO
          KBD$ = INKEY$
          SELECT CASE KBD$
               CASE CHR$(0) + "H":   J = 2: GOTO 109
               CASE CHR$(0) + "P":   J = 1: GOTO 109
               CASE CHR$(0) + "K":   K! = K! - q: GOTO 109
               CASE CHR$(0) + "M":   K! = K! + q: GOTO 109
               CASE "q", "Q": GOTO 999
               CASE "+": q = q * 2
               CASE "-": q = q / 2
               CASE ELSE
          END SELECT
          IF INKEY$ = CHR$(27) THEN GOTO 999
          IF q < 1 THEN q = 1
          FOR weight = 1 TO 600
          NEXT weight
        LOOP
109
IF J = 1 THEN GOTO 111:  ELSE IF J = 2 GOTO 119
111
IF K > 620 THEN K = 6
     IF K < 6 THEN K = 6
     KP = K - 6
     T! = 294 - (200 * (avl!(GJ%, K!) / bit!(3, GJ%)))
     IF T! < 10 THEN
     T! = 10
     ELSEIF T! > 294 THEN
     T! = 294
     END IF
     PUT (N1!, s!), CROSS%, XOR 'ERASE OLD CIRCLE
     PUT (KP, T!), CROSS%, XOR 'NEW CIRCLE
     LOCATE 2, 5
     PRINT USING "###.##^^^^"; avl!(2, K!)
     LOCATE 2, 42
     PRINT USING "###.#"; avl!(1, K!) * (180 / PI)
     LOCATE 2, 20
     PRINT USING "###.####^^^^"; avl!(GJ%, K!)
     GOTO 900
```

```
119     IF K > 620 THEN K = 6
        IF K < 6 THEN K = 6
        KP = K - 6
        T! = 294 - (180 * (avl!(2, K!) / bit!(3, 2)))
        IF T! < 10 THEN
        T! = 10
        ELSEIF T! > 310 THEN
        T! = 310
        END IF
        PUT (N1!, s!), CROSS%, XOR'ERASE OLD CIRCLE
        PUT (KP, T!), CROSS%, XOR'NEW CIRCLE
        LOCATE 2, 5
        PRINT USING "###.##^^^^"; avl!(2, K!)
        LOCATE 2, 42
        PRINT USING "###.#"; avl!(1, K!) * (180 / PI)
        LOCATE 2, 20
        PRINT USING "###.####^^^^"; avl!(GJ%, K!)
        GOTO 900

900
 N1! = KP
 s! = T!
LOOP
999
LOOP
CLS
COLOR 7, 0
'** Error trapping
HANDLER:
        NUMBER = ERR
        IF NUMBER = 6 THEN
        pp = 300:  pp1 = pp: H1 = H: NF2nd! = 10: MF2nd = 10: RESUME NEXT
        ELSE
        RESUME NEXT
        END IF
END
1000
```

```
SUB CREVICE
 CLS 0
' define shared variables
        ma = bit!(1, 2)
        D = bit!(4, 3)
        N = bit!(4, 6)
        Hg = bit!(4, 10)
        Ta = bit!(4, 11)
        TAK = Ta + 275


' SUB for crevice & abs/des emissions
' Model to Calculate Top Land Crevice flow and Gas Temperature
'   Version 1 leakage to 2nd land and ring groove 5/1/94
' define constants, all are sufix C
 CONST CX = 12, CY = 2
' crank shaft throw = r and con rod length = L
 R = bit!(4, 4) / 2
 L = bit!(4, 2)
' define mol Wt of mixture = MOr
' Univ. gas const = Ro  kJ/kg
' Mfu= Mr fuel, Mair= Mr air        Molar mass kg/kmol
 CONST RO = 8.314, PI = 3.1415927#, Mair = 28.96, Mfu = 170
 ratio = bit!(4, 5)' COMPRESSION RATIO FROM MAIN
CLS
D2 = .09946
 CLS
 PRINT "Please wait while the crevice flow is calculated."
' Calculate sub functions, Ma  mass air in chamber.
 Mp = bit!(1, 1)
'**********************
'** DEFINE MOLE WEIGHT**
'**********************
' ring groove clearance volumes and initial mass
' DEFINE TEMP VALUE OF  Tp and CRANK ANGLE x.
 p1 = 100000
'************************
'**CALC CREVICE VOLUMES**
'************************
 CONST Ring1T = .002485  'RING 1 THICKNESS
 CONST Ring1W = .0049    'RING 1 WIDTH
 CONST Ring2W = .0049    'RING 2 WIDTH
 CONST L2nd = .0099     ' 2ND LAND HEIGHT
'********** RING GROVE DIMS
 CONST RGD = .089871, RG1T = .002577, RG2T = .002577
' 2nd land vol
 C1la = PI * (bit!(4, 9) ^ 2 - bit!(4, 8) ^ 2) / 4
 C2la = PI * (bit!(4, 9) ^ 2 - bit!(4, 15) ^ 2) / 4
' Land = C2lv * L2nd * 1.6
```

```
 C1lv = C1la * bit!(4, 14)' + BIT!(4, 16) REQUIRED FOR ADDDITIONAL TOP
VOL
 C2lv = C2la * L2nd + bit!(4, 16)
 ' volume behind rings Rvol1 & Rvol2
 RVol1 = (bit!(4, 9) - 2 * Ring1W - RGD) * PI * RGD * RG1T
 RVol2 = (bit!(4, 9) - 2 * Ring2W - RGD) * PI * RGD * RG2T
 ' total 2nd land volume
 Vol2 = C2lv
 ' initial mass in crevice volumes
' PRINT Mp, Rvol1, Ro, ma, BIT!(4,17)
 M1st = bit!(1, 1) * C1lv / ((RO / Mair) * 1000 * bit!(4, 17))
 M1rg = bit!(1, 1) * RVol1 / ((RO / Mair) * 1000 * bit!(4, 17))'behind top
 MO3 = bit!(1, 1) * C2lv / ((RO / Mair) * 1000 * bit!(4, 17))       '2nd land
 mo4 = bit!(1, 1) * RVol2 / ((RO / Mair) * 1000 * bit!(4, 17))      'behind 2nd
 ' initial mass in total 2nd land volume M2i
 M2nd! = MO3 + mo4
 V2ND = RVol2 + C2lv
 'M2nd! = mo3
 'M2nd! = C2lv
 ' define constants for ring groove flow, viscosity of gas, mu
 ' top ring side clearance ht, area normal to flow, Af
 mu = 3.3E-07 * bit!(4, 17) ^ .7
 ht = RG1T - Ring1T
 Af = ht * PI * bit!(4, 3)

 ' area of piston = A  RING GAP(FROM mw) AND Cd
 CONST ringgap = .00041, Cd = .86
 A = (PI * bit!(4, 3) ^ 2) / 4
 A2 = ringgap * (bit!(4, 9) - bit!(4, 8)) / 2
 K = A2 / A
 ' ring end gap
 ' Calculate sub functions
 'Crankshaft rotation (w)
  tdp = 1 / (bit!(4, 6) * 360)
  tdp = bit!(4, 6)
  w = bit!(4, 6) * PI * 2 / 60
 ' top land crevice volume,CA + ring groove volume Rvol1
 CA = PI / 4 * (bit!(4, 9) ^ 2 - bit!(4, 8) ^ 2) * bit!(4, 14)
 CK = CX * bit!(4, 6) * tdp
 ' constant values for crevice mass flow rate
 P1Rg = avl!(2, 35)'bit!(1, 1)
 P2RG = avl!(2, 35)'bit!(1, 1)
 Prg = avl!(2, 35)'bit!(1, 1)
 PV1 = .0003
 nt1 = -.0004
' adtot = 0 ' reset  total
'****************
 ' START OF LOOP
'****************
```

```
 FOR Oi = 35 TO 360 ' DATA STARTS AT 180 DEG
   dp = avl!(2, Oi) - avl!(2, Oi - 1)
   dpp = avl!(2, Oi) + avl!(2, Oi - 1)
   dp3 = avl!(2, Oi) - avl!(2, Oi - 2)
   dp4 = avl!(2, Oi - 1) - avl!(2, Oi)
   ' Piston Displacement = PX, Velocity = PCO
   '  Vol Displacement by Piston = PV
          CE1 = L ^ 2 / R ^ 2 - (SIN(avl!(1, Oi))) ^ 2
          CE = SQR(CE1)
   PX = R * ((1 - COS(avl!(1, Oi))) + L / R - CE)
          PC1 = .5 * SIN(2 * avl!(1, Oi)) / CE
   PCO = w * R * (SIN(avl!(1, Oi)) + PC1)
   PV = PX * A
   VOL = PV + VSW / ratio
   m1 = M
'****************************************
'** define molar weight of mixture (MOr) **
'****************************************
 'NO OF KILOGRAMME MOLES AIR
        Nair = bit!(1, 2) / Mair
        '*****************
        '** fuel moles****
        '*****************
        IF MOR!(2, Oi) < .0517 THEN : Nmole = Nair: MOR = Mair: GOTO 157
        Mfuel = avl!(8, Oi)
        IF Mfuel > 0 THEN
        GOTO 151
        ELSE
        Nmole = Nair
        MOR = Mair
        GOTO 157
        END IF
151
Nfuel = Mfuel / Mfu   ' kilogramme moles of fuel
Nmole = Nfuel + Nair  ' kilogramme moles of air
FuelMolf = Nfuel / Nmole
avl!(22, Oi) = FuelMolf
'************************************
'** MOr = molar weight in comb chamber
MOR = (1 / Nmole) * ((Mfu * Nfuel) + (Mair * Nair))
157
MOR!(1, Oi) = MOR
```

```
'*****************
' MOr at crevice is time aligned by injdegs = MOR!(1,Oi-INJDEGS)
'*****************
Crg = ht ^ 2 * Af / ((24 * (RG1T - Ring1T) * mu * (RO / MOR!(1, Oi - injdegs)) *
bit!(4, 17) * 1000))
CJ = (MOR!(1, Oi - injdegs) * CA) / (RO * 1000 * bit!(4, 17))
          IF avl!(2, Oi) < 1.3 THEN
          GOTO 216
         ELSE
          GOTO 165
165   END IF
  Rho = avl!(2, Oi) * MOR!(1, Oi) / (avl!(3, Oi) * RO * 1000)
  ' Crevice mass Flow = m, Units of mass flow g/s.
  ' Calc crevice flow velocity = Cv
 'MASS  IN 1ST LAND  M1st
  IF dp < 0 THEN
          M = CJ * dp4
          Cv = CK * dp3 / dpp
          M1st = M1st - M
          MOR1st = (NF1st / (NF1st + NA1st) * Mfu) + (NA1st / (NF1st + NA1st) *
Mair)
          NF1st = NF1st - ((M - ((((NA1st / (NF1st + NA1st))) * (M / MOR1st))) *
Mair) / Mfu)
          ELSE
          M = CJ * dp
          Cv = CK * dp / dpp
          M1st = M1st + M
          MOR1st = ((avl!(22, Oi - injdegs) * Mfu) + ((1 - avl!(22, Oi - injdegs)) *
Mair))
          NF1st = NF1st + ((M - (((1 - avl!(22, Oi - injdegs)) * (M / MOR))) * Mair) /
Mfu)
  END IF
  '**  MOLECULAR WEIGHT OF MIXTURE IN 1ST LAND Mor1st
  NA1st = (M1st - (NF1st * Mfu)) / Mair
  avl!(14, Oi) = M1st
  '** fuel mole fraction in 1 land = Fmf1 = NF1st/(NF1st+NA1st)
  Fmf1 = NF1st / (NF1st + NA1st)
  IF FuelMolf = 0 THEN NF1st = 0
  avl!(23, Oi) = NF1st
            '** GET PEAK VALUE OF M1st
            IF Oi < 3 GOTO 167
            IF bit!(3, 14) > avl!(14, Oi) THEN GOTO 167
            IF avl!(14, Oi) < avl!(14, Oi - 1) THEN bit!(3, 14) = avl!(14, Oi - 1)
```

```
167
                '** GET PEAK VALUE OF NF1st
                IF Oi < 3 GOTO 177
                IF bit!(3, 23) > avl!(23, Oi) THEN GOTO 177
                IF avl!(23, Oi) < avl!(23, Oi - 1) THEN bit!(3, 23) = avl!(23, Oi - 1)
177
  '** PRINT NF1st
  '*********************************
  ' allow for leakage BEHIND 1ST RING
  '*********************************
  IF avl!(2, Oi) < P1Rg THEN
    Dp1R = P1Rg - avl!(2, Oi)
    M1r! = (Dp1R * Crg) / bit!(4, 6) * 6
    M1rg = M1rg - M1r
    MOR1rg = (NF1rg / (NF1rg + NA1rg) * Mfu) + (NA1rg / (NF1rg + NA1rg) *
Mair)
    NF1rg = NF1rg - ((M1r - (((1 - (NF1rg / (NF1rg + NA1rg))) * (M1r /
MOR1rg))) * Mair) / Mfu)
   ELSE
    Dp1R = avl!(2, Oi) - P1Rg
    M1r! = (Dp1R * Crg) / bit!(4, 6) * 6
    M1rg = M1rg + M1r
    MOR1rg = (NF1rg / (NF1rg + NA1rg) * Mfu) + (NA1rg / (NF1rg + NA1rg) *
Mair)
    NF1rg = NF1rg + ((M1r - ((((NA1st / (NF1st + NA1st))) * (M1r / MOR1st))) *
Mair) / Mfu)
  END IF
  NA1rg = (M1rg - (NF1rg * Mfu)) / Mair
  avl!(9, Oi) = NF1rg
  avl!(11, Oi) = M1rg
                '** GET PEAK VALUE
                IF Oi < 3 GOTO 173
                IF bit!(3, 11) > avl!(11, Oi) THEN
                GOTO 173
                ELSE
                bit!(3, 11) = avl!(11, Oi)
                END IF
173
                '** GET PEAK VALUE   NF1rg
                IF Oi < 3 GOTO 183
                IF bit!(3, 9) > avl!(9, Oi) THEN
                GOTO 183
                ELSE
                bit!(3, 9) = avl!(9, Oi)
                END IF
```

```
183
  P1Rg! = M1rg * (RO / MOR!(1, Oi - injdegs)) * 1000 * bit!(4, 17) / RVol1
  avl!(21, Oi) = P1Rg!
  '** GET MAX VALUE
            IF bit!(3, 21) > avl!(21, Oi) THEN GOTO 236
            IF avl!(21, Oi) < avl!(21, Oi - 1) THEN bit!(3, 21) = avl!(21, Oi - 1)
236
  '*********************************************
  ' FLOW INTO 2ND LAND   M2nd = MASS IN SECOND LAND  NF2nd = FUEL
MOLES 2ND LAND
  IF avl!(2, Oi) - P2RG > 0 THEN
      DP2nd = avl!(2, Oi) - P2RG
      SQ1 = SQR((2 * DP2nd) / (Rho * (1 - K ^ 2)))
      M2l = Cd * A2 * SQ1 / bit!(4, 6) * 6
      M2nd! = M2nd! + M2l
      MOR2nd = (NF2nd! / (NF2nd! + NA2nd) * Mfu) + (NA2nd / (NF2nd! +
NA2nd) * Mair)
      NF2nd! = NF2nd! + ((M2l - (((1 - (NF2nd! / (NF2nd! + NA2nd))) * (M2l /
MOR1st))) * Mair) / Mfu)
      ELSE
      DP2nd = P2RG - avl!(2, Oi)
      SQ1 = SQR((2 * DP2nd) / (Rho * (1 - K ^ 2)))
      M2l = Cd * A2 * SQ1 / bit!(4, 6) * 6
      M2nd! = M2nd! - M2l
      MOR2nd = (NF2nd! / (NF2nd! + NA2nd) * Mfu) + (NA2nd / (NF2nd! +
NA2nd) * Mair)
      'ORIGINAL MOR2nd = ((Fmf1 * MFU) + ((1 - Fmf1) * Mair))
      NF2nd! = NF2nd! - ((M2l - (((NA2nd / (NF2nd! + NA2nd)) * (M2l /
MOR2nd))) * Mair) / Mfu)
  END IF
  NA2nd = (M2nd! - (NF2nd! * Mfu)) / Mair
  avl!(12, Oi) = M2nd!
  avl!(24, Oi) = NF2nd!
      '** GET PEAK VALUE OF M2nd!
      IF Oi < 3 GOTO 192
            IF bit!(3, 12) > avl!(12, Oi) THEN
            GOTO 192
            ELSE bit!(3, 12) = avl!(12, Oi)
            END IF
192
      '** GET PEAK VALUE OF NF2nd!
      IF Oi < 3 GOTO 202
            IF bit!(3, 24) > avl!(24, Oi) THEN
            GOTO 202
            ELSE bit!(3, 24) = avl!(24, Oi)
            END IF
```

```
202
  '**********************
  'CALC 2ND LAND PRESSURE
  P2RG = M2nd! * (RO / MOR!(1, Oi - injdegs)) * 1000 * bit!(4, 17) / V2ND
  avl!(13, Oi) = P2RG
                '** GET PEAK VALUE
                IF Oi < 3 GOTO 200
                IF bit!(3, 13) > avl!(13, Oi) THEN
                GOTO 200
                ELSE
                bit!(3, 13) = avl!(13, Oi)
                END IF
200
  Mtot = M2nd! + M1rg
  avl!(10, Oi) = Mtot
                '** GET PEAK VALUE
                IF Oi < 3 GOTO 216
                IF bit!(3, 10) > avl!(10, Oi) THEN
                GOTO 216
                ELSE
                bit!(3, 10) = avl!(10, Oi)
                END IF
216
  '**********************************
  '**CALCULATE ADSORPTION / DESORPTION
  '**********************************
  'CONSTANTS   LINER TEMP TK
  'idle 355 1600/2.86 364 1600/5.72 368 1600/8.59 375 2500/7.49 395
  CONST AD1 = -.0001972, AD2 = -.432, AD3 = 1.1304, TK = 368'TEMP
  'AD1,AD2 + AD3 FROM KOREMESU
  'MOLECULAR WEIGHTS  OIL = OW FUEL = FD MOLE FRACTION NMOLE
  ' OIL DENSITY OD
  CONST OD = 857, FD = 170, OW = 550

  OHC = bit!(4, 13) / 1000000
  '******* HENRY CONST
  HC2 = -1.82 + .0125 * (TK - 300)
  HC1 = 10 ^ HC2
  HC = HC1 * 101.3
  '*** CALC CM
  CM = AD1 + AD3 * tdp
  DYS = PX / (2 * R)
  DY = y - Y1 + bit!(4, 14)
  '** C EQUILIBRIUM
  CEQ = (FD * avl!(2, Oi)) * avl!(22, Oi - injdegs) / (OW * HC)
  CMY = CM + AD2 * DYS
 DMF = CMY * PI * bit!(4, 3) * OHC * OD * CEQ * DY * 1000
  Y1 = y
316
```

```
'**********************
  '** total ads des = adtot
  adtot = DMF
        IF avl!(1, Oi) <= 4.5 THEN
                PEND! = avl!(21, Oi)
                ELSE
                PDIF! = avl!(21, Oi - 1) - avl!(21, Oi)'p1 - p2

        END IF

        IF PEND! = avl!(21, Oi) THEN GOTO 333

        PRAT! = PDIF! / PEND!


        avl!(17, Oi) = PRAT! * adtot

333
'           '** GET PEAK VALUE
'           IF Oi < 3 GOTO 336
'           IF bit!(3, 17) > avl!(17, Oi) THEN GOTO 336
'           IF avl!(17, Oi) < avl!(17, Oi - 1) THEN bit!(3, 17) = avl!(17, Oi - 1)
'336
NEXT Oi
bit!(4, 19) = adtot 'TOTAL

' *** This code ensures that no  more that what goes in comes out ***
FOR Oi2 = 35 TO 360
  IF avl!(17, Oi2) > 0 THEN totads = totads + avl!(17, Oi2)
  IF avl!(17, Oi2) < 0 THEN negads = negads + avl!(17, Oi2)
NEXT Oi2
   PRINT bit!(3, 17), totads; negads
   DO WHILE INKEY$ = ""
   LOOP
FOR Oi3 = 35 TO 360
  IF avl!(17, Oi3) < 0 THEN avl!(17, Oi3) = avl!(17, Oi3) * ABS(totads / negads)
  IF avl!(17, Oi3) > 0 THEN totads2 = totads2 + avl!(17, Oi3)
  IF avl!(17, Oi3) < 0 THEN negads2 = negads2 + avl!(17, Oi3)

                '** GET PEAK VALUE
                IF Oi3 < 3 GOTO 336
                IF bit!(3, 17) > avl!(17, Oi3) THEN GOTO 336
                IF avl!(17, Oi3) < avl!(17, Oi3 - 1) THEN bit!(3, 17) = avl!(17, Oi3 -
1)
```

```
NEXT Oi3
  PRINT bit!(3, 17), totads2; negads2
  DO WHILE INKEY$ = ""
  LOOP



END SUB

SUB FILEIN

'*********************************************
'**********  INPUT SCREEN FOR SELECTING   ***
'**********    FILE TYPES                 ***
'**********  working version 11-3-95      ***
'*********************************************
EXT$ = "PRN"
30
'**  Clear PWY$
ERASE PWY$
CLS
'** Shell to DOS and write directory to temp file
SHELL "CD C:\UTILS\MODEL\DATA"    ' The authors data directory use for
default
SHELL "DIR *." + EXT$ + " /b/O> C:\DIRFILE.TMP"'/b for file name only /O =
ORDER
PWINC = 1
'** Read in directory listing
OPEN "C:\DIRFILE.TMP" FOR INPUT AS #1
DO WHILE NOT EOF(1)
     INPUT #1, DD$
    PWY$(PWINC) = LEFT$(DD$, 12)   ' read in file names
    PWINC = PWINC + 1
 LOOP
CLOSE #1
 '*************
 'GET DIRECTORY
 '*************
DIRSTP = 0
 SHELL "DIR XX*.XXX > C:\DIRFILE3.TMP"
OPEN "C:\DIRFILE3.TMP" FOR INPUT AS #3
        DO WHILE NOT EOF(3)
        INPUT #3, DIRP$
        DIRSTP = DIRSTP + 1
        IF DIRSTP = 4 THEN DIRPATH$ = DIRP$: GOTO 332
```

```
        LOOP
332
        CLOSE #3
DISPATH$ = RIGHT$(DIRPATH$, LEN(DIRPATH$) - 13)    'THE CURRENT
DIRECTORY
        '*****************************************
        '**   Draws the Input screen and allows    **
        '**   modifications to  Certain Parameters **
        '*****************************************
CLS
 SCREEN 9
 COLOR 7, 1
 LOCATE 2, 2: PRINT "F1 TO CHANGE FILE TYPE    CURRENT EXTENSION
*." + EXT$
 LOCATE 3, 2: PRINT "F5  TO CHANGE DIRECTORY   CURRENT
DIRECTORY " + DISPATH$
 LOCATE 4, 2: PRINT "F10 TO QUIT              ENTER TO SELECT &
CONTINUE"
 st = 0
 FOR H = 1 TO 14 STEP 13
 FOR N = 6 TO 22 STEP 2
' LOCATE N, H * 3
 LINE ((H * 24) - 16, (N * 14) - 15)-STEP(230, 15), 7, BF'n*24
' PRINT NAM$(1, ((N - 4) / 2) + st)
 ' ***DRAW RED BOX
 IF N = 6 THEN IF H = 2 THEN LOCATE 6, 24: LINE ((24 * 8) - 16, (6 * 14) - 15)-
STEP(85, 15), 6, BF
 LOCATE N, (H * 3) + 10
 PRINT PWY$(((N - 4) / 2) + st)
 NEXT N
 st = 9
 NEXT H

 K = 6: KS = 6
 J = 13: JS = 13
 LS = 1
DO

        DO
                KBD$ = INKEY$
                SELECT CASE KBD$
                CASE CHR$(0) + "H":  K = K - 2: GOTO 3129
                CASE CHR$(0) + "P":  K = K + 2: GOTO 3129
                CASE CHR$(0) + "K":  J = 13: SST = 0: GOTO 3129
                CASE CHR$(0) + "M":  J = 52: SST = 9: GOTO 3129
                CASE CHR$(13): FILENAME$ = PWY$(LS): GOTO 399
                CASE CHR$(0) + CHR$(59): LOCATE 2, 28: INPUT "NEW FILE
SPEC       *.", EXT$: GOTO 30
```

```
                CASE CHR$(0) + CHR$(63):  GOTO 799  ' F5 TO CHANGE
DIRECTORY
                CASE CHR$(0) + CHR$(68):  bit!(1, 4) = 99: GOTO 3999' F10 TO
QUIT
                CASE ELSE
                END SELECT
          LOOP
3129     'SCREEN CONTROL
         IF K <= 5 THEN K = 22
         IF K >= 23 THEN K = 6
'**  erase red box
 LOCATE KS, JS
         LINE ((JS * 8) - 24, (KS * 14) - 15)-STEP(120, 15), 7, BF
         PRINT PWY$(LS)
'**  draw red box and display data
 LOCATE K, J
         LINE ((J * 8) - 24, (K * 14) - 15)-STEP(120, 15), 6, BF
         LI = ((K - 4) / 2) + SST
         PRINT PWY$(LI)

 JS = J
 KS = K
 LS = LI

 LOOP
399
 CLS
GOTO 3999
799
ERASE PWY2$
PWY2$(1) = ".."

         CLS
         SHELL "DIR /A:D /B >C:\DIRFILE2.TMP" '/b for file name only /A:D FOR
DIRECTORYS
         PWINC = 2
         IF LEN(DISPATH$) < 4 THEN PWINC = 1 'CHECK FOR ROOT
DIRECTORY
         OPEN "C:\DIRFILE2.TMP" FOR INPUT AS #2
         DO WHILE NOT EOF(2)
              INPUT #2, DD$
            PWY2$(PWINC) = LEFT$(DD$, 8)   ' read in file names
            PWINC = PWINC + 1
         LOOP
      CLOSE #2
 FOR STP = 1 TO 10
 NEXT STP

 CLS
```

```
 SCREEN 9
 COLOR 7, 1
 LOCATE 2, 2: PRINT "F10 TO QUIT              CURRENT DIRECTORY " +
DISPATH$
 LOCATE 3, 2: PRINT "ENTER TO SELECT & CONTINUE"
 st = 0
 FOR H = 1 TO 14 STEP 13
 FOR N = 6 TO 22 STEP 2
' LOCATE N, H * 3
 LINE ((H * 24) - 16, (N * 14) - 15)-STEP(230, 15), 7, BF'n*24
 ' ***DRAW RED BOX
 IF N = 6 THEN IF H = 2 THEN LOCATE 6, 24: LINE ((24 * 8) - 16, (6 * 14) - 15)-
STEP(85, 15), 6, BF
 LOCATE N, (H * 3) + 10
 PRINT PWY2$(((N - 4) / 2) + st)
 NEXT N
 st = 9
 NEXT H

 K = 6: KS = 6
 J = 13: JS = 13
 LS = 1
DO

        DO
                KBD$ = INKEY$
                SELECT CASE KBD$
                CASE CHR$(0) + "H":  K = K - 2: GOTO 229
                CASE CHR$(0) + "P":  K = K + 2: GOTO 229
                CASE CHR$(0) + "K":  J = 13: SST = 0: GOTO 229
                CASE CHR$(0) + "M":  J = 52: SST = 9: GOTO 229
                CASE CHR$(13): DIRNAME$ = PWY2$(LS): GOTO 309
                CASE CHR$(0) + CHR$(68):  bit!(1, 4) = 99: GOTO 3999' F10 TO
QUIT
                CASE ELSE
                END SELECT
         LOOP
229.    'SCREEN CONTROL
        IF K <= 5 THEN K = 22
        IF K >= 23 THEN K = 6
'**  erase red box
 LOCATE KS, JS
        LINE ((JS * 8) - 24, (KS * 14) - 15)-STEP(85, 15), 7, BF
        PRINT PWY2$(LS)
```

```
'**  draw red box and display data
 LOCATE K, J
        LINE ((J * 8) - 24, (K * 14) - 15)-STEP(85, 15), 6, BF
        LI = ((K - 4) / 2) + SST
        PRINT PWY2$(LI)

 JS = J
 KS = K
 LS = LI

 LOOP
309
   CHDIR DIRNAME$
   GOTO 30
3999


END SUB

SUB INSCREEN
        '*****************************************
        '**   Draws the Input screen and allows    **
        '**   modifications to  Certain Parameters **
        '*****************************************
10
   '**  Swap data for first model run
        IF inflag = 1 THEN GOTO 47
         FOR Z% = 1 TO 22
         bit!(4, Z%) = bit!(2, Z%)
         NEXT Z%
         inflag = 1
47
 CLS
 SCREEN 9
 COLOR 7, 1
 LOCATE 2, 2: PRINT "F1 RESTORE DEFULT   F5  TO CONTINUE"
 LOCATE 3, 2: PRINT "F10 TO QUIT          ENTER TO EDIT"
 st = 0
 FOR H = 2 TO 15 STEP 13
 FOR N = 6 TO 22 STEP 2
 LOCATE N, H * 3
 LINE ((H * 24) - 16, (N * 14) - 15)-STEP(230, 15), 7, BF'n*24
 PRINT NAM$(1, ((N - 4) / 2) + st)
 ' ***DRAW RED BOX
 IF N = 6 THEN IF H = 2 THEN LOCATE 6, 24: LINE ((24 * 8) - 16, (6 * 14) - 15)-
STEP(85, 15), 6, BF
 LOCATE N, (H * 3) + 18
 PRINT bit!(4, ((N - 4) / 2) + st)
 NEXT N
```

```
st = 9
NEXT H

K = 6: KS = 6
J = 24: JS = 24
LS = 1
DO

        DO
                KBD$ = INKEY$
                SELECT CASE KBD$
                CASE CHR$(0) + "H":  K = K - 2: GOTO 129
                CASE CHR$(0) + "P":  K = K + 2: GOTO 129
                CASE CHR$(0) + "K":  J = 24: SST = 0: GOTO 129
                CASE CHR$(0) + "M":  J = 63: SST = 9: GOTO 129
                CASE CHR$(13): LOCATE K, J: PRINT "       ": LOCATE K, J:
INPUT "", bit!(4, LS)
                CASE CHR$(0) + CHR$(59): inflag = 0: GOTO 10' F1 RESET
VALUES
                CASE CHR$(0) + CHR$(63):  GOTO 699  ' F5 TO CONTINUE
                CASE CHR$(0) + CHR$(68):  bit!(1, 4) = 99: GOTO 1999' F10 TO
QUIT
                CASE ELSE
                END SELECT
        LOOP
129     'SCREEN CONTROL
        IF K <= 5 THEN K = 22
        IF K >= 23 THEN K = 6
'**  erase red box
 LOCATE KS, JS
        LINE ((JS * 8) - 16, (KS * 14) - 15)-STEP(85, 15), 7, BF
        PRINT bit!(4, LS)
'**  draw red box and display data
 LOCATE K, J
        LINE ((J * 8) - 16, (K * 14) - 15)-STEP(85, 15), 6, BF
        LI = ((K - 4) / 2) + SST
        PRINT bit!(4, LI)

 JS = J
 KS = K
 LS = LI

 LOOP
699
 CLS


1999
END SUB
```

```
SUB OXIDAT
'calculate the oxidation of the crevice and desorbed gas
' calculate the crevice mole fractions
'mole weights of the fuel(MWf) and its products and reactants
CLS
PRINT "The Final Values And"
PRINT "Oxidation Rates Are Being Calculated"
'RO = 8.314' GAS CONSTANT
        MWf = 170.34 'MOLECULAR WEIGHT OF FUEL
        CARBON = 12  'NO OF FUEL CARBON ATOMS
        HYDRO = 26   ' NO OF HYDROGEN ATOMS
        MIXR = .6   'NEEDS A PROPER INPUT
        WTFUEL = (12.011 * CARBON) + (1.00797 * HYDRO)
        molair1 = (CARBON + (.25 * HYDRO))
        molair2 = CINT(CARBON + (.25 * HYDRO))
'** DETERMINE NO OF MOLES OF AIR FOR COMBUSTION
IF molair1 > molair2 THEN
        MOLAIR = (molair1) + (1 - (molair1 - molair2)): GOTO 16
        ELSE
        MOLAIR = (molair2)
16
END IF
'WEIGHT OF AIR
'*************
        WTAIR = MOLAIR * 4.76
'DETERMINE THE MOLE WT OF REACTANTS
'**********************************
        WTREAC = (1 / (WTAIR + 1)) * (WTFUEL + (WTAIR * 28.96))
'DETERMINE NUMBER OF MOLES OF COMBUSTION PRODUCTS
        MOLPRD = CARBON + (.5 * HYDRO) + (3.76 * MOLAIR) + (((2 *
MOLAIR) - (2 * CARBON) - (.5 * HYDRO)) / 2)
'************
'* MOLE WEIGHT OF PRODUCTS = WTPRD
        WTCO2 = (CARBON * 43.991)  'WEIGHT CO2
        WTH2O = ((HYDRO / 2) * 18.015) 'WEIGHT H2O
        WTO2 = ((MOLAIR) - ((CARBON) + (HYDRO / 4))) * 15.99  'WEIGHT O2
        WTPRD = (1 / MOLPRD) * (WTCO2 + WTH2O + WTO2 + (MOLAIR *
3.76 * 14.0067))'WEIGHT PRODUCTS
'***********
'SET TEMP OF FREEZING
'PRINT BIT!(1, 1), BIT!(4, 12) * 100!  '100 = mbar TO N/M^2
        TOSF1 = .02 * LOG(1.4 * 100 * bit!(1, 1) / bit!(4, 12) * 100!)
        TOSF = 1320 / (1 + TOSF1)
'***********
'CALC MOLE FRACTIONS
        '**PERCENT HC "MFHC"
        MFHC = 1 / (WTREAC + MIXR * WTPRD)
        '** PERCENT O2 "MFO2"
```

```
        MFO2 = moleair1 / (WTREAC + MIXR * WTPRD) 'moleair1 is corect mole
number
        '** PERCENT ADSORBED HC "MFAHC"
        MFAHC = 1 / (1 + MIXR * .8 * WTPRD)
        'COMBINED MOLE FRACTION "CMF"
        CMF = WTREAC * MIXR + WTPRD * (1 - MIXR)
'CALC GAS CONSTANT "RMIX"
        RMIX = RO / CMF
'*********************
'START OF LOOP
FOR OXI = 80 TO 468
        '*************
        ' MIXED GAS TEMP "MGT"
        ' MGT = ((MIX RATIO * GAS TEMP) + PISTON TEMP)/RATIO
        MGT! = (MIXR * avl!(3, OXI)) + bit!(4, 17) / (MIXR + 1)
' CREVICE MASS FLOW HC  = CMFHC  PER SECOND
'PRINT AVL!(10, OXI), AVL!(17, OXI)
'CMFHC = DX 1LAND + DX 2LAND + DX 1RING
        CMFHC = ((avl!(14, OXI) - avl!(14, OXI - 1)) + (avl!(11, OXI) - avl!(11, OXI
- 1)) + (avl!(12, OXI) - avl!(12, OXI - 1))) / (bit!(4, 6) * 6)'SUM OF CREVICE
FLOWS
'INSTANT MOLE FRACTION
  ' PRINT CMFHC, MFHC, MFCHANGE, CHCMR, MFAHC, AVL!(17, OXI),
CMFHC, MFCHANGE, AVL!(17, OXI)
        IMFHC = (CMFHC * MFHC + mfchange * CHCMR + MFAHC * avl!(17,
OXI)) / (CMFHC + mfchange + avl!(17, OXI))
   '**********
   'SET LIMITS
   '**********
        IF avl!(1, OXI) > 7.6 THEN GOTO 433
        IF MGT! > TOSF THEN
        DXIMFHC = IMFHC * .5: OXFLAG = .1
        ELSE
        DXIMFHC = IMFHC * .01: OXFLAG = .9
        END IF
'***************
' CREVICE HC MASS RESIDUALS "CHCMR"
433
        CHCMR = IMFHC - DXIMFHC
'PRINT CHCMR
'*********************
' MOLE FRACTION CHANGE
        mfchange = mfchange + avl!(17, OXI) + CMFHC
'PRINT mfchange
' total step mole fraction change
        MFTOT = MFTOT + DXIMFHC
        avl!(20, OXI) = MFTOT
        IF bit!(3, 20) > avl!(20, OXI) THEN
        GOTO 94
```

```
        ELSE
        bit!(3, 20) = avl!(20, OXI)
        END IF
94
        avl!(18, OXI) = mfchange
'***************************
'** GET PEAK VALUE
        IF bit!(3, 18) > avl!(18, OXI) THEN
        GOTO 97
        ELSE bit!(3, 18) = avl!(18, OXI)
        END IF
97
'************************************
'** MASS OF HC UNBURNED MHCU miligramme
'************************************
        '* TO CONVERT kg.mol to kg multiply by Molar mass 170 for fuel
        '* TOTAL UN OXIDISED HC NF1ST + DES, DES IN MGRAMME THUS
170E-9
NhcU! = ((avl!(23, OXI) * 170) + (avl!(24, OXI) * 170) + (avl!(17, OXI) * 1.7E-10))
* OXFLAG
        '* un odiised NF1st**
'NhcU = (AVL!(23, OXI - 1) - AVL!(23, OXI)) * OXFLAG
        '* UN OXIDISED ADS-DES **
'NhcU = NhcU + (((AVL!(17, OXI - 1) - AVL!(17, OXI)) * 170e-9#)) * OXFLAG
IF NhcU < 0 THEN NhcU = 0
avl!(19, OXI) = NhcU!  'THE MAIN ANSWER
        '**MAX VALUE
        IF bit!(3, 19) > avl!(19, OXI) THEN
        GOTO 115
        ELSE
        bit!(3, 19) = avl!(19, OXI)
        END IF
115
'PRINT AVL!(18, OXI)
                '*** get max VALUE
                IF bit!(3, 18) > avl!(18, OXI) THEN GOTO 444
                IF avl!(18, OXI) < avl!(18, OXI - 1) THEN bit!(3, 18) = avl!(18, OXI -
1)
444
NEXT OXI
END SUB

SUB SPRAY
PRINT "The fuel values are being calculated"
        CONST OXY = 20.95, RO = 8.314, MIO2 = 32, PI = 3.1415926#
'SOOT CALC CONSTANTS
        CONST ASF = .08, ASCC = .0000000000000001#
'**CALC ORIGINAL NUMBER OF O2 MOLES
        MO2 = bit!(1, 2) * (OXY / 100)
```

```
        NMO2 = MO2 / MIO2
'**CALC FINAL O2 MOLES
        MO3 = bit!(1, 2) * (bit!(4, 18) / 100)
        FMO2 = MO3 / MIO2
'**************************
' CALC THE NUMBER OF O2 MOLES
' GIBBS DALTON LAW
'**************************
  FOR SP1 = 1 TO 640
    ' CALC FOR SWEPT VOL
    VSW = (PI * bit!(4, 3) ^ 2 * bit!(4, 4)) / 4
    ' Calcs to define cylinder volume
    V2S! = SQR(L ^ 2 / R ^ 2 - (SIN(avl!(1, SP1)) ^ 2))
    PV! = PI / 4 * bit!(4, 3) ^ 2 * (bit!(4, 4) / 2) * ((1 - COS((avl!(1, SP1)))) + L /
(bit!(4, 4) / 2) - V2S!)
    VOL! = PV! + (VSW / (bit!(4, 5) - 1))

'**** PARTIAL PRESSURE OF O2= PPO2
PPO2 = RO * avl!(3, SP1) / VOL! * ((NMO2 - ((NMO2 - FMO2) * avl!(6, SP1) /
100)))
'**** SOOT FORMATION = DMSF
        IF avl!(3, SP1) = 0 THEN GOTO 28
        DMSF = ASF * (avl!(8, SP1) - avl!(8, SP1 - 1)) * avl!(2, SP1) ^ .5 * EXP(-
6313 / avl!(3, SP1))
'**** SOOT CONSUMPTION = DMSC
        DMSC# = ASCC * avl!(15, SP1 - 1) * PPO2 * avl!(2, SP1) ^ 1.8 * EXP(-
7070 / avl!(3, SP1))
        IF DMSC# < 0 THEN DMSC# = 0
'**** TOTAL SOOT FORMED PER DEGREE = SOOT = AVL!(15,
SOOT# = DMSF - DMSC#
'PRINT USING "##.####^^^^"; DMSF; DMSC#; AVL!(15, SP1 - 1)
avl!(15, SP1) = SOOT# + avl!(15, SP1 - 1)
IF avl!(15, SP1) < 0 THEN avl!(15, SP1) = 0
                'GET PEAK VALUE
                IF SP1 < 3 GOTO 28
                IF bit!(3, 15) > avl!(15, SP1) THEN
                GOTO 28
                ELSE
                bit!(3, 15) = avl!(15, SP1)
                END IF
28
        '******************
        '** SET INJ LIMITS**
        IF avl!(8, SP1) < 1E-10 THEN GOTO 32
        IF avl!(1, SP1) > 7.33 THEN GOTO 31
'**********************************
' RATE OF HEAT RELEASE WHITEHOUSE***
'**********************************
        '*** FUEL PREPERATION FPR
```

```
        '**** CONSTANTS
        CONST KD = 1.2E+09, XC = .01, ZC = .4'KD OLD = 1.2E+9 MINE =
2.3937E8
        FPR# = KD * avl!(8, SP1) ^ (1 - XC) * (avl!(8, 638) - avl!(8, SP1)) * PPO2 ^
ZC
        '*** FUEL BURN RATE FBR
        '*** CONSTANTS
        CONST EA = -15000!, K = .008
        IF avl!(3, SP1) < .00001 THEN GOTO 32
        FBR2 = (FPR# - IFBR#) + FBR2
        FBR1 = EXP(EA / avl!(3, SP1)) * FBR2
        fbr# = (K / (bit!(4, 6) * 6 * PI / 180)) * (PPO2 / SQR(avl!(3, SP1))) * FBR1
31
        avl!(16, SP1) = fbr#
        IFBR# = fbr#
                'GET PEAK VALUE
                IF SP1 < 3 GOTO 32
                IF bit!(3, 16) > avl!(16, SP1) THEN GOTO 32
                IF avl!(16, SP1) < avl!(16, SP1 - 1) THEN bit!(3, 16) = avl!(16, SP1 -
1)

32
'SOF level by nakajima et al "Relationship between"
' RHOsof = (0.267*RHOhc) + 0.01304 =g/m^3
RHOsof = (.267 * avl!(16, SP1) / VOL!) + .01304
  avl!(7, SP1) = RHOsof
            'GET MAX VALUE OF SOF DENSITY
                IF SP1 < 3 GOTO 33
                IF bit!(3, 7) > avl!(7, SP1) THEN GOTO 33
                IF avl!(7, SP1) < avl!(7, SP1 - 1) THEN bit!(3, 7) = avl!(7, SP1 - 1)
33
NEXT SP1
REM PRINT massfpr
END SUB
```

Reducing the Environmental Impact of Vehicles - Replacement verses Refurbishment

L. Holloway, M. Bassett & P. W. Yates
Sheffield Hallam University
United Kingdom

96EN031

Synopsis

This work looks at the evolution of a typical family saloon car over recent years in terms of functional, aesthetic and environmental performance. The energy required in each stage of the vehicles life-cycle is calculated. A comparison of the environmental effects of replacing or refurbishing vehicles in terms of energy usage is carried out. It is suggested that although there are savings to be made by refurbishment or recycling the adoption design strategies which lead to a reduction in fuel consumption may result in the greatest life-cycle energy savings.

Introduction

For many years the effects that vehicles have on our environment have become increasingly obvious, particularly in urban areas. In an attempt to minimise these effects the main thrust of research and development has been directed towards reducing engine emissions, leading to the adoption of catalytic converters and lead free fuels.

Current concerns may indicate that we should reassess our strategies for reducing the environmental impact of vehicles. Materials selection, recycling and life extension have been demonstrated to produce real environmental benefits. Therefore it is essential that a complete life-cycle design approach which takes these factors into account is adopted.

Allied to the increase in concern for the environment, consumers want vehicles which display better performance in terms of safety, handling, power and comfort. This has resulted in an increase in the weight of vehicles due to the increased levels of trim, safety features, extra sound-proofing and use of electrically operated components. The trend of upsizing vehicle models in order to increase interior space has also contributed .

A comparison was made between the unladen vehicle weights for several 1981 model vehicles and their 1992 counterparts, Table 1, **Bladon** (1993), **Blunden** (1982)

1982		1992	
Austin Mini 1000	615 kg	Mini Cooper	706 kg
Austin Metro HLE 1.0	757 kg	Rover Metro 1.1C	815 kg
Austin Metro 1.3 Automatic	801 kg	Rover Metro 1.3	840 kg
Ford Fiesta XR2	785 kg	Ford Fiesta XR2	890 kg
Ford Fiesta 1.3S	775 kg	Ford Fiesta 1.4 Ghia	890 kg
Ford Escort XR3	895 kg	Ford Escort XR3i	1090 kg
BMW 316 (1.8)	1020 kg	BMW 318i	1260 kg
BMW 323i	1135 kg	BMW ~~235i~~ 325i	1330 kg
BMW 528i	1319 kg	BMW 535i	1525 kg

Table 1. Comparison of Vehicle Weights - 1982 and 1992

From Table 1 it can be clearly observed that in all the cases shown the modern equivalent is heavier. This increase in weight has numerous implications in terms of material usage and life-cycle energy requirement.

Environmental Effects in Vehicles Life Cycles

The life-cycles of automobiles are very long and complex and result in a number of environmental effects. It is difficult therefore to compare different scenarios of vehicle life and in many Environmental Impact Analysis studies Multiple Criteria Analysis has been used, **Diakoulaki & Koumoutsos**(1991). It has also been shown that using energy balancing a simple and relatively accurate measure of environmental performance can be established, **Fussler & Krummenacher** (1991). Each vehicle will have a very large and complex energy system, as it requires energy to extract materials, manufacture components, assemble and power the vehicle. Energy is also required to dispose of the vehicle after use, however some of this may be recovered.
For the purpose of this work the energy inherent in materials and also the energy used in manufacture etc. is summed to give a single figure for total life energy usage and this figure is used as a basis for environmental comparison.

NB The values used in this paper are approximate averages of different operations and a intended only as guidelines to demonstrate the apparent differences.

This study will consider 3 stages of the vehicles life-cycle defined as:
1. Material extraction/Manufacture
2. Usage
3. Disposal/refurbishment

The energy requirement for each of these life-cycle stages are calculated using data presented in previous works.

Materials/Manufacture

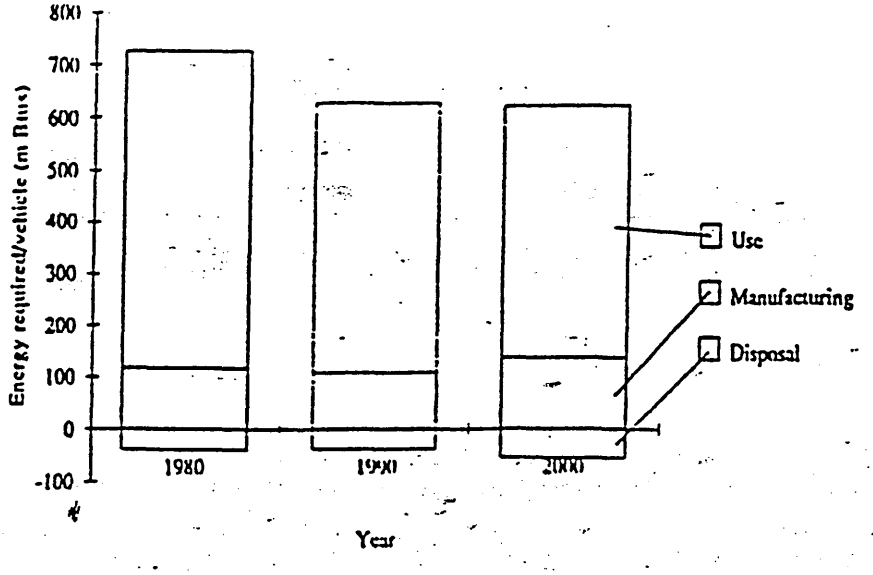

Figure 1. Energy Requirements of Typical Automobiles

In the initial stages of a vehicles life-cycle energy is used in extracting and refining raw materials and then in their conversion to useable components. Table 2. shows a breakdown of a standard family saloon in terms of material consumption and resulting energy content. The overall material composition of vehicles is shown in figure 1. Hendrickson (1994).

Material	Average part energy / kg	Weight as % of total vehicle	Weight Kg	Energy as % of total	Energy Total (MJ)
Polymers	80	9	101.25	9.8	8100
Aluminium	293	9	101.25	36	29666
Non-Ferrous	35	18	202.5	8.6	7087.5
Ferrous	54	61	697.5	45.6	37665

Table 2. Material and energy requirement of the average family saloon

Use

It is the use of a vehicle which will consume the greatest amount of energy in the form of hydrocarbon based fuels. The amount of fuel consumed by a vehicle is dependent on factors such as engine size, aerodynamics etc. as discussed previously but is probably most directly affected by weight, the more weight you add to a vehicle the more the fuel consumption increases. Wheeler (1982) showed that the weight of a material and it's life-cycle energy usage are directly related. Therefore for a given weight of vehicle the amount of energy consumed in fuel, through out its life-cycle may be calculated:

Average weight of saloon car = 1125kg
Average fuel consumption = 10.8 Km/litre
Average vehicle life mileage = 190,000km

This vehicle, therefore, will use 17,593 litres of fuel in its life time. In terms of energy content, assuming a calorific value of fuel of 32 MJ/litre, this corresponds to
562976 MJ or 563 GJ.

Fussler & Krummenacher also showed that by increasing the weight of a car, with a constant engine size, will result in the use of an extra 9 litres of fuel per 150,000 km. In this case each Kg added will result in an extra 11.5 litres of fuel being consumed over the complete life cycle. This increase in weight is prevalent in newer vehicles, as a result of a number of factors discussed previously.

Disposal

Disposal of vehicles will also in itself use energy, but if the materials within the vehicle are recycled an overall net energy gain will be achieved.

For example, an aluminium sump weighing 6.6 kg will have an overall energy content for the component of 1934 MJ Kamprath (1987). When this component has been recycled the energy balance is 1247 MJ. This is the energy content of the raw materials produced as a result of recycling minus the recycling process energy requirement. Table 3 shows the energy recycling balances for different materials in an automobile weighing approximately 1125kg.
As can be seen from this table over 40% of the energy inherent in the materials of an automobile could be recovered if it was completely recycled.

Total Energy Requirement

By adding the energy required in all three stages of the life-cycle a full life energy requirement may be calculated: Table 4.

Material	Average part energy / kg	Weight as % of total vehicle	Weight Kg	Energy Total (MJ)	Recycling energy balance (MJ)
Polymers	80	9	101.25	8100	2268
Aluminium	293	9	101.25	29666	19283
Non-Ferrous	35	18	202.5	7087.5	2481
Ferrous	54	61	697.5	37665	9793
				82518.5	33825

Table 3. Energy Recovery form Recycling in Disposal

Materials and Manufacture	Use (190,000 KM)	Disposal	Total (MJ)
82518.5 MJ	562976	- no recycling	645494.5
82518.5 MJ	562976	-16912.5 (50% recycling)	628582
82518.5 MJ	562976	-33825 (100% recycling)	611669.5

Table 4. Total Life Energy Requirement.

Even with 100% recycling the overall energy saving is just over 5%. It must be remembered that these figures do not take into account the energy required to re-manufacture the materials recovered into new components.

Refurbishment

Another option available when a vehicle has reached the end of its life is that of refurbishment. Many of the components within a vehicle will outlast others. Components such as engine, transmission, brakes and certain parts of the suspension will wear out while others such as the chassis, wheels and the majority of he interior and bodywork will still deliver many more years of service. **Waterman** (1983) shows a breakdown of the average family saloon in terms of weights of components. Although at present more plastics are being used in cars the main areas of concern for refurbishment have a very similar material composition. The main parts replaced during a refurbishment of a vehicle and the energy requirement as a result of this are shown in table 5.

It must be noted that this refurbishment does not include items such as tyres, exhaust systems, batteries and other 'consumables'.
If an extra 10% is added to the energy requirement figure to allow for repairs to body work etc. the total energy requirement of a refurbishment will be 30,576 MJ.

When this is compered to the energy required to make a new vehicle - 82,518 MJ it can be seen that refurbishment uses only 37% of that amount, Table 6. shows the total energy requirement of a vehicle which has been refurbished (i.e. requirement for its second life-cycle).

Component(s)	Average weight (Kg)	Material composition by Weight (%)	Energy Requirement (MJ)
Power plant	170	75 steel / 25 aluminium	19312
Cooling system	6	50 Al / 10 Polymer / 40 Other	1011
Front suspension	35	100 steel	1883
rear suspension	21	100 steel	1130
Wheels	27	100 steel	1453
Steering	10	90 steel / 10 aluminium	782
Brakes	42	95 steel / 5 other	2220
		Total	27796

Table 5. Energy requirements for vehicle refurbishment

Materials and Manufacture	Use (190,000 Km)	Disposal	Total (MJ)
30576	562976	- no recycling	593552
30576	562976	- 16912.5 (50% Rec.)	576639.5
30576	562976	-33825 (100% Rec.)	559727

Table 6. Energy requirement of a refurbished vehicle (second life-cycle)

Compared to a manufacturing a vehicle form new materials a refurbishment saves over 8% in the total life energy requirement. A further reduction in energy requirement is made if the refurbished vehicle is recycled at the end if it's second life-cycle.

As can be seen from the data in these tables by far the largest percentage of energy requirement is within the use stage of the vehicle life-cycle. It may therefore be more beneficial in environmental terms to make the issues effecting fuel economy a key consideration in the life-cycle design strategy.

Factors Effecting the Fuel Economy

Listed below are the five major factors that effect vehicle fuel economy.

1) Engine Efficiency.
2) Air Resistance.
3) Rolling resistance.
4) Vehicle Weight.

Each of these will be discussed in turn.

Engine Efficiency

The efficiency of an Internal Combustion (I.C.) engine is governed by the energy losses incurred during the conversion of chemical energy into mechanical work. Nagesh et al. (1992) catergorise the inefficiences associated with the production of mechanical work by burning fuel within an I.C. engine into the following groups:-

i) *Cycle Efficiency* - The heat energy available is not fully converted into useful mechanical work. Nagesh et al. (1992) state that typical cycle efficiency is about 45 to 50%. They go on to

state that it is possible to improve the cycle efficiency of an Otto-cycle engine by increasing the Compression Ratio (CR) or the Expansion Ratio (ER), or by increasing both simultaneously. In a spark ignition engine, increasing CR is restricted by the onset of detonation.

ii) *Mechanical Efficiency* - Which can be split into two types of parasitic losses; Frictional losses and Pumping losses. Frictional loss occurs in the bearings, at the piston ring to bore wall interface, valve components and other mechanical parts of the engine and engine accessories such as oil and water pumps. **Nagesh et al.** (1992) suggest that mechanical efficiency of a typical automotive engine is of the order of 85 to 90%. Pumping losses are caused by the work done in pumping gas into and out of the engine, past the throttle, valves and through the manifolds. Therefore the mechanical efficiency is highly dependant upon throttle position. As the engine is increasingly throttled, mechanical efficiency decreases, eventually to zero at idle operation.

Air Resistance

At 120 km/h drag is responsible for about 70% of the total vehicle resistance. However the majority of journeys made by passenger cars are low speed (i.e. below 50 km/h) where aerodynamic drag typically accounts for less than 1/3 of the vehicles resistance. Modern styling trends can produce an aerodynamically efficient body shape.

Rolling Resistance

The vehicle's rolling resistance is comprised of:

i)Tyre rolling resistance
ii) Frictional losses

Tyre Rolling Resistance

As a vehicles wheels rotate, the tyres deform, the portion in contact with the ground being flattened by the vehicles weight. Hystersis of the rubber compound of the tyre causing energy loss. Figure 2. from **Salerno** (1983) depicts the power required at different speeds by a typical small car. It can be seen that at high speeds the loss from the tyres forms a small percentage of the vehicle drag, however at low speeds, it can contribute as much as 40% of the total power required to maintain constant speed.

Whilst low hystersis rubber compounds or minimising deformation in the areas in which energy loss is greatest can help to reduce tyre rolling resistance. **Gerresheim** (1983) mentions that it is also necessary to ensure that wet skid resistance, handling behaviour, aquaplaning, noise and wear resistance are not seriously affected.

The rolling resistance is also dependant upon the wheel load and inflation pressure, which will determine the magnitude of deformation during rolling.

Frictional Losses

All moving components incur frictional losses at their interface where there is a discontinuity in velocity of the components. This can be minimised by the use of lubricants or surface treatments. In a typical saloon car a large proportion of such energy loss occurs in the engine, which is taken into account as part of the overall engine efficiency. There are also losses in the gearbox, differential, brake components and the wheel bearings.

Vehicle Weight

Increased vehicle weight has a direct effect on the vehicle fuel economy (as discussed earlier). The increased weight also has other detrimental effects, e.g. a heavier car will need a more powerful engine to attain the same acceleration rates. The increased power of the engine will

necessitate the use of a stronger, heavier gearbox and drive line components. Suspension components will need to be stronger/stiffer, also power steering may be required. It is clear therefore that a increase in vehicle body weight may result in other design alterations which increase weight further. If extra mass is added to rotating components (crankshaft, flywheel, propshaft, wheels etc.) the extra rotational inertia of these components will yield an added performance deficit when accelerating.

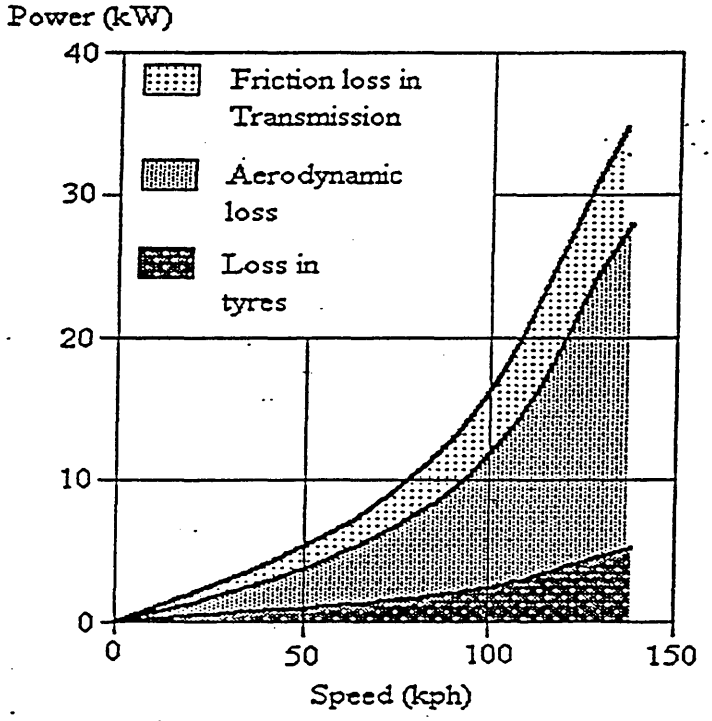

Figure 2. Power Required to Overcome Frictional and Aerodynamic Losses

Conclusions

Manufacturing, using and disposing of vehicles requires large amounts of energy. This energy requirement has been shown to be a good measure of environmental performance.
A new vehicle from virgin materials uses only 13% of the total life-cycle energy requirement in the materials and manufacturing stage, the remaining 87% being consumed during the vehicles operation. Benefits can be achieved by recycling and refurbishment, but as this work has shown refurbishing a vehicle saves only 8% in terms of life-cycle energy usage. In this case the energy saved is in the materials and shifts the balance of in-use energy requirement further still to 95%.
The main aim of studies attempting to reduce environmental impact is to identify the biggest problem area and address it first, as this is the biggest opportunity for environmental gain. As this paper has attempted to show, the use of vehicles is by far the largest contributor to their overall environmental effect and as such this is the life-cycle stage which should be considered in the greatest detail.
By studying the areas outlined and attempting to reduce the fuel consumption of vehicles their impact on the environment may be reduced significantly.

References

Bladon, S. (1993) *Observer's Cars.*, Penguin Books Limited,.

Blunden, J. (1982) *The Observer's Book of Automobiles*, Frederick Warne (Publishers) Ltd., London.

Diakoulaki, A. & Koumoutsos, N. K. (1991) Comparative Evaluation of Alternative Beverage Containers with Multiple Criteria Analysis. *Resources, Conservation and Recycling*, pages 241 - 252. Elsevier Science Publishers.

Fussler, C. & Krummenacher, B. (1991) Ecobalances: a key to better environmental material choices in automobile design. *Materials and Design*, Vol. 12 No. 3 June.

Gerresheim, M. (1998) Dependence of Vehicle Fuel Consumption on the Tyre-Wheel Assembly. *Automobile Wheels and Tyres*. Institute of Mechanical Engineers. ISBN 0 85298 524 X

Hendrickson et al. (1994) Green Design, *National Academy of Engineering Workshop "Engineering Within Ecological Constraints,"* April 19 - 21. Washington, DC

Kamprath, A. (1987) Kunststoff - *Motorolwanne fur den Porsche 944 - Grun Satzuntersuchungen an Prototypbauteilen*. VDI, page 85.

Nagesh, M. S., Govinda Mallan, K. R. & Gopalakrishnan, K. V. (1992) Experimental Investigation on Extended Expansion Engine (EEE) *SAE Paper No. 920452*..

Salerno, P (1983) Considerations on Fuel Consumption and Performance of a Vehicle Fitted with Low Rolling Resistance Tyres. *Automobile Wheels and Tyres*. Institute of Mechanical Engineers. ISBN 0 85298 524 X

Waterman, N. A. (1983) *Materials Substitution in the Mass Produced Automobile*. Issued by the Materials Forum. Institute Mechanical Engineers, UK.

Wheeler, M. A. (1982) Lightweight Materials and Life Cycle Energy Use. *SAE Technical Paper No. 820148*, Detroit.

AUTOTECH 95
C498/2/038

The Determination of the Hydrocarbon Species Present in the Particulate SOF, from a Turbocharged Diesel Engine

P Yates BEng, D Douce BSc and P W Foss, Sheffield Hallam University and
D H Tidmarsh, University of Central England and M Willcock, AE Goetze Ltd, UK

I MECH E
INSTITUTION OF MECHANICAL ENGINEERS
1 Birdcage Walk
London SW1H 9JJ
Tel: 0171 222 7899
Fax: 0171 222 4557
Registered charity number 206882

Abstract

A direct injection diesel engine using reference fuel and oil was subjected to steady state emission testing. The methods and equipment used are discussed. The particulate matter was collected using a dilution tunnel and the Soluble Organic Fraction(SOF) extracted and separated into functional groups by liquid chromatography. Gas chromatography with mass spectrometry was used to identify the hydrocarbon species present in each group. The results show that as the air fuel mixture increases, the distribution and quantity of hydrocarbon species present in the SOF diminish for all functional groups analysed.

Test Equipment

The engine used to generate the particulate matter was a in line 4 cylinder, 4 litre, non inter cooled direct injection engine with a turbo charger. The fuel pump was a Lucas DPA with the fuel injection timing set to 12° BTDC. Throughout all tests the fuel and oil used was of reference quality and from the same batch to retain the same hydrocarbon species distribution, the oil being Silkolene RL 139 and the fuel CCRF03. The chromatogram for the fuel is shown in figure 1. Gas phase exhaust gases were sampled from the exhaust

system at a point 1m from the turbo charger exit. These were transported by a heated sample line at 180°C to a multi gas analyser to determine the CO, CO_2 and NOx. The uHC levels were obtained using a flame ionisation detector. To allow repeatability of test data the engines cooling water, exhaust gas, inlet manifold, oil temperatures and the cylinder pressures were measured and recorded. The cylinder pressure data was recorded by piezo electric pressure transducers placed adjacent to the injector nozzle.

Origins of Hydrocarbon Emissions form a Diesel Engine.

The hydrocarbon emissions from diesel engines(C.I.) are typically lower than those from a spark ignition (S.I.) engine, but with exhaust after treatment the exhaust gas from a S.I. engine that enters the atmosphere contains comparable levels. Oxidation catalysts (3 way) that are fitted to S.I. engines will not function on C.I. engines because of the lower exhaust gas temperatures, the possibility of blockage through soot and the quantity of oxygen present in the exhaust gas. Oxidation catalysts have been developed for diesel engines, but any sulphur dioxide(bp -10°C) present in the exhaust gas is oxidised further to sulphur trioxide(bp 44.7°C), thus any sulphur compounds collected by a dilution tunnel would be 25% heavier and in greater quantities because the boiling point of the compound is nearer the maximum allowable sampling temperature (52°C).

Combustion in a C.I. engine is in three general stages:

1. Delay (the time between the start of injection and the start of combustion).
2. Rapid combustion (the burning of the fuel injected during the delay period) .
3. Controlled combustion (fuel burning as it is injected).

The unburnt hydrocarbon(UHC) formation mechanisms for each of these stages are different. The speculated routes have been shown by Yu[1], figure 2 does not show the effects of the system boundaries, i.e. wall quench and adsorption desorption of the fuel into the lubricating oil. Daniel and Whitehouse[2, 3] used in-cylinder sampling on a S.I. engine to determine the distribution of hydrocarbons. Their tests showed that as the sample point neared the cylinder wall the hydrocarbon concentrations increased, indicating wall quench. Multi spray C.I. diesel engines delivering high fuel quantities can allow the fuel spray to penetrate too far into the combustion chamber so that it impinges onto the cylinder wall or piston crown. Conditions in this area are relatively cool with poor or no air swirl and the fuel will not ignite. Lyn and Valdmanis[4] varied injector hole size, nozzle

type and its geometry, with none of these affecting the ignition delay. When the hole size was doubled and the injection pressure remained constant, the fuel flow rate increased by a factor of four and the droplet size increased by approximately 30 percent.

A source of UHC also associated with the injector is that of the fuel remaining in the injector nozzle after injection. This is most significant at low fuel injection volumes where there is little overmixing. Greeves[5] found that a $1mm^3$ nozzle sac volume gave 350 ppm C_1, and he also stated that $1mm^3$ of fuel gave 1660 ppm C_1. He postulated that the volume may not be filled with fuel and the higher boiling point fractions of the fuel remained in the nozzle. The relationship between nozzle sac volume and exhaust HC is linear, with its intercept for zero HC at $-1.8mm^3$ for a speed range of 1700 - 2800 rpm. The rate of fuel injection in the majority of production diesel engines is assumed constant after the injector needle has attained its fully open condition. Vollenweider[6] completed a series of tests using a two spring injector. This style of injector allowed a small amount of fuel to be injected before the main quantity and this reduced the heat release within the premixed combustion stage. The net result in emissions was a reduction of HC and NOx but an increase in particulates. In a study of "in use" motor vehicles Williams(7) reported that injectors that had a lower opening pressure than the standard specification produced higher levels of emitted particulate matter. This is because the lower kinetic energy of the particle allows it to slow in the air stream, removing its supply of oxygen.

The highest concentrations of soot within the combustion chamber of a diesel engine are in the core region of each of the fuel sprays. This is where the local equivalence ratios are very rich. The formation of the soot particle initiates with a fuel molecule containing 12 to 22 carbon atoms and a H/C ratio of approximately 2 and progresses through the two stages proposed by Haynes[8],

i) Particle formation - the first condensed phase of the material formed by oxidation and pyrolysis. The typical components of these are unsaturated hydrocarbons i.e. acetylene and multiples of $C_{2n}H_2$, and polycyclic aromatic hydrocarbons (PAH). These particles are very small($d < 2nm$).

ii) Particle growth - by surface growth (gas phase material condensing and being incorporated) and agglomeration of smaller particles.
Studies[9] with combustion bombs have shown three different paths to soot formation

depending on combustion temperature. At the lowest temperatures (>1700 °C) only aromatics or highly unsaturated aliphatic compounds of high molecular weight are very successful in forming solid carbon through pyrolysis. At intermediate temperatures typical of diffusion flames (<1800 °C), all normally used hydrocarbon fuels produce soot if burned at a significantly rich mixture. At very high temperatures (above the range found in diesel engines) a nucleation process utilising carbon vapour is the primary formation mechanism.

Particulate Sampling

The exhaust gas immediately leaving the tailpipe of a diesel engine is composed primarily of elemental carbon and organic compounds, and at normal in cylinder temperatures these exist separately. The purpose of a dilution tunnel is to simulate the mixing of the exhaust gas with the external air cooling the exhaust and allowing the organic compounds to condense onto the elemental carbon. The maximum permissible sampling temperature for a dilution tunnel is 52°C. This is the mid point between the boiling points of pentane(Bp 36.1°C) and hexane(Bp 68.7°C). To reduce the sample gas temperature further to the boiling point of pentane, the dilution ratio would have to be increased to a region above that of the optimum ratio for the collection of the extractable fraction. The dilution ratio for the collection of the maximum amount of the extractable organic fraction is approximately 5:1. The reasons for this are that, as the dilution ratio increases from unity, the effect of the decreasing temperature on the number of active sites dominates the condensation process. When the dilution ratio becomes higher the decreasing partial pressure causes the extractable mass to fall again. Condensation will occur whenever the vapour pressure of the gaseous phase hydrocarbons exceeds its saturated vapour pressure. Increasing the dilution ratio decreases the hydrocarbon concentrations and hence the vapour pressure. The total exhaust flow from the engine at high speeds and loads was in excess of the quantity required by the Weslake dilution tunnel for collection of the maximum quantity of the SOF, therefore a diverter system was used to remove the unwanted exhaust gas.

Solvent extraction.

Because of the small amount of material collected for the majority of the test points, the optimum method to determine the amount of material removed by the extraction process is to weigh the filter before and after the process. Because the filter can contribute to the weight difference, blank filters will also have to be subjected to the extraction process.

The overall calculation for the soluble organic fraction by weight loss will be :-

SOF(filter weight loss) = (Wbe - Wae - Avb)
Wbe = Weight before extraction
Wae = Weight after extraction
Avb = Average weight loss of blank filters

The choice of solvent used for extraction influences the group or groups of hydrocarbons removed from the sample, dichloromethane was used for the results presented in this paper, a more aggressive solvent favoured by some researchers is a 4:1 mixture of distilled benzene and methanol[10]. To remove the solvent and to stop any mutation or oxygenation of the remaining matter prior to weighing, the papers were dried in a nitrogen atmosphere. Before any weighing of the filter papers can be undertaken they must be subjected to the same ambient conditions. It is recommended that the papers are stored in temperature and humidity controlled conditions for four hours to equilibrate.

Isocratic Eluant	Group
Hexane	Alkanes
Dichloromethane	Polycyclic Aromatic Hydrocarbons (PAH)
Acetronitrile	Polar PAH & Nitro PAH
Acetronitrile & Methanol (3:1)	Very polar PAH

Table 1

SOF analysis

Clean up procedure[11].

A high performance liquid chromatography(HPLC) system using a alumina column-activated, basic, Brockmann 1 (150 mesh, 250 x 5 mm). This was used to separate the hydrocarbons of interest, i.e. C_8 to C_{30} from any other emitted by the engine, i.e. aromatic and substituted aromatic compounds known to be released by incomplete combustion. Fractionation was achieved on a Varion isocratic HPLC system using a UV detector set at 254 nm. To separate the sample into these groups, low pressure liquid chromatography utilising different elutants was used. Table 1 shows the eluant with the corresponding group

Capillary GC/MSD Analysis

The residual weights of the test samples varied with the speed load conditions i.e. depending upon the contribution to the total collected weight of the soluble fraction, these samples were then diluted with Dichloromethane to give similar concentrations. A 1µl. sample of this was then used for analysis, the instrument used was a Hewlett Packard 5890 (Series II) coupled with a HP 5971A Mass Selective Detector. Electron impact mass spectra were obtained at 70eV and processed using a HP ChemStation data system. The GC conditions used are shown in table 2.

Gas Capillary Chromatographic Conditions	
Carrier gas	Helium
Analytical column	18m x 0.25mm (id), 5% biphenyl fused silica
Film thickness	0.25µm
Oven temperature program	50°C (2 mins) ramped at 10°C/min to 280°C (5 mins)
Volume injected	1µl. splitless

Table 2

The identification of the abundance peaks on the chromatograms produced was initially by the comparison to the retention times of a standard. The hydrocarbon species present in the exhaust and not the calibration sample were identified using a library search on the data system.

Results

The chromatograms shown were obtained by separating the sample into four groups by liquid chromatography. For ease of analysis the group that has undergone the closest scrutiny is the alkanes. This is the first group extracted from the organic fraction and thus has the least chance to degrade or mutate. The compounds that are recognised as the

most harmful are in the second group, these being benzo[*a*]pyrene and possibly 7,12-dimethylbenz[*a*]anthracene. These compounds were recognised as being carcinogens in 1933 and are both polycyclic aromatic hydrocarbons. These compounds are not cancer forming until they form a diol-epoxide.

The chromatogram plots show that as the engine load increases the quantity of carbon atoms present in the most abundant peak also increases. When the load is increased beyond half rated power the two lightest species diminish below a level that can be accurately quantified. The alkane species that are presented are the lightest of those shown on all plots. There is a greater distribution of species present at lower speeds, i.e. there are both heavier and lighter species detected at idle than those detected at 75% of rated power. As the combustion temperatures and pressures increase so does the degree of fuel pyroliysis, therefore, the heavier fuel molecules break down into lighter components; these components have lower vapour pressures and auto ignition temperatures and are oxidised easier. The size of the most abundant species also increases with the temperature and pressure. A simplified illustration of the chromatograms for the abundance of n-alkanes is shown in figure 3. The concentrations of gas phase uHC's present just prior to the exhaust turbine inlet and a 1 meter from the outlet are shown in figure 4 for comparison. The survivability's of the PAH do not follow this trend (fig 5), the abundance of PAH increases with load and the most probable cause is the increase in oil consumption giving a higher initial quantity of PAH present in the exhaust. The speciation of the lubricating oil by gas chromatography does not produce clear and identifiable peaks, the oil with usage produces clearer peaks this is probably due to fuel contamination[10].

Conclusions

The identification and quantification of the species of hydrocarbon present in the particulate SOF will assist in determining the methods that exhaust pipe uHC has avoided oxidation or pyrolysis. The higher temperatures with increasing load reduce the quantity and carbon number distribution of the species present in the SOF but there is a greater quantity and larger spectrum of the PAH present. The speciation of the uHC present in the exhaust gas stream will be a fundamental method of achieving the ever tightening emission laws.

Acknowledgements

The authors wish to thank AEGoetze for the funding, technical assistance and provision of resources received during this research period, and the School of Science at Sheffield Hallam University for the use of their equipment to analyse the particulate matter.

References

1) Yu R.C., Wong V.W. and Shahed S.M.: " Sources of hydrocarbon emissions from direct injection engines. S.A.E Paper 800048 1980.

2) Daniel, W.A., Wentworth, J.T.: " Exhaust gas hydrocarbons Genesis and Exodus". S.A.E. 486B ,1962.

3) Whitehouse, N.D., Clough, E., and Uhunmwangho, S.O.: " The development of some gaseous products during diesel engine combustion". SAE Paper 800028, 1980.

4) Lyn, W.T., and Valdmanis, E.: "Effects of physical factors on ignition delay". S.A.E. 680102, 1968.

5) Greeves, G., Khan, I.M. , Wang, C.H.T. and Fenne, I.: " Origins of hydrocarbon emissions from diesel engines". SAE Paper 770259.

6) Vollenweider, J.:" Emission-optimised fuel injection for large diesel engines-expectations, limitations and compromises ". Proc IMechE C448/003, 1990.

7) Williams, D.J., Milne, J.W, Quigley, S.M.and Roberts, D.B.: "Particulate emissions from "in use" motor vehicles-II Diesel Vehicles". Atmospheric Environment Vol 23, No12, pp 2647-2661 1989.

8) Haynes, B.S. and Wagner, H.G.: "Soot formation" Prog Energy Combustion Science, Vol 7, pp 229 - 273, 1981.

9) Amann, C.A., and Siegla, D.C.: "Diesel particulates-What they are and why." Aerosol Science Technology, vol , pp 73-101, 1982.

10) Abbass, M.K., Andrews, G.E., Ishaq, R.B. and Williams, P.T.: "A comparison of the particulate composition between turbocharged and naturally aspirated D.I. diesel engines". SAE Paper 910733, 1991.

11) Ciccioli, P et al. Journal of Chromatography, 351 (1986) pp 451 - 464

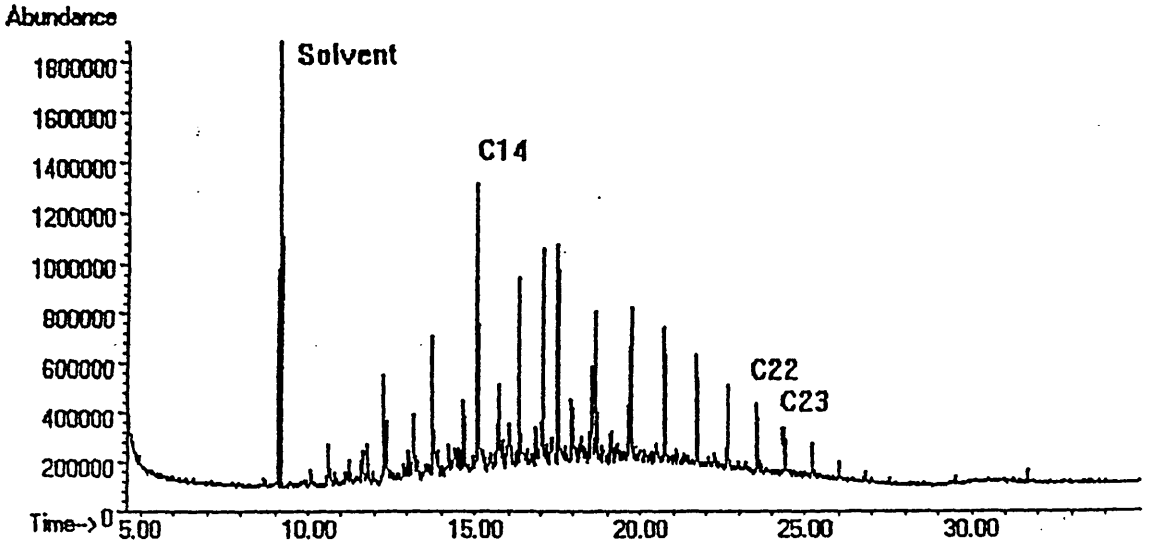

Chromatogram showing all hydrocarbon species

Figure 1

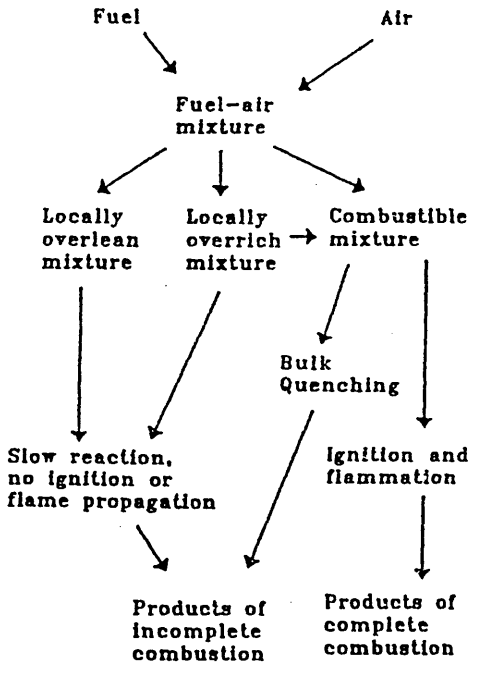

Fuel injected during the delay period

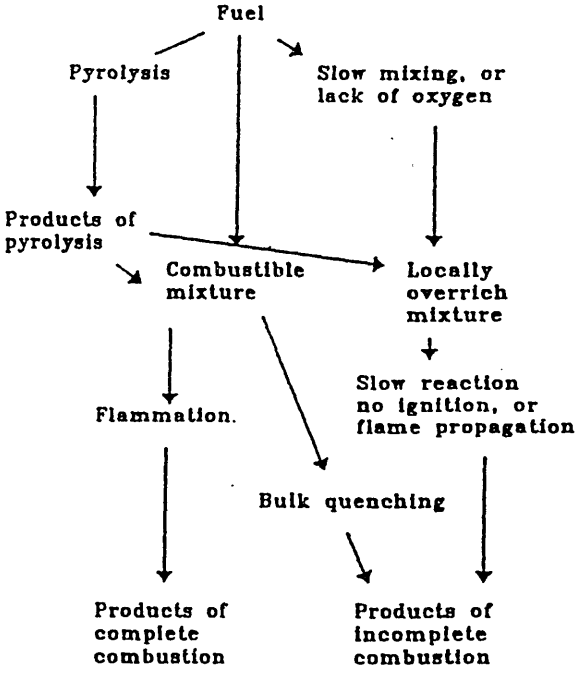

Fuel injected while combustion is occurring

Figure 2

Showing the change in distribution with load

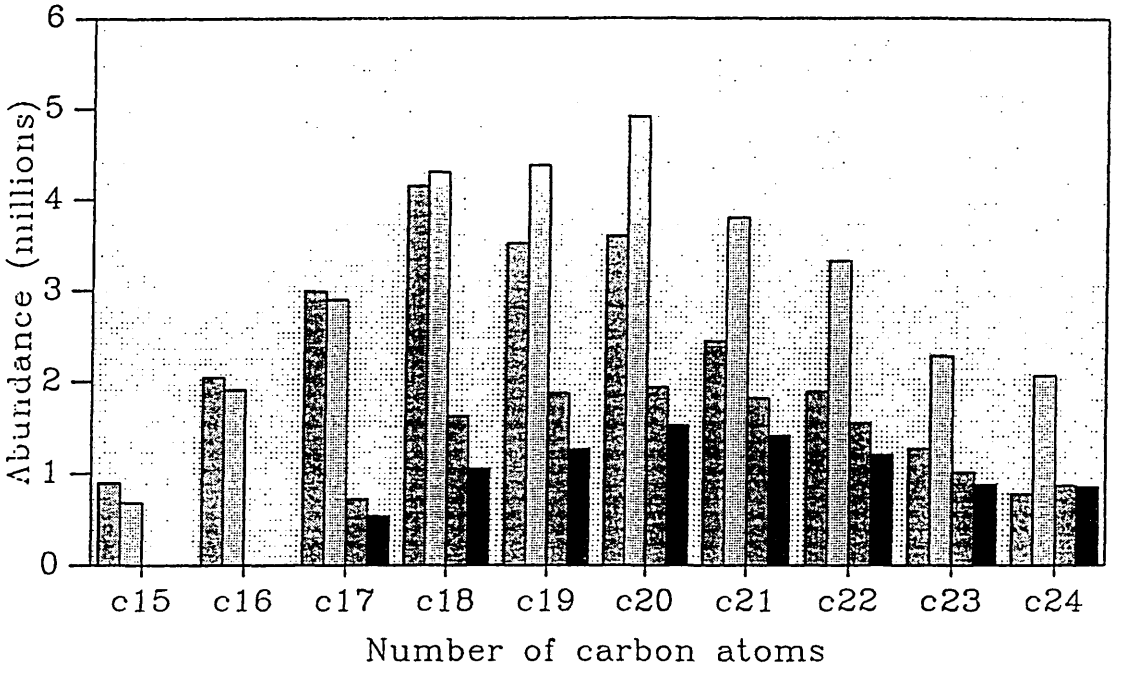

Figure 3

Hydrocarbon Emission with Load

Pre-turbo + 1 meter

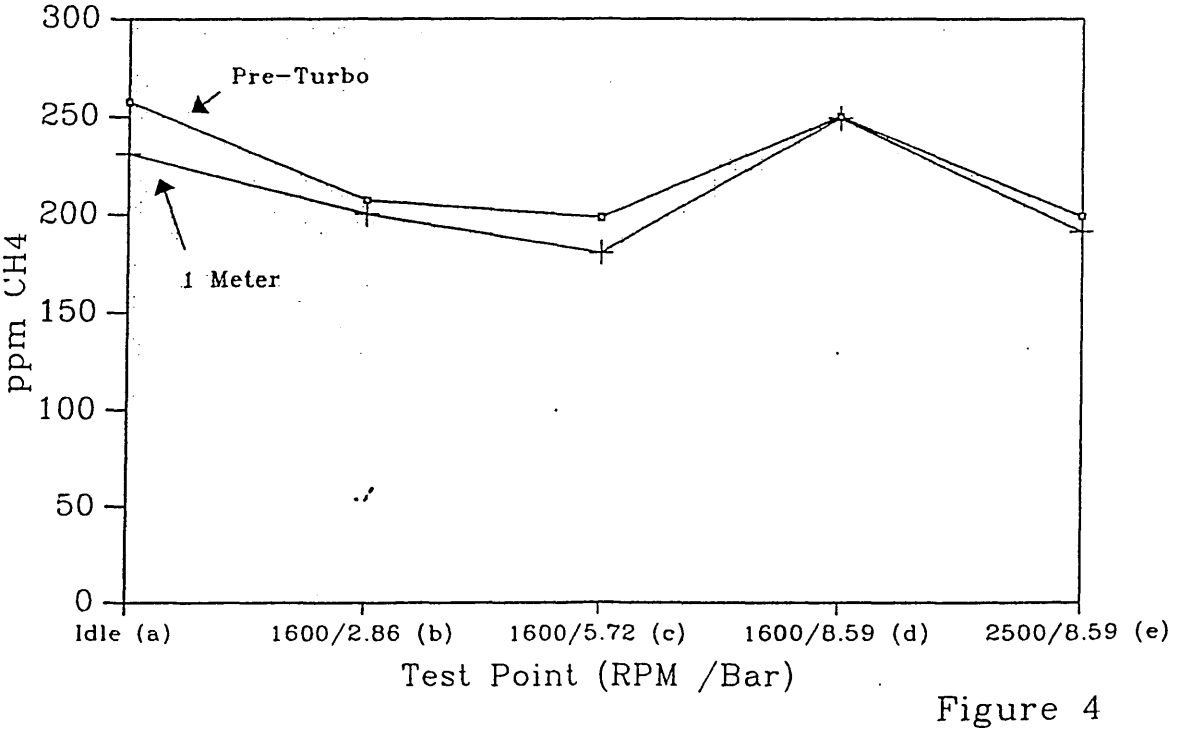

Figure 4

Abundance of PAH
Showing the change in distribution with load

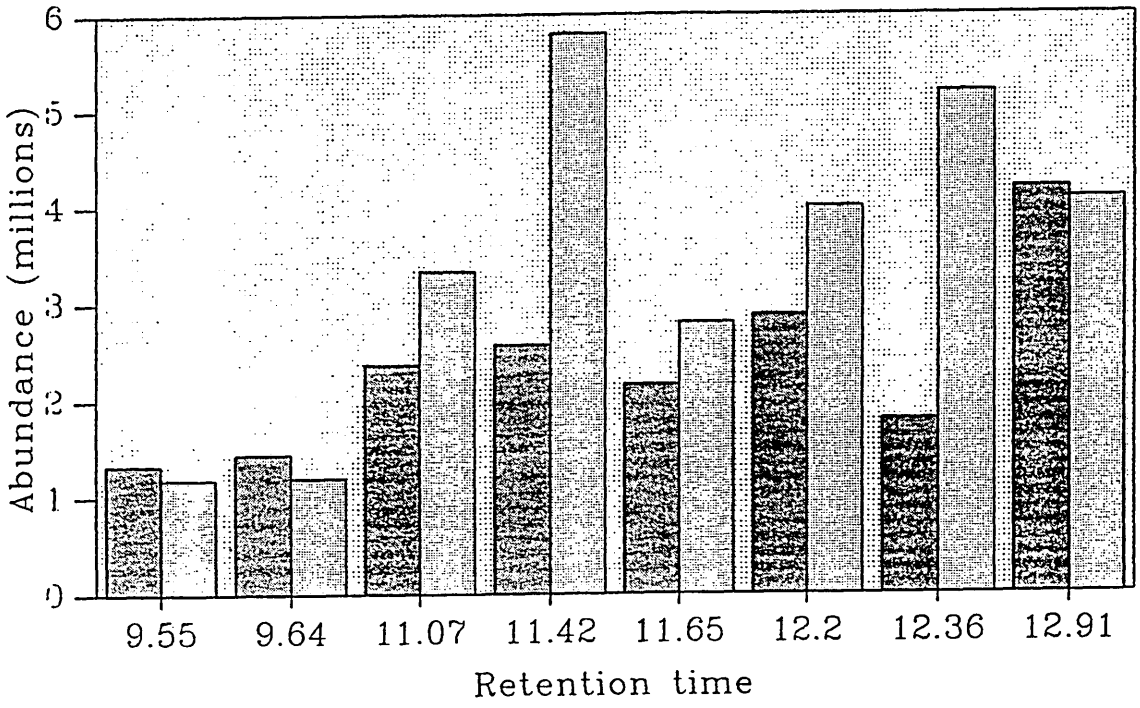

Figure 5

AUTOTECH 95
C498/2/038

I MECH E
INSTITUTION OF MECHANICAL ENGINEERS
1 Birdcage Walk
London SW1H 9JJ
Tel: 0171 222 7899
Fax: 0171 222 4557
Registered charity number 206882

The Determination of the Hydrocarbon Species Present in the Particulate SOF, from a Turbocharged Diesel Engine

P Yates BEng, D Douce BSc and P W Foss, Sheffield Hallam University and
D H Tidmarsh, University of Central England and M Willcock, AE Goetze Ltd, UK

Abstract

A direct injection diesel engine using reference fuel and oil was subjected to steady state emission testing. The methods and equipment used are discussed. The particulate matter was collected using a dilution tunnel and the Soluble Organic Fraction(SOF) extracted and separated into functional groups by liquid chromatography. Gas chromatography with mass spectrometry was used to identify the hydrocarbon species present in each group. The results show that as the air fuel mixture increases, the distribution and quantity of hydrocarbon species present in the SOF diminish for all functional groups analysed.

Test Equipment

The engine used to generate the particulate matter was a in line 4 cylinder, 4 litre, non inter cooled direct injection engine with a turbo charger. The fuel pump was a Lucas DPA with the fuel injection timing set to 12° BTDC. Throughout all tests the fuel and oil used was of reference quality and from the same batch to retain the same hydrocarbon species distribution, the oil being Silkolene RL 139 and the fuel CCRF03. The chromatogram for the fuel is shown in figure 1. Gas phase exhaust gases were sampled from the exhaust

system at a point 1m from the turbo charger exit. These were transported by a heated sample line at 180°C to a multi gas analyser to determine the CO, CO_2 and NOx. The uHC levels were obtained using a flame ionisation detector. To allow repeatability of test data the engines cooling water, exhaust gas, inlet manifold, oil temperatures and the cylinder pressures were measured and recorded. The cylinder pressure data was recorded by piezo electric pressure transducers placed adjacent to the injector nozzle.

Origins of Hydrocarbon Emissions form a Diesel Engine.

The hydrocarbon emissions from diesel engines(C.I.) are typically lower than those from a spark ignition (S.I.) engine, but with exhaust after treatment the exhaust gas from a S.I. engine that enters the atmosphere contains comparable levels. Oxidation catalysts (3 way) that are fitted to S.I. engines will not function on C.I. engines because of the lower exhaust gas temperatures, the possibility of blockage through soot and the quantity of oxygen present in the exhaust gas. Oxidation catalysts have been developed for diesel engines, but any sulphur dioxide(bp -10°C) present in the exhaust gas is oxidised further to sulphur trioxide(bp 44.7°C), thus any sulphur compounds collected by a dilution tunnel would be 25% heavier and in greater quantities because the boiling point of the compound is nearer the maximum allowable sampling temperature (52°C).

Combustion in a C.I. engine is in three general stages:

1. Delay (the time between the start of injection and the start of combustion).
2. Rapid combustion (the burning of the fuel injected during the delay period) .
3. Controlled combustion (fuel burning as it is injected).

The unburnt hydrocarbon(UHC) formation mechanisms for each of these stages are different. The speculated routes have been shown by Yu[1], figure 2 does not show the effects of the system boundaries, i.e. wall quench and adsorption desorption of the fuel into the lubricating oil. Daniel and Whitehouse[2, 3] used in-cylinder sampling on a S.I. engine to determine the distribution of hydrocarbons. Their tests showed that as the sample point neared the cylinder wall the hydrocarbon concentrations increased, indicating wall quench. Multi spray C.I. diesel engines delivering high fuel quantities can allow the fuel spray to penetrate too far into the combustion chamber so that it impinges onto the cylinder wall or piston crown. Conditions in this area are relatively cool with poor or no air swirl and the fuel will not ignite. Lyn and Valdmanis[4] varied injector hole size, nozzle

type and its geometry, with none of these affecting the ignition delay. When the hole size was doubled and the injection pressure remained constant, the fuel flow rate increased by a factor of four and the droplet size increased by approximately 30 percent.

A source of UHC also associated with the injector is that of the fuel remaining in the injector nozzle after injection. This is most significant at low fuel injection volumes where there is little overmixing. Greeves[5] found that a $1mm^3$ nozzle sac volume gave 350 ppm C_1, and he also stated that $1mm^3$ of fuel gave 1660 ppm C_1. He postulated that the volume may not be filled with fuel and the higher boiling point fractions of the fuel remained in the nozzle. The relationship between nozzle sac volume and exhaust HC is linear, with its intercept for zero HC at $-1.8mm^3$ for a speed range of 1700 - 2800 rpm. The rate of fuel injection in the majority of production diesel engines is assumed constant after the injector needle has attained its fully open condition. Vollenweider[6] completed a series of tests using a two spring injector. This style of injector allowed a small amount of fuel to be injected before the main quantity and this reduced the heat release within the premixed combustion stage. The net result in emissions was a reduction of HC and NOx but an increase in particulates. In a study of "in use" motor vehicles Williams(7) reported that injectors that had a lower opening pressure than the standard specification produced higher levels of emitted particulate matter. This is because the lower kinetic energy of the particle allows it to slow in the air stream, removing its supply of oxygen.

The highest concentrations of soot within the combustion chamber of a diesel engine are in the core region of each of the fuel sprays. This is where the local equivalence ratios are very rich. The formation of the soot particle initiates with a fuel molecule containing 12 to 22 carbon atoms and a H/C ratio of approximately 2 and progresses through the two stages proposed by Haynes[8],

i) Particle formation - the first condensed phase of the material formed by oxidation and pyrolysis. The typical components of these are unsaturated hydrocarbons i.e. acetylene and multiples of C_{2n} H_2 , and polycyclic aromatic hydrocarbons (PAH). These particles are very small($d < 2nm$).

ii) Particle growth - by surface growth (gas phase material condensing and being incorporated) and agglomeration of smaller particles.
Studies[9] with combustion bombs have shown three different paths to soot formation

depending on combustion temperature. At the lowest temperatures (>1700 °C) only aromatics or highly unsaturated aliphatic compounds of high molecular weight are very successful in forming solid carbon through pyrolysis. At intermediate temperatures typical of diffusion flames (<1800 °C), all normally used hydrocarbon fuels produce soot if burned at a significantly rich mixture. At very high temperatures (above the range found in diesel engines) a nucleation process utilising carbon vapour is the primary formation mechanism.

Particulate Sampling

The exhaust gas immediately leaving the tailpipe of a diesel engine is composed primarily of elemental carbon and organic compounds, and at normal in cylinder temperatures these exist separately. The purpose of a dilution tunnel is to simulate the mixing of the exhaust gas with the external air cooling the exhaust and allowing the organic compounds to condense onto the elemental carbon. The maximum permissible sampling temperature for a dilution tunnel is 52°C. This is the mid point between the boiling points of pentane(Bp 36.1°C) and hexane(Bp 68.7°C). To reduce the sample gas temperature further to the boiling point of pentane, the dilution ratio would have to be increased to a region above that of the optimum ratio for the collection of the extractable fraction. The dilution ratio for the collection of the maximum amount of the extractable organic fraction is approximately 5:1. The reasons for this are that, as the dilution ratio increases from unity, the effect of the decreasing temperature on the number of active sites dominates the condensation process. When the dilution ratio becomes higher the decreasing partial pressure causes the extractable mass to fall again. Condensation will occur whenever the vapour pressure of the gaseous phase hydrocarbons exceeds its saturated vapour pressure. Increasing the dilution ratio decreases the hydrocarbon concentrations and hence the vapour pressure. The total exhaust flow from the engine at high speeds and loads was in excess of the quantity required by the Weslake dilution tunnel for collection of the maximum quantity of the SOF, therefore a diverter system was used to remove the unwanted exhaust gas.

Solvent extraction.

Because of the small amount of material collected for the majority of the test points, the optimum method to determine the amount of material removed by the extraction process is to weigh the filter before and after the process. Because the filter can contribute to the weight difference, blank filters will also have to be subjected to the extraction process.

The overall calculation for the soluble organic fraction by weight loss will be :-

SOF(filter weight loss) = (Wbe - Wae - Avb)
Wbe = Weight before extraction
Wae = Weight after extraction
Avb = Average weight loss of blank filters

The choice of solvent used for extraction influences the group or groups of hydrocarbons removed from the sample, dichloromethane was used for the results presented in this paper, a more aggressive solvent favoured by some researchers is a 4:1 mixture of distilled benzene and methanol[10]. To remove the solvent and to stop any mutation or oxygenation of the remaining matter prior to weighing, the papers were dried in a nitrogen atmosphere. Before any weighing of the filter papers can be undertaken they must be subjected to the same ambient conditions. It is recommended that the papers are stored in temperature and humidity controlled conditions for four hours to equilibrate.

Isocratic Eluant	Group
Hexane	Alkanes
Dichloromethane	Polycyclic Aromatic Hydrocarbons (PAH)
Acetronitrile	Polar PAH & Nitro PAH
Acetronitrile & Methanol (3:1)	Very polar PAH

Table 1

SOF analysis

Clean up procedure[11].

A high performance liquid chromatography(HPLC) system using a alumina column-activated, basic, Brockmann 1 (150 mesh, 250 x 5 mm). This was used to separate the hydrocarbons of interest, i.e. C_8 to C_{30} from any other emitted by the engine, i.e. aromatic and substituted aromatic compounds known to be released by incomplete combustion. Fractionation was achieved on a Varion isocratic HPLC system using a UV detector set at 254 nm. To separate the sample into these groups, low pressure liquid chromatography utilising different elutants was used. Table 1 shows the eluant with the corresponding group

Capillary GC/MSD Analysis

The residual weights of the test samples varied with the speed load conditions i.e. depending upon the contribution to the total collected weight of the soluble fraction, these samples were then diluted with Dichloromethane to give similar concentrations. A 1µl. sample of this was then used for analysis, the instrument used was a Hewlett Packard 5890 (Series II) coupled with a HP 5971A Mass Selective Detector. Electron impact mass spectra were obtained at 70eV and processed using a HP ChemStation data system. The GC conditions used are shown in table 2.

Gas Capillary Chromatographic Conditions	
Carrier gas	Helium
Analytical column	18m x 0.25mm (id), 5% biphenyl fused silica
Film thickness	0.25µm
Oven temperature program	50°C (2 mins) ramped at 10°C/min to 280°C (5 mins)
Volume injected	1µl. splitless

Table 2

The identification of the abundance peaks on the chromatograms produced was initially by the comparison to the retention times of a standard. The hydrocarbon species present in the exhaust and not the calibration sample were identified using a library search on the data system.

Results

The chromatograms shown were obtained by separating the sample into four groups by liquid chromatography. For ease of analysis the group that has undergone the closest scrutiny is the alkanes. This is the first group extracted from the organic fraction and thus has the least chance to degrade or mutate. The compounds that are recognised as the

most harmful are in the second group, these being benzo[*a*]pyrene and possibly 7,12-dimethylbenz[*a*]anthracene. These compounds were recognised as being carcinogens in 1933 and are both polycyclic aromatic hydrocarbons. These compounds are not cancer forming until they form a diol-epoxide.

The chromatogram plots show that as the engine load increases the quantity of carbon atoms present in the most abundant peak also increases. When the load is increased beyond half rated power the two lightest species diminish below a level that can be accurately quantified. The alkane species that are presented are the lightest of those shown on all plots. There is a greater distribution of species present at lower speeds, i.e. there are both heavier and lighter species detected at idle than those detected at 75% of rated power. As the combustion temperatures and pressures increase so does the degree of fuel pyroliysis, therefore, the heavier fuel molecules break down into lighter components; these components have lower vapour pressures and auto ignition temperatures and are oxidised easier. The size of the most abundant species also increases with the temperature and pressure. A simplified illustration of the chromatograms for the abundance of n-alkanes is shown in figure 3. The concentrations of gas phase uHC's present just prior to the exhaust turbine inlet and a 1 meter from the outlet are shown in figure 4 for comparison. The survivability's of the PAH do not follow this trend (fig 5), the abundance of PAH increases with load and the most probable cause is the increase in oil consumption giving a higher initial quantity of PAH present in the exhaust. The speciation of the lubricating oil by gas chromatography does not produce clear and identifiable peaks, the oil with usage produces clearer peaks this is probably due to fuel contamination[10].

Conclusions

The identification and quantification of the species of hydrocarbon present in the particulate SOF will assist in determining the methods that exhaust pipe uHC has avoided oxidation or pyrolysis. The higher temperatures with increasing load reduce the quantity and carbon number distribution of the species present in the SOF but there is a greater quantity and larger spectrum of the PAH present. The speciation of the uHC present in the exhaust gas stream will be a fundamental method of achieving the ever tightening emission laws.

Acknowledgements

The authors wish to thank AEGoetze for the funding, technical assistance and provision of resources received during this research period, and the School of Science at Sheffield Hallam University for the use of their equipment to analyse the particulate matter.

References

1) Yu R.C., Wong V.W. and Shahed S.M.: " Sources of hydrocarbon emissions from direct injection engines. S.A.E Paper 800048 1980.

2) Daniel, W.A., Wentworth, J.T.: " Exhaust gas hydrocarbons Genesis and Exodus". S.A.E. 486B ,1962.

3) Whitehouse, N.D., Clough, E., and Uhunmwangho, S.O.: " The development of some gaseous products during diesel engine combustion". SAE Paper 800028, 1980.

4) Lyn, W.T., and Valdmanis, E.: "Effects of physical factors on ignition delay". S.A.E. 680102, 1968.

5) Greeves, G., Khan, I.M. , Wang, C.H.T. and Fenne, I.: " Origins of hydrocarbon emissions from diesel engines". SAE Paper 770259.

6) Vollenweider, J.:" Emission-optimised fuel injection for large diesel engines-expectations, limitations and compromises ". Proc IMechE C448/003, 1990.

7) Williams, D.J., Milne, J.W, Quigley, S.M.and Roberts, D.B.: "Particulate emissions from "in use" motor vehicles-II Diesel Vehicles". Atmospheric Environment Vol 23, No12, pp 2647-2661 1989.

8) Haynes, B.S. and Wagner, H.G.: "Soot formation" Prog Energy Combustion Science, Vol 7, pp 229 - 273, 1981.

9) Amann, C.A., and Siegla, D.C.: "Diesel particulates-What they are and why." Aerosol Science Technology, vol , pp 73-101, 1982.

10) Abbass, M.K., Andrews, G.E., Ishaq, R.B. and Williams, P.T.: "A comparison of the particulate composition between turbocharged and naturally aspirated D.I. diesel engines". SAE Paper 910733, 1991.

11) Ciccioli, P et al. Journal of Chromatography, 351 (1986) pp 451 - 464

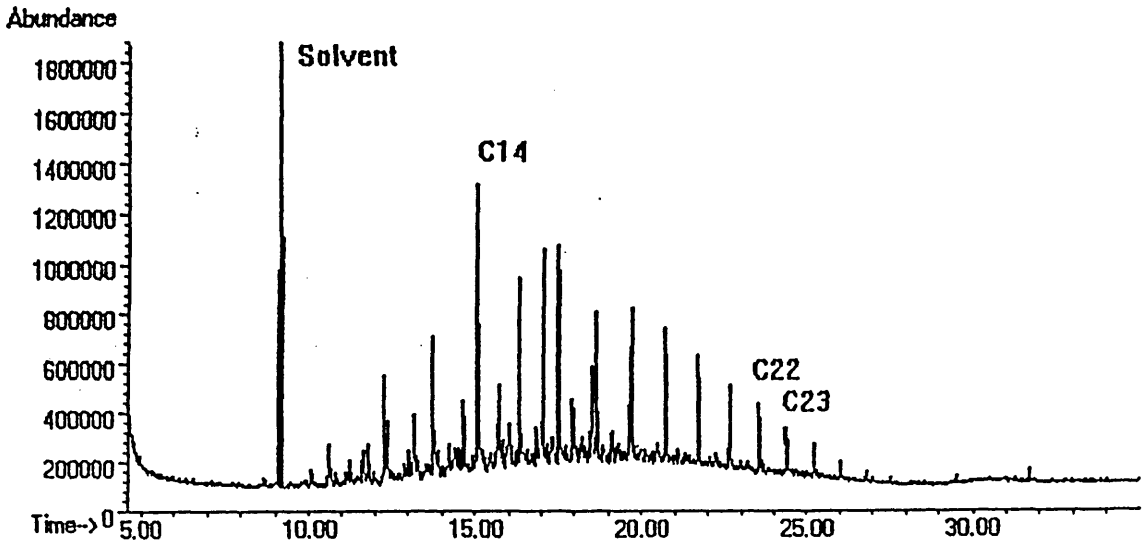

Chromatogram showing all hydrocarbon species

Figure 1

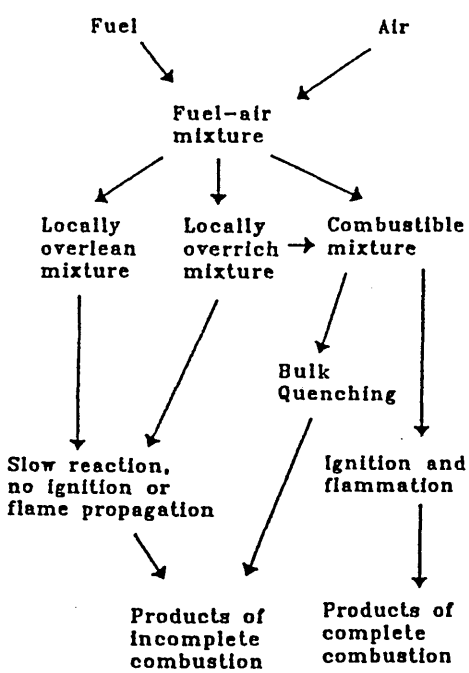

Fuel injected during the delay period

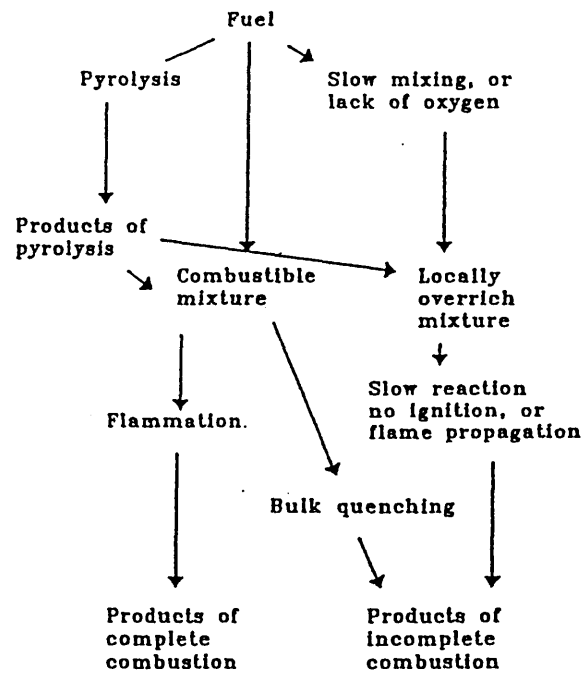

Fuel injected while combustion is occurring

Figure 2

Showing the change in distribution with load

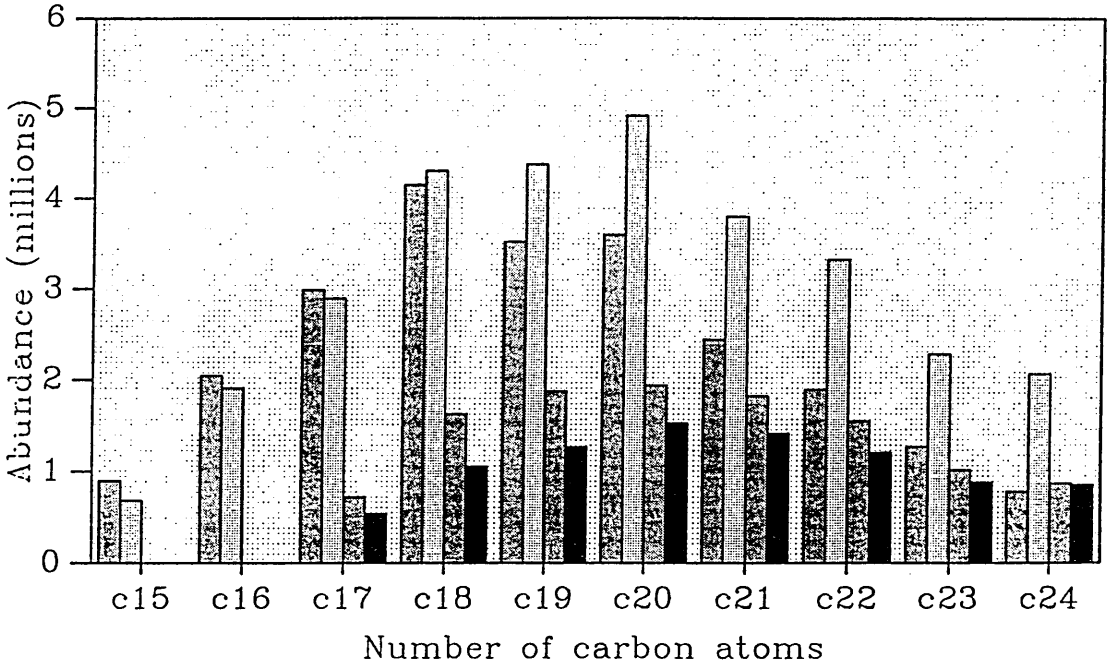

Figure 3

Hydrocarbon Emission with Load

Pre-turbo + 1 meter

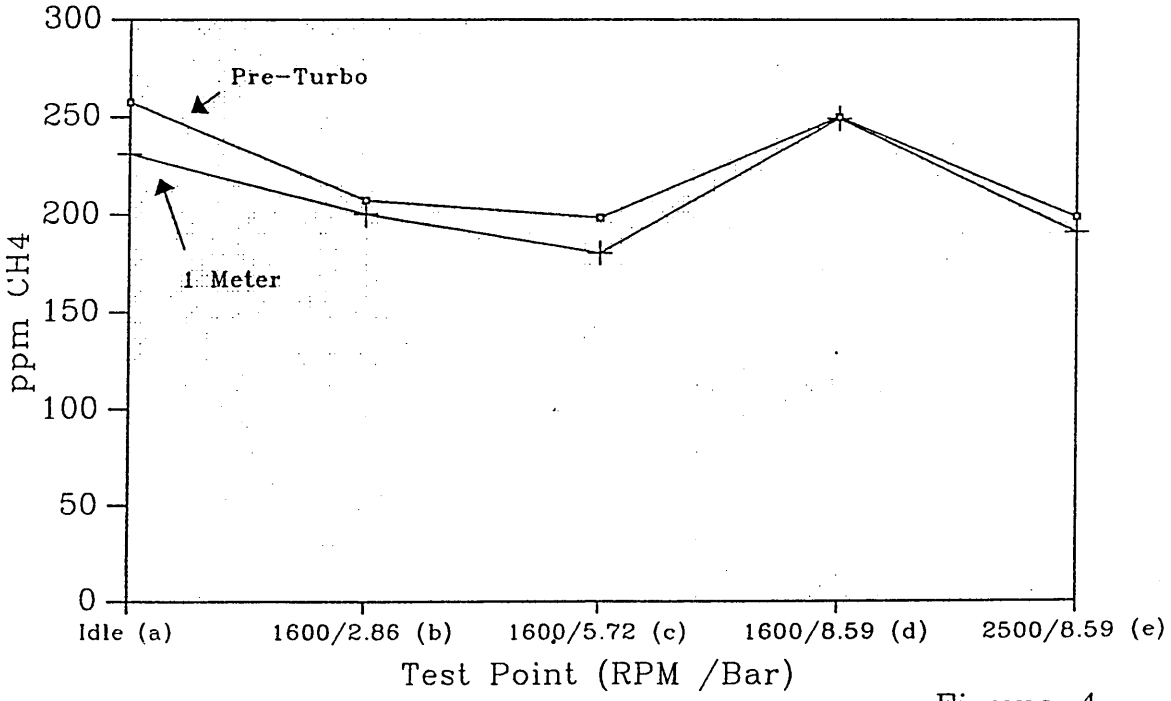

Figure 4

Abundance of PAH

Showing the change in distribution with load

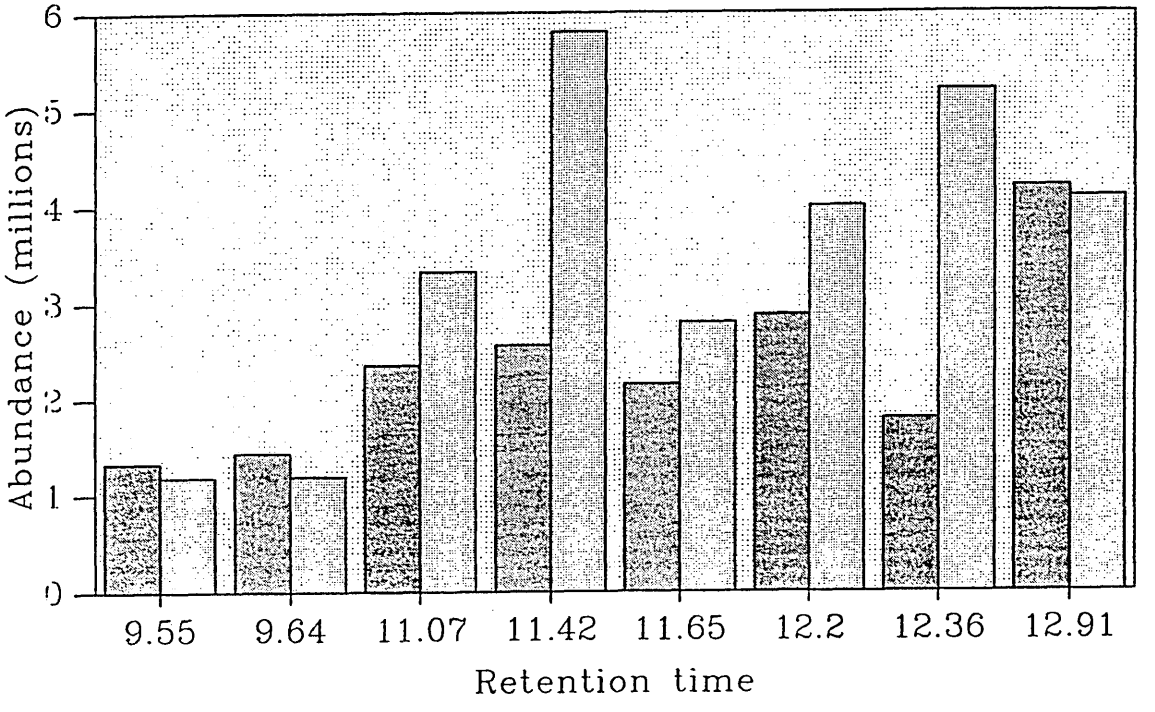

Figure 5

INTERNAL COMBUSTION ENGINES AND COMBUSTION

Proceedings of the
XIV National Conference on I C Engines and Combustion
Institute of Armament Technology
Pune - 411025
December 8-10, 1995

Editor
V. RAMANUJACHARI

Tata McGraw-Hill Publishing Company Limited
New Delhi

McGraw-Hill Offices
New Delhi New York St Louis San Francisco Auckland Bogotá Guatemala
Hamburg Lisbon London Madrid Mexico Milan Montreal Panama
Paris San Juan São Paulo Singapore Sydney Tokyo Toronto

THE MEASUREMENT AND ANALYSIS OF THE PARTICULATE MATTER FROM A TURBO CHARGED DIESEL ENGINE

P.W. YATES, M.D. BASSETT and P.W. FOSS

School of Engineering, Sheffield Hallam University

D. DOUCE

School of Science, Sheffield Hallam University

A direct injection diesel engine using reference fuel and oil was subjected to steady state emission testing. The methods and equipment used are discussed. The particulate matter was collected using a dilution tunnel and the Soluble Organic Fraction(SOF) extracted and separated into functional groups by liquid chromatography. Gas chromatography with mass spectrometry was used to identify the hydrocarbon species present in each group. The results show that as the air fuel mixture increases, the distribution and quantity of hydrocarbon species present in the SOF diminish for all functional groups analysed.

Test Equipment

The engine used to generate the particulate matter was a in line 4 cylinder, 4 litre, non inter cooled direct injection engine with a turbo charger. The fuel pump was a Lucas DPA with the fuel injection timing set to 12° BTDC. Throughout all tests the fuel and oil used was of reference quality and from the same batch to retain the same hydrocarbon species distribution, the oil being Silkolene RL 139 and the fuel CCRF03. The chromatogram for the fuel is shown in figure 1. Gas phase exhaust gases were sampled from the exhaust system at a point 1m from the turbo charger exit. These were transported by a heated sample line at 180°C to a multi gas analyser to determine the CO, CO_2 and NOx. The uHC levels were obtained using a flame ionisation detector. To allow repeatability of test data the engines cooling water, exhaust gas, inlet manifold, oil temperatures and the cylinder pressures were measured and recorded. The cylinder pressure data was recorded by piezo electric pressure transducers placed adjacent to the injector nozzle.

Origins of Hydrocarbon Emissions form a Diesel Engine.

The hydrocarbon emissions from diesel engines(C.I.) are typically lower than those from a spark ignition (S.I.) engine, but with exhaust after treatment the exhaust gas from a S.I. engine that enters the atmosphere contains comparable levels. Oxidation catalysts (3 way) that are fitted to S.I. engines will not function on C.I. engines because of the lower exhaust gas temperatures, the possibility of blockage through soot and the quantity of oxygen present in the exhaust gas.

Combustion in a C.I. engine is in three general stages:

1. Delay (the time between the start of injection and the start of combustion).
2. Rapid combustion (the burning of the fuel injected during the delay period) .
3. Controlled combustion (fuel burning as it is injected).

The unburnt hydrocarbon(UHC) formation mechanisms for each of these stages are different. The speculated routes have been shown by Yu[1], figure 2 does not show the effects of the system boundaries, i.e.

wall quench and adsorption desorption of the fuel into the lubricating oil. Daniel and Whitehouse[2, 3] used in-cylinder sampling on a S.I. engine to determine the distribution of hydrocarbons. Their tests showed that as the sample point neared the cylinder wall the hydrocarbon concentrations increased, indicating wall quench. Multi spray C.I. diesel engines delivering high fuel quantities can allow the fuel spray to penetrate too far into the combustion chamber so that it impinges onto the cylinder wall or piston crown. Conditions in this area are relatively cool with poor or no air swirl and the fuel will not ignite. Lyn and Valdmanis[4] varied injector hole size, nozzle type and its geometry, with none of these affecting the ignition delay. When the hole size was doubled and the injection pressure remained constant, the fuel flow rate increased by a factor of four and the droplet size increased by approximately 30 percent.

A source of UHC also associated with the injector is that of the fuel remaining in the injector nozzle after injection. This is most significant at low fuel injection volumes where there is little overmixing. Greeves[5] found that a $1mm^3$ nozzle sac volume gave 350 ppm C_1, and he also stated that $1mm^3$ of fuel gave 1660 ppm C_1. He postulated that the volume may not be filled with fuel and the higher boiling point fractions of the fuel remained in the nozzle. The relationship between nozzle sac volume and exhaust HC is linear, with its intercept for zero HC at $-1.8mm^3$ for a speed range of 1700 - 2800 rpm.
The rate of fuel injection in the majority of production diesel engines is assumed constant after the injector needle has attained its fully open condition. Vollenweider[6] completed a series of tests using a two spring injector This style of injector allowed a small amount of fuel to be injected before the main quantity and this reduced the heat release within the premixed combustion stage. The net result in emissions was a reduction of HC and NOx but an increase in particulates. In a study of "in use" motor vehicles Williams(7) reported that injectors that had a lower opening pressure than the standard specification produced higher levels of emitted particulate matter. This is because the lower kinetic energy of the particle allows it to slow in the air stream, removing its supply of oxygen. The highest concentrations of soot within the combustion chamber of a diesel engine are in the core region of each of the fuel sprays. This is where the local equivalence ratios are very rich. The formation of the soot particle initiates with a fuel molecule containing 12 to 22 carbon atoms and a H/C ratio of approximately 2 and progresses through the two stages proposed by Haynes[8],

i) Particle formation - the first condensed phase of the material formed by oxidation and pyrolysis. The typical components of these are unsaturated hydrocarbons i.e. acetylene and multiples of $C_{2n}H_2$, and polycyclic aromatic hydrocarbons (PAH). These particles are very small($d < 2nm$).

ii) Particle growth - by surface growth (gas phase material condensing and being incorporated) and agglomeration of smaller particles.

Studies[9] with combustion bombs have shown three different paths to soot formation depending on combustion temperature. At the lowest temperatures (>1700 °C) only aromatics or highly unsaturated aliphatic compounds of high molecular weight are very successful in forming solid carbon through pyrolysis. At intermediate temperatures typical of diffusion flames (<1800 °C), all normally used hydrocarbon fuels produce soot if burned at a significantly rich mixture. At very high temperatures (above the range found in diesel engines) a nucleation process utilising carbon vapour is the primary formation mechanism.

Particulate Sampling

The exhaust gas immediately leaving the tailpipe of a diesel engine is composed primarily of elemental carbon and organic compounds, and at normal in cylinder temperatures these exist separately. The purpose of a dilution tunnel is to simulate the mixing of the exhaust gas with the external air cooling the exhaust and allowing the organic compounds to condense onto the elemental carbon. The maximum permissible sampling temperature for a dilution tunnel is 52°C. This is the mid point between the boiling points of pentane(Bp 36.1°C) and hexane(Bp 68.7°C). To reduce the sample gas temperature further to the boiling point of pentane,

the dilution ratio would have to be increased to a region above that of the optimum ratio for the collection of the extractable fraction. The dilution ratio for the collection of the maximum amount of the extractable organic fraction is approximately 5:1. The reasons for this are that, as the dilution ratio increases from unity, the effect of the decreasing temperature on the number of active sites dominates the condensation process. When the dilution ratio becomes higher the decreasing partial pressure causes the extractable mass to fall again. Condensation will occur whenever the vapour pressure of the gaseous phase hydrocarbons exceeds its saturated vapour pressure. Increasing the dilution ratio decreases the hydrocarbon concentrations and hence the vapour pressure. The total exhaust flow from the engine at high speeds and loads was in excess of the quantity required by the Weslake dilution tunnel for collection of the maximum quantity of the SOF, therefore a diverter system was used to remove the unwanted exhaust gas.

Solvent extraction.

Because of the small amount of material collected for the majority of the test points, the optimum method to determine the amount of material removed by the extraction process is to weigh the filter before and after the process Because the filter can contribute to the weight difference, blank filters will also have to be subjected to the extraction process. The overall calculation for the soluble organic fraction by weight loss will be :-

SOF(filter weight loss) = (Wbe - Wae - Avb)
Wbe = Weight before extraction
Wae = Weight after extraction
Avb = Average weight loss of blank filters

The choice of solvent used for extraction influences the group or groups of hydrocarbons removed from the sample, dichloromethane was used for the results presented in this paper, a more aggressive solvent favoured by some researchers is a 4:1 mixture of distilled benzene and methanol[10]. To remove the solvent and to stop any mutation or oxygenation of the remaining matter prior to weighing, the papers were dried in a nitrogen atmosphere. Before any weighing of the filter papers can be undertaken they must be subjected to the same ambient conditions. It is recommended that the papers are stored in temperature and humidity controlled conditions for four hours to equilibrate.

SOF analysis

Clean up procedure[11].

A high performance liquid chromatography(HPLC) system using a alumina column- activated, basic, Brockmann 1 (150 mesh, 250 x 5 mm). This was used to separate the hydrocarbons of interest, i.e. C_8 to C_{30} from any other emitted by the engine, i.e. aromatic and substituted aromatic compounds known to be released by incomplete combustion. Fractionation was achieved on a Varion isocratic HPLC system using a UV detector set at 254 nm. To separate the sample into these groups, low pressure liquid chromatography utilising different elutants was used. Table 1 shows the eluant with the corresponding group.

Isocratic Eluant	Group
Hexane	Alkanes
Dichloromethane	Polycyclic Aromatic Hydrocarbons (PAH)
Acetronitrile	Polar PAH & Nitro PAH
Acetronitrile & Methanol (3:1)	Very polar PAH

Table 1

Capillary GC/MSD Analysis

The residual weights of the test samples varied with the speed load conditions i.e. depending upon the contribution to the total collected weight of the soluble fraction, these samples were then diluted with Dichloromethane to give similar concentrations. A 1µl. sample of this was then used for analysis, the instrument used was a Hewlett Packard 5890 (Series II) coupled with a HP 5971A Mass Selective Detector. Electron impact mass spectra were obtained at 70eV and processed using a HP ChemStation data system. The GC conditions used are shown in table 2.

Gas Capillary Chromatographic Conditions	
Carrier gas	Helium
Analytical column	18m x 0.25mm (id), 5% biphenyl fused silica
Film thickness	0.25µm
Oven temperature program	50°C (2 mins) ramped at 10°C/min to 280°C (5 mins)
Volume injected	1µl. splitless

Table 2

The identification of the abundance peaks on the chromatograms produced was initially by the comparison to the retention times of a standard. The hydrocarbon species present in the exhaust and not the calibration sample were identified using a library search on the data system.

Results

The chromatograms shown were obtained by separating the sample into four groups by liquid chromatography. For ease of analysis the group that has undergone the closest scrutiny is the alkanes. This is the first group extracted from the organic fraction and thus has the least chance to degrade or mutate. The compounds that are recognised as the most harmful are in the second group, these being benzo[*a*]pyrene and possibly 7,12-dimethylbenz[*a*]anthracene. These compounds were recognised as being carcinogens in 1933 and are both polycyclic aromatic hydrocarbons. These compounds are not cancer forming until they form a diol-epoxide.

The chromatogram plots show that as the engine load increases the quantity of carbon atoms present in the most abundant peak also increases. When the load is increased beyond half rated power the two lightest species diminish below a level that can be accurately quantified. The alkane species that are presented are the lightest of those shown on all plots. There is a greater distribution of species present at lower speeds, i.e. there are both heavier and lighter species detected at idle than those detected at 75% of rated power. As the combustion temperatures and pressures increase so does the degree of fuel pyroliysis, therefore, the heavier fuel molecules break down into lighter components; these components have lower vapour pressures and auto ignition temperatures and are oxidised easier. The size of the most abundant species also increases with the temperature and pressure. A simplified illustration of the chromatograms for the abundance of n-alkanes is shown in figure 3. The concentrations of gas phase uHC's present just prior to the exhaust turbine inlet and a 1 meter from the outlet are shown in figure 4 for comparison. The survivability's of the PAH do not follow this trend (fig 5), the abundance of PAH increases with load and the most probable cause is the increase in oil consumption giving a higher initial quantity of PAH present in the exhaust.

References

1) Yu R.C., Wong V.W. and Shahed S.M.: " Sources of hydrocarbon emissions from direct injection engines. S.A.E Paper 800048 1980.

2) Daniel, W.A., Wentworth, J.T.: " Exhaust gas hydrocarbons Genesis and Exodus". S.A.E. 486B ,1962.

3) Whitehouse, N.D., Clough, E., and Uhunmwangho, S.O.: " The development of some gaseous products during diesel engine combustion". SAE Paper 800028, 1980.

4) Lyn, W.T., and Valdmanis, E.: "Effects of physical factors on ignition delay". S.A.E. 680102, 1968.

5) Greeves, G., Khan, I.M. , Wang, C.H.T. and Fenne, I.: " Origins of hydrocarbon emissions from diesel engines". SAE Paper 770259.

6) Vollenweider, J.:" Emission-optimised fuel injection for large diesel engines- expectations, limitations and compromises ". Proc IMechE C448/003, 1990.

7) Williams, D.J., Milne, J.W, Quigley, S.M.and Roberts, D.B.: "Particulate emissions from "in use" motor vehicles-II Diesel Vehicles". Atmospheric Environment Vol 23, No12, pp 2647-2661 1989.

8) Haynes, B.S. and Wagner, H.G.: "Soot formation" Prog Energy Combustion Science, Vol 7, pp 229 - 273, 1981.

9) Amann, C.A., and Siegla, D.C.: "Diesel particulates-What they are and why." Aerosol Science Technology, vol , pp 73-101, 1982.

10) Abbass, M.K., Andrews, G.E., Ishaq, R.B. and Williams, P.T.: "A comparison of the particulate composition between turbocharged and naturally aspirated D.I. diesel engines". SAE Paper 910733, 1991.

11) Ciccioli, P et al. Journal of Chromatography, 351 (1986) pp 451 - 464

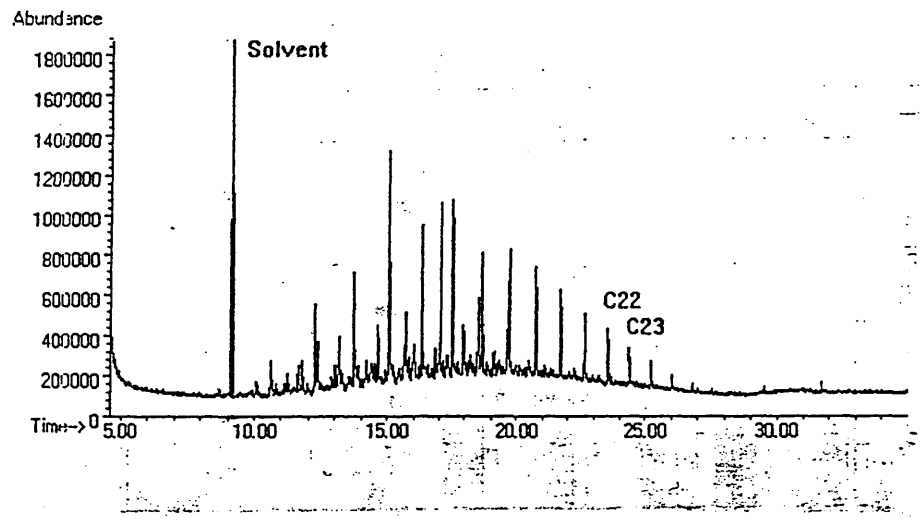

Figure 1 Chromatogram Of Diesel Fuel

Hydrocarbon Emission with Load

Pre-turbo + 1 meter

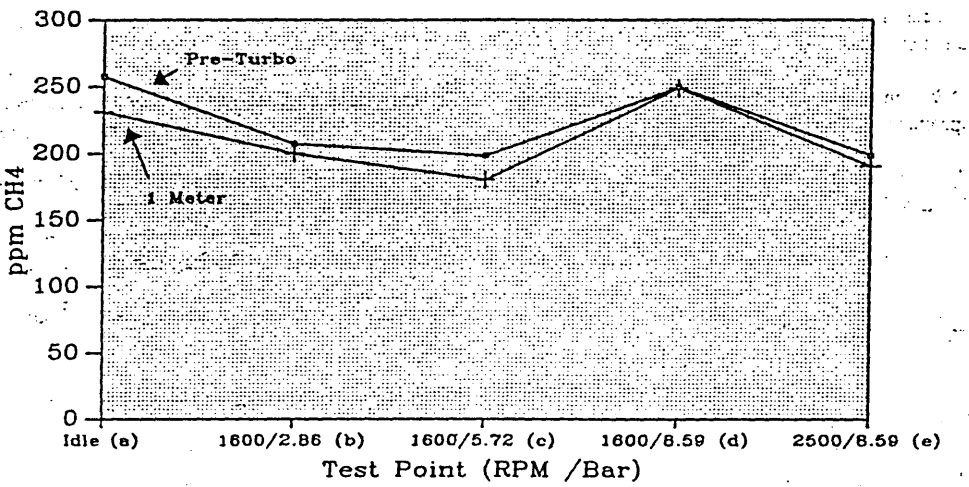

Figure 4

Abundance of PAH

Showing the change in distribution with load

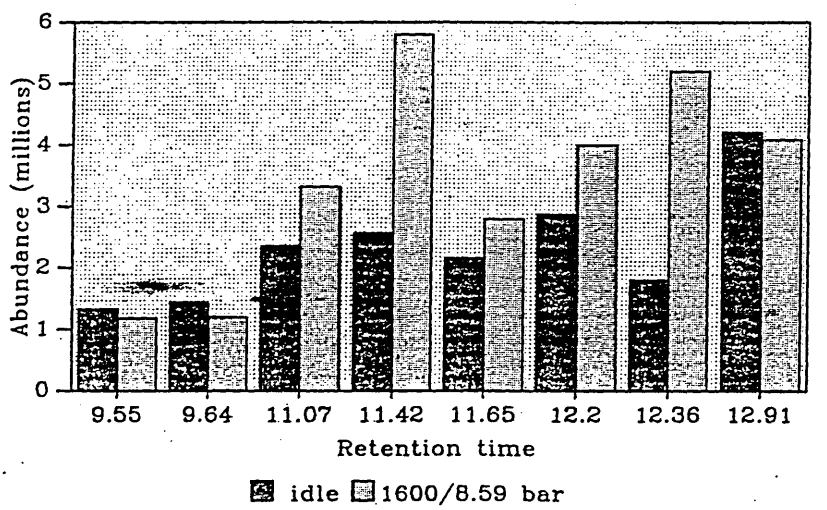

Figure 5

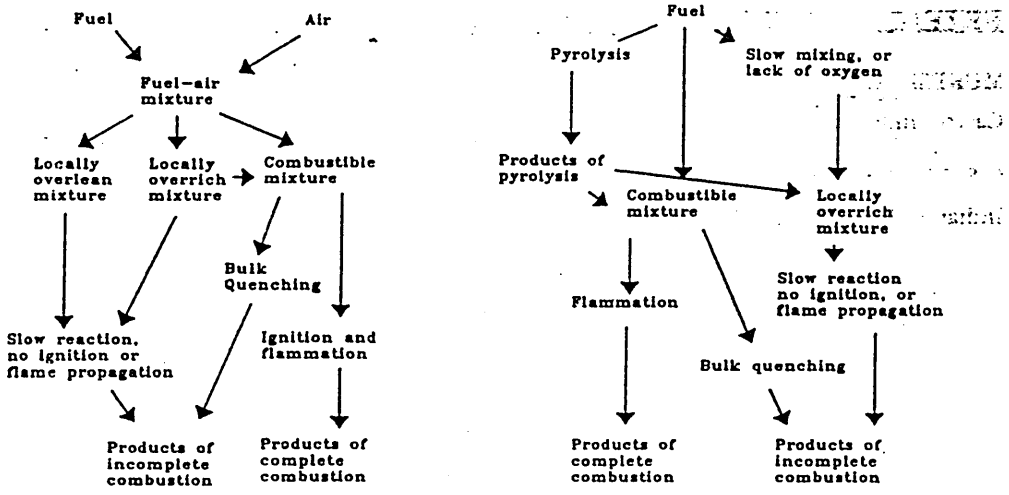

Figure 2

Abundance of n–Alkanes
Showing the change in distribution with load

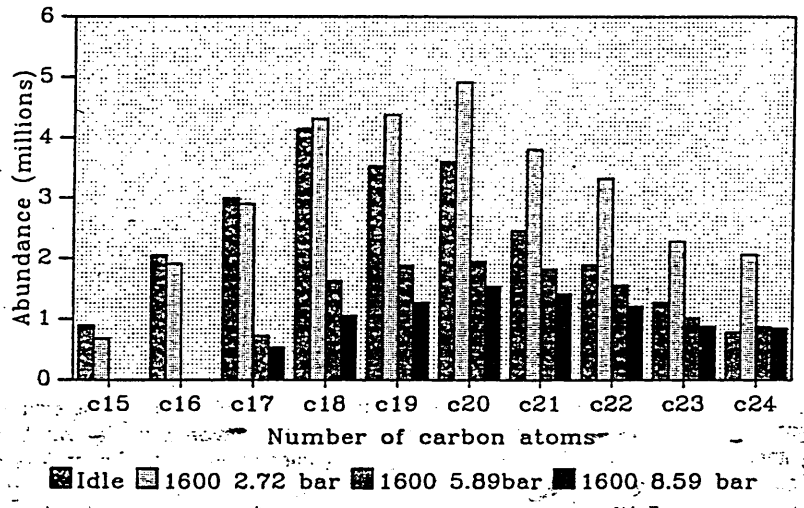

Figure 3

IMPROVED AUTOMOTIVE PART LOAD FUEL ECONOMY THROUGH LATE INTAKE VALVE CLOSING

S.C. BLAKEY and P.W. FOSS

Senior Lecturers, School of Engineering,
Sheffield Hallam University, S1 1WB, England

M.D. BASSETT and P.W. YATES

Research Assistants, School of Engineering,
Sheffield Hallam University, S1 1WB, England

Key factors limiting conventional four stroke S.I. engine efficiency have been identified as the energy lost pumping sub-atmospheric intake gases, drawn past a part open throttle valve, frictional losses between moving components and finally limitations on compression ratio due to the onset of knock. The late intake valve closing (LIVC) load control concept provides a means to eliminate most of the pumping work energy loss. Experimental and theoretical studies have shown that the fuel saving with such a load control system can be as much as 7%. If LIVC is combined with a variable compression ratio (VCR) device, further fuel savings can be realised. Results of up to 20% over a conventional engine, at low loads/speeds have been reported. A simple two-state LIVC control mechanism is proposed. This system is currently under development/evaluation at Sheffield Hallam University.

Introduction

The Otto-cycle engine has been with us since 1876 in varying forms. Saunders (1984) has attributed its consistent popularity as an automotive power unit to its relatively low cost, high power to weight ratio and flexible performance. However he suggests that its weaknesses include the harmful exhaust emissions and relatively high fuel consumption, especially at light loads, where an irreversible loss occurs, resulting from the extra work required to draw air past the part open throttle valve. During recent years automotive aero-dynamics has improved, as has tyre technology, resulting in vehicles that require less power to maintain a given speed due to reduced areo-dynamic drag and rolling resistance. Whilst the output power of a given displacement engine has increased multi-fold. For example, Elrod and Nelson (1986) state that a modern intermediate sized automobile requires about 15bhp to maintain a speed of 100 kilometres per hour on a level road, though typically such vehicles in this class have engines ranging up to about 130bhp capacity. Hence the passenger car now spends most of its life operating at only a fraction of its maximum output power, the reserve of power being required for hill climbing, overtaking and joining of carriageways.

Over the last twenty years or so, increasing energy awareness and legislation (notably the U.S. Federal Corporate Average Fuel Economy (CAFE) Standards) have dictated that motor manufacturers have tried to produce vehicles that are more fuel efficient. Blackmore and Thomas (1977) suggest four areas which engineers strive to improve during engine development :-

- Driveability.
- Power per unit weight/displacement.
- Lower emissions.
- Improved fuel economy.

These have been regarded as conflicting demands, requiring the engineer to use his judgement to 'balance' the performance compromises. It has however been possible to produce engines that are much improved simultaneously in all of the four facets mentioned above, due to improvements in engine control systems and combustion chamber design.

Fuel Efficiency

In order to improve the fuel economy of future engines, current causes of efficiency loss must be identified, then

addressed. Nagesh *et al.* (1992) categorise the inefficiencies associated with the production of mechanical work by burning fuel within an IC engine into the following groups:-

i) **Cycle Efficiency** - The heat energy available is not fully converted into useful mechanical work. Nagesh *et al.* state that typical cycle efficiency is about 45 to 50%. They go on to state that it is possible to improve the cycle efficiency of an Otto-cycle engine by increasing the Compression Ratio (CR) or the Expansion Ratio (ER), or by increasing both simultaneously. In a spark ignition engine, increasing the CR is restricted by the onset of detonation.

ii) **Mechanical Efficiency** - Which can be split into two types of parasitic losses; *Frictional losses* and *Pumping losses*. Frictional loss occurs in the bearings, at the piston ring to bore wall interface, valve components and other mechanical parts of the engine and engine accessories such as the oil and water pumps. Nagesh *et al.* suggest that the mechanical efficiency of a typical automotive engine is typically of the order of 85 to 90 percent. Mechanical losses increase as a proportion as load decreases. Pumping losses are caused by the power lost in pumping gas into and out of the engine, past the throttle, valves and through the manifolds. Pumping loss increases as load reduces due to the increased throttle restriction. Therefore the mechanical efficiency is highly dependant upon throttle position. As the engine is throttled, mechanical efficiency decreases, eventually to zero at idle operation.

The largest potential benefits could be achieved at part load by the removal/reduction of the need to use the throttle valve to regulate the mass of the incoming charge, thus reducing the associated irreversible pumping loss caused by the presence of the throttle valve itself.

Late Intake Valve Closing (LIVC)

The LIVC concept allows the intake charge mass retained in the cylinder for combustion to be controlled without the need for a throttle valve. The trapped charge mass is reduced by keeping the intake valve open during a portion of the compression stroke. Excess induced charge is expelled back into the intake manifold. Thus the engine load control is achieved with the charge at approximately atmospheric pressure throughout the induction process. Figure 1, from Ma (1986), shows typical pressure-volume diagrams for both a conventionally throttled engine and a LIVC controlled engines. The shaded area on the diagrams depicts the losses caused by pumping work. With the conventionally throttled engine this area will increase as output is reduced, due to the increased restriction at the throttle (throttling work). The difference in area between the two shaded portions represents the direct efficiency improvement brought about by using LIVC control. However as will be discussed later this improvement can be offset somewhat by a reduction in combustion efficiency.

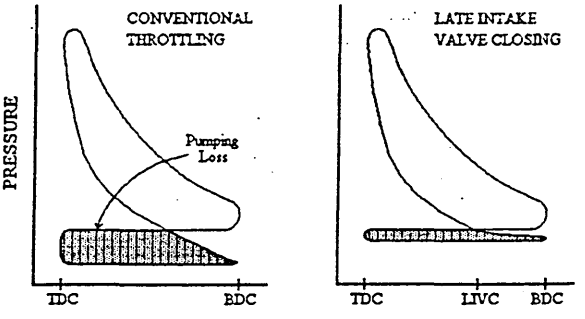

Figure 1 - Part Load Modulation by Late Intake Valve Closing.

Variable Valve Timing (VVT) for LIVC Control

Any VVT mechanism intended to control the output of the engine by LIVC needs to be able to alter the valve duration. Several VVT mechanisms have been put into mass production by major vehicle manufacturers. Traditionally the profile of the lobes on a camshaft have been designed to suit the application of the engine. Lancefield *et al.* (1993) explain that ideally at idle the valve opening durations should be short to trap the intake gas, minimise residual fraction and perform maximum compression work on the mixture to improve mixture preparation and burn the charge efficiently. As the load on the engine increases, the opening times should be duly extended to improve volumetric efficiency. As the engine speed increases, the valve opening duration should be further extended and the valve timing retarded for maximum power. One such mass produced mechanism that has been developed to overcome the restraints of fixed valve

timing is Rover's variable valve control system, as featured in Automotive Engineer (1995), allows the point of valve opening and closing to be altered using an eccentric mechanism. A simpler two-state system developed by Honda, called VTEC, described by Hosaka and Hamazaki (1991), consists of a camshaft with both 'high speed' and 'low speed' lobes. Depending upon operating conditions the most suitable lobe profile is hydraulically selected.

Many excellent papers have been written on the subject of VVT for optimised engine performance. It is not proposed to duplicate that work here. For a comprehensive description of the array of complex and costly mechanisms devised, the reader is advised to refer to the papers by Dresner & Barkan (1989), Nelson & Elrod (1987) or Ahmad & Theobald (1987). It is sufficient to say here that any such mechanisms devised for performance optimisation purposes can typically alter valve phasing or duration about 30°, however as will be discussed later, for pure LIVC operation, valve timing alterations in excess of 100° are required, thus requiring more convoluted and complex VVT mechanisms. However in view of the potential of LIVC operation to reduce brake specific fuel consumption (BSFC) there have been numerous attempts to develop VVT systems capable of controlling engine output by the LIVC method.

Previous LIVC Studies

Recent interest in LIVC began with the work of Tuttle (1980) who tested the LIVC concept on a single cylinder research engine. Variable valve timing was achieved by replacing the production camshaft with a splined shaft which allowed cam lobes with different dwells at maximum lift to be installed. Tuttle used four intake cam profiles which had 0° (standard timing), 60°, 88° and 96°CA dwell. All tests were conducted at an engine speed of 1600rpm, with an air/fuel ratio of 14.7:1 with minimum advance for best torque (MBT) spark timing, unless knock occurred, when the spark timing was retarded to borderline knock.

Tuttle (1980) observed from his experiments that as the conventional engine is increasingly throttled, the pumping mean effective pressure (PMEP) of the engine continually increases. The PMEP values for the LIVC engine are virtually the same as those of the conventional engine operating at WOT. However set against this benefit the rate of decrease in indicated thermal efficiency with decreasing load was significantly greater for the LIVC engine. The combined effect of lower pumping losses and reduced indicated thermal efficiency still result in the LIVC engine having a higher net thermal efficiency than the conventional engine, giving rise to a net specific fuel consumption of up to 6.5% less than the conventional engine at the same light load. The reduction in indicated thermal efficiency is mostly caused by a reduction in the effective compression ratio of the engine with increasing LIVC. The effective compression ratio is defined by Tuttle as the effective cylinder volume at intake-valve closing divided by the clearance volume. As the CR is reduced the combustion deteriorates, leading to a burn rate reduction. This is attributed to the lower gas temperature at the end of the compression stroke of the LIVC engine due to the lower CR. The in-cylinder gas temperatures are found to be lower for the LIVC engine, even though the LIVC engine has a higher charge intake temperature, which is up to 50°C higher than that of the standard engine, caused by the back flow of heated charge into the intake manifold with increasing valve dwell. This is offset somewhat by the conventional engine having a larger residual fraction due to its lower intake manifold pressure, caused by a pressure drop across the throttle valve, which causes an expansion of the incoming charge and also encourages exhaust back-flow through the cylinder into the inlet manifold during the valve overlap period.

Specific emissions of NO_x measured by Tuttle (1980) show that at equal load, the NO_x emissions from the LIVC engine are appreciably less than those from the conventional engine. This is attributed to the LIVC engine's lower peak cylinder pressures and gas temperatures. Specific emissions of unburned hydrocarbons (HC) were found to be similar for both types of engine.

Tuttle found that with an intake valve dwell of 96°CA power output was reduced to 33% of maximum, which he states would not provide a sufficient range of control for vehicular usage. Further increases in intake valve dwell would result in an unacceptably large decrease in the indicated thermal efficiency of the engine. The LIVC concept of load control would have to be combined with a traditional variable density throttle control. In order to maximise the effectiveness of the LIVC mechanism, the throttle valve should only be used to further reduce output after maximum LIVC has been applied.

Saunders (1986) used a comprehensive computer based engine simulation package to model the performance of a single and a four cylinder engine, operating on both the standard Otto cycle and with the LIVC load control strategy. This simulation predicted a 2% reduction in fuel consumption, at low loads, for the single cylinder LIVC engine

compared to the throttled Otto engine. This improvement was calculated to be 6% in the case of the four cylinder LIVC engine, the extra improvement with the four cylinder engine resulting from a beneficial inlet manifold effect. Saunders & Rabia (1986) implemented an LIVC system on an Austin A-Series engine. The switch between LIVC and throttle load control could be achieved within a short time interval, so that other engine parameters such as wear do not alter significantly between tests. In order to directly control the intake valve closure timing they mounted a second camshaft above the rocker arms, as shown in Figure 2. A variable geometry timing belt drive from crankshaft achieves LIVC of up to 90°CA. The valve lift profile of the two camshafts had to be altered to avoid an unacceptable discontinuity on transfer between the cams. They report a maximum fuel economy gain of about 11% at half load. However at lower loads the gain becomes smaller or even negative. This pattern is reported to be consistent throughout the speed range, although less marked at higher speeds and is brought about by the low CRs and hence low in-cylinder temperatures which are damaging to combustion.

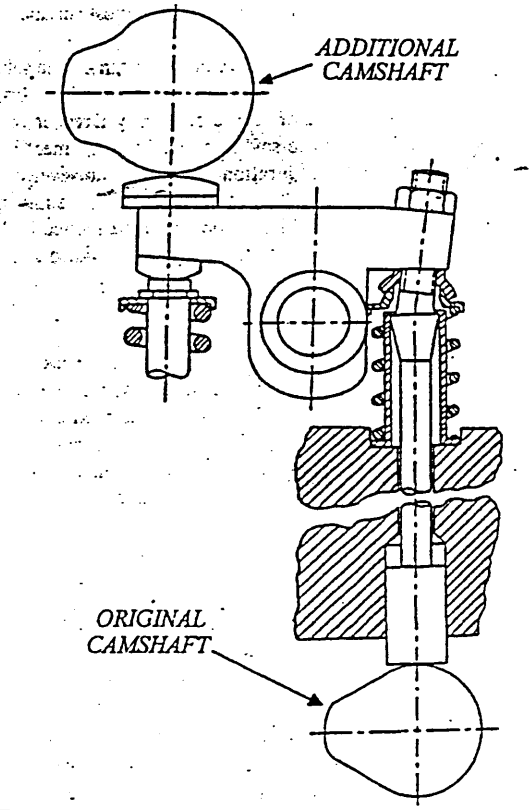

Figure 2 - Valve Drive Train, Developed by.Saunders & Rabia (1986).

Elrod & Nelson (1986) developed a device that could phase shift the valve timing of an engine sufficiently to control it by LIVC. The engine used for this test program was a four cylinder Fiat DOHC engine. The exhaust camshaft remained unaltered, but the intake camshaft was redesigned such that each original lobe was replaced by a paired set of half width adjacent cam lobes. One of each of these paired lobes was attached rigidly to the timed camshaft, the other half lobes are mounted on an inner hexagonal shaft controlled by an electric motor via a harmonic gearbox, which can be rotated relative to the timed shaft. When these half cam lobes are aligned the manufacturer's original profile is maintained. The phasing is variable between 0 and 88°CA. The motor and gearbox unit rotate with the camshaft, electrical connections are made using a slip-ring and brush block assembly. During trials with this LIVC system, they found that charge was being returned to the carburettor and re-enriched during subsequent intake events, causing the engine to run with an over-rich mixture. This problem was cured by fitting a reed-valve between the carburettor and the intake manifold, to prevent air returning to the carburettor. Elrod & Nelson (1986) claim that although this engine may have a reduced effective CR, caused by the delayed closing of the intake valve, no reduction in CR occurs relative to the standard engine operating at the same load/speed point. They argue that during throttled operation the standard engine induces charge at sub-atmospheric pressure and hence the portion of the compression process that is above atmospheric pressure is comparable with the complete compression process of the LIVC engine, thus giving them both the same in-cylinder pressures. However, Saunders & Abdul-Wahab (1989) observe during a motored compression test conducted at 2000rpm, that with about 85°CA of LIVC the nominal CR of the engine must be about 20:1 to maintain the same in-cylinder peak pressure as the standard engine with a nominal CR of 8.7:1.

A cam-less engine featuring electronically controlled, pneumatic valve actuators was developed for experimental purposes by Gould *et al.* ((1991). Their test program concentrated primarily upon the optimisation of the valve event for conventionally throttled engines, but they did use this engine for investigations into LIVC for power modulation. The engine used in this study was a Ford 1.9 litre EFI unit. They give a performance comparison between the standard engine and their LIVC engine both operating at 5000rpm and producing a bmep of 2.62bar. To achieve this load condition the intake valve closing was delayed by 75°CA. A bsfc reduction of 4.4% was observed. Brake specific NO_x emissions were reduced by 60%, whilst HC and CO emissions increased. The increases in HC and CO emissions are stated by Gould *et al.* (1991) to be indicative of incomplete combustion, which they suggest is likely to be due to the short comings of LIVC; poor fuel vaporisation and lower in-cylinder gas temperatures, which all lead to longer combustion durations.

Blakey *et al.* (1991) set out to design a production feasible LIVC controlled engine, based on a Ford 2.0 litre DOHC 16 valve engine. The LIVC mechanism adopted was a development of the two camshaft arrangement used by Saunders & Rabia (1986). The inlet camshaft remains in its standard location and operates one of the two inlet valves from each cylinder. The exhaust camshaft then operates the exhaust valves, as well as the remaining inlet valve from each cylinder via a rocker arm, shown in Figure 3. The intake camshaft can be phase-shifted relative to the engine, the combined opening duration of the two inlet valves per cylinder thus being able to give an extended valve opening event. However the design of a suitable phase-shift mechanism was not included as part of their project remit. Phase-shifting was achieved during testing using a vernier timing pulley, which required the engine to be stopped between tests. Tests were conducted with stoichiometric fuelling and MBT spark timing. The maximum value of LIVC used was 75°CA, as greater amounts of LIVC prevented the engine from re-starting. The largest bsfc reduction, 6.7%, was recorded with 75°CA of LIVC, at 1000rpm. Above 3250rpm the bsfc consumption with LIVC was worse than the conventionally throttled engine.

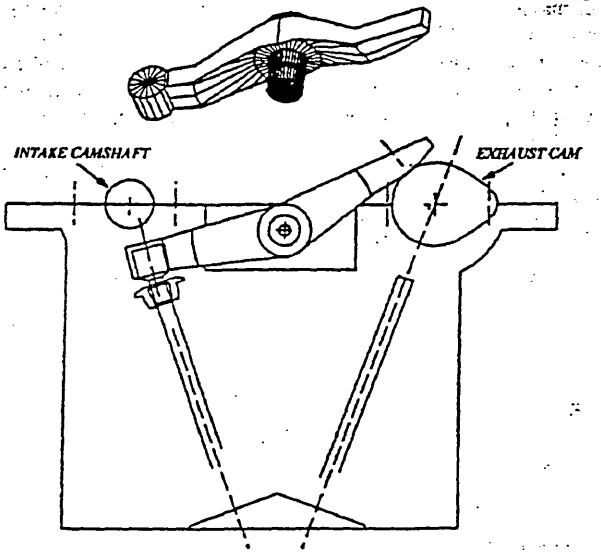

Figure 3 - Diagram of the Rocker Arm that Operates the Inlet Valve, Activated by the Exhaust Camshaft, as Developed by Blakey et al. (1991).

Haugen *et al.* (1992) studied the benefits of LIVC using an Oldsmobile 2.3 litre, sixteen valve, DOHC four cylinder engine. The LIVC mechanism adopted for this study operates on the same principal as that of the one built by Blakey *et al.* (1991), in that each of the two inlet valves from each cylinder are operated by separate camshafts, one of which can be phase-shifted relative to the engine. This was achieved by the addition of a third camshaft, placed directly above the standard intake camshaft. The original intake camshaft operates one valve per cylinder in the conventional manner, the new upper camshaft operates the remaining intake valves via push rods that straddle the original camshaft. The upper shaft is driven from the lower via a phase-shift mechanism, details of which are not given. They also give no details of the extra frictional losses encountered by the addition of a third camshaft. The fuel injection system control was based on a "speed density" strategy, which determines the estimated fuel requirements and desired spark timing from look-up tables, based on engine speed and manifold absolute pressure (MAP) and then refines the fuel metering by O_2 sensor feedback. Obviously with LIVC load control the MAP signal would become meaningless (i.e. about atmospheric for all loads). Thus an external signal was used to simulate the MAP sensor signal. This was found to be sufficient to allow the engine to operate in the closed loop, O_2 feedback mode, however they suggest that a mass air-flow (MAF) system may be preferable for future LIVC applications. A maximum reduction in bsfc of 6.3% was observed with 105°CA of LIVC at 1500rpm. NO_x emissions were reduced, whilst HC emissions tended to be higher.

The Otto-Atkinson Cycle

In order to improve the poor indicated thermal efficiency of an LIVC controlled engine, brought about by the reduction in effective compression ratio, Luria, Taitel & Stotter (1982) proposed the Otto-Atkinson engine. So called because it combines the advantages of the Otto cycle engine with those of the Atkinson cycle engine. James Atkinson developed a number of engines during the latter half of the last century. His most successful of these, built in 1886, he named the 'Cycle' engine, which featured a longer expansion stroke than compression stroke. When properly implemented, the combustion products should be expanded to almost atmospheric pressure.

The Otto-Atkinson cycle proposed by Luria *et al.* (1982) is intended to combine the efficiency of the Atkinson cycle, with the higher specific output power of the Otto cycle. The concept is basically an LIVC controlled engine, whose compression ratio at light loads is restored by a Variable Compression Ratio (VCR) device which reduces the clearance

volume. Luria *et al.* used a modified air standard cycle to analyse the improvements obtainable with this system. They calculated that with a stoichiometric air/fuel ratio, at 25% of full load, the Otto-Atkinson engine's indicated thermal efficiency is 59% higher than that of a standard throttled Otto cycle engine operating under the same conditions. This theory was also experimentally tested by Luria *et al.* using a 1098cc Austin A-Series engine. LIVC was achieved by changing the camshafts to ones with identical valve timing, except for the delay in intake valve closing. Three camshafts were used as well as the standard one, giving 55°, 83° and 91°CA of LIVC. The effective compression ratio was maintained by reducing the clearance volume in the cylinder head. At certain speed/load conditions the Otto-Atkinson engine showed a BSFC improvement of 19%, when compared to the standard engine. Luria *et al.* report that analysis of the exhaust emissions from the Otto-Atkinson engines showed a reduction in CO, which they attribute to the longer expansion stroke providing a greater possibility for the CO to oxidise to CO_2. Also NO_x emissions showed a reduction of about 50%. They offer no explanation for the discrepancy between the calculated and measured BSFC improvements for the Otto-Atkinson engines, one possible factor is the reduced turbulence of incoming charge with the Otto-Atkinson engine, due to the absence of the throttle valve, which could reduce the laminar flame speed during combustion, thus reducing the anticipated indicated thermal efficiency. It still remains that the Otto-Atkinson engine offers a fuel saving of up to 19% whilst having substantially reduced emissions.

It was mentioned in the previous section that Saunders (1986) used a computer based engine simulation package to model the performance with LIVC load control. He also used this package to model the performance of these two engines operating on the Otto-Atkinson cycle, which predicted up to a 20% reduction in fuel consumption for both the single and four cylinder Otto-Atkinson engines compared with the conventional units. This is well in excess of the fuel economy improvements for both the single and the four cylinder LIVC controlled engines. It is interesting to note that Saunders (1986) calculated that the economy improvement available by optimising the CR to the knock limit is of the order of 5%, thus the combination of LIVC + VCR in the Otto-Atkinson cycle gives an increase in efficiency higher than the sum of the improvements given by LIVC or VCR when used separately.

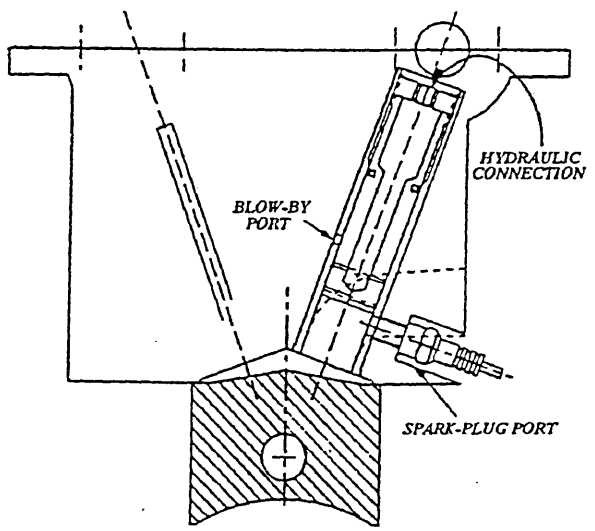

Figure 4 - Diagram of the Hydraulically Activated Auxilary Piston Device, Developed by Blakey et al. (1991).

Saunders & Abdul-Wahab (1989) have tested the Otto-Atkinson cycle experimentally using an Austin A-Series engine. The LIVC system used was that developed by Saunders & Rabia (1986), variable compression ratio was achieved by altering the clearance volume in the cylinder head. This was accomplished by the use of several cylinder heads, as well as by the use of spacers placed between the head and block. Using LIVC alone they recorded a 13% reduction in bsfc at half load and 2000rpm when compared to the conventional engine. With the effective compression ratio increased such that the effective CR remains similar to the CR of the conventional engine this bsfc reduction was improved to 20%.

As an integral part of the study undertaken by Blakey *et al.* (1991) mentioned previously, they also set out to design a VCR device, in order to achieve an Otto-Atkinson cycle engine. The VCR device built consisted of an auxiliary piston that was located in place of one of the exhaust valves from each cylinder, as shown in Figure 4, from Blakey *et al.* (1991). Control of the auxiliary piston is by hydraulics which make use of the engine lubricating oil. It is a two-position system and was designed to give either the nominal (10:1) or an increased (13:1) CR. The VCR device was incorporated into their LIVC engine, and tested up to loads of 5 bar bmep. However troublesome hydraulic leaks prevented any conclusive bsfc results from being obtained from this test rig.

Future Work In This Field

It is apparent from the previous studies reviewed here that when implemented alone LIVC load control offers a bsfc reduction in the region of 7%, at very light loads. To comply with emissions regulations this would need to be implemented on a fuel injected engine, Haugen *et al.* (1992) suggest that a management system monitoring load using a MAF sensor would be best suited for this. The mechanism developed by Blakey et al. (1991) was packaged within the engines original castings, and is neat and robust system suited to mass production, that requires a minimum of modification to a standard engine. However this system requires a mechanism to phase shift the inlet camshaft. Any system used is likely to add a prohibitive cost to this concept. It is also important to consider with all the mechanisms described here that the marginal benefit offered by LIVC must be offset against the added energy required to operate additional components.

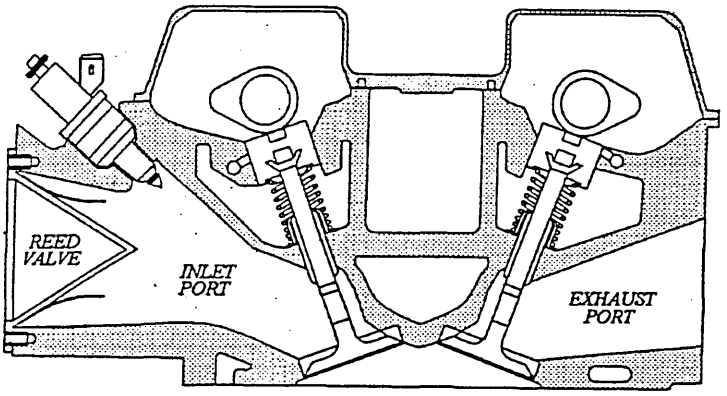

Figure 5 - Diagram Showing the Intended Location of the Reed Valve in the Proposed System.

At Sheffield Hallam University our aim is to develop a cheap and simple mechanism that will allow two state LIVC control, with the remainder of the load control being achieved with a conventional throttle valve. The LIVC device would allow the engine to operate with wider than normal throttle settings at low load, and hence reduce pumping losses. The proposed system is depicted in Figure 5, which consists of an intake camshaft with a profile causing late closing of the intake valve at all times. For full load operation a reed valve situated in the intake manifold prevents the charge from being rejected from the cylinder. At low loads the reed valve is by-passed to allow charge to return freely to the inlet manifold. A successful installation will require that reed valve is sited as close as possible to the inlet valve, whilst leaving sufficient space for the by-pass.

In view of the extra bsfc reductions (around 20%), the Otto-Atkinson cycle is a much more attractive proposition for future exploitation. It is felt that the two-state LIVC device described above will be ideal for use in conjunction with a two-state VCR device, similar to that developed by Blakey *et al.* (1991).

Conclusion

The LIVC concept offers bsfc reductions in the region of 7%, whilst also reducing NO_x emissions. However a number a detrimental effects have also been observed, such as poor fuel vaporisation and lower in-cylinder gas temperatures, which all degrade the combustion event. Tuttle (1980) observed no significant increase in specific emissions of hydrocarbons with his LIVC engine, compared with the conventional engine, whilst both Gould *et al.* (1991) and Haugen *et al.* (1992) found HC emissions to increase with LIVC operation. Saunders (1986) observed a beneficial manifold effect in a 4-cylinder engine which may help to offset these draw-backs. Haugen *et al.* (1992) suggest that if fuel injection is to be used with LIVC then a management system monitoring MAF would be best suited. For sufficient load control for automotive purposes, LIVC must be combined with a conventional throttle valve. The Otto-Atkinson cycle is a more attractive proposition as it produces bsfc reductions in the region of 20%, but requires much greater modification of the engine hardware.

References

Ahmad, T.; Theobald, M.A. 'A Survey of Variable-Valve-Actuation Technology.' SAE paper no. 891674, 1989.

Automotive Engineer, PP52-53, Vol.20 No.2, 1995, ISSN 0307-6490.

Blackmore, D.R.; Thomas, A. 'Fuel Economy of the Gasoline Engine.' The Macmillan Press Ltd, 1977.

Blakey, S.C.; Saunders, R.J.; Ma, T.H.; Chopra, A. 'A Design and Experimental Study of an Otto-Atkinson Cycle Engine Using Late Intake Valve Closing.' SAE paper no. 910451, 1991.

Dresner, T.; Barkan, P. 'A Review and Classification of Variable Valve Timing Mechanisms.' SAE paper no. 890674, 1989.

Dresner, T.; Barkan, P. 'A Review of Variable Valve Timing Benefits and Modes of Operation.' SAE paper no. 891676, 1989.

Elrod, A.C.; Nelson, M.T. 'Development of a Variable Valve Timed Engine to Eliminate the Pumping Losses Associated with Throttled Operation.' SAE paper no. 860537, 1986.

Gould, L.A.; Richeson, W.E.; Erickson, F.L. 'Performance Evaluation of a Camless Engine Using Valve Actuators with Programmable Timing.' SAE paper no. 910450, 1991.

Haugen, D.J.; Blackshear, P.L.; Pipho, M.J.; Esler, W.J. 'Modifications of a Quad 4 Engine to Permit Late Intake Valve Closure.' SAE paper no. 921663, 1992.

Hosaka, T.; Hamazaki, M. 'Development of the Variable Valve Timing and Lift (VTEC) Engine for the Honda NSX.' SAE paper no. 910008, 1991.

Lancefield, T.M.; Gayler, R.J.; Chattopadhay, A. 'The Practical Application and Effects of a Variable Event Valve Timing System.' SAE paper no. 930825, 1993.

Luria, D.; Taitel, Y.; Stotter, A. 'The Otto-Atkinson Engine - A New Concept in Automotive Economy.' SAE paper no. 820352, 1982.

Ma, T. 'Recent Advances in Variable Valve Timing.' International Symposium on Alternative Engines and Advanced Automatics, Toronto 1986.

Nagesh, M.S.; Govinda Mallan, K.R.; Gopalakrishnan, K.V. 'Experimental Investigation on Extended Expasion Engine (EEE).' SAE paper no. 920452, 1992.

Nelson, M.T.; Elrod, A.C. 'Continuous-Camlobe Phasing: An Advanced-Valve-Timing Approach.' SAE paper no. 870612, 1987.

Saunders, R.J. 'Atkinson Cycle Spark Ignition Engines.' International Journal of Vehicle Design, IVAD congress volume 4, 1984.

Saunders, R.J. 'Part Load Control of Spark Ignition Engines to Improve Fuel Economy (Atkinson Type Cycles).' Report to the Science and Engineering Research Council, 1986.

Saunders, R.J.; Rabia, S.M. 'Part Load Efficiency in Gasoline Engines.' Proc. Seminar on Practical Limits of Efficiency in Engines, I.Mech.E. PP. 55-62, 1986.

Saunders, R.J.; Abdul-Wahab, E.A. 'Variable Valve Closure Timing for Load Control and the Otto-Atkinson Cycle Engine.' SAE paper no. 890677, 1989.

Tuttle, J.H. 'Controlling Engine Load by means of Late Intake-Valve Closing.' SAE paper no. 800794, 1980.